AN INVESTIGATION OF THE RELATIONSHIP BETWEEN BEAM AND GLOBAL IRRADIATION WITH THE DEVELOPMENT OF NUMERICAL SOLAR RADIATION MODELS

A THESIS
Presented to
The Faculty of the Division of Graduate Studies

By

Constantinos Agelou Balaras

In Partial Fulfillment
of the Requirements for the Degree
Doctor of Philosophy

The George W. Woodruff School of Mechanical Engineering
Georgia Institute of Technology
June, 1988

AN INVESTIGATION OF THE RELATIONSHIP BETWEEN BEAM AND GLOBAL IRRADIATION WITH THE DEVELOPMENT OF NUMERICAL SOLAR RADIATION MODELS

Approved:

S. M. Jeter, Chairman

W. L. Chameides

J. I. Craig

C. G. Justus

W. J. Wepfer

Date Approved by Chairman May 26, 1988

To my parents,

Christina and Agelos

Thank you for sharing my dreams and
for your help in reaching my goals

ACKNOWLEDGEMENTS

The author is indebted to many people who have assisted him both directly and indirectly in preparation of this work.

To my academic advisor, Dr. Sheldon M. Jeter, I extend my sincere gratitude for his wise guidance throughout this endeavor, patience, continuous encouragement, and time invested that made the completion of this thesis possible. Special thanks are also extended to the committee members of this thesis, Drs. W. Chameides, J. Craig, C. Justus, and W. Wepfer, for their many useful comments and suggestions.

This work was performed under the financial support of the Georgia Power Company. My own research, and indeed solar energy research within the School of Mechanical Engineering, could not have been possible without this generous support which manifests this organization's concern for secure and economical energy resources in the future. In particular, the support and encouragement of Mr. E. J. Ney, Manager of Solar Operations, is gratefully acknowledged.

Finally, the author would like to thank his family, and friends, for their continued love, support and encouragement. This work is especially dedicated to my parents as a small token for all their sacrifices, and above all for nurturing me with their highest ideals.

TABLE OF CONTENTS

Appendixes Page

Appendixes

Appendixes Page

LIST OF TABLES

LIST OF FIGURES

Figure Page

Figure Page

Figure Page

Figure Page

NOMENCLATURE

a, b	regression coefficients
AST	apparent solar time
AU	astronomical unit
b_n	seasonal factor
c	distance from the center of the earth's orbit to a focus of its elliptical orbit
CF	percent cloud fraction
CVLT	local standard time
d	time in days in Universal Time since the standard epoch
d.f.	degrees of freedom
e	eccentricity of earth's orbit
E_T	equation of time
F	F-statistic
F_5	basic Shenandoah five-year model
F_m	regression model for month m
G_{sc}	solar constant
H	daily global radiation
H_d	daily dome radiation
H_o	extraterrestrial daily horizontal radiation
I	hourly total radiation
I_{bn}	hourly beam normal radiation
I_d	hourly scattered radiation on the horizontal (dome radiation)

I_o	hourly extraterrestrial horizontal radiation
I_{on}	hourly extraterrestrial normal radiation
K	atmospheric extinction coefficient
k_d	daily or hourly dome fraction
k_t	daily or hourly clearness index
l	depth of atmosphere
LST	local sidereal time
L_{st}	standard longitude
L	local longitude
m	optical air-mass
M	mean anomaly
M_o	mean anomaly at standard epoch
MS_E	mean sum of squares for the residual
MS_R	mean sum of squares for the regression
MST	mean solar time
n	number of observations
N	day of the year
p	atmospheric path length
q	number of parameters
r^2	coefficient of determination
r_e	effective radius of cloud droplet
R	prevailing sun-earth distance
RA	right ascension
R_{ave}	average sun-earth distance
R_m	mean sun-earth distance

RSS	sum of squares of the observations about regression
S_{xx}	sum of squares of the x's about their mean
S_{xy}	sum of products of the deviations of the x's and y's from their respective means
SSR	sum of squares of regression about the mean
SYY	sum of squares of the observations about their mean
TM	eccentric anomaly
w	liquid water content
W	liquid water path
x	observed value of the independent variable
y	observed value of the dependent variable
x_{oi}	lower limit of clearness index (k_t) bands
y_{oi}	regression model at x_{oi}
X_i	predicted value of the independent variable
Y_i	predicted value of the dependent variable

Greek Symbols

α	solar altitude (sun elevation)
β	longitude of perihelion
β_i	regression coefficient
β_o, β_1	parameter estimates of regression coefficients
γ	vernal equinox

γ_s	azimuth angle
δ	earth's declination
Δt	time interval
Δz	cloud depth
$\Delta\tau_b$	variable defined as $(\tau_{bc}-\tau_b)$
ε	data residual
η	temporal variation coefficient
θ_z	solar zenith angle
κ	normalized extinction coefficient
λ	sun's ecliptic-true longitude
τ_b	atmospheric beam transmittance
τ_{bc}	limiting clear sky beam transmittance
τ_c	cloud optical thickness
ϕ	local latitude
ω	hour angle

Subscripts

ave	average value
b	beam radiation
c	clear sky conditions
d	sky radiation on the horizontal (dome)
H	alternative hypothesis
i	band coefficient

j	datum
n	radiation on normal plane
o	extraterrestrial radiation
o	null hypothesis when used in statistics
s	sky radiation
T	radiation on tilted plane

SUMMARY

A number of improved numerical models have been developed to predict the beam radiation from global radiation data. The analysis was based on five years of hourly radiation data collected at the Solar Total Energy Project in Shenandoah, Georgia.

Previously developed empirical correlations relate hourly values of the beam transmittance, τ_b - beam normal radiation over the extraterrestrial normal radiation, to clearness index, k_t - global radiation over the extraterrestrial global radiation. The relationship of τ_b-k_t, though, is not deterministic. Some the observed variation was explained by a seasonal dependence. Improved performance was achieved by introducing a third variable, either the atmospheric air-mass (m), or the temporal variation coefficient, η, a new dimensionless parameter used to describe the sky condition without using any meteorological information.

Seasonal effects on solar radiation caused by cloudiness and air quality were found to be significant and two methods were developed to account for this phenomenon. The air-mass dependence of solar radiation was examined through a study of the relationships between (τ_b-m) and (k_t-m). A simple clear sky beam transmittance model was developed for the region,

although it was shown that clearest skies are not necessarily site specific.

Two improved beam radiation models were developed, relating three variables at a time - namely (k_t,m,τ_b) and (k_t,η,τ_b). These correlations have significantly increased the predictive powers of the beam radiation model, without compensating for additional input information. These models can predict different values of beam radiation for a given day and over the year, for the same value of global radiation which is what is observed. Several surface fitting techniques were used to generate the response surface among which are, a best RMS triangulation method, an inversely weighted fit method, and a fifth-degree polynomial fit.

The work satisfies a major deficiency in solar radiation modeling by providing the most accurate up-to-date models for the southeast United States. The proposed models were validated with data from the National Observatory of Athens, Greece. The good performance of the models is reassuring of their wide applicability.

CHAPTER I

INTRODUCTION

Solar Energy has developed substantially in the last two decades. Technological advances in the area continuously open new horizons, and exciting opportunities for different applications are being found. This chapter is intended to provide a brief overview of the significance of solar energy and outline the goals to be accomplished by this work.

1.1 The Solar Energy Option

Solar Energy is a superficially new branch of technology which has hopefully and auspiciously appeared on the international stage.

The beginning of the exploitation of solar heat can be traced throughout the ages. One should connect it with the existence of the oracles. As Plutarch says, the light of the altar at the oracles should be transmitted from "a clean and immaculate flame" that only the sun could offer with the help of the "σκαφεια", the concave mirrors the Hestiades virgins used in order to focus the solar rays.

Much later there appears the man, who became famous in mechanics and was praised by all to the highest degree -

Archimedes - who burned the attacking Roman fleet at Syracuse in 212 BC, by using the sun's power. In the Byzantine period the exploits of Archimedes were duplicated during a siege of Constantinoples, by the mathematician and Neoplatonic philosopher Proclus, who it appears was unaware of Archimedes' feat.

It is of course not possible to enumerate everything that occurred in between those distant dates and our days, which in any event is not within the scope of this work. There is only one observation to be made: Why did that old idea remain unexploited for so many centuries?

One of the reasons, most certainly, is that during the centuries that have elapsed, our present day needs did not exist in their pressing forms. Another reason that has also contributed is that we rarely refer to the past. One should not oversee the fact that several times old and forgotten methods, brought back from oblivion, have been discovered as concealing useful knowledge and ingenious ideas which, applied and perfected, can in many cases benefit modern man.

One can only wonder what perfection the present times would have reached if a systematic exploitation of solar energy had begun long ago. Still, a bright future lies ahead of us. Upcoming developments of this branch of technological endeavor will no doubt lead to new exciting ways to use solar energy, and hereby promote human welfare and happiness.

Why shouldn't the same thing happen with solar energy as occurred with electricity? The pioneers of electrical energy considered electricity as a means of conducting experimental research and they may have dimly foreseen in it a source of light. They certainly did not imagine that it would produce the endless series of modern applications, and in such a comparatively short time.

Although the energy crisis of the 1970's was ignited by political reasons, a new and even more severe problem will soon evolve. Fossil fuel reserves, according to Tabor (1985) and others, will last decades, not centuries. Thus, it is of utmost importance for the human race that alternative energy sources be considered.

At an annual increase of world energy consumption of about five percent, the proven reserves of the three major fossil fuels - oil, gas, and coal - would last about a century, while the ultimate reserves, including sources not considered exploitable at present, would extend this a further century.

Tabor (1985) believes that renewable sources are the only options available to solve the forthcoming energy shortages. Limitations on the development of solar energy, of course, exist. There should be no excuse though for not exploiting solar energy whenever possible.

1.2 Problem Statement

Radiation from the sun is the primary source of most energy used by mankind. The life expectancy of fossil and nuclear reserves are difficult to determine with accuracy. However, the earth's supply of fuels is limited and severe shortages of this form of fuel are possible within the near future.

The technologies of solar energy show promise for applications in all major economic sectors - residential, commercial, industrial, transportation, and utility. At the present stage though, and for the future economic viability of this technology, every application must show good performance. For that reason, one needs to be successful in the initial design stage (i.e. site selection, performance prediction of active or passive solar systems) before a design weakness results in a costly aftermath.

Local solar radiation data can provide a complete picture of the solar potential for the region of interest. Such information is of capital importance to anyone involved in the preliminary design, analysis, and modeling of solar energy systems.

Several other disciplines, such as architecture and environmental engineering, require knowledge of the availability of local solar radiation. Radiation information is also greatly needed for agricultural purposes (a key factor

in evaluating the soil moisture status, which greatly affects agricultural yields).

There is indeed a wide spectrum of applications for solar radiation data. However, the complexity and cost of a reliable radiation measuring network may prohibit their deployment. Worldwide, there is a limited number of stations with many regional gaps. As a result, many users are forced to collect their own solar radiation data. Such data collection efforts can delay solar energy applications or related projects for a considerable amount of time.

Thus, it is desirable to have other alternatives available that can provide accurate information on the local solar radiation data and in addition, substantiate and/or complement observations. This situation has made the development of models for estimating the solar radiation components a high priority among solar energy researchers.

1.3 Objective

The main objective of this work is to develop the most accurate, up-to-date numerical models for the Southeast region of the United States to predict the solar radiation components. Such information is generally needed in order to calculate the radiation on tilted surfaces (such as thermal or photovoltaic solar collectors) and assessing the performance of concentrating collectors.

This work has been intentionally established upon the simplest possible practical basis, the dependable and commonly measured global radiation. The developed empirical correlations were based on five years of data collected at the Solar Total Energy Project, which is located in Shenandoah, Georgia (33.4042° N, 84.7478° W).

The development of our models proceeded through a series of sequential steps. The first step examined annual, and seasonal variations in the relationship between τ_b (the beam transmittance, defined as the ratio of the beam normal to the extraterrestrial normal radiation), and k_t (the clearness index, defined as the ratio of global to extraterrestrial global radiation) based on the available five year data. The next step looked for clues which would clarify the effect of parametric variables on the relationship between τ_b and k_t.

The analysis of the developed correlations may be used to provide an insight on how easily measured and/or calculated variables can be related to other useful but usually unavailable solar radiation components (beam or diffuse). It should be noted though, that all of the work is limited to solar radiation information, with meteorological and other variables being used only to substantiate either observations or conclusions made during the progress of the analysis.

In the conclusion of this work, the best correlation should incorporate information that qualifies to explain the physics of the phenomenon which links the beam and global

radiation but does not overcomplicate the model. Our intention is to keep the developed model more accurate than other available correlations, but at the same time minimizing the amount of input information required to facilitate future implementation.

The development of the proposed solar radiation network by the Southern Company across the southeast United States will provide a complete data base for the region in the near future. This network is to provide hourly global radiation measurements from several unattended remote stations, scattered in the region.

The procedures presented in this work may then be used to decompose the global radiation to its components, depending on the nature of the application. Thus, it becomes evident that our search for dependable correlations to predict beam radiation is bounded by our objective to limit required input to only solar radiation data. This is a condition that the final product of this work must satisfy.

CHAPTER II

SOLAR RADIATION PRINCIPLES

The sun's structure and characteristics determine the nature of the energy that it radiates into space. This chapter is intended to provide some basic information on solar radiation and related terminology. The various components of solar radiation are introduced, along with other fundamentals that are provided as background for the proceeding discussion.

2.1 Theoretical Fundamentals of Solar Radiation

The sun is a giant nuclear fusion reactor, converting 4 million tons of hydrogen to helium per second, and emitting about 39.06 10^{25} W of energy (short wavelength radiation) towards the earth every year. There are conflicting reports in the literature on periodic variations of intrinsic solar radiation. According to measurements conducted during the last 60 years, there are small variations (within approximately $\pm$1 percent) with different periodicities and variation related to sunspot activities, Sabatino, Demarque, and Endal (1985).

Measurements from Nimbus and Mariner satellites over periods of several months showed variations within limits of $\pm$ 0.2 percent, Frohlich (1977), over a time when sunspot activity was very low. For the purposes of this work, and until reliable measurements indicate otherwise, the energy emitted by the sun can be considered constant.

In any event, such changes of solar irradiance cannot produce a detectable effect on earth. These changes are less than those due to the eccentricity of earth's orbit, and far less than the day-to-day fluctuations of solar flux due to global changes in cloud cover. For more information on solar variability, the reader is referred to Studies in Geophysics (1982).

Although the earth intercepts but a minute fraction of the energy released by the sun, that falling on the earth's atmosphere occurs at the rate of 5.4 10^{24} Joules per year, or 170 trillion Kilowatts. This is some 27000 times the energy produced by all human-made systems in the world.

From that energy, according to recent estimates, about 6% is either reflected or scattered back into space by the atmosphere, 20% is reflected by clouds, 3% is absorbed by clouds and 16% by the atmosphere, and 51% heats the earth's surface. Finally, 4% of the incoming radiation is reflected back into space from the earth's surface, presumably without any effect on the earth or its atmosphere.

Earth, of course, radiates away an equivalent amount of energy, in the form of longwave or infrared radiation, thus maintaining the earth's average temperature at around 45° F. About 30% of the sun's energy is reflected without affecting the earth's temperatures. Of the remaining 70%, 6% flows from the earth's surface directly into space, another 15% heats the atmosphere, and 59% is radiated into space (e.g. by delivery of the latent heat in water vapor, and rising warm air masses).

Exact measurements of the energy flow have been made historically from satellites and balloons. It is expected though that the new Earth Radiation Budget Satellite, deployed by the shuttle Challenger during its late 1984 mission, will produce data that, when combined with readings from the unmanned weather satellites of the National Oceanic and Atmospheric Administration (NOAA), will provide the most complete measurements to date.

On the average, 99% of the sun's radiation reaching the earth falls in the spectral range between 0.29 μm and 4 μm, Dogniaux et al. (1984). The radiation occurring in this spectrum is referred to as solar radiation. Radiation in the spectral range longer than 4 μm dominates the terrestrial radiation emitted by the earth.

Results also presented also by Bird (1981) indicate that for a reasonable range of cloud-free atmospheric conditions, the broad band incoming solar radiation is attenuated by

atmospheric constituents in the following order: aerosols attenuate the most, molecular scattering is next in importance and water vapor absorption is third. Attenuation by ozone, carbon dioxide, and oxygen is nominal.

The energy from the sun, per unit time, received on a unit area of surface of the radiation, at the earth's mean distance from the sun (one Astronomical Unit=1.495 10^{11} m), outside of the atmosphere, is called the solar constant (G_{SC}). In the past, measurements to determine the value of the solar constant were made from ground based instruments (that is, after parts of the incoming solar radiation had been absorbed or scattered).

Later on, additional measurements were made from high peak mountains that helped to better estimations of its value. Initially, the value assigned to G_{SC} by C.G. Abbot and his colleagues at the Smithsonian Institution was 1322 W/m^2. Johnson (1954) updated this value to 1395 W/m^2.

Several attempts have been made to measure accurately the exact value of the constant and investigate its seasonal variation. There is still, though, disagreement between researchers on its absolute value, Thekaekara (1976). Some of the values that have been historically assigned to G_{SC} are listed in Table 2.1, adapted from Lowry (1980). There will be some time before one can say with certainty how much of the variability of the published values of G_{SC} is due to observational error, to errors of extrapolation from within to out-

side the earth's atmosphere, or to actual temporal variability of the sun's power.

Table 2.1

A Sample of Published Values for the Solar Constant

Published by	Value ($W\ m^{-2}$)	Notes
Kondratyev, 1969	1255 to 1269	Various Soviet authors 1952-60
Kosters et al, 1969	1334	Three balloon soundings
Shaw, 1930	1350	
Godske et al, 1957	1353	
Willson et al, 1980	1368	Rocket sounding in June 1976
Willson et al, 1980	1373	Rocket sounding in November 1978
Hickey et al, 1980	1376	Nimbus 7 satellite
Smith et al, 1977	1392	Nimbus 6 satellite
Raschke and Bandeen, 1970	1350 to 1430	Various U.S. authors 1954-68

The value of the solar constant to be used in this work is 1367 W/m^2, adopted by the World Meteorological Organization (1978). Knowledge of the exact value of the solar constant is not fundamentally important for our study. In our analysis, the solar constant is only a normalizing

factor and the adopted value should be continued to be used in relation to this work.

2.2 Solar Radiation Components

In the literature, solar radiation arriving on a surface is variously termed irradiation (or radiant exposure), insolation, radiation, irradiance, radiance, intensity, radiant flux, radiant flux density, etc. It is necessary to adopt a minimum set of terms and explain their meaning, since there are distinctions between terms expressing the quantity of energy and those denoting the rate of energy.

Irradiation, J m^{-2}, refers to the incident energy per unit area on a surface during a given period of time (usually an hour or a day). Insolation is an alternative term, and applies specifically to solar energy irradiation, but has fallen into indefinite usage. It is customary to use the symbol "I" for hourly or other shorter period irradiation values, while "H" denotes daily values. In both cases, H and I, can represent any component of solar radiation, and can be on surfaces of any orientation.

Irradiance, W m^{-2}, is the same as radiant flux density or flux. It refers to the rate at which radiant energy is incident upon a surface, per unit area of that surface. Usually the symbol "G" is used, with appropriate subscripts to denote the appropriate component and reference surface of solar radiation.

Radiation is employed in a generic sense, and its meaning should be obvious from the context. Intensity, $W/m^2/sr$, refers to the irradiance from a particular direction and contained within a unit solid angle, on an area normal to the direction of radiation.

The solar (total) radiation is composed of the beam and scattered radiation. Each of these terms is defined as follows and illustrated in Figure 2.1.

Beam Radiation (I_{bn}) is the component of solar radiation received from the sun with minimal or no scattering by the atmosphere. It is composed of the direct and the near circumsolar radiation components. According to Grether et. al. (1975), from measurements made at Berkeley, California, the amount of irradiance from the immediate vicinity of the sun (near circumsolar, within 3° of the sun-earth vector) was typically 1.75 percent of the direct irradiance. In practice, beam radiation is measured with a standard pyrheliometer.

Scattered Radiation is the component of solar radiation received from the sun after its direction has been changed due to scattering by the atmosphere or clouds (the so-called, sky radiation) and ground reflected radiation (the so-called, foreground radiation). As a result of these interactions, part of the incoming solar radiation is diffused anisotropically. In practice, scattered radiation is measured with a shaded pyranometer. The sky radiation when measured on the horizontal is called dome radiation. This is what is referred

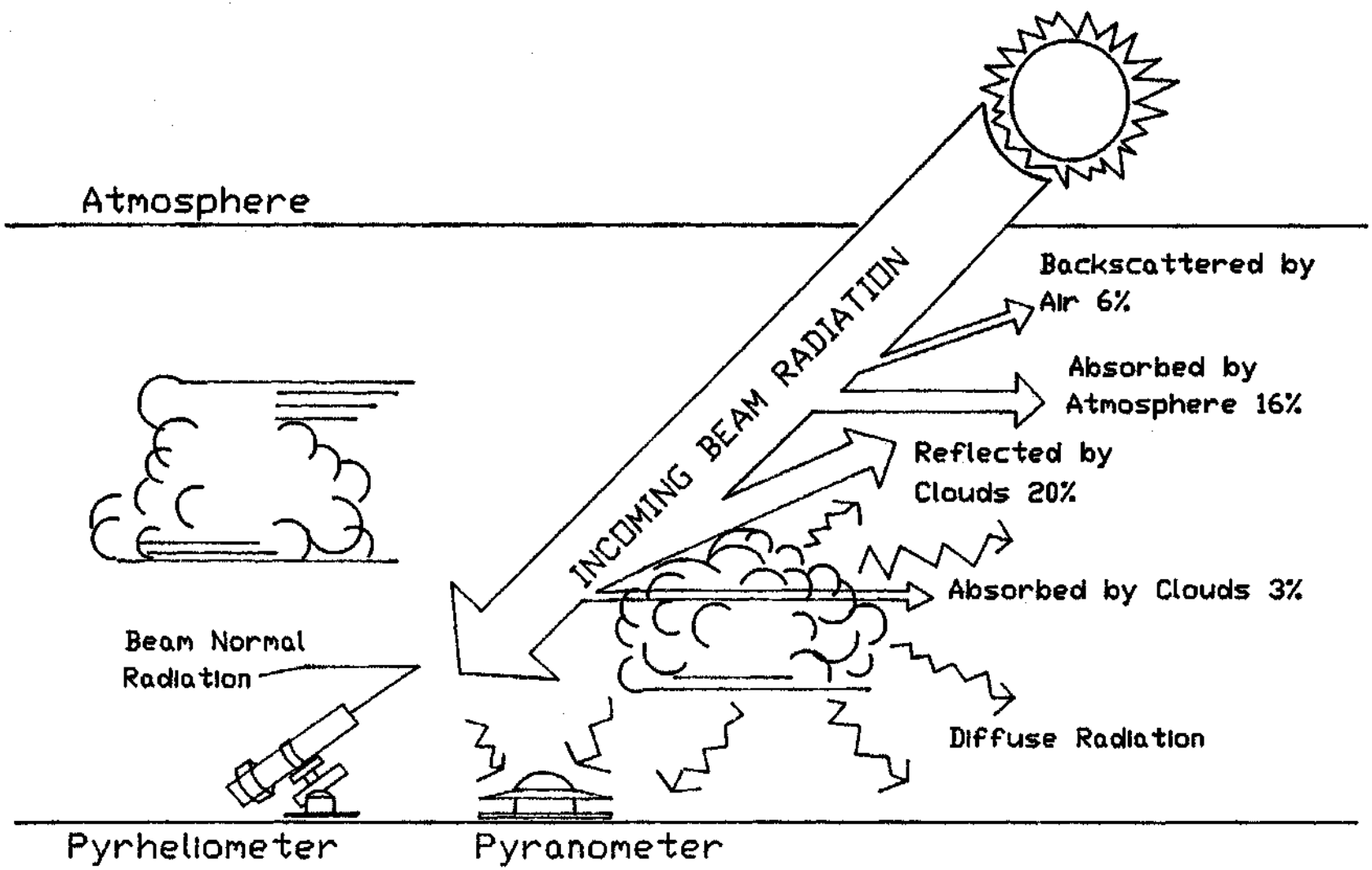

Figure 2.1 Components of Incoming Solar Radiation

to in literature as diffuse radiation, a term that actually describes the nature of the process for both sky and foreground radiation. The term "dome" for full sky radiation allows the retention of the standard mnemonic subscript, "d".

Total Radiation (I) is the sum of the beam and scattered radiation received on a surface. In practice, the total radiation is measured with a pyranometer. These measurements can be made on the horizontal (the so-called, global radiation), on a tilted plane (usually at the latitude angle), or on a tracking plane.

Accepted notation of different subscripts used on G, H, and I are as follows:

"o" refers to radiation above the earth's atmosphere (extraterrestrial radiation),

"b" and "d" refer to beam and sky radiation on the horizontal (the latter is the dome radiation), and

"T" and "n" refer to radiation on tilted or normal planes. If neither T or n appear, the radiation is on a horizontal plane.

Historically, global radiation has been measured in several parts of the world, as well as the United States. Experience has also proved that global radiation values are the most dependable measurements.

On the other hand, the consistently adequate operation of pyrheliometers, being a tracking instrument, is demanding on time and other resources (e.g., frequent adjustment). As a

result, exact and reliable beam normal radiation data is not so readily available as global, pyranometer, data. As a matter of fact, many meteorological stations have not recorded beam normal radiation, probably due to the instrument's complexity. Available sources of solar radiation data are reviewed in Chapter 4.

CHAPTER III

SOLAR ASTRONOMY

The availability of solar energy at the earth's surface is not uniform. It depends primarily on the optical state of the atmosphere and the apparent daily motion of the sun across the celestial vault. This chapter reviews some principles of solar astronomy and the sun's apparent motion about an observer on earth.

Balaras (1985) developed a FORTRAN algorithm called HELGO (Appendix A) based on the so-called low precision formulas to calculate the position of the sun. HELGO provides an acceptable level of precision and accuracy. For the purpose of this work, where we are dealing with solar radiation analysis, an accuracy of $\pm$ 0.5 to 1.0 degrees is satisfactory. The following discussion reviews the principles that have been implemented in HELGO.

3.1 The Position of the Sun

The position of the sun relative to a specific point on the earth, varies throughout the day and season, due to the spin of the earth around its axis and to its orbit around the sun. The earth revolves around the sun in an elliptical orbit

of small eccentricity.

The earth's motion about the sun is affected primarily by the gravitational attraction between the earth and the sun. For simplicity, we will ignore any other influences of the other planets and assume that the earth is the only celestial object orbiting the sun.

Since the sun has a much greater mass than the planets, one can assume that the sun remains approximately stationary as the earth moves in its orbit. According to Kepler's First Law (Law of Ellipse-1609) the orbit of each planet is an ellipse, with the sun located at one of the focuses, as indicated in Figure 3.1. The amount by which the orbit deviates from circularity, that is, the eccentricity (e) of the ellipse, is very small, and can be defined as:

$$e = \frac{c}{a} \tag{3.1}$$

where c = distance from the center to a focus, and

a = semimajor axis.

In Figure 3.1 the eccentricity of the earth's orbit is exaggerated for purposes of illustration.

The fixed plane containing the earth's orbit is called the ecliptic plane. The earth's axis of rotation is tilted at 23°26.5' (1984 value) with respect to the ecliptic plane (Figure 3.1). This angle is called the obliquity of the

ecliptic, ε, and can be considered fixed for our purposes. The actual decrease is approximately 47 arc-sec per century.

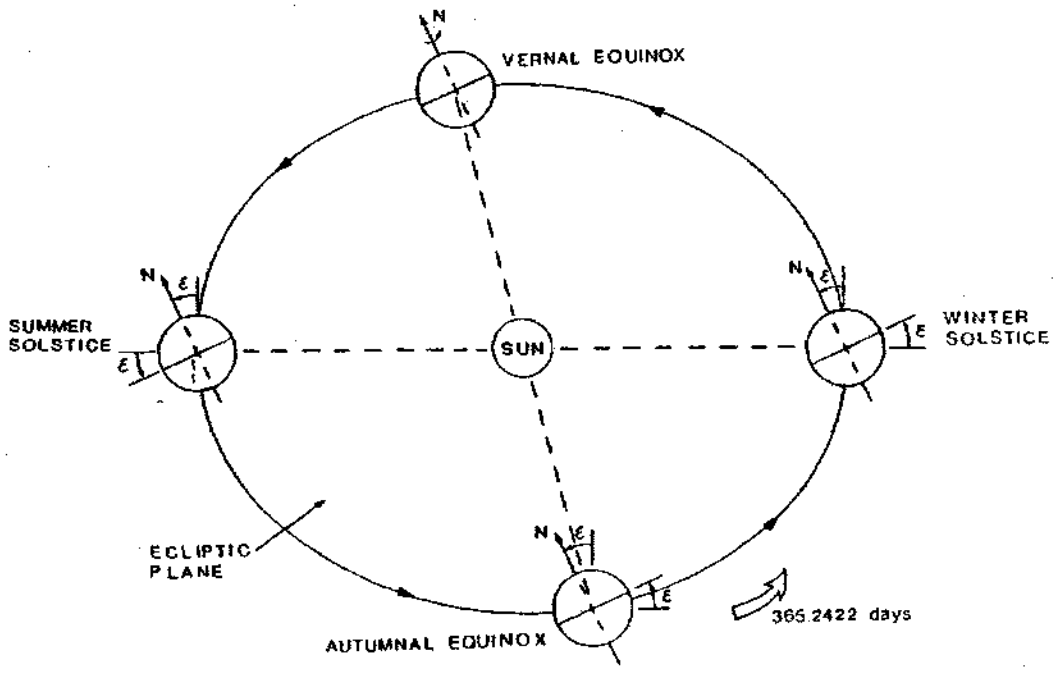

Figure 3.1 Earth's Elliptical Orbit Around the Sun

3.2 The Motion of the Earth

Let S be the sun's center and OEO' the ellipse, with S at one focus, in which the earth makes its annual revolution as illustrated in Figure 3.2. Consider the circle CE'C' (same area) with its center at S and its radius SE'= 1/2 (OO')=α. This is a hypothetical circular orbit.

The earth, E, orbiting the sun on an elliptic orbit is called eccentric earth, while E' orbiting the sun on a circular motion is called mean earth. The mean earth is assumed

to revolve about the sun with the same period as the eccentric earth.

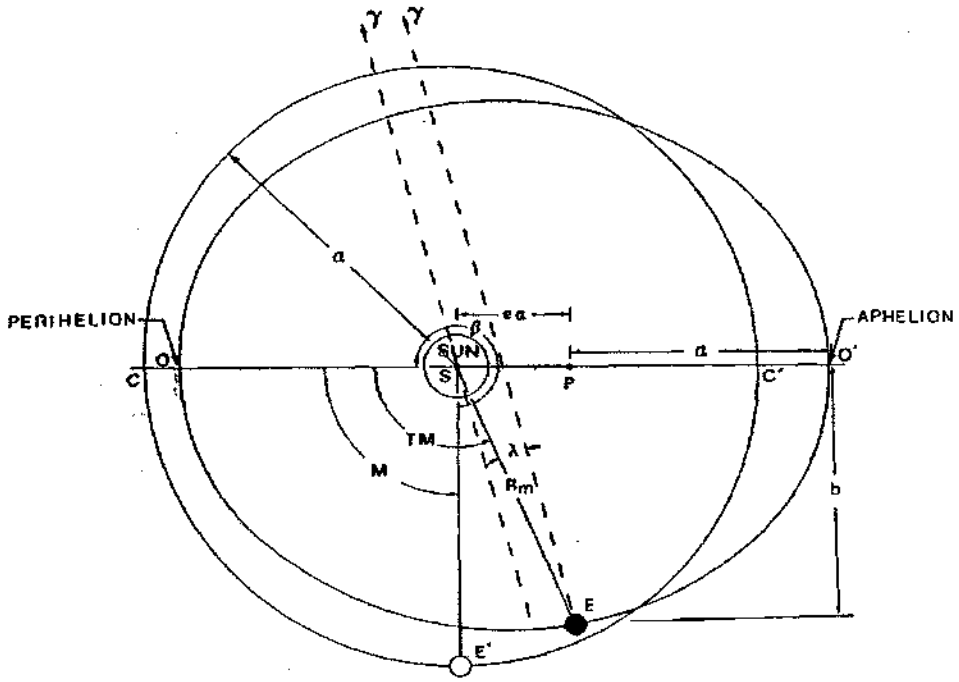

Figure 3.2 Variation in the Motion of the Mean and Eccentric Earth

There are two angles of interest, namely $O\hat{S}E$ and $C\hat{S}E'$. These angles are called respectively, eccentric anomaly (TM) and mean anomaly (M). The orbital velocities according to Kepler's Second Law are non-uniform, but vary in an angular fashion (Law of Equal Areas - 1609). The farther the earth is from the sun, the more slowly it moves in its orbit. The speed of the planet is actually inversely proportional to the square of the distance at the Aphelion and the Perihelion.

The eccentric earth returns to the Perihelion in an interval called the anomalistic year (365.2596 mean solar days), which is slightly longer than the time it takes for the earth to make one complete circuit of its orbit (360°) relative to the stars (the so-called sidereal year). Earth's sidereal year is equal to 365.25634 ephemeric days (or $3.155815\ 10^7$ seconds). This is due to the influence of the planets on the axis of the earth's orbit.

The mean earth completes its orbit during the same period, but it travels at a constant angular rate. As a result, when both the eccentric and mean earth make a complete revolution about the sun, they are again aligned with the sun's position at the Perihelion. Since the anomalistic year is 365.2596 days, the mean anomaly (M) is:

$$M = M_o + \left(\frac{360}{365.2596}\ \text{days}\right) d \qquad (3.2)$$

where M_o = mean anomaly at standard epoch, and

d = time in days in Universal Time since the standard epoch.

An epoch is simply another aspect of time, and is no more than a point of time selected as a fixed reference. It so happens that a scholar named Joseph Scaliger in 1582 first conceived the idea and proposed the Julian System. This system takes as the arbitrary initial epoch 12:00 Universal

Time (UT) January 1, 4713 BC. The Julian Date (JD) at this instant was by definition zero.

It is obvious that such an early starting epoch creates large numbers laborious to handle in calculations. Various other fundamental epochs have been suggested and in many cases the standard epoch is considered to be 12:00 UT January 1, 2000 (or indicated as J 2000). Then Equation 3.2 becomes:

$$M = 357.528 + 0.985600\ d. \qquad (3.3)$$

Equation 3.3 is better than the "low precision" formulas given by Watt (1978) and Cooper (1969), and is equivalent to the equation included in the Almanac for Computers (1984). Equation 3.3 should be accurate to 0.01° until year 2050.

The time of a phenomenon in days since 0 January 0^h UT, d, is calculated from:

$$d = \frac{N + (6^h - \lambda)}{24} \quad \text{(morning), or} \qquad (3.4)$$

$$d = \frac{N + (29^h - \lambda)}{24} \quad \text{(evening)} \qquad (3.5)$$

where N = Day of the year,

β = Longitude of Perihelion, and

λ = Sun's true longitude, $\lambda = TM + \beta$, in hours.

It is desirable that we have available an expression to calculate the earth-sun distance, since the solar radiation

arriving at the top of the earth's atmosphere varies with the square of the distance to the sun. Roberts and Boksenberg (1985) provide a relation based on the mean anomaly:

$$R_m = 1.00014 - 0.01671 \cos(M) - 0.00014 \cos(2M) \quad (3.6)$$

For 1983, the daily values of the mean distance of sun-earth, R_m in astronomical units, were calculated, with the following characteristic values:

$(R_m)_{min} = 0.98329$ AU on January 3, 1983, and

$(R_m)_{max} = 1.01699$ AU on July 6, 1983.

The variation of the sun-earth distance, ± 1.685 percent, is due to the eccentricity of the earth's orbit around the sun. The principal result is a ± 3.4 percent variation in the amount of radiation that reaches the earth's outer atmosphere.

The units of R_m (the mean distance between the earth and the sun) are in astronomical units (AU). The astronomical unit is defined as the length of the radius of the unperturbed circular orbit of a body of negligible mass (compared to the sun) moving around the sun with a sidereal angular velocity of 0.017202098950 radian per day of 86400 ephemeris seconds (1AU=1.4959787 10^{11} meters).

3.3 The Celestial Vault

For many purposes, star positions may be represented by points on the surface of an imaginary sphere of arbitrary

radius, centered at the earth's center. Such a unit sphere is called the Celestial Vault. The rotation axis of the earth intersects this sphere at the north and south celestial poles. The projection of the earth's equatorial plane onto the celestial vault and containing the center, is called the celestial equator or the equinoctial (Figure 3.3).

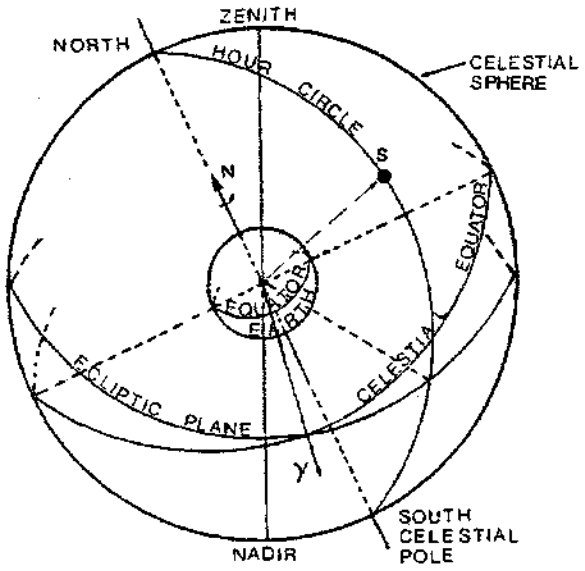

Figure 3.3 Basic Lines and Points of the Celestial Vault

The equator's plane is perpendicular to the axis of apparent rotation of the celestial vault and it is everywhere 90° from both celestial poles. The intersection of the great circle of the celestial sphere, in which the sun appears to perform its annual movement (the ecliptic), with the celestial equator provides two fixed points on the celestial equator 180° apart (since both are great circles). These

intersections are the equinoctial points (Vernal and Autumnal equinoctial points) or equinoxes.

The points on the ecliptic that are 90° from the equinoxes are the solstitial points or solstices. An alternative term for the Vernal equinox is the First Point of Aries (γ). The great circle normal to the celestial equator and passing through the sun, is called the hour circle.

3.3.1 Celestial Coordinate Systems

The position of the stars on the celestial vault can be defined by two perpendicular or curvilinear coordinates. There are four available reference planes:

A. The Ecliptic System,

B. The Equatorial System,

C. The Hour Angle System, and

D. The Horizontal System.

A. The Ecliptic System. The primary reference plane is the ecliptic and the secondary is the ecliptic meridian of Aries (Figure 3.4). The direction of the sun, point S, can be defined by the ecliptic latitude and the ecliptic longitude. The ecliptic latitude, β, is the angular distance between the direction of the observer to the sun and the ecliptic measured in the ecliptic meridian of S from 0° to 90°. It is positive when measured northward and negative southward. The complement of the true latitude is the true polar distance. The true (or ecliptic) longitude, λ, is the angle between the

ecliptic meridian of the sun and that of the equinox measured from the vernal equinox, γ, to the east, in the ecliptic from 0° to 360°.

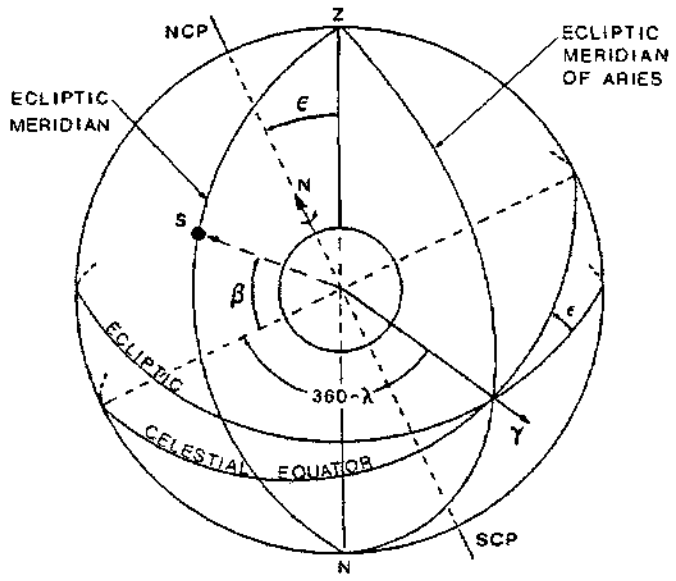

Figure 3.4 The Ecliptic System of Coordinates (β and λ)

B. The Equatorial System. The primary reference plane is the celestial equator and the secondary is the plane defined by the NCP and SCP on the celestial vault - the equinoctial colure (Figure 3.5). Let S be the arbitrary position of the sun on the celestial vault. Its direction is given by the declination, δ, and the right ascension, RA. The right ascension is the angle between the hour angle of S and the equinoctial colure, measured from the vertical equinox, γ, to the east in the plane of the celestial equator from 0^h to 24^h or from 0° to 360°.

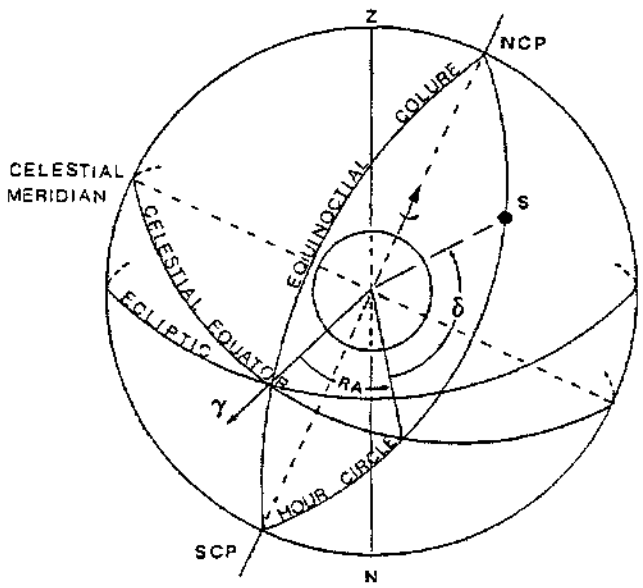

Figure 3.5 The Equatorial System of Coordinates (δ and RA)

C. The Hour Angle System. The primary reference is the celestial equator and the secondary is the hour circle containing the observer's celestial meridian (Figure 3.6). The direction of the sun, located at S, can be defined by the hour angle and declination. The hour angle, ω, is the angular distance between the hour circle and the observer's meridian. It is positive when measured westward from the observer. The declination, δ, is the angular distance from the celestial equator to the sun measured on the hour circle. It is taken with a positive sign on the northern half of the celestial sphere and with a negative sign on the southern half.

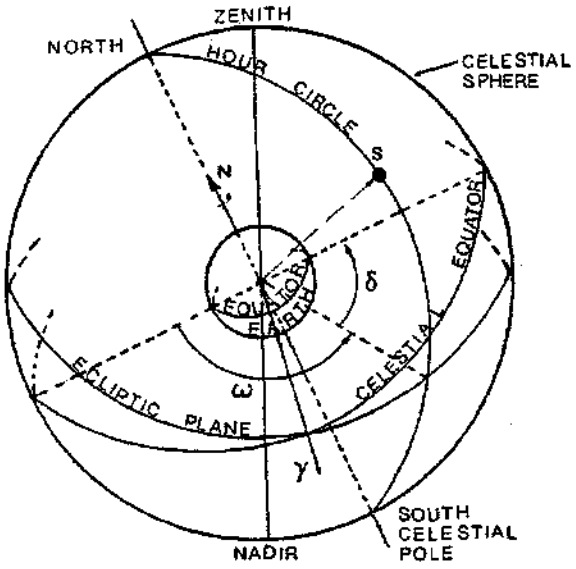

Figure 3.6 The Hour Angle System of Coordinates (δ and ω)

D. The Horizontal System. The primary plane is the celestial meridian (Figure 3.7). The direction of the sun, located at point S, can be defined by the elevation and the azimuth. The elevation, α, is the angular distance between the direction of the observer and the sun and the celestial horizon measured from 0° to 90° in the plane of the vertical circle through the position of the sun. It is considered positive above the horizon. Its compliment is the zenith angle, θ_z. The azimuth angle, γ_s, is the angular distance between the vertical plane of the sun and the celestial meridian of the observer measured from the direction of the north point to the east in the celestial horizon from 0° to 360°.

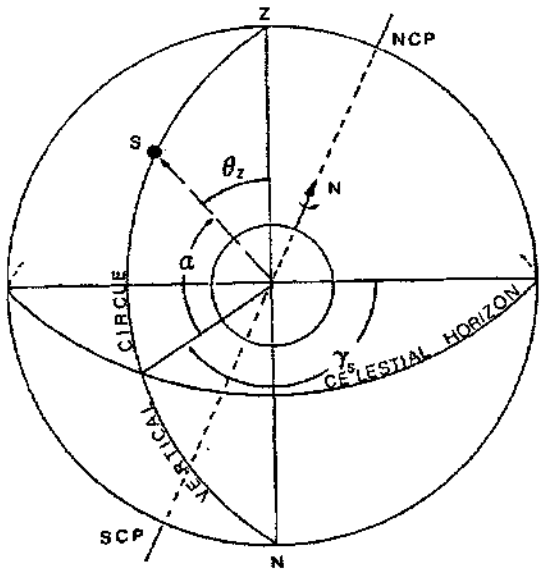

Figure 3.7 The Horizontal System of Coordinates (α and γ_S)

3.3.2 Conversions Between Equatorial and Ecliptic Systems

Consider a celestial vault composed of the equatorial and ecliptic systems (Figures 3.4 and 3.5). One can note that for the north ecliptic pole RA=270° and the longitude of the north celestial pole is 90°. The following relations may be obtained by applying the Laws of sine, cosine and the five elements of spherical trigonometry on the spherical triangle between NEP, NCP, and S. The resulting sets of equations are according to McNally (1974):

$$\cos\delta \cos(RA) = \cos\beta \cos\lambda \qquad (3.7)$$

$$\sin\delta = \cos\beta \sin\lambda \sin\varepsilon + \sin\beta \cos\varepsilon \qquad (3.8)$$

$$\cos\delta \sin(RA) = \cos\beta \sin\lambda \cos\varepsilon - \sin\beta \sin\varepsilon \quad (3.9)$$

$$\cos\beta \cos\lambda = \cos\delta \cos(RA) \quad (3.10)$$

$$\sin\beta = -\cos\delta \sin(RA) \sin\varepsilon + \sin\delta \cos\varepsilon \quad (3.11)$$

$$\cos\beta \sin\lambda = \cos\delta \sin(RA) \cos\varepsilon + \sin\delta \sin\varepsilon \quad (3.12)$$

If the ecliptic parameters ε, λ, β are known, the right ascension, RA, is found by dividing Equation 3.9 by Equation 3.8, i.e.

$$\tan(RA) = \tan\lambda \cos\varepsilon - \tan\beta \frac{\sin\varepsilon}{\cos\lambda} \quad (3.13)$$

and δ is given by Equation 3.8.

If the equatorial parameters RA, δ, ε are known, then λ is found by dividing Equation 3.12 by 3.10, i.e.

$$\tan\lambda = \tan(RA) \cos\varepsilon + \tan\delta \frac{\sin\varepsilon}{\cos(RA)} \quad (3.14)$$

and β is given by Equation 4.11. To determine the appropriate quadrant of RA or λ one can check the corresponding sines and the signs of the cosines.

3.3.3 Conversions Between Hour Angle and Equatorial Systems

For practical calculations the hour angle is more useful than the right ascension, since it accounts for the observer's local meridian and changes with the diurnal motion of the rotating earth. Declination is a common parameter for the hour angle and equatorial systems since both systems use the

equatorial plane as their primary reference.

Let us consider the celestial equator viewed from the north pole shown in Figure 3.8.

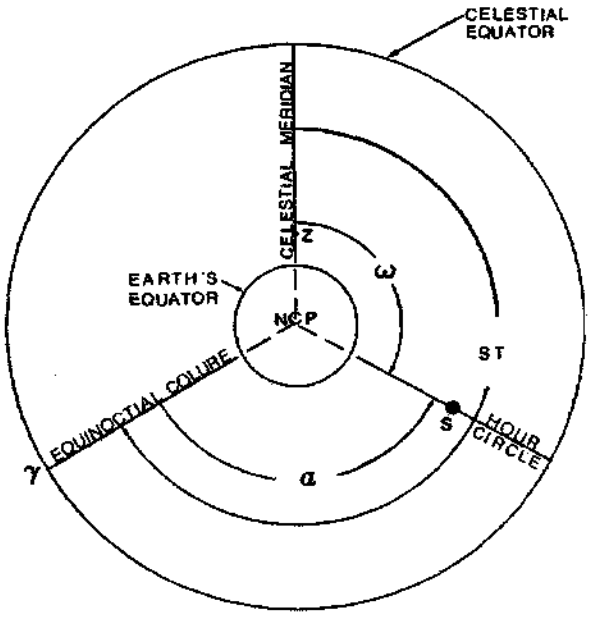

Figure 3.8 Relations Between the Hour Angle and Equatorial Systems

We can identify the Local Sidereal Time (LST) defined as the hour angle of the vernal equinox:

$$LST = \omega + RA \qquad (3.15)$$

Depending on the known parameters one may solve Equation 3.15 for either the right ascension or the hour angle.

3.3.4 Conversions Between Horizontal and Hour Angle Systems

Consider a celestial vault composed of the horizontal and hour angle systems (Figures 3.6 and 3.7). The relations

between the parameters of the horizon and the hour angle, derived from basic laws of spherical trigonometry, have been presented by McNally (1974) as follows:

$$\sin\theta_z \sin\gamma_s = -\cos\delta \sin\omega \tag{3.16}$$

$$\cos\theta_z = \sin\delta \sin\phi + \cos\delta \cos\omega \cos\phi \tag{3.17}$$

$$\sin\theta_z \cos\gamma_s = \sin\delta \cos\phi - \cos\delta \cos\omega \sin\phi \tag{3.18}$$

$$\cos\delta \sin\omega = -\sin\theta_z \sin\gamma_s \tag{3.19}$$

$$\sin\delta = \cos\theta_z \sin\phi + \sin\theta_z \cos\gamma_s \cos\phi \tag{3.20}$$

$$\cos\delta \cos\omega = \cos\theta_z \cos\phi - \sin\theta_z \cos\gamma_s \sin\phi \tag{3.21}$$

where

ϕ = astronomical or geographical latitude of a plane on the earth's surface, which is the complement of the acute angle between the astronomical vertical and the earth's axis of rotation, positive (negative) in the northern (southern) hemisphere. The astronomical vertical (ZN) is a line determined by the direction of the local gravitational field.

If the hour angle parameters ω, δ, and ϕ are known, then the azimuth angle is found by dividing Equation 3.16 by Equation 3.18, i.e.

$$\tan\theta_z = -\frac{\cot\delta \sin\omega}{\cos\phi} + \tan\omega \sin\phi \tag{3.22}$$

and the zenith angle is given by Equation 3.17.

If the horizon parameters θ_z, γ_s, and ϕ are available, then the hour angle is found by dividing Equation 3.19 by 3.21, i.e.

$$\tan\omega = -\frac{\tan\theta_z \sin\gamma_s}{\cos\phi} + \frac{\tan\gamma_s}{\sin\phi} \qquad (3.23)$$

and the declination is given by Equation 3.20.

3.4 An Algorithm for Calculating the Position of the Sun

The preceding discussion was intended to facilitate the reader in understanding the fundamental relations incorporated by the FORTRAN algorithm HELGO (Appendix A). HELGO, named after the Greek words HELiaci-GOnia (solar angle), is primarily based on subprograms written at McDonnell Douglas Corporation by Johnson (1984), to control the tracking of a high performance modular dish collector system with an advanced heat engine receiver. Some of the added refinements, though, include a correction for atmospheric refraction, an expression for the change in the orbital eccentricity, and an expression for the change in obliquity.

3.4.1 Basic Equations for Calculating the Sun's Position

The basic equations used by HELGO are essentially the so-called "lower precision" formulae from the Almanac of Computers. HELGO can efficiently and accurately perform the calculations necessary to determine the position of the sun.

The algorithm's primary functions are computations of the declination, δ, the equation of time, E_T, and the distance of sun-earth. Function GAST, is a subprogram that computes the Greenwich Apparent Sidereal Time, using the

equation of Equinoxes. Finally, Function XJDAY computes the Julian date. A listing of all three codes is provided in Appendix A.

The irregularities in the earth's rate of rotation make Universal Time (the local mean time of the prime meridian) unsuitable for the comparison of theory with observation. This fact created the obvious need to be able to define with precision, on a uniform time scale, the instant of some phenomenon or observation. That was previously called an epoch (J 2000). The time interval elapsed between two epochs measured in units of some time scale, is the so called time interval, and for this system:

$$d = JD - TREF \tag{3.24}$$

where TREF = 2451545, or

$$d = -5479.5 - N + \frac{UT}{24} \tag{3.25}$$

where N = number of whole days since 0 UT, 0 January 1985.

The world is divided into twenty-four zones each having a width of 15 degrees (one hour) of longitude, in each of which the same standard time is kept. The meridian of Greenwich is taken as the reference point and namely zone zero. Zones to the east are numbered negative and zones to the west are numbered positive, according to the number of

hours to be added to the local standard time (CVLT). Thus,

$$UT = CVLT + ZONE \tag{3.26}$$

The STEP site is located five zones west of Greenwich, for which ZONE=5. Since 1966, for six months each year the time in each zone is advanced one hour, thus defining the daylight savings time (DST). One should always use standard time to avoid confusion.

To determine δ and ω a change should be made from the horizontal plane to the equatorial reference system. The calculation of ω from the RA was analyzed in the previous sections of this chapter. As a point of caution, one must always make sure that the hour angle is in the correct quadrant. To eliminate the ambiguity of sign or quadrant, use of the two argument arctangent function is suggested. Once the value of ω is calculated in degrees, one can easily obtain the apparent solar time (AST)

$$AST = \omega + 12^h \tag{3.27}$$

so at ω=0, AST=12 noon. Similarly, the mean solar time (MST)

$$MST = LST + (L_{st} - L) \tag{3.28}$$

where LST = local standard time,

L_{st} = standard longitude, 75° W, and

L = longitude of the locality, 84.7076° W.

The difference between the apparent and mean solar time is called the equation of time (E_T). Thus,

$$E_T = AST - MST \qquad \text{(in minutes)} \qquad (3.29)$$

The equation of time may also be defined as the quantity which must be added to the mean longitude of the sun to give the sun's right ascension. Knowledge of E_T allows one to account for both the eccentricity and the obliquity of the earth's orbit in time related calculations.

The apparent and mean solar time agree four times a year.For example, at Greenwich the apparent solar noon varies between $11^h\ 44^m\ 05^s$ and $12^h\ 14^m\ 19^s$. Maximum contribution from earth's orbital eccentricity is approximately eight minutes; from earth's obliquity is approximately ten minutes.

The apparent solar time, numerically measured by the hour angle of the sun plus 12^h, is no longer of importance in time keeping. In the American Ephemeris and the British Astronomical Ephemeris, since 1965, the equation of time was eliminated and replaced by the Ephemeris Time of transit of the sun, and no reference was any longer made to the apparent solar time.

However, in applications to solar engineering, navigation, and surveying, there is still need for means to determine the hour angle of the sun. In such cases one should recall that AST is a time scale paced to the apparent sun, such that:

$$\omega = (AST - 12)\ 15^\circ \text{ per hour} \qquad (3.31)$$

In this time scale, ω equals zero when AST equals 12:00 (solar noon) or when the apparent sun is due south.

The overall performance of the algorithm HELGO was evaluated by Balaras (1985). Accordingly, HELGO and the commonly used equations for declination by Cooper (1969), and equation of time by Whilier (1979), see Duffie and Beckman (1980), were compared against the 1983 Nautical Almanac at 12:00 noon local Greenwich time, Figure 3.9.

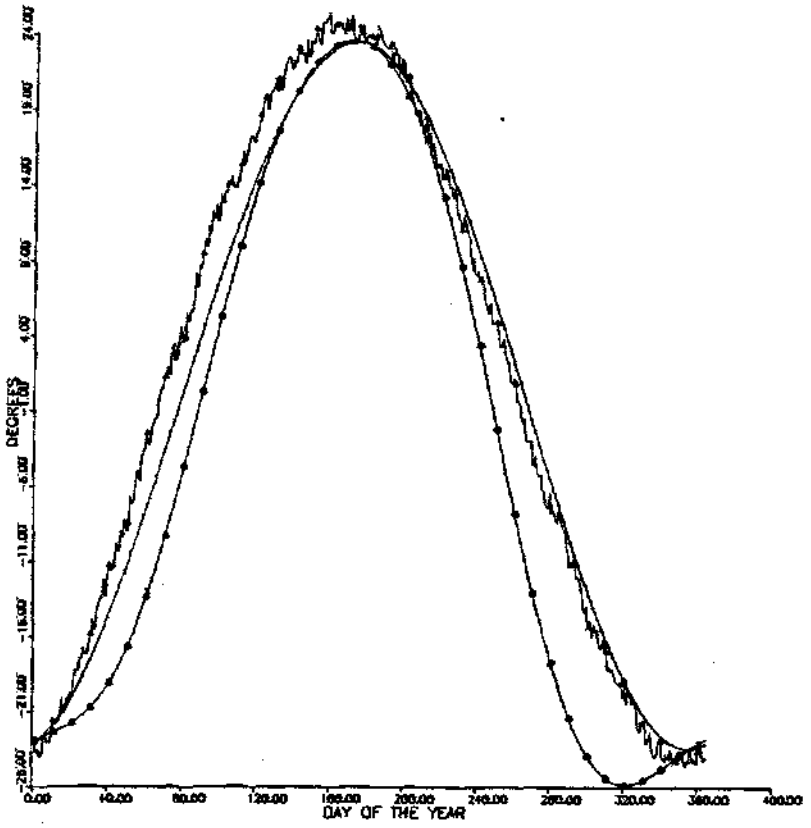

Figure 3.9 Comparison of Calculated Annual Values of Declination, from Subroutine HELGO (Distorted Curve), and Cooper's Equation (Solid Curve with "o"), with 1983 Nautical Almanac (Solid Smooth Curve)

HELGO produced a maximum error of 0.006° for declination and 0.057 minutes for the equation of time, while Cooper's equation resulted in 1.196° maximum error for the declination and Whilier's equation of time produced an error of 1.581 minutes.

3.5 Extraterrestrial Solar Radiation

HELGO is a relatively straight-forward algorithm that calculates the declination, equation of time, and the mean sun-earth distance, with an extremely small error. Along with accurate latitude and longitude information for a specific site, one can very accurately calculate the corresponding extraterrestrial radiation values.

For each hour it is possible to calculate the extraterrestrial normal irradiation as follows:

$$I_{on} = G_{sc} \frac{1}{R_m^2} \Delta t \qquad (3.32)$$

where G_{sc} = solar constant, 1367 W m^{-2},

R_m = mean sun-earth distance, R/R_{ave},

R = prevailing sun-earth distance,

R_{ave} = average sun-earth distance, and

Δt = time interval, for example 1 hour, adjusted for sunrise and sunset.

The extraterrestrial horizontal irradiation can be calculated according to the following expression:

$$I_o = \frac{12}{\pi} G_{sc} \frac{R_{ave}^2}{R^2} (\cos\phi \cos\delta (\sin\omega_2 - \sin\omega_1) + (\omega_2 - \omega_1) \sin\phi \sin\delta) \quad (3.33)$$

where ϕ = latitude of the locality,

δ = solar declination, and

ω_1, ω_2 = hour angle at start, end of the period (hour).

Algorithm EXTRAD has been developed to perform the above calculations and provide the user with accurate hourly values of I_{on} and I_o. The algorithm is listed in Appendix A.

Note that all the calculations are performed at the middle of each hourly period. HELGO has been used extensively over the past few years and is believed to be free of errors and very dependable. The algorithm was used for the development of the data basis for this study, and its application is illustrated in the following chapter.

CHAPTER IV

SOLAR RADIATION DATA

Proper design of a solar energy system requires knowledge of the amount and reliability of solar energy. For example, all design methods used to size solar energy systems (even sophisticated models like TRNSYS or f-chart) require radiation data. "Best" data are measured data at the site of the proposed solar energy system. However, complexity and cost of a reliable radiation measuring network dictates the need for developing alternatives that can substantiate and/or complement observations. Dependable solar radiation models can successfully satisfy this need.

This chapter is intended to provide a brief overview of existing measured data bases. The present work was based on the Shenandoah five year data base, collected at Shenandoah, Georgia (33.4042° N, 84.7478° W). To assure the highest possible accuracy, a data quality control procedure was developed and summarized in this chapter. A detailed literature review of models for predicting the solar radiation components is also presented.

4.1 Measured Solar Radiation Data

Throughout the years, it has become quite obvious to the scientific solar community that accurate information on solar radiation data is essential in order to assess the availability of solar energy on the earth. The most direct way to generate such information is by collecting accurate data at the specific site of interest.

In Chapter II we mentioned briefly the most commonly used instruments associated with measuring the three principal solar radiation fluxes - beam, scattered, and total radiation. The instruments for measuring solar radiation are of two basic types. A concise description of each instrument follows.

The pyrheliometer is an instrument using a collimated detector for measuring the beam solar radiation at normal incidence. The instrument is usually attached to an electrically driven equatorial mount for tracking the sun. Among the popular field instruments used for routine measurement of beam normal irradiance are the Eppley normal-incidence pyrheliometer (NIP), mostly used in North America, and the Kipp and Zonen actinometer, mostly used in Europe, Africa, and Asia.

The pyranometer is an instrument for measuring total hemispherical (complete sky dome) solar radiation, either on a horizontal surface or tilted at a latitude angle (in which

case it will receive the ground-reflected radiation). A pyranometer with a shading devise (ring or disk) measures scattered irradiance within a solid angle of 2π (sky-dome), with the exception of the solid angle subtended by the sun's disk. There are a number of manufacturers of pyranometers. Very popular are the black and white, and the spectral precision pyranometer (manufactured by Eppley Laboratory in the United States), the Kipp and Zonen pyranometers (manufactured in the Netherlands), and the less expensive (but with a lower accuracy) Li-Cor photovoltaic pyranometers.

Due to the operational complexity of pyrheliometers, being a tracking instrument, attempts have been made to develop other means for measuring the beam radiation. A method has been recently proposed by Faiman et. al. (1987), that incorporates a set of fixed pyranometers tilted in various orientations to collect, among other information, beam radiation data. The errors introduced to the data are of the order of the measurements errors of the individual instruments, although the collected data need to be compared with dependable pyrheliometer data for a final evaluation,.

Lamm and Adler (1987) have also proposed a new method. They use two static pyranometers which measure total radiation, mounted at different orientations to yield data for a set of equations that may be solved for the beam normal radiation under clear sky conditions. The tilt angle was for latitude and an appropriate angle to minimize effect of

errors, 80 degrees North-facing, was proposed. The basic assumption was that the time interval must be chosen such that one can reasonably assume that measured insolations do not vary significantly during the interval. Latitude variations are important and the method has to be tested before it is employed at the site of interest.

Appelbaum and Bergshtein (1987) presented a relative simple solar radiation distribution sensor that can supply the common solar radiation data of the conventional instruments. At the same time, the solar radiation data on various tilt and azimuth angles, and the solar radiation distribution from the sky and from reflected surfaces are measured. The sensor is static and it includes several individual directional solar radiation detectors (solar cells) oriented radially around a hemisphere surface and individually shielded so as to simultaneously intercept only directional solar radiation. Although the apparatus requires precise construction and calibration, it can be used to provide accurate information on the sky anisotropy.

These are of course positive steps towards the solution of the problem. That is, in the event that one needs to collect data at a remote location. It is impractical to use a tracking pyrheliometer when regular adjustments are not possible. In addition, if only one pyrheliometer was available at a monitoring station one needs some means of checking collected data. The above methods may be considered as

possible solutions.

Measuring instruments are calibrated internationally. Since 1981 the official scale is the World Radiometric Reference (WRR). The World Meteorological Organization (1971) classifies pyrheliometers according to their accuracy and the accuracy of their auxiliary equipment. The various criteria for accuracy and sensitivity are stability of the calibration factor, maximum error due to variations in ambient temperature, errors due to spectral response of the receiver, nonlinearity of response, opening angle, time constant of the system, and effect of auxiliary equipment.

The World Radiation Center at Davos, Switzerland, maintains a group of absolute pyrheliometers, Brusa and Frohlich (1975). Against this group, the reference standard pyrheliometers are calibrated and maintained at different designated regional centers around the world and also in some national centers. The secondary instruments are in turn calibrated against the reference pyrheliometers.

The calibration constant of a reference standard instrument is the ratio of radiative flux measured by the absolute instrument to the signal response of the reference standard instrument. Such a constant is determined from a number of average readings of each instrument and can vary with the level of radiant flux.

Unlike pyrheliometers, there are no absolute pyranometers. All pyranometers are calibrated instruments. There

are a number of methods of calibrating pyranometers using the sun or laboratory sources. Two methods commonly used are calibrating directly against a reference standard pyrheliometer using the sun as source, and calibrating against a reference pyranometer that has already been calibrated.

For a more detailed discussion of instruments, calibration procedures, their use and the associated terminology, the reader is referred to Robinson (1966), Kondratyev (1969), WMO (1971), Coulson (1975), Thekaekare (1976), Yellott (1977), Duffie and Beckman (1980), and Iqbal (1983).

Knowing solar radiation distribution on the earth's surface can be proven very useful. Global solar radiation information may be sufficient to satisfy the needs of many solar energy users. However, for many applications the global information alone is not sufficient. It is often very important to know the amount of solar radiation coming directly from the sun.

The beam component is indicative of the maximum energy that could be collected using concentrating collectors. Prime examples are the high temperature collectors needed for electric power generation, or arrays of tracking photovoltaic devices. Beam and global radiation data can also be used to accurately calculate the amount of solar radiation incident upon tilted surfaces.

While there are numerous locations in the United States where the global insolation has been observed, continuous

records of the beam component are very limited. Prior to 1977 only seven sites in the U.S. had digitized data, with the exception of Albuquerque, where four years of data were available, and Maynard, Massachusetts, with nine years of data, McDaniels (1987).

In the United States the National Weather Service (NWS) operated about 60 sites that record global solar radiation. However, only five sites recorded beam radiation. About two-thirds recorded daily data only, the remaining one-third reported both hourly and daily totals. After many years of less than perfect data collection, the NWS has recently upgraded the solar radiation network by equipping 35 sites with both pyranometers and pyrheliometers. A map showing the network is presented in Figure 4.1.

In 1978 corrected data tapes of hourly meteorological information (including global solar radiation) for 26 stations over a period of 23 years (1953-1975) were made available. These data are maintained by the National Climatic Center (NCC) of the National oceanic and Atmospheric Administration (NOAA). The data tapes are referred to as the SOLMET (SOLar METeorological) tapes described in detail in the SOLMET User's Manual (1978).

The main difficulty with the older solar radiation data is that the data were usually presented only as daily totals. For many solar applications daily data does not provide enough information about short-term variations; hourly data

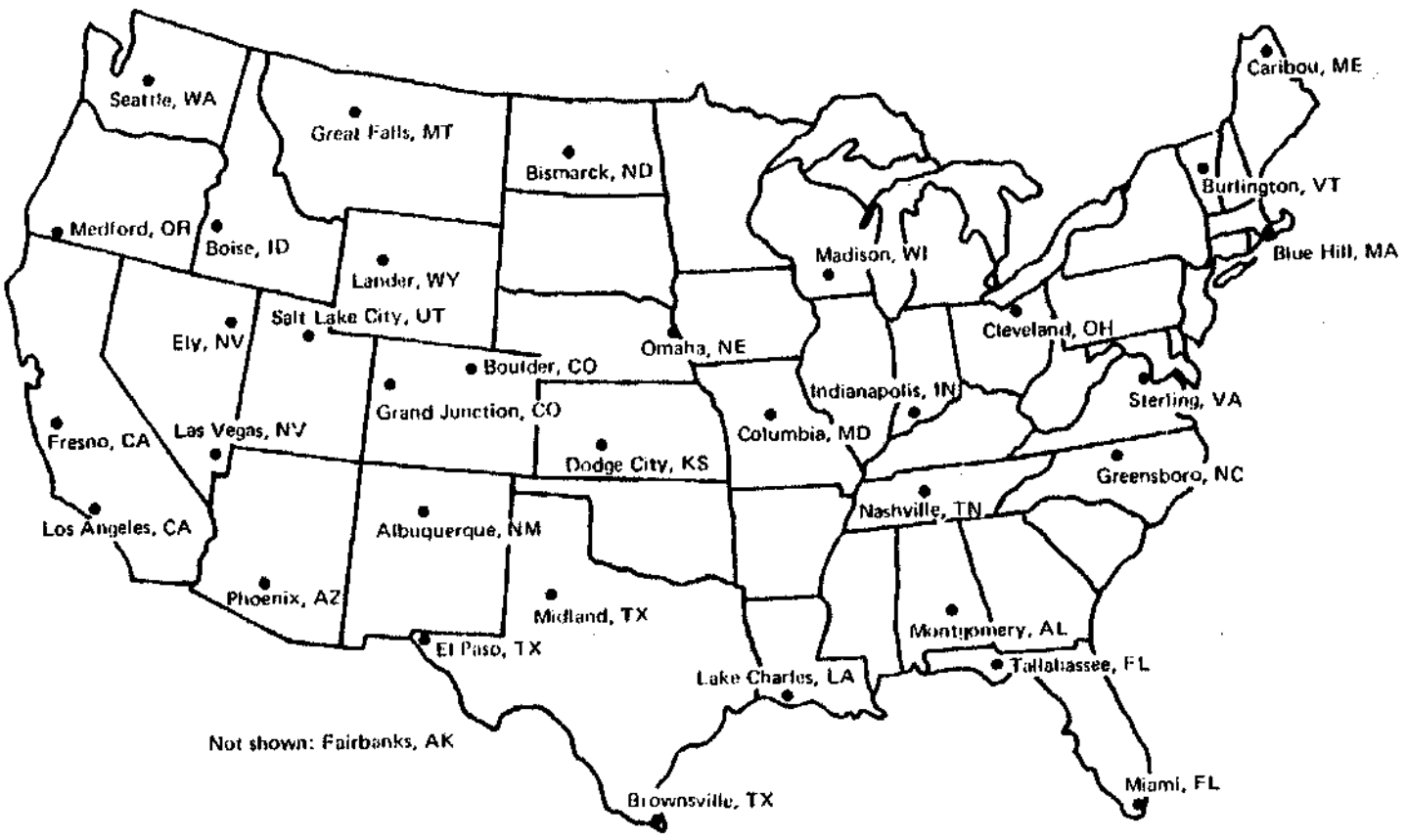

Figure 4.1 New NWS Network Recording Both Total and Direct Solar Radiation. Adapted from Kreith and Kreider (1978).

is essential.

There is also a real need for long-term data. The daily and annual solar radiation at a given site will vary considerably from year to year. For example, the National Weather Service has measured at Maynard, Massachusetts, beam radiation over a nine year period. These results, summarized by McDaniels (1987), indicate that the difference between the lowest and the highest annual average was 18 percent of the nine year average and the root-mean-square deviation was 6 percent of the average.

Clearly, information of this type is much needed and will take years to accumulate. Statistical studies have shown that the amount of data needed to characterize the solar radiation at a particular location requires periods up-to 15 years. Surface temperature records in the United States show periodicities of up-to 24 years. Similar time periods are expected to be necessary to characterize the incoming solar radiation.

An excellent report has been published by the Solar Energy Institute (1983) that describes 32 representative national, regional, and multistate networks and data sets. The report describes among others the type of data collected and provides a contact list. Some of these data collection efforts that were described in the SERI report include the following:

The Aerospace Corporation with Aerospace Insolation Data Base. A collection of measurements used used to construct the Aerospace Direct Insolation Prediction Algorithm (ADIPA) used in SOLMET data rehabilitation, and is available for five locations.

The Department of Energy (DOE) Solar Energy and Meteorological Research Training Sites (SEMRTS) Program. Funded by DOE, in 1975 eight universities began a research quality monitoring network representative of the full range of climatic regions in the U.S., collecting high resolution (1 minute) data. Part of the SEMRTS data, for Region 3, was collected at the Georgia Institute of Technology, and was kindly provided to the author by Dr. Justus.

The data were recorded on a minute basis and compiled into a monthly minute data base. Several automatic and manual quality control procedures were applied to the data and then compounded into an Hourly Data Base for each month. The data contain a variety of solar radiation and meteorological observations, and is referred as the HDB data base from here on. For a detailed description of the station and the data base the reader is referred to Justus et. (1979).

The Electrical Power Research Institute, West Associates Solar Resource Evaluation Project. Western Energy Supply and Transmission (WEST) Associates established a monitoring network in 1976 to evaluate solar resources available in the southwest United States. Data from 50 stations through 1979

have been collected. The data consist of 15-minute averages of global and direct normal solar radiation.

The NOAA-SOLMET Rehabilitated Data. These data include hourly integrated values of measured horizontal solar radiation, derived estimates of direct normal radiation, and collateral surface weather observations, for a total of 27 stations.

Additional information on available solar radiation data in the U.S. and throughout the world, have been published by Bahm (1980). Also included are, a review of some problems with these data and suggestions on avoiding or correcting these problems. Historical solar radiation data have also been collected by the National Observatory of Athens (NOA), Greece, since 1961. The author has obtained three years of data from NOA to be used in our study. The measured values include hourly global and sky irradiation data.

A data base comprising five years (1979-1983) of hourly global and beam solar irradiation has been prepared for west central Georgia by Jeter and Balaras (1986). Measured data were collected at a primary site at the Shenandoah, Georgia, Solar Total Energy Project (STEP). To complete the record, various methods of interpolating, inferring, and modeling missing data were used. A brief description of the STEP project, instrumentation, and data quality controls employed to assure the validity of the collected data, are presented in the next sections. The reader is also referred to Phan

(1980), Jeter and Phan (1981), and Dischinger (1984).

4.1.1 The Solar Total Energy Project

The Solar Total Energy Project (STEP) at Shenandoah, Georgia (33.4042° N, 84.7478° W) is a cooperative effort between the United States Department of Energy and Georgia Power Company, to further the search for new sources of energy. The project is a prototype solar thermal total energy plant, being in operation since early 1982. The site is composed of 114 parabolic solar dish collectors (each, 7 meters in diameter).

Each parabolic dish at the Shenandoah plant, acts as a concentrator producing a concentration ratio of 250. The concentrated rays heat the circulating silicone transfer fluid to 750° F. The heat transfer fluid is then pumped to a heat exchanger, where it boils water and superheats steam. The superheated steam drives a turbine generator, producing electricity. Medium pressure steam is extracted from the turbine for knitwear pressing at a near-by factory. Low pressure steam exhausted from the turbine is used to produce chilled water for air-conditioning.

4.1.2 Instrumentation

A meteorological station at the site, operated by the Georgia Institute of Technology, constantly monitors the amount of solar energy available. The solar radiation and surface weather instruments make it one of the most sophi-

sticated stations in America for gathering data about the sun and is considered to be a pioneer of a modern automated station. It has been recently renovated and substantially upgraded.

The basic data set assembled at the STEP, for the period between 1979 to 1984, includes irradiation values integrated over fifteen minute periods and recorded at the end of each period. The pertinent instruments at the site are an Eppley precision spectral pyranometer (PSP), to measure the global irradiation and two Eppley normal incidence pyrheliometers (NIP) on a common polar mount to measure beam normal irradiation.

During 1984 the solar monitoring station was reconfigured. Two global pyranometers were employed for redundancy. Redundancy in the beam normal measurements was enhanced by a third pyrheliometer on the common mount being converted from measurements in the infrared band to full spectrum measurements.

A fourth pyrheliometer was added on a separate mount for complete redundancy, and in late 1984 this mount was converted to reliable PV power via a DC to AC from an adjacent PV array with battery storage. One should note that the inverter powered unit shows poor performance, due to poor temperature stability. The station has again been under another reconstruction that includes improvements in the data acquisition system, instrumentation, and process of collected data. It is

expected to return in operation within 1988.

The pyranometer and the NIP are not self-checking or absolute instruments. Their sensitivity should be determined by comparing them with some other "standard" instruments. Thus, all instruments have been periodically calibrated. The NIP's were calibrated by comparison with a TMI MK VI absolute cavity radiometer traceable to the World Radiation Reference (WRR). No significant calibration adjustments have been necessary for any of the NIP's deployed in this station since operations began in 1977.

Calibration adjustments from the original calibration for the two principal instruments average only 0.8% and -0.3% respectively. The PSP for the global irradiation measurement has been calibrated by comparison with the carefully maintained NBS-traceable Eppley PSP. Its average deviation from initial calibration has been -1.5%. The PSP has shown a slight trend of degradation in response, which has been fully compensated by recalibration. The NIP's show no trend in response degradation.

4.1.3 Data Quality Control

It is of capital importance to prepare a high-quality data base since, as demonstrated by Jeter and Balaras (1985), spurious data can have a substantive effect on the resulting correlation. A rather intensive routine data quality control procedure developed by Phan (1980), has been instituted for

the Shenandoah data.

The procedure involves an automated quality-control algorithm which computes a set of redundancy, limit, and consistency checks and flags any suspicious data. These outliers are a peculiarity and indicate a data point which is not at all typical of the rest of the data. Automatic rejection of outliers is not always a very wise procedure, Anscombe (1960). Sometimes the outlier is providing information which other data points cannot due to the fact that it arises from an unusual combination of circumstances which may be of vital interest. Actually the vast majority of such suspicious data was found to be valid. Thus, no measurements are confirmed as erroneous without manual inspection of computer generated plots of the data.

After these checks the data was assembled in monthly files including the confirmed error flags. The unflagged data is expected to be highly reliable; however, to prevent any residual poor data from contaminating the results, additional screening was instituted.

A daily validation test was instituted to eliminate certain days from further consideration. Days that were mostly overcast were rejected primarily because little beam radiation occurs on such days and secondarily because it is difficult to verify the pyrheliometer data on such days. Additionally, days with one-half or more of their periods flagged as unreliable were totally excluded as a conservative

measure to preclude erroneous data.

For this daily screening only periods with solar altitudes greater than 6 degrees were considered. No data with lower altitude is used in the beam radiation model to avoid the consequent refraction effects on tracking accuracy. Also it is felt that beam radiation at low solar altitudes has little practical significance but might confuse the model because of the effects of the large intervening air-mass.

The resulting data was tested by comparing annual scatter plots of the daily diffuse versus global radiation with published correlations (Collares-Pereira and Rabl (1978), Liu and Jordan (1960), and Speigel (1981)). Significant deviations from the model would have indicated a severe problem such as a malfunction tracker. The good agreement obtained was an encouraging verification of the preceding quality controls.

Next, an hourly data base was assembled from fifteen-minute data. The criterion used in this step is that at least three of the four intervals used in calculating the hourly value passed the previous quality checks. The results of this procedure was the development of a new data base containing only good hourly irradiation values for the year.

A final check on the hourly data was a comparison of the beam radiation against empirical upper and lower bounds for a given global radiation value. This step was instituted as a final verification of the previous checks. As detailed in

Dischinger (1984), a scatter plot of the hourly values for 1980 was used to establish empirical bounds for hourly data. Upper and lower boundary curves were estimated and then adjusted until data just outside the curves was found on close inspection likely to be spurious and any data just inside the curves was found likely to be reliable. Only a very few isolated errors caused by intermittent radiometer or tracker problems were discovered.

The empirical error bound test was instituted primarily as a proof against grossly erroneous data. Only eighteen hours from 2477 in the entire set were excluded for 1980. This close inspection confirms the reliability of the data.

4.1.4 Shenandoah Five Year Data Base

The resulting data base is a set of hourly irradiation values closely screened for reliability excluding data from predominantly overcast days and excluding data for very low solar altitudes (i.e. less than 6 degrees). Data from year 1982 was excluded due to a series of electronic and mechanical failures which degraded the performance of the monitoring system substantially. Only 41 days out of the whole year were classified as good days and from these, only 270 hourly periods passed all the checks.

Consequently, five annual data sets were available for further analysis, which combined generate the five-year useable hourly data base (with a total of 8112 periods).

The important information included in this data base are:

1. The date, namely year, month, day, hour, and minute,
2. The radiation data, namely the hourly beam and global irradiation,
3. The clearness index (calculated dimensionless value for the global radiation), and beam transmittance (calculated dimensionless value for the beam radiation), and
4. The percent of 15-minute periods, and their identification, that were missing from the hour of interest.

It is believed that the Shenandoah five year data base, Jeter and Balaras (1986), constitutes one of the few long term, accurate sources of available solar radiation data in the United States. In view though of the limited availability of such data extensive work has been conducted by researchers in developing other methods for predicting solar radiation components. Numerous models are available in the literature and are reviewed in the following sections.

4.2 Modeled Solar Radiation Data

Although the quest for accurate solar radiation data has intensified in recent years, there are still inadequacies of current observational networks, such as limited coverage, and length of records. Thus, it becomes desirable to have alter-

natives that can substantiate and/or complement observations, in order to satisfy the need for such data.

If solar energy were clearly economical at the present time, the performance assessment would not be so critical. Solar techniques though, are only now becoming competitive with more traditional forms of providing low grade heat. Thus, it is necessary in most cases to optimize the design of the solar system in order to obtain an economic advantage over traditional techniques.

Knowledge of the direct beam component of solar radiation is essential for modeling many solar energy systems. This is particularly critical for applications that concentrate the incident energy to attain high thermodynamic efficiency achievable only at the higher temperature. In order to estimate the performance of concentrating systems it is necessary to know the intensity of the beam radiation, as only this component can be concentrated. Accurate predictions of beam radiation are of critical importance at this case.

For nonconcentrators, one typically wants to convert horizontal global (commonly measured quantity) to global radiation on a tilted surface, hence requiring a knowledge of the beam and scattered components separately. Empirical correlations are often used to extract beam and scattered radiation components from measured global values. The sensitivity of the final result to errors in the beam fraction will be compensated by an opposite error in the scattered

component. Thus, accuracy in this case is not as critical.

Precise methods of estimation are therefore necessary at the moment to provide an honest indication of systems' performance. In addition, the complexity and cost of a reliable monitoring network point to the desirability of an independent approach whose findings can substantiate and/or complement observations. This requires the use of sophisticated simulations with the complexities that accompany them.

Although models can not replace good measured data, they can be used to generate solar radiation data sets which closely imitate the actual data. Availability of dependable and accurate models can ease the need for detailed, high cost and time demanding hourly local insolation measurements.

Thus, several investigators and research groups are working on improved models for the beam and scattered irradiation based on other easily measured quantities (i.e. global radiation). There are basically two categories of correlations available in the literature, namely a group of parametric and a group of decomposition models. A literature review of such available correlations is presented in the following sections.

A number of these models have performed poorly and one needs to investigate and verify their applicability at different geographical regions. Several such studies have been made utilizing different models and their results are also discussed.

4.2.1 Parametric Models

When meteorological observations are available it is possible to estimate the solar radiation components by a number of existing models. The meteorological parameter frequently used as a predictor is the fractional sunshine (FS), the ratio of the hours of bright sunshine to the length of the day from sunshine to sunset.

Models using this approach are initially developed for locations for which both sunshine and solar radiation measurements exist. One then expects that the developed regression relationships would be valid over the surrounding regions. Estimates, though, of the solar radiation can be obtained when only sunshine measurements are available. The accuracy would be governed by the length and accuracy of the record of solar radiation and sunshine measurements, and regional climatology (e.g. type, amount, and distribution of clouds, atmospheric turbidity and moisture content).

The monthly average daily radiation fraction can be expressed as a function of the monthly average daily values of bright sunshine hours and maximum possible sunshine hours. Iqbal (1978) using physical arguments, has suggested such a correlation. Several researchers like Collares-Pereira and Rabl (1979), Iqbal (1979), and Hay (1979) have determined values of the correlation coefficients for various locations.

Rao et. (1984) developed regression relationships for Corvallis, Oregon, utilizing insolation and sunshine measurements made over a three year (1980-1982) period. Atmospheric water vapor content can be used along with sunshine duration to obtain a relation to estimate the global irradiation, Hussain (1984). The method was also extended to calculate the dome irradiation.

Sherry and Justus (1984) have presented a simple hourly all-sky solar radiation model based on the modified Suckling and Hay (1976) cloud sky model, and the cloud transmissivity concept by Haurwitz (1948). Rapp and Hoffman (1976) presented a study of the relation between insolation and climatological data collected at Fort Worth, Texas that resulted in a correlation that can be used for estimating solar radiation from sky cover and visibility data. In another approach based on Canadian data, Davies and McKay (1982) used a polynomial rather than exponential expression to define partial transmittances which were specified in terms of air-mass, zenith angle, ozone, precipitable water, temperature, and pressure parameters.

One highly regarded statistical model was developed by Cotton (1979), who has presented simple linear regression equations of hourly global solar radiation for clear sky conditions which were then modified by cloud effects. Regression coefficients are provided by Cotton for a number of locations across the United States. This model can estimate

the hourly global irradiation from common surface observations. Finally, a number of non-spectral transmissivity models are presented and compared by Carroll (1985) based on radiation and meteorological data collected at Davis, CA.

In the last decade satellite data have been used to estimate global radiation at the earth's surface, Vonder Haur and Ellis (1975). Tarpley (1979) developed an algorithm for estimating surface solar radiation from geostationary data. Satellite measurements of upwelling radiation from the earth-atmosphere system have also been used by Gautier et. al. (1980) to calculate global irradiation. The effects of variations in both cloud amount and transmittance are contained in the satellite's radiation measurements.

The difficulty of distinguishing cloud reflection from snow reflection has precluded the use of Gautier's model in winter. An improvement in the representation of the physical process in the atmosphere was achieved by Pinker and Ewing (1985), although their approach has to be adjusted according to limitations of satellite observations.

4.2.2 Decomposition Models

Development of correlation models that predict beam radiation using other solar radiation measurements is also possible. This group of models usually requires information only on the global radiation and consequently maybe referred to as decomposition models.

The accuracy to which the beam values can be determined from these correlations is highly dependent on the precision of the global measurements. Any error in the global data translates into twice the error from the calculated beam values because to a close approximation the beam value is proportional to the square of the global value (the reader may want to refer to Figure 4.2 and verify this by noting the magnitude of the corresponding τ_b and k_t values). This problem is particularly severe with global data collected with second class pyranometers which tend to exhibit systematic errors which vary with time and year. The validity of the beam values becomes much more uncertain when they are derived from global values calculated from meteorological models.

The distribution of the dome solar radiation is very irregular, both in time and in space, due to the variability of the weather. Nevertheless the average characteristics of the dome radiation are quite regular and can be correlated with an effective transmission coefficient of the atmosphere.

This was first recognized by Liu and Jordan (1960) who developed a daily correlation for predicting the dome irradiance from measurements of global irradiation using results obtained from Blue Hill, MA. The correlation was expressed in terms of the daily dome fraction (k_d) defined as,

$$k_d = \frac{H_d}{H_o} \qquad (4.1)$$

where H_d = daily dome radiation,

H_o = extraterrestrial daily horizontal radiation,

and the daily clearness index (originally referred to by Liu and Jordan as cloudiness index) defined as,

$$k_t = \frac{H}{H_o} \qquad (4.2)$$

where H = daily global radiation.

Normalizing the daily (or hourly) global solar radiation in terms of extraterrestrial solar irradiation on a horizontal surface, has become usual practice. That way one may account for the dependence of the global radiation on the available solar energy at the top of the atmosphere. Similarly, by considering the clearness index rather than the radiation incident upon the surface of the earth, one eliminates the effect of the time dependence of extraterrestrial radiation.

The wide spread applicability of the Liu and Jordan (1960) correlation has been questioned by some researchers. Ruth and Chant (1976) and Hay (1976) concluded that the Liu and Jordan correlation exhibits a latitude dependence and suggested some modifications. Iqbal (1980) found that the

correlation developed for data from Canada and France did not agree with the results of Liu and Jordan. Various authors, among which Page (1961), Choudhury (1963), and Tuller (1976) have suggested that there is a dependence of the Liu and Jordan correlations on other variables such as latitude, cloud cover and surface albedo. Rabl (1979) confirmed the validity of the Liu and Jordan approach and identified the sources for the numerical inaccuracies of the original correlations.

Although the daily Liu and Jordan (1960) correlation has been used on an hourly basis, there is evidence that it is not suitable for this purpose (the reader is referred to Ruth and Chant (1977), Orgill and Hollands (1977), Bugler (1977), Collares-Pereira and Rabl (1979), Iqbal (1980), Erbs, Klein and Duffie (1982), Spencer (1982), and Rao et. al. (1984)). Following the Liu and Jordan method, other researchers have developed hourly correlations. A widely used model of this form is due to Orgill and Hollands (1977) and also Bruno (1978). More recent results have been presented by Erbs, Klein, and Duffie (1982), and by Spencer (1982).

Page (1961) developed correlations between daily total and scattered radiation for ten widely-spread sites in the 40° N to 40° S latitude belt. His model was verified and found to have widespread applicability in a number of locations like in Canada by Iqbal (1979), India by Choudhury (1963) and Modi (1979), Israel by Stanhill (1966), Zimbabue

by Lewis (1983), Australia by Norris (1966), and the United States by Vignola and McDaniels (1984). Finally, Lewis (1987) tested the applicability of a number of correlations for the estimation of the dome radiation against measured values in Huntsville, Alabama. The model proposed by Page (1961) was found to perform the best.

In each of these models the proposed equations were devised by empirically correlating measured data. Hollands (1985) proposed a theoretical approach for relating k_d to k_t, using a model for the radiative processes in the atmosphere. The atmosphere is modeled as having two homogeneous non-selectively absorbing layers. The model according to Hollands is simple but is consistent with the known physics and capable of giving a reasonable fit to measured data. A revised model, Hollands (1987), accounts for the effect of multiple interreflections between the atmosphere and the ground, and includes the ground reflectance as a parameter.

A problem though arises in the event that there is no data on either global radiation or any of its components. Then, in order to predict the dome radiation one may use the approach proposed by Iqbal (1978), which requires information on bright sunshine hours, or first predict the monthly average daily global radiation using an Angstrom (1924) type correlation.

Angstrom assumed the following linear relationship:

$$H = H_C \left(a + (1-a) \frac{n}{N}\right) \qquad (4.3)$$

where H = daily global radiation,

H_C = daily global radiation under clear skies,

a = constant,

n = number of sunshine hours during that day, and

N = maximum possible number of sunshine hours during that day.

The original form proposed by Angstrom is not widely used although it forms the foundation of many recent models, as in the case of Barbaro et. al. (1979). Rietveld (1978) modified the Angstrom correlation and he has examined the variation of the parameters throughout the world and found that they varied with the fractional bright sunshine in a predictable manner. Although Rietveld has not claimed general validity for his model, Ma and Iqbal (1984) imply this possibility. A comprehensive review of the above approaches and a number of other methods, can be found in Davies , Abdel-Wahab, and McKay (1984).

One may then use the predicted global radiation value in a correlation that relates the scattered component to the global radiation (Page (1961), Iqbal (1979), Erbs (1982) or Rao et. al. (1985)). Massaquoi (1987) concluded that it is more accurate to predict the global radiation value using an Angstrom-type equation and then calculate the dome radiation,

instead of a direct relation between the dome radiation and a meteorological parameter like sunshine hours.

An important alternative model is constructed by defining a modified clearness index based on an independent model for the clear day global irradiance. Stauter and Klein (1980) developed a correlation in terms of hourly global to clear sky irradiation to the ratio of hourly dome to global irradiation. Correlations of this format, with quite similar results have been also presented by Turner and Salim (1984).

Hottel (1976) developed a convenient method for estimating the transmittance of beam solar radiation through clear skies but which also requires some additional information such as air-mass, altitude, visibility, and climate. The model was based on data by McClatchey et. al. (1972). Clear day models and comparisons of these different models are included in Mujahid and Turner (1980).

Historically, the most common approach has been to use the correlation between the dome fraction and global solar radiation to first determine the scattered component on a horizontal surface. The direct component on the horizontal surface could then be obtained by subtraction and the beam radiation determined by a straight forward procedure. Another approach, and the one taken here, is to calculate the beam radiation directly using a beam-global correlation.

Beam-global and dome-global correlations are related because on an instantaneous basis the direct component on the

horizontal surface (easily obtained by subtracting the dome component from the global value) is equal to the beam insolation times the cosine of the angle of incidence. For hourly values the beam intensity can be fairly accurately calculated by dividing the average horizontal direct value by the average of the cosine over that hour.

However, if this method is applied to daily data, according to Vignola and McDaniels (1986), a systematic error will result because the atmosphere significantly attenuates the beam intensity during the morning and evening hours and this affect is not taken into account by the simple average procedure. It is possible of course to remove this error by properly weighting the cosine over the day, it is simpler and more accurate just to use a correlation between the beam and global values.

Such relationships are expressed in terms of the irradiations which are the time integrals (i.e. one hour) of the radiant flux or irradiance. A convenient representation is the relationship between two dimensionless numbers, the beam transmittance of the atmosphere (according to Liu and Jordan (1960) and Beckman et. al. (1978)),

$$\tau_b = \frac{I_{bn}}{I_{on}} = f(k_t) \qquad (4.4)$$

where I_{bn} = hourly or short period beam normal radiation,

I_{on} = corresponding extraterrestrial normal radiation,

and the hourly or short period clearness index,

$$k_t = \frac{I}{I_o} \qquad (4.5)$$

where I = hourly or short period global radiation,

I_o = corresponding extraterrestrial global radiation.

We should recall that the clearness index was also expressed in terms of daily values, through Equation 4.2. For the remaining of this study, and unless otherwise specified, reference to clearness index implies that the variable was calculated according to Equation 4.5. A similar hourly expression may be provided for the hourly dome fraction (k_d), defined as the ratio of hourly dome radiation to hourly extraterrestrial horizontal radiation.

Correlations of this form have special intuitive appeal since one expects the beam transmittance to increase monotonically with clearness index. Especially notable among this work are the pioneering efforts by Boes et. al. (1977), and the highly regarded results of Randall and Whitson (R-W), 1977, concisely restated by Boes (1981) and Maxwell (1987).

The Randall and Whitson (1977) algorithm, or the so called Aerospace model, is based on composite hourly data of five U.S. climatic stations: Albuquerque, NM; Fort Hood, TX; Livermore, CA; Maynard, MA; and Rayleigh, NC. These data represent 65 months of simultaneous hourly global and beam

radiation measurements. The model has been used for generating the hourly beam radiation for 26 U.S. SOLMET (1979) stations, which had previously recorded only global radiation. Rabl (1981) also used these data to develope the yearly collectible energy correlations.

A model to predict the beam normal irradiation from measured global solar radiation is also available by Turner and Mujahid (1985). In the development of the model, statistical regression tests were conducted over a range of solar altitude angles. The model was compared to the R-W model, and overall the two models were found very similar with the Aerospace model believed though to be the best available model.

Jeter and Balaras (1986) have also prepared a similar model based on the hourly clearness index, useful for decomposing hourly global irradiation into beam and dome radiation components. The beam transmittance and clearness index for each hour were computed according to Equations 4.4 and 4.5, respectively. Based on the Shenandoah five year data base, HELGO (Appendix A) was used to accurately calculate the sun's position, while the hourly k_t and τ_b values were calculated using SUBI (a listing of the algorithm is presented in Appendix B).

A statistical analysis was then performed to the Shenandoah data. The principal result was a piecewise linear regression for the five years of data. For consistency, the same bands were selected as were used by R-W. For each band

the regression model which assures continuity is,

$$(\tau_{bj} - y_{oi}) = \beta_i (k_{tj} - x_{oi}) + \varepsilon_j \qquad (4.6)$$

where x_{oi} = lower limit of band i,

y_{oi} = regression model at x_{oi},

β_i = regression coefficient,

ε_j = residual error for data (k_{tj}, τ_{bj}).

The analysis was performed separately for all five annual cases and the aggregate five year set. Results of the linear regression analyses are given in Table 4.1. A more thorough discussion of the linear regression analysis can be found in Balaras (1985), and Jeter and Balaras (1986).

The so-called Basic Shenandoah Five-Year Model was shown to be preferable to any annual model from a constituent year, Jeter and Balaras (1986). A scatter plot of the combined five years is shown in Figure 4.2 with the resulting regression model superimposed along with the Randall and Whitson model.

The Basic Shenandoah five-year model was also shown to be similar to the Randall and Whitson model except in the highest range of clearness indices. Available evidence tends to support a preference for the Jeter and Balaras model in the region of disagreement, Jeter and Balaras (1986).

Table 4.1

Annual and Five-Year Regression Coefficients for Shenandoah STEP

INTERVALS of k_t	1979	1980	1981	1983	1984	5-YR
0.00-0.05	0.0000	0.0000	0.0000	0.0000	0.0000	0.0000
0.05-0.15	0.0000	0.0004	0.0032	0.0000	0.0000	0.0007
0.15-0.25	0.0168	0.0317	0.0511	0.0301	0.0310	0.0297
0.25-0.35	0.2564	0.2337	0.2591	0.2879	0.1733	0.2490
0.35-0.45	0.8562	0.8796	0.8851	1.0713	1.1740	0.9466
0.45-0.55	1.3511	1.3473	1.6430	1.5602	1.5111	1.4772
0.55-0.65	1.8084	1.3314	1.5253	1.4959	1.6393	1.5680
0.65-0.75	2.0174	2.1214	2.3527	2.0059	1.9325	2.0773
0.75-0.85	1.4478	2.2664	1.3337	0.8439	0.0000	1.3778

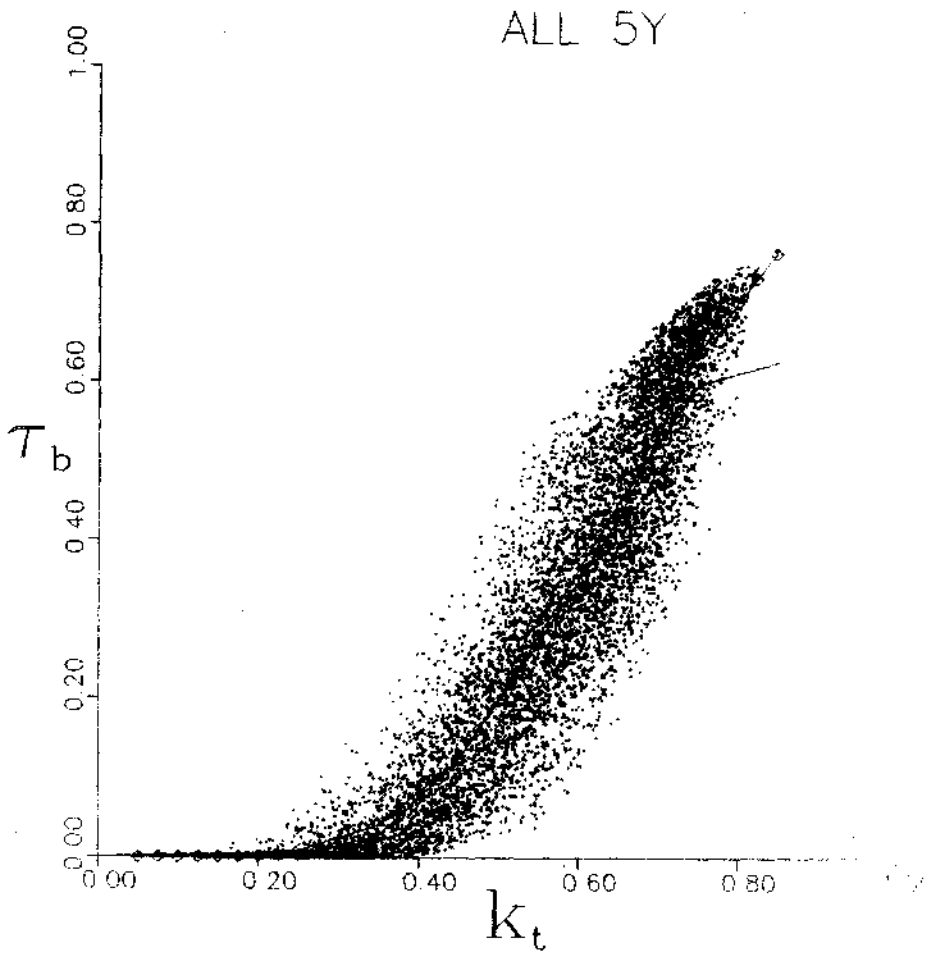

Figure 4.2 Scatter Plot of and Piecewise Regression on Shenandoah STEP Data for the Five Years. The R-W (1977) Model is Shown by the Plain Line.

High values of clearness index (clear sky conditions) are expected to result to high beam transmittance values. As illustrated by Figure 4.3, high k_t values are also expected to occur for high percent sunshine periods.

Using the HDB data base, we identified hourly periods of 100% sunshine with crosses, the range of 1% to 99% sunshine with polygons, and 0% to 1% with stars in a scatter plot of (τb-k_t) for the month of April 1980. The high sunshine

periods are concentrated at high clearness index and beam transmittance region, while the lowest sunshine periods occurred at a level of no significant beam radiation, as expected.

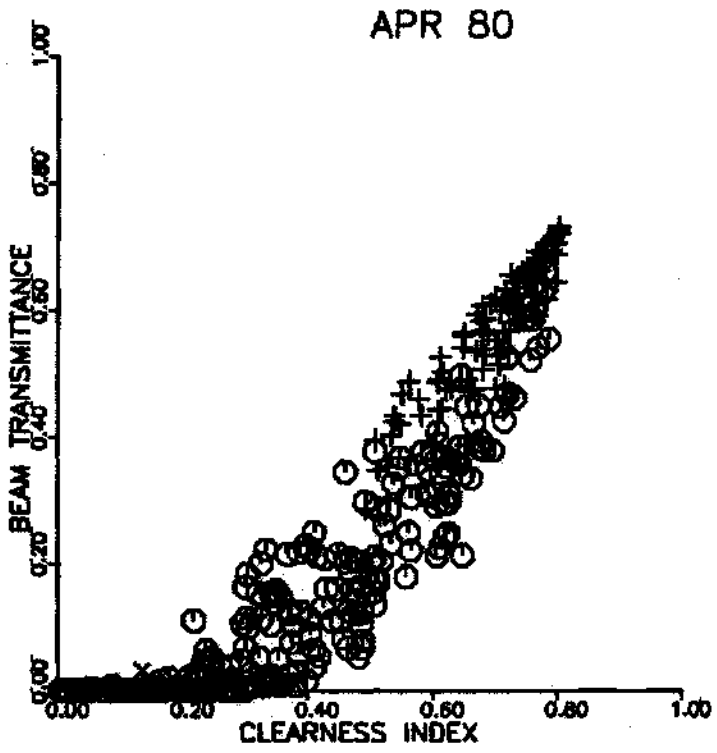

Figure 4.3 Scatter Plot of Hourly HDB Data for the Month of April 1980. Crosses Identify 100% Sunshine, Polygons are for 1% to 99% Sunshine, and Stars Represent 0% to 1% Sunshine Conditions.

In general, the beam radiation follows an inclined path in reaching the earth's surface. To take into account the effect of inclination on the length of the path traversed by the sun's ray through the atmosphere we define a dimensionless quantity, m, called the air-mass. It is defined as the

ratio of the mass of the atmosphere in the actual path of the beam radiation to the mass of the atmosphere which would exist if the sun were directly overhead. The value of air-mass equals unity when the sun is directly overhead.

For practical purposes, we may approximate air-mass by a flat earth model and a nonrefractive completely homogeneous atmosphere to relate m to the inverse of the sine of the solar altitude angle as follows,

$$m = \frac{1}{\sin\alpha} \qquad (4.7)$$

where α = solar altitude angle (complimentary of θ_z).

According to Kontratyev (1969) sufficient accuracy can be obtained using Equation 4.7, while Iqbal (1983) states that the error in this equation is 0.25 percent at a zenith angle of 60°, and increases to 10 percent at a zenith angle of 85°. Once the curvature of the atmosphere becomes significant, that is at low elevation angles, then a Lagrangian interpolation of air-mass from Table 4.2 should be substituted in place of Equation 4.7. An algorithm, called AMASS, has been developed to perform these calculations and is listed in Appendix B.

Table 4.2

Mean Air-Mass to Sun Elevation Angles
Adapted from Kreider and Kreith (1981)

Elevation (rad)	Air-Mass
0	22.0
0.017	20.0
0.035	18.0
0.052	15.6
0.070	12.5
0.087	10.4
0.105	9.0
0.122	8.0
0.140	7.185

Once we predict the hourly value of the beam transmittance one may calculate the hourly beam normal radiation through Equation 4.4. Then, the beam normal irradiation can related to the global and scattered horizontal irradiances by defining an hourly average incident cosine, $\cos\theta_z$, such that

$$I_{bn} = \frac{I - I_d}{\cos\theta_z} \qquad (4.7)$$

where θ_z = solar zenith angle.

Other correlations on the clearness index are also possible. The beam transmittance may be expected to follow a Bouguer's Law dependence, Kreith and Kreider (1978), on atmospheric extinction coefficient (K), due to absorption and scattering, and air-mass (m),

$$\tau_b = \exp(-K\ m) \qquad (4.8)$$

The extinction coefficient, or some suitably normalized function, from Equation 4.8, could then be correlated against the clearness index. This has been done by Dischinger (1984).

The so-called single regression models, as in the case of Randall and Whitson (1977) and Jeter and Balaras (1986), have some limitations due to inadequate representation of real world data. The dependence of beam transmittance on clearness index is not a deterministic function. Reference to Figure 4.2 indicates that, especially at intermediate clearness indices, there is a wide range of values assumed by τ_b for a given value of k_t. This is in part due to the differences in the transmissivities of the clouds making up the overcast. Thus,the single regression function of $\tau_b=f(k_t)$ can not be used to reproduce the variation of the data according to observed values.

An analogous assumption was made for the relationships between k_d and k_t. They made the deterministic-k_d assumption that for any given value of k_t, there can exist only one value of k_d. But as several workers have pointed out, Orgill

and Hollands (1977), Smietana et. (1979) and Hollands and Crha (1987), this function is not deterministic: for given k_t value, k_d can take on a range of values distributed about its average.

Indeed one would expect this to be the case on physical grounds, since there are a large number of combinations of cloud cover, aerosol content, air-mass, ground albedo, etc., that will yield the same value of k_t, but one can not also expect each combination to yield a unique value of k_d. The error associated with this assumption was evaluated by Hollands and Crha (1987). For flat plate collector output and scattered radiation on an inclined surface, using a non-isotropic sky model, it was found that the errors are modest. For concentrating collector outputs, the errors are more significant.

Along these lines, a new generation of more realistic models has been initiated. Recently, Hollands and Crha (1987) developed a probability density function governing the distribution of the observed values of k_d about their mean for a specified value of k_t. This probability was shown to depend on the specified value of k_t as well as the random variable k_d. The analysis was based on a 20 year record of historical data for two Canadian locations. The proposed function can be used to find more accurate estimates of long term averages, because one need not to make the deterministic-k_d assumption.

Stuart and Hollands (1987) presented an empirical equation which models the probability density function of monthly sets of the hourly beam atmospheric transmittance taken at a fixed time of day. The parameters included are the air-mass and mean values of the beam transmittance. The analysis was based on data from Toronto, Canada. Further work with climatologically different data is required before one can expect the equation to be universally applicable.

Similarly, Maxwell (1987) developed the Direct Insolation Simulation Code (DISC), based on a one year data set from Atlanta, Georgia. Maxwell suggests, among others, that air-mass is the dominant parameter affecting the relationship between beam transmittance and clearness index. DISC employs an exponential relationship between air-mass and clear transmittance, which is parametric in k_t. The model was validated using data from three different stations in the United States and seems to provide a satisfactory (τ_b-k_t) relationship.

4.2.3 Performance of Models

The previous literature review has clearly indicated that there is a great number of models already developed. Depending on the available information different models can be used. Some models require only solar radiation information while others may require knowledge of meteorological observations.

An additional criteria for selecting available models may be imposed by the complexity of these models. Precision of predicted values is of great importance in applications dealing with concentrating systems. Simpler models, with less accuracy, maybe best candidates for passive solar designing.

The most important factor, though, for one to consider is the applicability of the model at the site of interest. The accuracy of several correlations has been questioned by several investigators. Since the development of such models is based on data collected at a specific locality, their performance at different sites can be poor. Of course locally developed models will outperform any other candidates.

Several researchers have reported comparative studies on the performance of various models for a number of applications. For example, it is of interest to know how large of an effect the choice of diffuse fraction correlation will have on calculated solar system performance.

According to Erbs et. al. (1982), for simulations involving a flat-plate collector system the results obtained with different correlations were generally within 5 percent of each other. For a concentrating collector system though, the Liu and Jordan (1960) daily scattered correlation resulted in significantly higher estimates of system performance.

One important practical value of the hourly τ_b-k_t correlation is predicting the yearly collectible energy for solar collector system from a data base of hourly horizontal

global radiation only. Using one-to-one correlations of beam transmittance and clearness index, knowing k_t one can then predict the beam transmittance and then solve for the beam irradiation value. To determine how accurate is the value of the beam irradiation so calculated, one can use calculated and measured hourly beam radiation values as input data to a computer simulation of solar system performance, as it has been done by Erbs, Klein, and Duffie (1982).

Gordon and Hochman (1984), preferred to plot the yearly collectible energy against threshold, which compares the data-based result with the result based on the hourly (τ_b-k_t) correlation. The resulted differences were not significant for the case of a flat plate collector. For a two-axis tracking concentrating collector the differences are small but not insignificant (0.2 to 0.3 GJ/yr/m^2) over the range of collector operating thresholds typical to realistic solar systems. The above method can also be sued to provide useful information for the performance of a correlation used to predict yearly collectible energy, without resorting to computer simulations.

Tuner and Mujahid (1985) conducted comparisons of models that predict hourly beam radiation from hourly measurements of global radiation and generally when clouds are present. They obtained the individual data sets used in the Aerospace model and used each data set from each location in making comparisons. As one would expect, the Randall and Whitson

(1977) model proved to be superior to all models for these data bases.

The accuracy of models developed from hourly data improves if longer periods, such as a month, are considered. As with most solar radiation models, the prediction for a particular hour on a given day maybe poor. Although individual hourly predictions may look bad the statistical results, considering both positive and negative errors should average out to give good long-term results (for an hourly simulation study) if the model is valid. Overall the yearly average percent for the Randall and Whitson model ranged from -7 to 1 percent. Constantly though, on an annual basis, it underpredicted the beam radiation for all locations except for Maynard, Massachusetts (where it over predicted by 1%).

A study for clear sky models was performed by Mujahid and Turner (1980). Based on data collected at Blytheville, Arkansas all models overpredicted the beam normal solar radiation for each month over the entire recording period. Available data from Houston, Texas was also used.

The Randall and Whitson model consistently overpredicted every month ranging from 1.7 to 46 percent for Blytheville and -21 to 11 percent for Houston data. The results for the spring and summer months are reasonably good (about 6 percent) but overpredicts in fall (14%) and winter (24%). Unfortunately no explanations were given on the observed behavior and the significant positive and negative swings.

In conclusion, development of different models can prove to be beneficial in several ways. First, these models become the most accurate tools for the region they were developed for. They can provide dependable solar radiation data necessary for a variety of applications, such as solar systems simulation. Powerful enough correlations may also be applicable to other regions with similar climate.

Second, once such a model is available one can verify the accuracy and evaluate the performance of different models, or challenge their predictive power. Results of that nature could increase the confidence on some models or caution future users to utilize them with caution due to their poor performance.

Third, a solar radiation model also facilitates an investigation of a wide range of conditions which affect solar radiation. It provides efficient and cost effective means to simulate observations by incorporating parameters that have a dominant affect on the solar radiation components under study. Finally, further investigation on the subject could improve the accuracy of models by incorporating better modeling techniques.

CHAPTER V

STATISTICAL PRINCIPLES

The main objective of this work is to develop numerical models to predict the beam radiation through a regression analysis of empirical data. However, the reader should always bear in mind that such models are no more than what the word implies - generally considered as a means of creating representations of real world data.

A model is not a reality, and in a sense all models involve some uncertainty. To properly understand the power of a model we require the methods of statistics. In this chapter we summarize the basic areas of statistical theory and methods which were used throughout this study. Procedures for testing the goodness of fit of a model and for model selection between correlations with more than one independent variable, are also discussed.

5.1 Regression Analysis

A common problem in statistics is that of estimating the relationship that exists, if any, between two variables X and Y. The starting point is a set of n values of a dependent variable Y. The values themselves will be denoted by y_1, y_2,

... , y_n. The variable which enters into the specification of the dependent component is denoted by X, with individual values x_1, x_2, ... , x_n, and is called the independent (explanatory) variable.

Regression analysis is designed for situations where a variable is thought to be related to one or more of the measurements made. The available n pairs of measurements (x_i, y_i) are composed for this study by the Shenandoah five year data of clearness index and beam transmittance values, described in Chapter 4. If these data are plotted, one obtains the so-called scatter plot, illustrated in Figure 4.2. The objective is to fit a smooth curve through the points in such a way that the points are as "close" to the curve as possible.

Frequently, the type of curve to be fitted is suggested by the empirical evidence or theoretical arguments. A continuous piecewise linear model has been chosen for this study, suggested by Dischinger (1984). The term model is used rather broadly to describe the mathematical and statistical relationships that were developed between the dependent and independent variables.

5.1.1 The Linear Model

Let us again recall Figure 4.2 and observe the following. For any given clearness index there is a wide range of observed beam transmittance values and vice versa. Some of

this variation is due to errors of measurement of τ_b and k_t, but most of it is due to real variation between the dependent and independent variables. Thus, there is no unique relationship between τ_b and k_t.

However, the average observed clearness index for a given observed beam transmittance increases with increasing k_t, and the average observed clearness index for a given observed beam transmittance increases with increasing τ_b. The graph of the mean value of one variable for given values of other variable, when referred to the whole population is the regression curve also shown in Figure 4.2.

The method of estimating a linear regression, usually referred to as fitting a straight line to the data, is straight forward. We require to estimate the values of the parameters a and b in the equation,

$$Y_i = a + b\, x_i. \qquad (5.1)$$

Capital letters denote predicted or "mean" value of the dependent variable, while small letters denote an observed value.

There are several possible methods of estimating a and b, the so-called regression coefficients, in Equation 5.1. The one of most interest is called the Method of Least Squares. This consists of finding the value of the regression coefficients that minimize the sum squares of the deviations of the observed values from the line.

The estimated values of a and b will be denoted by β_o and β_1 respectively. If we denote the observations by (x_1,y_1), (x_2,y_2), ..., (x_n,y_n) then for any point x_i, the predicted value Y_i of y_i is $\beta_o+\beta_1 x_i$. The line of the form given in Equation 5.1 which has been fitted to a set of n points (x, y) by the method of least squares is called the line of regression of y on x or the line of prediction for y.

The vertical distance between actual y_i and predicted Y_i is therefore $y_i-(a+bx_i)$. The sum of the squares of all of the n such deviations is called the residual sum of squares (RSS) and is defined by,

$$RSS = \Sigma\{y-(a+bx)\}^2 = \Sigma\varepsilon_i^2 \qquad (5.2)$$

The vector of residuals is given by $\varepsilon_i=y_i-Y_i$. It is true that $\Sigma\varepsilon Y_i=0$, whatever the model, and also $\Sigma\varepsilon=0$. The values of a and b that minimize Equation 5.2 are the least square estimators of a and b.

Minimization is achieved in the usual manner; differentiate Equation 5.2 with respect to a and b and equate the differentials to zero. We obtain two equations for the parameter estimates β_o and β_1, of a and b respectively,

$$\beta_o = \frac{\Sigma y}{n} - \beta_1 \frac{\Sigma x}{n} = y_{ave} - \beta_1 x_{ave} \qquad (5.3)$$

$$\beta_1 = \frac{S_{xy}}{S_{xx}}$$

where S_{xy} = the sum of products of the deviations of the x's and y's from their respective means, $\Sigma xy-\Sigma x\Sigma y/n$,

S_{xx} = the sum of squares of the x's about their mean, $\Sigma x^2-(\Sigma x)^2/n$.

The variation about the regression, represented by the deviations of the observed y's from the regression line, must be less than the total variation of the observed y's about their mean. The extent by which it is less represents the amount of variation accounted for by the regression.

Consider now an observation (x_1, y_1) of the sample. The point on the regression line corresponding to x_1, given by substituting x_1 in the regression equation, is $Y_1=y_{ave}+\beta_1(x_1-y_{ave})$. The deviation of the actual observation y_1 from the regression can be expressed as the algebraic difference between two deviations, that of the deviation of the observation from the average, y_1-y_{ave}, and that of the deviation of the corresponding point on the regression from the average, Y_1-y_{ave}, that is

$$y_1 - Y_1 = (y_1 - y_{ave}) - (Y_1 - y_{ave}) \qquad (5.4)$$

Similar identities can be written down for each of the other n-1 deviations. Squaring each one and summing the equations we obtain the following expression for the sum of squares of the deviations from the regression:

$$\Sigma(y-Y)^2 = \Sigma(y-y_{ave})^2 - 2\Sigma(y-y_{ave})(Y-y_{ave}) + \Sigma(Y-y_{ave})^2$$

$$= \Sigma(y-y_{ave})^2 - 2\beta_o\Sigma(y-y_{ave})(x-x_{ave}) + \beta_o{}^2\Sigma(x-x_{ave})^2$$

$$= \Sigma(y-y_{ave})^2 - 2\beta_o{}^2\Sigma(x-x_{ave})^2 + \beta_o{}^2\Sigma(x-x_{ave})^2$$

$$= \Sigma(y-y_{ave})^2 - \beta_o{}^2\Sigma(x-x_{ave})^2$$

$$= \Sigma(y-y_{ave})^2 - \Sigma(Y-y_{ave})^2 \qquad (5.5)$$

Thus, we have the following identity,

Sum of squares of the observations about regression	=	Sum of squares of the observations about their mean	-	Sum of squares of regression about the mean

which can also be expressed as,

$$RSS = SYY - SSR. \qquad (5.6)$$

The sum of squares of the regression about the mean (SSR) represents the amount by which the total sum of squares of one variable is reduced when allowance is made for variations in the other variable. The alternative expression for $\Sigma(Y-y_{ave})^2$ is $b^2\Sigma(X-x_{ave})^2$.

The sum of squares about the regression (RSS) is based on n-2 degrees of freedom (d.f.). The degrees of freedom are defined as the number of available observations (n) minus the number of parameters estimated from the population. In our case, since two degrees of freedom have been used up in calculating the regression, we have d.f. equal to n-2. One d.f. for the mean value of y, and one d.f. for the regression coefficient b.

Dividing the sum of squares about the regression by the degrees of freedom gives an estimate of the variance about the regression. A typical analysis of variance (ANOVA) table contains the following information,

Source of Variation	Sum of Squares	d.f.	Mean Square
Due to Regression	$b^2\Sigma(X-x_{ave})^2$	1	MS_R
About Regression	$\Sigma(Y-y_{ave})^2 - b^2\Sigma(X-x_{ave})^2$	n-2	MS_E
Total	$\Sigma(Y-y_{ave})^2$	n-1	

If MS_R is judged significantly greater than MS_E, then the regression is statistically significant. That is the variates of y and x are probably connected by a genuine relationship. This idea is the basis of the so-called F-test which is discussed in the following section.

5.2 Testing Regression Models

A model of the form of Equation 5.1 can allow us to consider some of the variation of Y as due to a linear relationship, and some due to the error term ε. A measure of the relative importance of each source of variation is the coefficient of determination (r^2).

The coefficient of determination is the ratio of the sum of squares due to regression (explained by the regression) to

the sum of the squares about the mean, and is expressed as,

$$r^2 = \frac{SSR}{SYY} \qquad (5.7)$$

Let us examine two extreme cases. If the fit of the linear relationship is perfect, that is, if all the data fall on the regression line, then $r^2=1$. If on the other hand, the variation from the linear relationship is nearly as large as the variation about the mean, r^2 approaches zero. In the latter case, of course, the regression has little explanatory value. The value of r^2 is therefore a measure of the "explanatory" power of the regression.

One should note though that the coefficient of determination is a statistic, hence the particular value it takes is governed by chance. When samples are small in relation to the number of parameters being fitted, it is possible to get a large value of r^2 even when no linear relationship exists.

The success of a model is evaluated by its powers to reveal aspects of the situation being modeled that were previously hidden. Once a correlation is developed and is accepted as a useful predictive model, it is necessary to establish procedures for its validation and maintenance.

Among the various statistical tools that are available, the Fisher F-test (in honor of R.A. Fisher, who pioneered its many uses) has been singled out as the most successful one. The F-test can be applied to test the adequacy of two hypo-

thesis, namely the null and the alternative hypothesis. Each hypothesis represents a model that is believed to be more tenable based on the available data.

The null hypothesis is, as a rule, brought into the study to be rejected. It is the aim of the alternative hypothesis to prove the hypothesized model "null and void". We can reject the null hypothesis and accept the alternative hypothesis only if an authentic difference exists between the two hypotheses.

Let RSS_O and RSS_H represent the residual sum of squares for the null and alternative models, respectively. The corresponding degrees of freedom are designated by df_O and df_H. Then, the difference RSS_O-RSS_H represents the additional amount of scatter that was explained by the alternative model (or the hypothesized model, if RSS_O-RSS_H is less than zero). Consequently, the degrees of freedom are reduced by df_O-df_H.

The F-statistic, which is the ratio of the mean sum of squares for the regression (MS_R) to the mean sum of square for the residual (MS_E), is defined as follows,

$$F = \frac{MS_R}{MS_E} = \frac{\dfrac{RSS_O - RSS_H}{df_H - df_O}}{\dfrac{RSS_H}{df_H}}, \qquad (5.8)$$

where RSS_O = residual sum of squares for hypothesized model,

RSS_H = residual sum of squares for alternative model,

df_H = degrees of freedom for hypothesized model, n,

df_o = degrees of freedom for alternative model, n-q,

n = number of data points, and

q = number of parameters $\{\beta_i\}$.

In light of the identity provided by Equation 5.6, the numerator of the F-statistic can be expressed as an increment in the regression sum of squares,

$$F = \frac{\dfrac{RSS_H - RSS_o}{S_{yy}}}{\dfrac{RSS_H}{S_{yy}}} \quad \frac{df_H}{df_H - df_o} \qquad (5.9)$$

Equation 5.9 may also be expressed in terms of the coefficient of determination, r^2, from Equation 5.7, to obtain

$$F = \frac{(r_H)^2 - (r_o)^2}{1 - (r_H)^2} \quad \frac{df_H}{df_H - df_o} \qquad (5.10)$$

The F-statistic, follows an F distribution with (df_H-df_o, df_H) degrees of freedom. When the alternative model fits the data better than the null model, then the value of RSS_H is less than RSS_o. If the alternative hypothesis is true, then the expected value of the numerator in Equation 5.9 is greater than the expected value of the denominator.

The hypothesis testing is governed by a comparison of the calculated value of the F-statistic, according to

Equation 5.6, with tabulated values of $F(\alpha, df_H-df_O, df_O)$, where α is the confidence interval. Therefore, we should reject the null hypothesis for values of F that are "sufficiently" large.

Draper and Smith (1966) suggest that, as a working rule, the fitted correlation is probably an accurate predictor if $F>4F(\alpha, df_H-df_O, df_O)$. Then one may claim that there is a statistically significant improvement of the alternative model over the hypothesized model. This improvement should be reflected variously and equivalently in an increase in the regression sum of squares, and a decrease in the residual sum of squares.

The coefficient of determination may also be used to draw similar conclusions, since both r^2 and F are closely related. Observe from Equation 5.10 that if there is no significant change in the value of r^2 between two hypothesis, then F approaches zero. On the other hand, when r_H^2 approaches unity then F approaches infinity, which means that the best correlation with the highest r_H^2 is the alternative model.

Another statistical variable of importance is the probability $P(W<F)$, that a random variable W following the F distribution with degrees of freedom, df_H-df_O and df_O, would be less than the computed value for F. When this probability has a large value (approximately unity) then the value of the F-statistic is sufficiently large to guarantee that there is

essentially no chance that a hypothesized model would perform better than the alternative model.

A model according to Equation 5.1 will clearly be less than satisfactory if in fact Y is also significantly affected by a variable Z. In looking at past data the effects of Z will be contained in the error term, so some allowance is made for the possibility of such unknown factors. However, the neglect of Z may have undesirable effects.

When we do regression calculations on unplanned data (that is, data rising from continuing operations and not from a designed experiment) some potentially dangerous possibilities can arise, as discussed by Box (1966). The error in the model may well not be random but may result from the joint effects of several variables not incorporated in the regression equation nor even measured.

Due to the possibilities of bias in the estimates an observed false effect of a visible variable may, in fact, be caused by an unmeasured latent variable. Provided that the system continues to run in the same way as when the data were recorded this will not mislead. Because though the latent variable is not available its changes will not be seen or recorded and such changes may well cause the predicted equation to become unreliable.

In a later chapter we will investigate the need of adding additional parameters to the developed basic two variable model. Thus, we need to develop the tools for treat-

ing three (or more) variable models.

One always has to keep in mind that introducing additional variables to a model might statistically improve its accuracy, but at the same time the required input information increases. That could jeopardize applicability and usefulness of the model. We must be able to decide if the added complexity to the model is balanced by the significance of the improvement of the model.

For that purpose, one may choose to investigate a set of regressor variables to be used in the proposed model. We are interested in screening the candidate models to obtain the regression model that contains the "best" subset of independent variables. We would like the final model to contain enough independent variables so that it may perform successfully.

On the other hand, we would like the model to use as few independent variables as possible. The proposed model should require readily available information in order to be widely applicable. The compromise between these conflicting objectives is what we call finding the "best" model.

However, there will be no algorithm that will always produce data that exactly represents actual data for any given locality. Therefore, one has to use some judgement for selecting an appropriate model with appropriate independent parameters depending on the nature of the application and the desired accuracy. We will now briefly summarize some of the

most popular model comparison techniques, when the correlations involve a number of parameters.

Use of the r^2 statistic was previously mentioned. This is perhaps the most commonly used criterion. The analysis proceeds by starting with the most simple model, calculating its r^2, and proceeding with the more complicated models calculating the corresponding coefficient of determination values. Typically, one examines these values for a consistent pattern and may choose the model that results in the highest r^2 next to the one with the least change.

Use of the residual mean square, s^2, provides an estimate based on n-p degrees of freedom of the variance about the regression for the p-variable model. Generally, $MS_E(p)$ decreases as p increases, but this is not necessarily so. If the addition of a variable to the model with p-1 terms does not reduce the error sum of squares in the new p term model by an amount equal to the error mean square in the old p-1 term model, $MS_E(p)$ will increase, due to the loss of one degree of freedom for error (Hines and Montgomery, 1980).

A plot of the $s^2(p)$ against p is usually quite informative and may provide a helpful first guide line. The mean square error about the regression is usually flat in the vicinity of the minimum number of p. Thus, we could choose p such that adding more variables to the model produces only very small reductions in the $MS_E(p)$.

Use of a modified coefficient of determination that accounts for the number of variables (p) in the model, is also attractive. This statistic is called the adjusted coefficient of determination (r_a^2), and according to Draper and Smith (1986) is defined as,

$$r_a^2 = 1 - \frac{n-1}{n-p}(1 - r_p^2). \qquad (5.12)$$

The adjusted r^2 is closely related to the C_p statistic. Note that r_a^2 may decrease as p increases if the decrease in $(n-1)(1-r^2)$ is not compensated for by the loss of one degree of freedom in n-p. One should select a regression model that has the maximum value of r_a^2. However, this is equivalent to the model that minimizes the mean sum of square errors for a model with p variables $MS_E(p)$, since an alternative expression for r_a^2 is,

$$r_a^2 = 1 - \frac{n-1}{n-p}\frac{RSS(p)}{SYY}$$

$$= 1 - \frac{n-1}{SYY} MS_E(p). \qquad (5.13)$$

The stepwise regression is also a widely used regression model selection technique. The procedure calls for an investigation of a sequence of regression models by adding or removing variables. The criterion for adding or removing a

variable is expressed in terms of a partial F-test. Let F^+ be the value of the F-statistic for adding a variable to the model, and F^- the value of the F-statistic for removing a variable from the model. We must have F^+ greater or equal to F^- and usually F^+ equals F^-.

Step wise regression begins by first considering one independent variable, usually chosen such that the regressor variable has the highest correlation with the response variable, say $Y=f(X_1)$. This will be the variable producing the largest F-statistic value. If no F-statistic exceeds F^+, the procedure terminates.

The second highest partial correlation coefficient, say X_2, is selected next and a second correlation $Y=f(X_1, X_2)$ is developed. The overall regression is checked for significance, the improvement in r^2 value is noted and the partial F values for both variables now in the equation are examined. The lower of these two partial F's is then compared with an appropriate F percentage point, and the corresponding predictor variable is retained in the equation or rejected according to whether the test is significant or not significant.

This testing of the least useful predictor currently in the equation is carried out at every stage of the step wise procedure. A predictor that may have been the best entry candidate at an earlier stage may, at a later stage, be superfluous because of the relationships between it and other

variables already included in the correlation. To check on this, the partial F criterion for each variable in the regression at any stage of the calculation is evaluated, and the lowest of these partial F values is then compared with a pre-selected percentage point of the appropriate F-distribution.

This provides a judgement on the contribution of the least valuable variable of the regression at that stage, treated as though it had been the most recent variable entered, irrespective of when it was actually entered into the model. If the tested variable provides a non-significant contribution, it should be removed from the model and the appropriate fitted regression equation is then computed for all the remaining variables still in the model.

The best of the variables not currently in the model is then checked to see if it passes the partial F entry test. If it passes, it is entered and we return to checking all the partial F's for variables in. If it fails, a further removal is attempted. Eventually, when no variables in the current equation can be removed and the next best candidate variable can not hold its place in the equation, the process stops. As each variable is entered into the regression, its effects on r^2, is usually recorded to be used as first indicator on the significance of the variable on the correlation.

The forward selection procedure is a simplification of the step wise regression. It is based on the principle that

variables should be added to the model one at a time until there are no remaining candidate variables that produce a significant increase in the regression sum of squares. That is, variables are added as long as F-statistic is greater than F^+. The procedure does not account for the effect that adding a variable at the current step has on the variables added at earlier steps.

Similar conclusions may be achieved by using all p candidate variables in the model as the starting condition. The variable with the smallest partial F-statistic is deleted, if this F-statistic is insignificant, that is, if the F value is less than F^-. Next, the model with p-1 variables is estimated, and the next variable for potential elimination is identified. The procedure terminates when no further variables can be excluded.

According to the above discussion pertinent statistics are calculated and recorded at the end of each upcoming section that deals with the development of new regression models. Finally, these information are to be used for the selection of the "best" model at the end of this work.

CHAPTER VI

SEASONAL EFFECTS ON SOLAR RADIATION

Seasonal variations in the (k_t-τ_b) relation persist. Such differences are caused by seasonal changes in factors that affect the beam component - air mass, cloudiness and air quality (turbidity, moisture). In this chapter, the seasonal dependence of the correlation of the hourly beam irradiation on the hourly global irradiation is examined with respect to the Shenandoah data. Two methods for presenting this dependence are developed; sets of monthly regression models and a seasonal factor to modify a basic model. The latter procedure results in an especially concise presentation. This method provides a convenient means of including the seasonal effects in a regression model for the beam transmittance as in the case of the basic Shenandoah five-year model.

6.1 Method of Analysis

We recall from Figure 4.2 that a $\tau_b=f(k_t)$ correlation may be sufficient to account for the small data variations under either clear or overcast skies. However, for intermediate clearness indices a one-to-one relationship between τ_b and k_t is not sufficient to describe the large variations of

measured beam radiation data for a given clearness index.

Some of this variation can be explained by a seasonal variation. Accordingly, we proceeded with an investigation of the seasonal effects by collecting the (k_t, τ_b) Shenandoah data for the same month averaged over the five year period. The standard least-square error fit to a homogeneous linear model was applied over k_t bands, for each monthly data base, resulting in a regression model of the form:

$$\tau_{bj} = F_m(k_{tj}) + \varepsilon_j \qquad (6.1)$$

where $F_m(k_{tj})$ = regression model for month m, at the given clearness index k_{tj}, and

ε_j = residual for datum (k_{tj}, τ_{bj}).

The algorithm used to calculate regression models for monthly data bases has been presented in detail by Balaras (1985).

Representative results are illustrated for three months in Figures 6.1-6.3, where the corresponding monthly model is plotted against the Jeter and Balaras (1986) basic Shenandoah five-year model. Based on these figures, one may observe that the beam transmittance is higher for winter than summer months. This could be expected on account of the prevalent sky conditions.

During winter, the typical condition for middling clearness index is periodic cloudiness in an otherwise clear sky. This results in intermittent beam radiation. In contrast, the

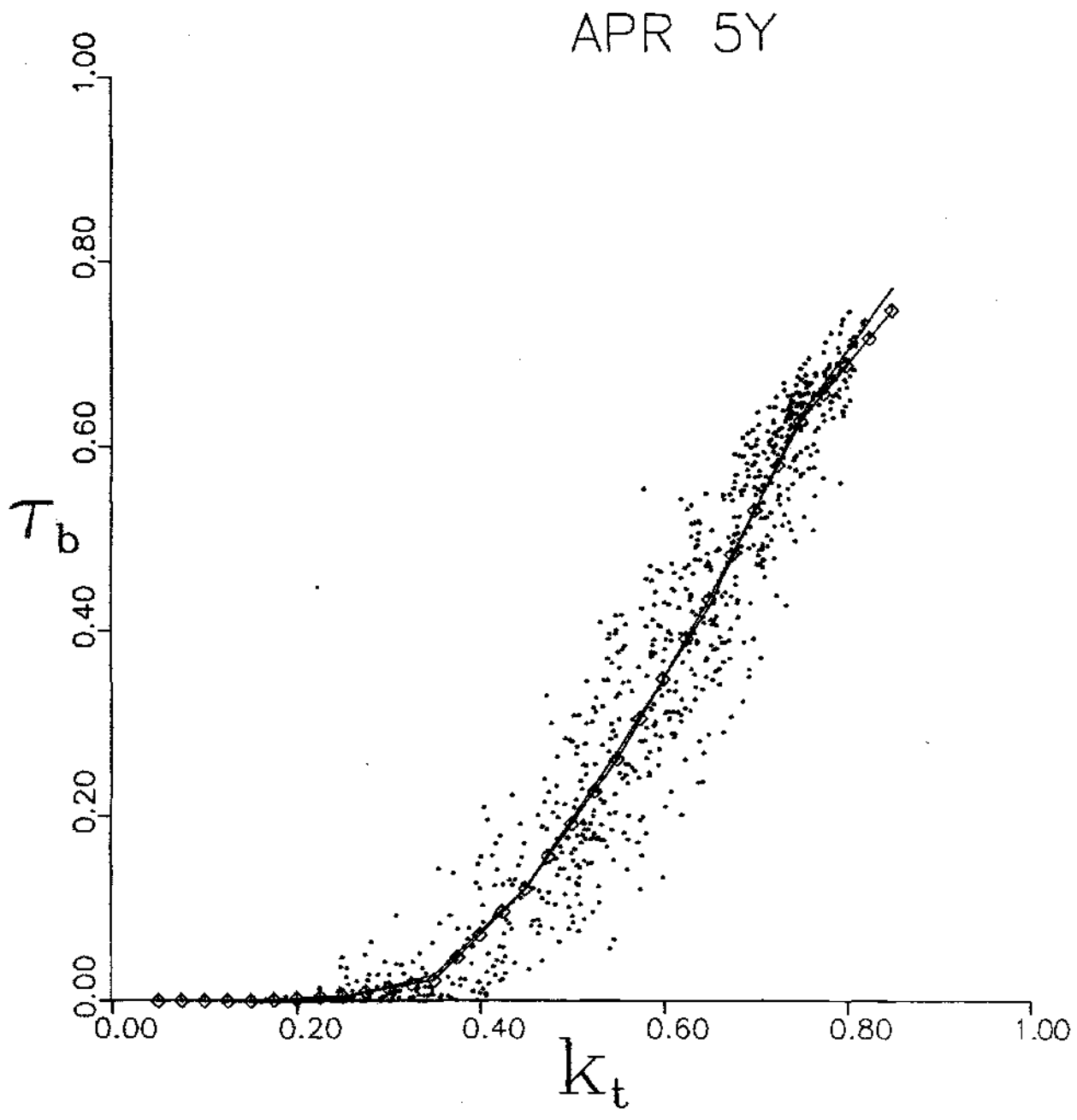

Figure 6.1 Scatter Plot of and Piecewise Regression on Shenandoah STEP Data for the Five Aprils. The Basic Shenandoah Five-Year Model is Shown by the Plain Line.

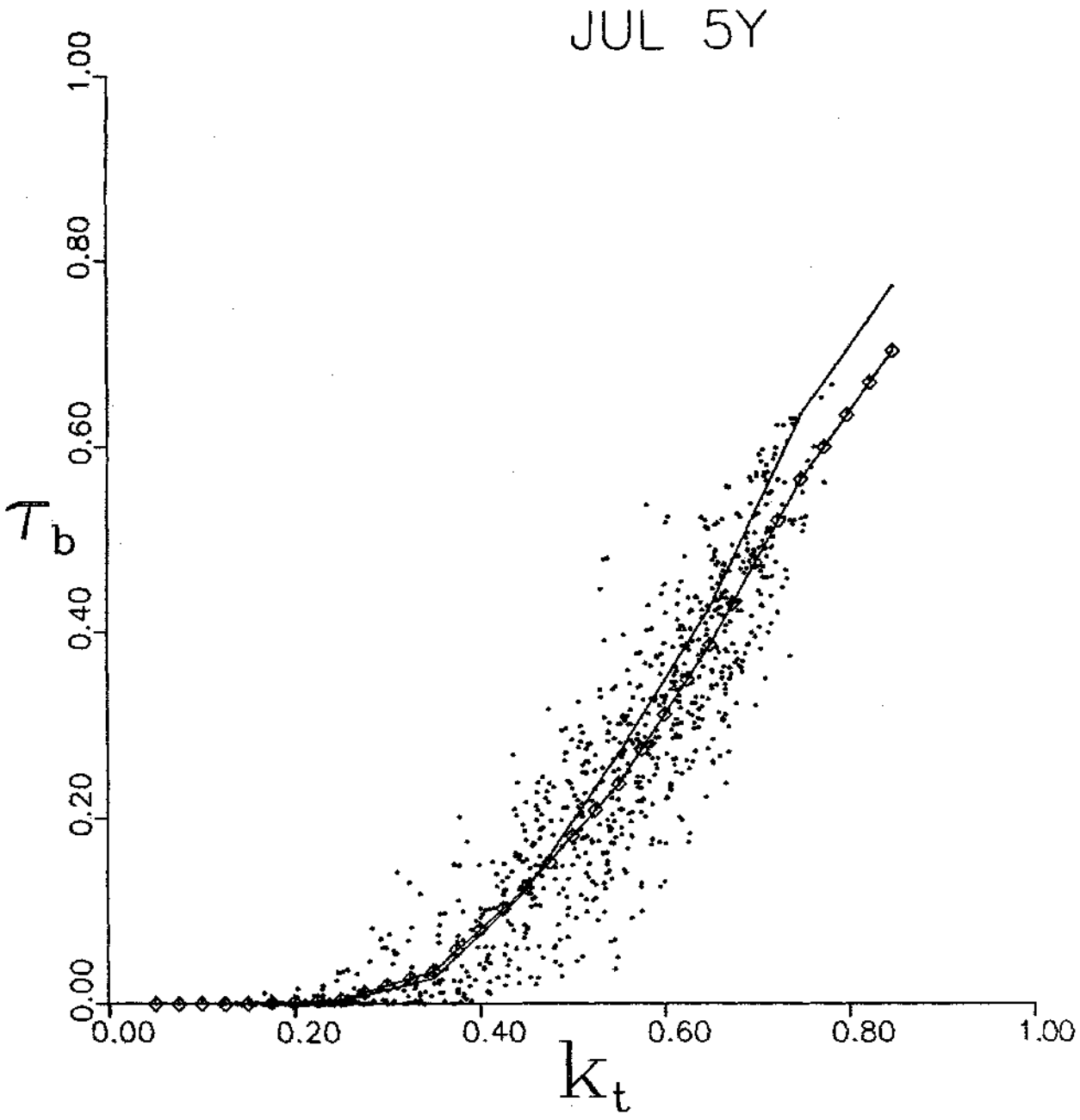

Figure 6.2 Scatter Plot of and Piecewise Regression on Shenandoah STEP Data for the Five Julys. The Basic Shenandoah Five-Year Model is Shown by the Plain Line.

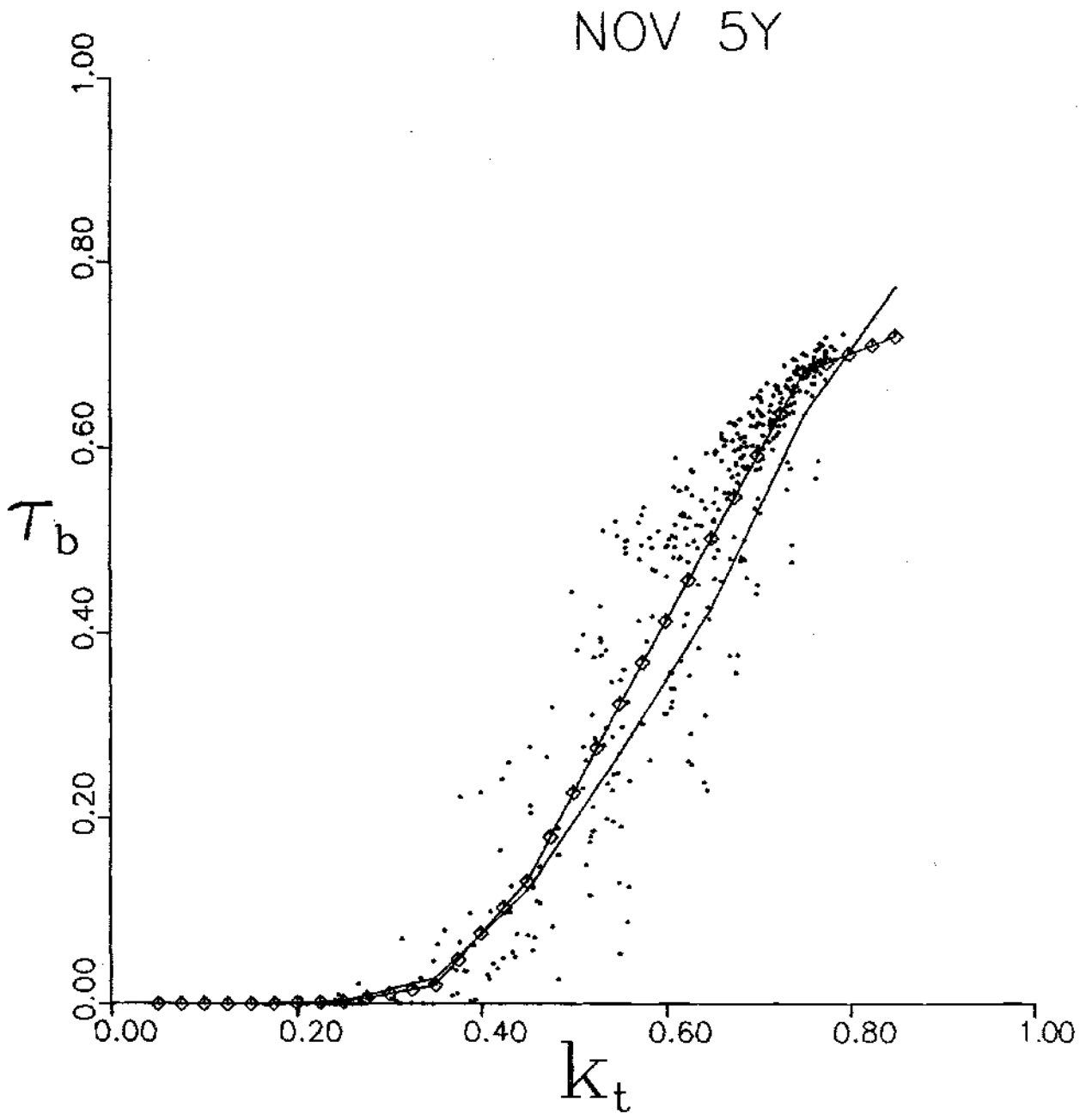

Figure 6.3 Scatter Plot of and Piecewise Regression on Shenandoah STEP Data for the Five Novembers. The Basic Shenandoah Five-Year Model is Shown by the Plain Line.

typical summertime intermediate k_t is a hazy condition with much greater attenuation of the beam radiation.

In addition, note that the beam transmittance reaches higher values for clear skies during winter. This is explained by the reduced water vapor and turbidity in the cold continental air masses that dominate clear weather conditions during winter in the southeastern United States.

A summary of the regression coefficient for all twelve months and for the basic Shenandoah five-year regression model is presented in Table 6.1. It is difficult to discern any trend from such a tabulation so the average of the regression coefficient in bands three through eight, the most important, has been computed. This average summarizes the steepness of the regression. The trend in steepness is basically smooth, declining from December to August. The coefficients for the last bands have to be used with caution. In some cases (Figure 6.3), due to the limited amount of data in these bands, outliers may influence the linear regression model to exhibit a slope not consistent with the previous regression trend.

6.1.1 Correlation Results

The monthly regression models clearly demonstrate a seasonal dependence in the correlation between beam transmittance and clearness index. This dependence cannot be a hidden effect of the optical path length since the air mass ratio is

Table 6.1

Monthly and Five-Year Regression Coefficients for Shenandoah STEP

k_t Interval	Piecewise Linear Regression Coefficients											
	JAN	FEB	MAR	APR	MAY	JUN	JUL	AUG	SEP	OCT	NOV	DEC
0.00-0.05	0.000	0.000	0.000	0.000	0.000	0.000	0.000	0.000	0.000	0.000	0.000	0.000
0.05-0.15	0.000	0.000	0.000	0.000	0.000	0.005	0.002	0.003	0.000	0.000	0.000	0.000
0.15-0.25	0.001	0.007	0.027	0.053	0.082	0.017	0.046	0.095	0.013	0.005	0.021	0.002
0.25-0.35	0.127	0.207	0.303	0.170	0.265	0.290	0.309	0.300	0.302	0.156	0.181	0.261
0.35-0.45	0.922	0.679	0.549	0.993	0.788	1.020	0.897	0.825	0.962	1.284	1.120	1.071
0.45-0.55	2.078	2.150	1.703	1.410	1.197	1.258	1.119	1.299	1.497	1.717	1.916	1.788
0.55-0.65	1.884	1.394	1.832	1.725	1.281	1.561	1.501	1.103	1.099	1.610	1.785	2.155
0.65-0.75	1.583	2.094	1.784	1.940	2.315	1.981	1.780	1.800	2.172	1.781	1.792	1.634
0.75-0.85	1.799	1.158	1.894	1.198	1.155	0.000	1.378	6.813	0.000	1.391	0.384	0.113
Average*	1.099	1.089	1.033	1.048	0.988	1.021	0.942	0.903	1.008	1.092	1.136	1.152

(*)Average regression coefficient for bands 3 through 8

higher in winter than in summer and by increasing the beam attenuation would cause a variation opposed to that actually observed.

There is also a possibility that a systematic error occurs in the calculation of the extraterrestrial radiation due to approximations in the analytic expression for the declination. This is ruled out, since the calculations for δ gives values are in very close agreement with those listed in the Nautical Almanac.

Temperature and cosine dependence of the measuring sensors could also affect the data in a systematic way, giving rise to seasonal variations. The temperature characteristics of the Eppley monitoring instruments are such that the sensitivity decreases at both high and low temperature (with respect to 0° C). In any event, the maximum effect is less than one percent during the few extremely low temperature days. Deviations due to cosine dependence are significant only during the winter months, but even then are less than two percent.

Consequently, these results do not support the assertion of Garrison (1984) that there is no seasonal dependence of the relationship. One explanation of this disagreement is that Garrison's data excluded hours for which the solar elevation exceeded 50°. As a consequence most winter hours are included but many summer hours around solar noon are excluded. This exclusion could have had a systematic impact

on his results because, in the southeast at least, one experiences many summertime days that are clear in early morning and late afternoon but cloudy in midday. Therefore, it may well be that summer hours when the elevation is less than 50° have sky conditions similar to winter hours.

Seasonal dependence has been noticed by other researchers reporting correlation studies using high quality solar radiation data. Collares-Pereira and Rabl (1979), and Erbs, Klein,and Duffie (1982) solved this problem by developing correlations for the winter and another for the rest of the year. A seasonal variation of the dome radiation was also reported by Rao et. (1984), but without any further treatment of this variation.

Vignola and McDaniels (1984), though, included a simple sinusoidal term dependent only on the year day in their dome-global correlation. The variance was significantly reduced and the seasonal dependence of the residuals was removed. Turbidity, water vapor and air-mass were identified as significant factors in the time dependence of the correlation.

A study of the beam-global correlations by Vignola and McDaniels (1986), yield the same seasonal trend. Using three years data from NOAA, their correlations, including the seasonal variation terms, appeared to work quite well. However, using data from Bet Dagan, Israel, collected by Gordon and Hochman (1984), they observed differences up to 20 percent, which clearly indicates that the correlation needs

to be tested with more data from other sites. Thus, it is suggested that their seasonally corrected correlations are not used outside the Pacific Midwest unless the variation in water vapor, turbidity and air mass is similar.

Collares-Pereira and Rabl (1979) proposed that changes in air-mass might be responsible for the differences in dome-global correlations found between summer and winter seasons. If air-mass, though, were the only cause, complete symmetry between summer and winter would be expected. But according to Vignola and McDaniels, the maximum deviations from the correlations occurred near the spring and fall equinoxes.

Vignola and McDaniels finally concluded that the observed seasonal variation is an intrinsic property of the data. This variation is most probably caused by the combined effects of air-mass, water vapor, and turbidity. Similarly, significant improvement can be achieved for the Shenandoah correlations by accounting for the seasonal variation using a single multiplicative factor. This analysis is presented in the following section.

6.1.2 Seasonal Variations

The monthly regressions should accurately account for the observed seasonal dependence. However, monthly models have some shortcomings. They are awkward to program and are not concise. On the other hand, a single variable accounting for the seasonal dependence would be easy to program and

concise in presentation.

Inspection of Figures 6.1 and 6.3 indicates that a simple multiplicative factor should be sufficient. This suggests a model of the form

$$\tau_{bj} = b_n F_5(k_{tj}) + \varepsilon_j \qquad (6.2)$$

where $F_5(k_{tj})$ = predicted value of beam transmittance by the basic five-year model by Jeter and Balaras (1986) from Equation 4.6, at the given clearness index k_{tj}.

ε_j = corresponding error between observed and predicted beam transmittance values at k_{tj}.

As usual, b_n is selected to minimize the unexplained variation. Therefore, for a given period, selected to be monthly, b_n is given by

$$b_n = \frac{\Sigma F_5(k_{tj}) \tau_{bj}}{\Sigma(F_5(k_{tj}))^2} \qquad (6.3)$$

Seasonal factors can be efficiently computed using monthly data bases and BCALCL presented in Appendix C. For the Shenandoah data the results tabulated in Table 6.2 and illustrated in Figure 6.4 are obtained.

The seasonal five-year model has been shown by Jeter and Balaras (1987) to be preferable to any of the annual models or the Shenandoah five-year model that has not been seasonal

Table 6.2

Seasonal Factors

Month	1979	1980	1981	1983	1984	5-YEAR
JAN	1.03214	1.059509	1.172972	-	1.287810	1.090281
FEB	0.99192	0.991142	1.123864	1.089944	-	1.032840
MAR	0.963483	0.962860	1.061209	0.988280	-	0.999403
APR	0.918130	0.990024	1.003169	1.025492	-	0.989392
MAY	0.724541	0.808086	-	0.981853	0.992495	0.885878
JUN	0.859448	0.900333	0.988580	1.011531	-	0.966864
JUL	0.885336	0.784846	0.913180	1.013243	0.817788	0.898174
AUG	0.884710	0.857430	0.848970	-	0.903891	0.875044
SEP	0.783950	0.849047	1.055425	-	1.003255	0.951085
OCT	1.046072	1.042244	1.127652	1.205805	1.046434	1.075994
NOV	1.092787	1.085864	-	1.158839	1.157031	1.112819
DEC	1.084911	-	1.227356	1.359432	1.163610	1.150584

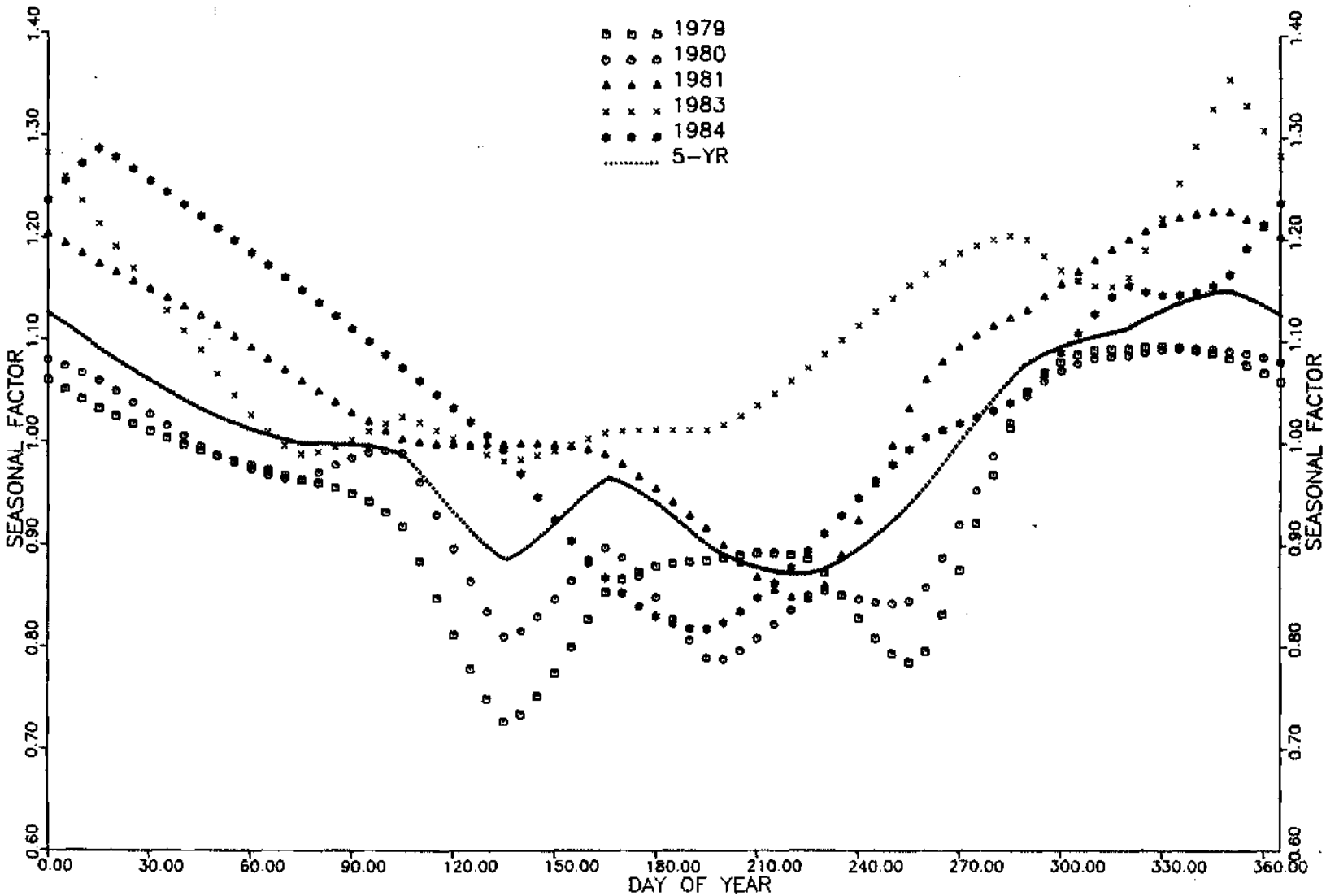

Figure 6.4 Seasonal Factors Computed from Five Years Data and Computed from Annual Data Bases

ly adjusted. This was, of course only to have been expected of a more flexible model.

The impact of this improvement can be much more important during days of longer length. As a result, increased amounts of extraterrestrial irradiation are available during summer. If the model overpredicts the beam transmittance during this season, the error is compounded.

Example results are illustrated in Figure 6.5. Here, beam irradiations inferred from historical global irradiations from Jeter et. (1979), are compared. The simple model underpredicts in winter and overpredicts in summer. Depending on the application, this could result in a poor design even though the annual totals are nearly equal.

In computing the results shown in Figure 6.5, algorithm BEAMNI was used (a listing is presented in Appendix C). The same interpolation routine used to plot the seasonal factor in Figure 6.4, was used to evaluate daily factors. Interpolation seems clearly preferable to a curve fit, especially since the asymmetry makes a simple sinusoid unsatisfactory.

6.2 Statistical Analysis

To quantify the results, pertinent statistics were computed for the seasonal five-year model, and each annual seasonal model as shown in Table 6.3. The information presented are in accordance to the discussion in Chapter 5.

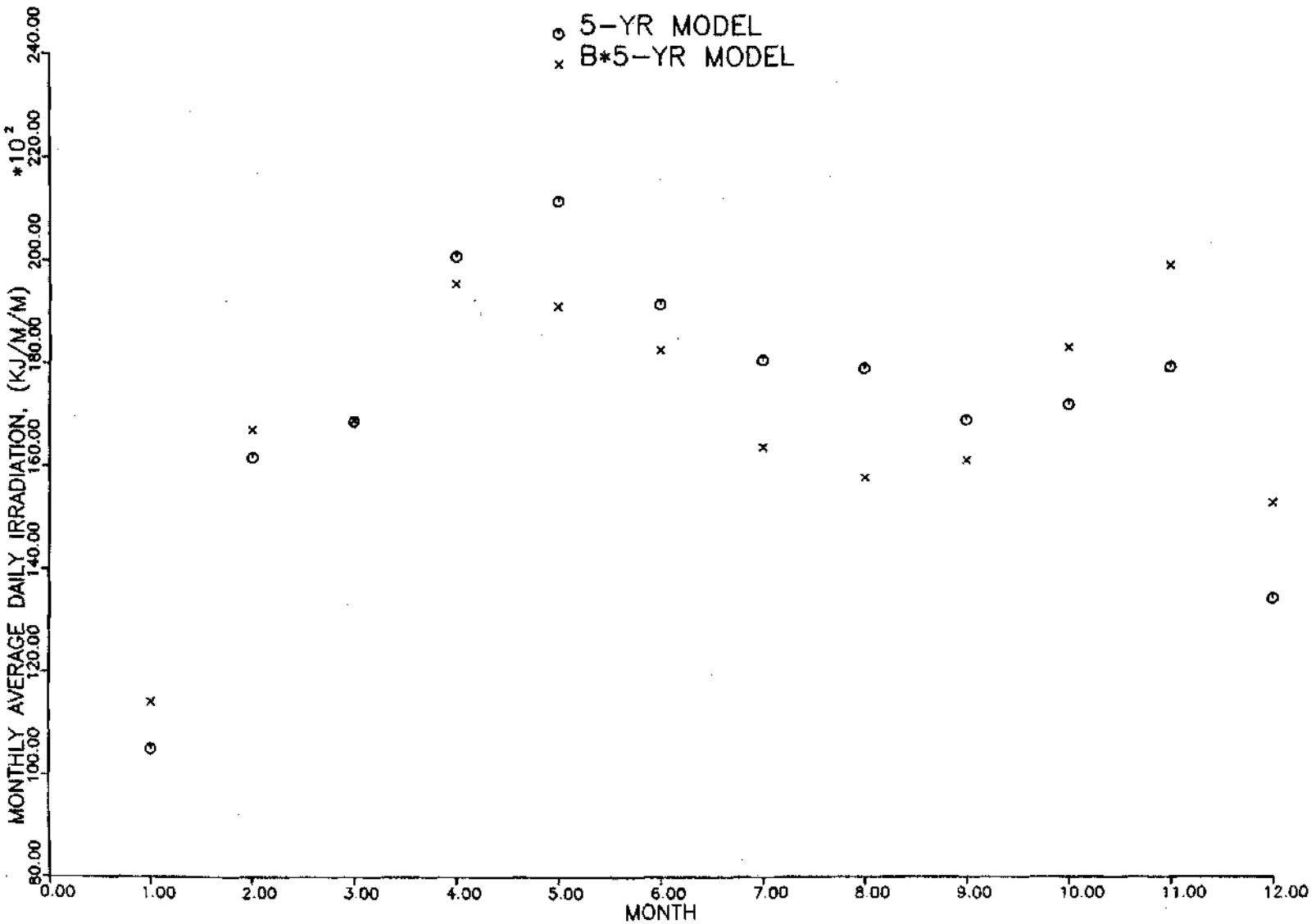

Figure 6.5 Comparison of Monthly Annual Daily Beam Irradiations Computed Using the Seasonal Model and the Basic Shenandoah Five-Year Model

Table 6.3

Statistical Analysis for the Five-Year Seasonal Model, the Simple Five-Year, Model, and the Annual Seasonal Models

Parameter	FIVE YEAR MODELS		Annual Seasonal Models				
	Seasonal	Simple	1984	1983	1981	1980	1979
No. Cases	8112	8112	8112	8112	8112	8112	8112
Total Variation	418.32	418.32	418.32	418.32	418.32	418.32	418.32
Residual Variation	40.36	47.47	52.40	55.59	44.72	44.13	47.94
Explained Variation	377.96	370.85	369.92	362.73	373.60	374.19	370.38
Coef. of Determination	0.9035	0.8865	0.8745	0.8671	0.8931	0.8945	0.8854
F-statistic	-	118.68	201.04	254.40	72.78	62.93	126.65
Probability	-	0.9999	0.9999	0.9999	0.9999	0.9999	0.9999

Table 6.3 indicates that the coefficient of determination has reached a value of 90.35% for the five-year seasonal model, from 88.65% for the simple five-year model. This slight improvement seems hardly worth any additional effort to implement, but it was previously illustrated (Figure 6.5) how this seasonal effect can regain importance.

Each of the less inclusive models was compared to the five-year seasonal model in order to determine the significance of the difference between the available models. For this decision-making procedure, the null hypothesis was that an annual seasonal model or the simple five-year model is tenable, while the alternative hypothesis was that the five-year seasonal model is more tenable based on the available five year data. The calculated F value was compared to the tabulated value of F(0.01,12,8) and found to be equal to 5.67. For all tests, the high values of the F-statistic tend to support the alternative hypothesis.

In summary, there is conclusive evidence of a seasonal dependence in the relationship between beam transmittance and clearness index. Variations of the beam intensity from different seasons within a given year can be as great as the variations from year to year. Either distinct seasonal regression models, or preferably an inclusive regression model modified by a seasonal factor, can be used to quantify this effect. The latter method was successful in improving the predictive powers of the basic Shenandoah five-year

model.

The performance of the model has increased, as one would expect since we have included additional variables. The iprovement was found to be significant to justify the seasonal five year model as better model in comparison to other correlations. However, since the multiplicative factors developed for our model are weather related, the model is not expected to perform as well outside the southeast United States in regions with distinctly different weather patterns.

Consequently, we need to develop a method that includes variables and information that are not directly weather dependent. Atmospheric air-mass is a prime candidate. No additional information are required for calculating the value of air-mass, than the information already included in the Shenandoah five year data base. The following chapters deal with the investigation of the dependence of beam and global radiation on air mass, and with the development of improved correlations for the beam transmittance.

CHAPTER VII

AIR MASS DEPENDENCE OF BEAM RADIATION

The intervening atmospheric air-mass is expected to exhibit a direct relationship with the beam transmittance. In this chapter, we will investigate the dependence of beam radiation on air-mass. Initially, a study of the relationship between τ_b and m would help us establish the limiting conditions of the beam transmittance under clear sky conditions. Such information may prove valuable for long term prediction of solar radiation. In order to isolate the effects of air-mass, new subsets of the Shenandoah five year data were formed. The dependence of the beam transmittance on air-mass is also assessed using a regression study with the development of (τ_b-m) correlations parametric in clearness index. Finally, for completeness, the (k_t-m) correlations parametric in τ_b are briefly discussed.

7.1 A Simple Clear Sky Model

Air-mass can be used to adequately predict the limiting value of beam radiation under clear sky. The method described here could be employed with data for a specific locality. However, after an investigation of independently developed

clear sky beam transmittance correlations, it is believed that clearest skies are not necessarily site specific. Accordingly, the proposed correlation may be applied generally for purposes such as prediciting extreme beam irradiance and removing the air-mass dependence in beam transmittance correlations.

7.1.1 Model Development

The atmosphere is not homogeneous, but contains a varying amount of water vapor molecules and particles (such as atmospheric pollutants), even under clear skies. As a result, beam radiation may be attenuated by scattering or absorption during its passage through the atmosphere. The interactions of the beam radiation with the molecules and particles present in the atmosphere are independent events.

Thus, considering an infinitesimal layer of the atmosphere, the net attenuation of the beam radiation is proportional to the incident irradiance and the atmospheric extinction, according to a Bouguer's Law type formulation. In Chapter 4, Equation 4.8 correlates the beam transmittance (τ_b) to atmospheric extinction coefficient (K) and air-mass (m). For convenience, let us restate the correlation that exhibits the dependence of τ_b on m, namely

$$\tau_b = \exp(-K\ m). \qquad (4.1)$$

The reader should recall at this point that the atmospheric

air-mass can be calculated from Equation 4.9 as a function of altitude alone. For our numerical calculations, m values were computed through AMASS, a routine found in Appendix B.

Hourly values of the beam transmittance and air-mass were also calculated for the Shenandoah five year data. The variation of τ_b versus m is illustrated in Figure 7.1. Note that air-mass values range from unity up to 6.5. Higher values of m were not attained, since at very low sun angles pyrheliometer data cannot be considered reliable on account of refraction and interference from objects near the horizon.

According to Figure 7.1, the beam transmittance distribution exhibits the expected variation. High τ_b values at low air-mass and progressively lower τ_b values occur as air-mass increases. This is in agreement with the fact that, as the energy attenuation caused by the atmosphere increases, the beam radiation decreases.

To identify the limiting values that represent the clearest sky conditions, the distribution was disaggregated into air-mass bands, each one being 0.1 wide. For each band (12 in total), the limiting beam transmittance values were identified. Consequently, these data represent the clear sky conditions for STEP. Using a minimization technique, the value of the extinction coefficient was estimated to be equal to 0.106. Thus, the expression for the clear sky beam transmittance becomes,

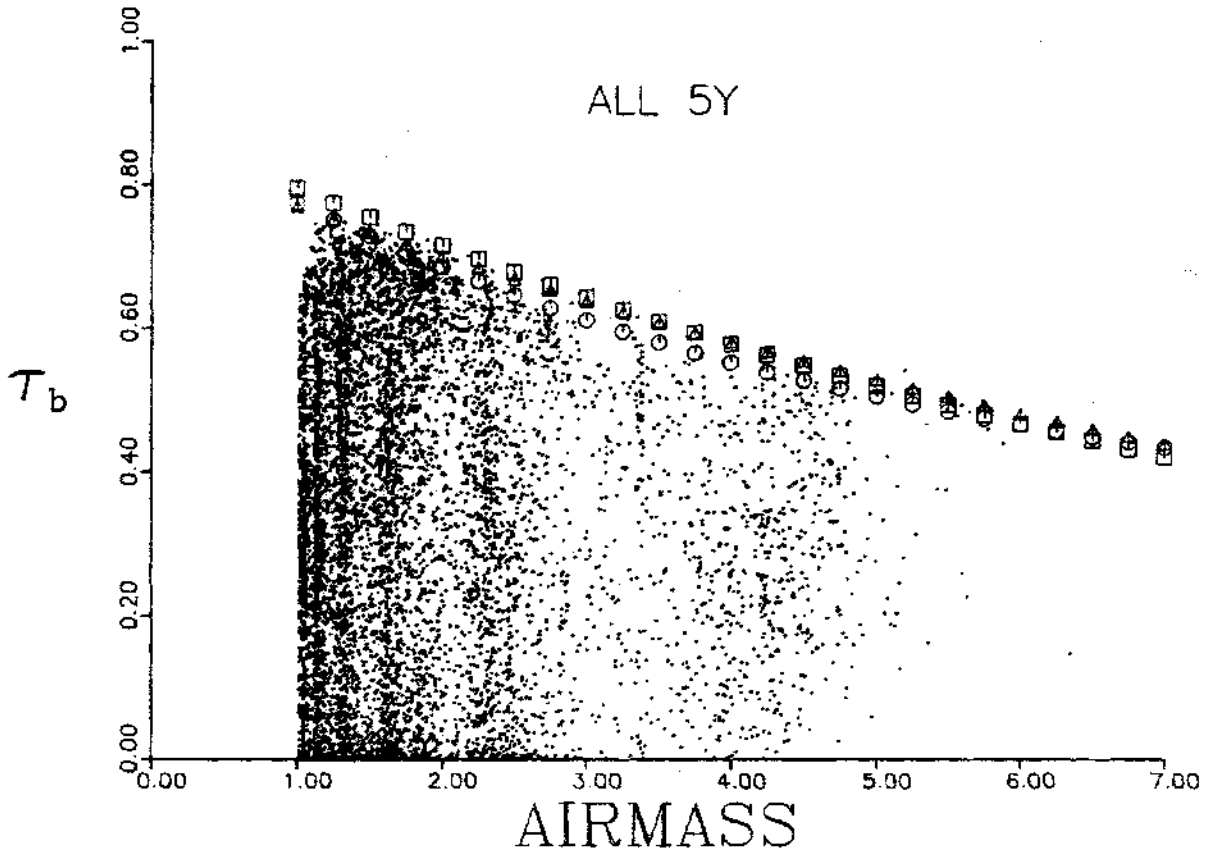

Figure 7.1 Beam Transmittance Dependence on Air-Mass Using Five Year Data From Shenandoah, Georgia. Triangles Indicate the Simple CSBT Model, Squares Indicate the Randall-Whitson Model, and Circles Indicate the Maxwell Model

$$\tau_{bc} = \exp(-0.106\ m) \qquad (7.1)$$

These calculations are performed by a routine called AIRMAS3 of which a listing is available in Appendix D.

Another way of expressing the dependence of beam transmittance on air-mass is to include an air-mass independent factor, τ_o, that is best justified for its improvement in fitting the statistical data. One then obtains the following formula for the beam transmittance:

$$\tau_b = \tau_o \exp(-K\ p) = \tau_o \exp(-\kappa\ m) \qquad (7.2)$$

where K = extinction coefficient (Km^{-1}),

p = path length (Km),

κ = normalized extinction coefficient,

m = air-mass ratio, m=p/l, or from Equation 4.9, and

l = depth of the atmosphere.

Using the data for the clearest sky conditions for a least square error curve fit, the following expression for the Clear Sky Beam Transmittance (CSBT) was determined,

$$\tau_{bc} = 0.8426 \exp(-0.0939\ m). \qquad (7.3)$$

The regression coefficients for the CSBT model were calculated by PLOTXY; a listing of this program can be found in Appendix D.

Similar expressions have also been developed by Randall and Whitson (R-W, 1977), and Maxwell (1987). The R-W model

was expressed as,

$$\tau_{bc(R-W)} = 0.8847 \exp(-0.106\ m) \qquad (7.4)$$

while Maxwell made a polynomial fit to clear sky values based on data from Atlanta, Georgia, to obtain an expression of the form,

$$\tau_{bc(M)} = a - b\ m + c\ m^2 - d\ m^3 + e\ m^4 \qquad (7.5)$$

where a=0.886, b=0.122, c=0.0121, d=0.000653, e=0.000014.

Figure 7.1 illustrates the scatter plot of the hourly five year STEP data, along with the resulting CSBT model, from Equation 7.3. Also illustrated are the R-W model, Equation 7.4, and the Maxwell model, Equation 7.5. Figure 7.1 which was generated using routine AIRMAS3 presented in Appendix D.

7.1.2 Model Validation

The previous analysis has provided us with all of the necessary information to calculate the beam radiation under clear skies. Once the beam transmittance value for clear skies (according to Equations 7.1 or 7.3) is known, one can simply express the clear sky beam radiation as follows,

$$I_{bnc} = I_{on}\ \tau_{bc} \qquad (7.6)$$

where I_{bnc} = periodic (e.g. hourly) beam irradiation under clear skies,

τ_{bc} = beam transmittance computed for the mid point of the period.

The modeled data from Equation 7.6 was compared with measured data for season representative clear days throughout the year of 1979. First, Equation 7.1 was used to calculate the τ_{bc} value. This resulted in a poor performance of the model, since at the beginning and ending periods of a day, the modeled data exceeded the measured clear sky beam radiation values.

This initiated a thorough investigation of the programming features for several routines that had been used upto that date. This is critical, because in the event, for example, that the air-mass values had been overpredicted, substantial errors may have been introduced. Such a problem would then play a critical role in the behavior of the model at low sun angles, possibly causing the observed erroneous behavior.

The fact that the problems occurred at the early and late periods of the day led us to a closer examination of the calculations performed during those intervals. One should recall that routine HELGO was used at the middle of each hourly period to calculate the position of the sun. This could potentially create a problem in the event that the calculated attenuation of the beam radiation is overestimated. This becomes especially critical at low sun

angles. Thus, a closer examination of these procedures was necessary in order to evaluate possible programming problems that may have resulted to loss of accuracy.

In accordance, average air-mass values were calculated using minute intervals and integrated to obtain hourly values. Even with half minute intervals, our results indicated no substantial differences between these integration methods and the previously obtained values using hourly intervals. Since no programming errors were found, one may conclude that the poor predictive powers of Equation 7.1 had caused these discrepancies.

Fortunately, the use of the CSBT model (Equation 7.3) to predict τ_{bc}, exhibited none of the above problems. On the contrary, the modeled data from Equation 7.6 plotted against season representative clear sky days from 1979, indicated that CSBT was indeed an accurate predictor of clear sky beam transmittance. This task was undertaken by routine IBN which can be found in Appendix D.

Example results are illustrated in Figure 7.2. The calculations are performed at the end of the hourly periods during November 14, 1979, using algorithm IBN listed in Appendix D. The triangles represent beam radiation values predicted by the CSBT model and the squares represent measured beam radiation values under clear skies. The general trend of the modeled data is in good agreement with the measured data. The CSBT model predicts slightly higher beam

radiation values since it represents the clearest sky conditions, or in other words, the limiting case.

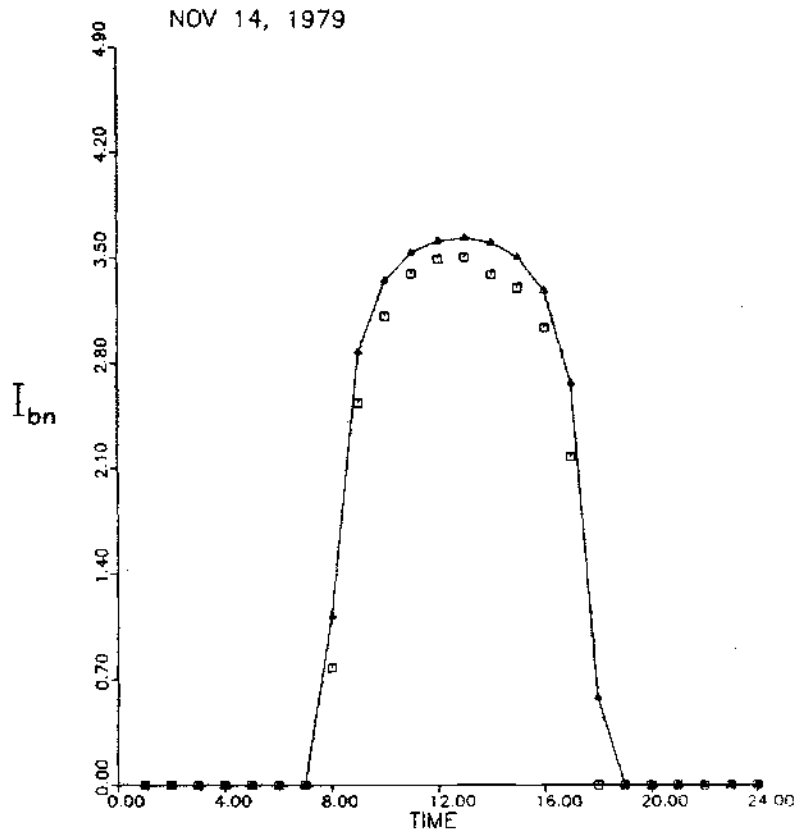

Figure 7.2 Hourly Beam Radiation Under Clear Skies During November 14, 1979 for Shenandoah, Georgia. Time is in Hours and the Beam Normal Irradiation in $KJ/m^2/hr$. The Solid Line Represents the CSBT Model and the Squares Represent the Measured Data

Finally, the reader should recall Figure 7.1 from which we may observe that in an absolute sense, the three curves vary by less than four percent. This is also illustrated by Table 7.1, which lists the corresponding values of τ_{bc} for different air-mass values according to all three correlations.

Table 7.1

Characteristic Values for the Clear Sky Beam Transmittance

Air-Mass	CSBT Model	R-W Model	Maxwell Model
1.0	0.7670	0.7960	0.7750
2.0	0.6983	0.7157	0.6854
3.0	0.6357	0.6437	0.6124
4.0	0.5788	0.5789	0.5534
5.0	0.5269	0.5207	0.5056
6.0	0.4797	0.4684	0.4670

This is a very important observation which shows that three models developed from distinctly different populations (with statistically different underlying distributions) are practically identical. In fact, either model could be applied with satisfactory results.

One can then conclude that clear sky conditions actually represent a universal behavior. Such models can then be used with confidence on different data bases for determining limiting sky conditions. Any observed discrepancies can be attributed to varying local climate, geographical variations, sampling techniques and/or instrumentation errors and variation that could bias the corresponding measurements.

For example, notice in Figure 7.1 that the Maxwell correlation underpredicted the values of τ_{bc}, for almost the whole m range, compared to the other two models. This is probably due to the fact that the Atlanta data, used by Maxwell, exhibits a certain degree of air-pollution that attenuates part of the beam radiation even under clear skies. Such a behavior should be expected at metropolitan areas.

7.1.3. Statistical Analysis

The analysis of variance for all three models was performed through CSMSTAT found in Appendix D. The data used were the maximum τ_b values from each of the 22 air-mass bands. The pertinent statistical results are summarized in Table 7.2, in accordance to the discussion in Chapter 5.

The coefficient of determination indicates that 94% of the variability in the Shenandoah data is accounted for by the CSBT model. The next highest value was achieved by the Maxwell model (88%), followed by the R-W model with 86%.

The F-statistic values are for testing two hypotheses, namely the null hypothesis (that the R-W or Maxwell model is tenable) and the alternative hypothesis (that the CSBT model is more tenable based on our data). The calculated F value was compared to the tabulated value of F(0.01,20,22) and found to be equal to 2.83. For both tests the alternative hypothesis is true. The CSBT model is preferred based on our statistical analysis, although all three models were in close

agreement as was previously graphically illustrated.

Table 7.2

Statistical Analysis for Testing the Clear Sky Beam Transmittance, Randall and Whitson, and Maxwell Models

Parameter	CSBT Model	R-W Model	Maxwell Model
Total Variation	0.06862	0.06862	0.06862
Residual Sum of Squares	0.00385	0.00963	0.00836
Explained Variation	0.06477	0.05899	0.06026
Coef. of Determination	0.94386	0.85959	0.87814
F-statistic	-	15.0103	11.7055
Probability	-	0.99999	0.99999

7.2 Dependence of Beam Transmittance on Air-Mass

In Chapter 4 we have discussed the dependence of beam transmittance on clearness index. To assess the effects of air-mass on the beam radiation a regression analysis can be used based on an alternative five year data base. These data must be created for the purpose of this study as described in the following section.

7.2.1 Model Development

The required information for the upcoming study are the hourly values of three variables, namely the clearness index,

air-mass, and beam transmittance. These data constitute an hourly five-year data base of the form (k_{ti}, m_i, τ_{bi}). The clearness index was calculated according to Equation 4.5, the air-mass values according to Equation 4.9, and the beam transmittance according to Equation 4.4.

Once the five year data (k_{ti}, m_i, τ_{bi}) were grouped together, the development of correlations for (τ_{bi}, m_i) proceeded as follows. First, the data were broken down to clearness intervals. For every group a continuous linear model was fitted in a least square sense, through air-mass bands of unit width (for computational details refer to algorithm CURVE2 in Appendix D). Such an approach is attractive since it would reveal the effects of air-mass on the beam transmittance under different clearness indices.

One expects that atmospheric air-mass would play a role in the attenuation of incoming beam radiation, since high air-mass indicates a long path through the atmosphere. The question that arises though, is whether this attenuation would be dependent on the sky condition or some other physical variable, and also the magnitude of the effect that air-mass exhibits on beam transmittance. Our analysis attempts to address these questions.

For each air-mass band the regression model which assures continuity is,

$$(\tau_{bj} - y_{oi}) = \beta_i (m_j - x_{oi}) + \varepsilon_j \qquad (7.7)$$

where x_{oi} = lower limit of band i,

y_{oi} = regression model at x_{oi},

β_i = regression coefficient, and

ε_j = residual error for data (m_j, τ_{bj}).

Results of the linear regression analyses are given in Table 7.3. Primary results of the analysis are the set of regression coefficients (β_i) for each clearness index case with representative results illustrated in Figures 7.3 to 7.6. The reader should observe that at high clearness indices - mostly clear winter conditions - beam transmittance increases with increasing air-mass for the interval of $1<m<2$, while for air-mass values greater than two, beam radiation is attenuated with increasing air-mass. For low k_t cases, typical of summer, hazy conditions, m has no direct effect on τ_b. One may then conclude that the intensity of beam radiation is rather weather related.

Based on these observations it was decided to perform a seasonal study. Following the same procedures the analysis was repeated for summer and winter seasons. Such an analysis should remove any seasonal dependence that could have affected our previous observations.

Representative results from the seasonal analysis are shown in Figures 7.7 to 7.10. The variation of the beam transmittance with air-mass did not exhibit any substantial deviation from the five year analysis. Thus, the observed τ_b-

Table 7.3

Functions for the Beam Transmittance - Air Massp pCorrelation

Clearness Index	Air-Mass Band 1<m<2	2<m<3	3<m<4	4<m<5	5<m<6
$0.0<k_t<0.1$	.00000	.00000	.00000	.00000	.00000
$0.1<k_t<0.2$	.00021+.00009m	-.00164	.00000	.00000	.00000
$0.2<k_t<0.3$	.01454-.00562m	.00127	-.00138	.00000	.00000
$0.3<k_t<0.4$	.04162-.00447m	.01698	.00081	.09641	.11253
$0.4<k_t<0.5$	.11174-.00558m	.07118	.00021	.07932	-.06462
$0.5<k_t<0.6$	.19862+.01962m	.13389	-.03122	.04263	.11513
$0.6<k_t<0.7$	.19205+.15512m	.02725	-.04531	-.06675	.49612
$0.7<k_t<0.8$	.43580+.11954m	-.14749	-.06730	.00000	.00000
$0.8<k_t<0.9$	.71281+.00253m	.00000	.00000	.00000	.00000

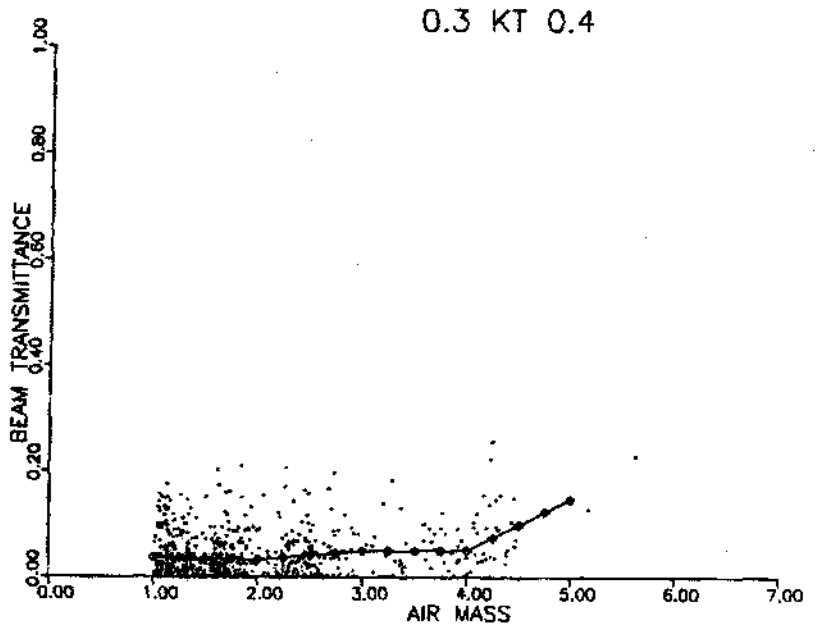

Figure 7.3 Scatter Plot of and Piecewise Regression on Shenandoah Data for a Clearness Index Range of 0.3 to 0.4

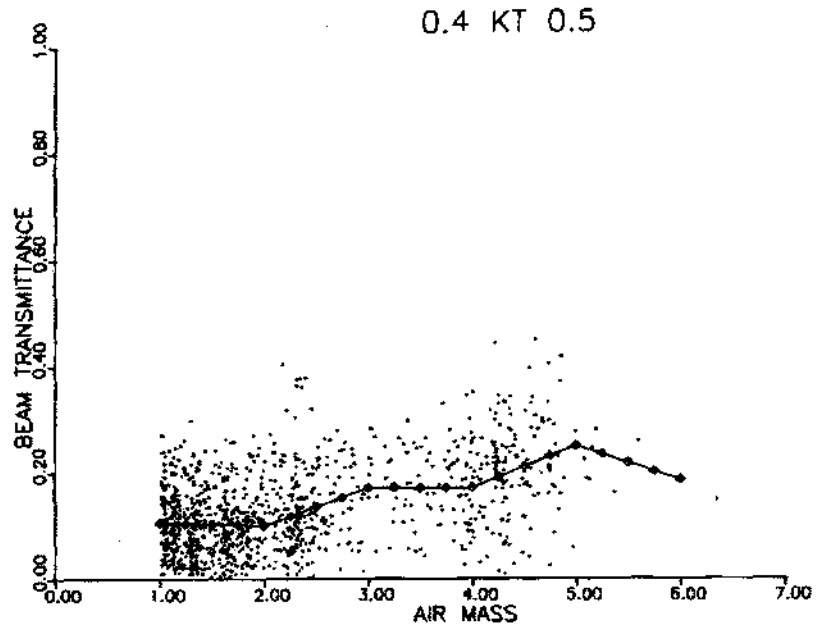

Figure 7.4 Scatter Plot of and Piecewise Regression on Shenandoah Data for a Clearness Index Range of 0.4 to 0.5

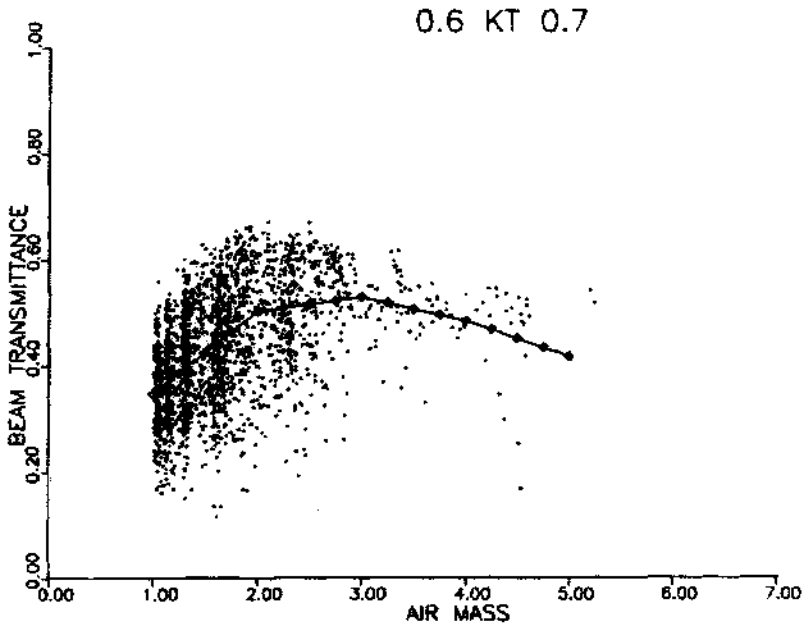

Figure 7.5 Scatter Plot of and Piecewise Regression on Shenandoah Data for a Clearness Index Range of 0.6 to 0.7

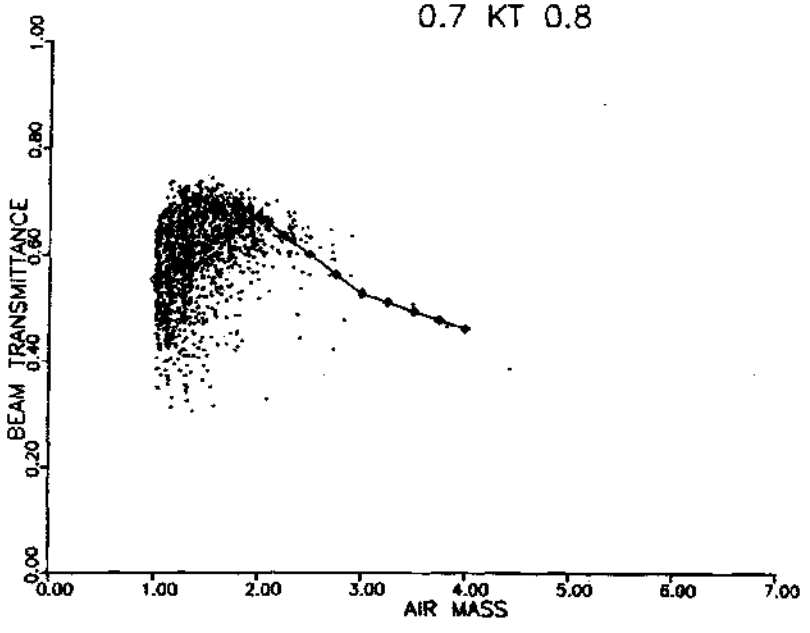

Figure 7.6 Scatter Plot of and Piecewise Regression on Shenandoah Data for a Clearness Index Range of 0.7 to 0.8

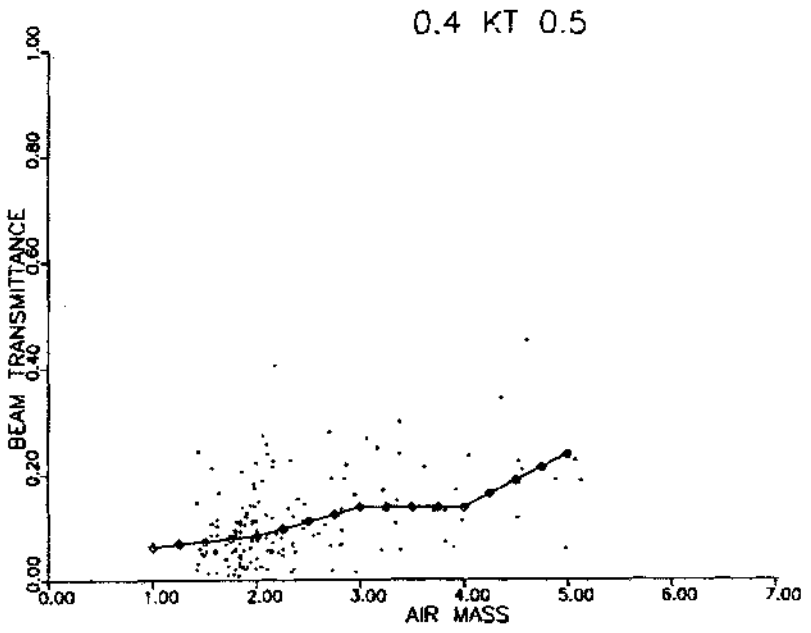

Figure 7.7 Scatter Plot of and Piecewise Regression on Shenandoah Data for a Clearness Index Range of 0.4 to 0.5 for Winter Seasons

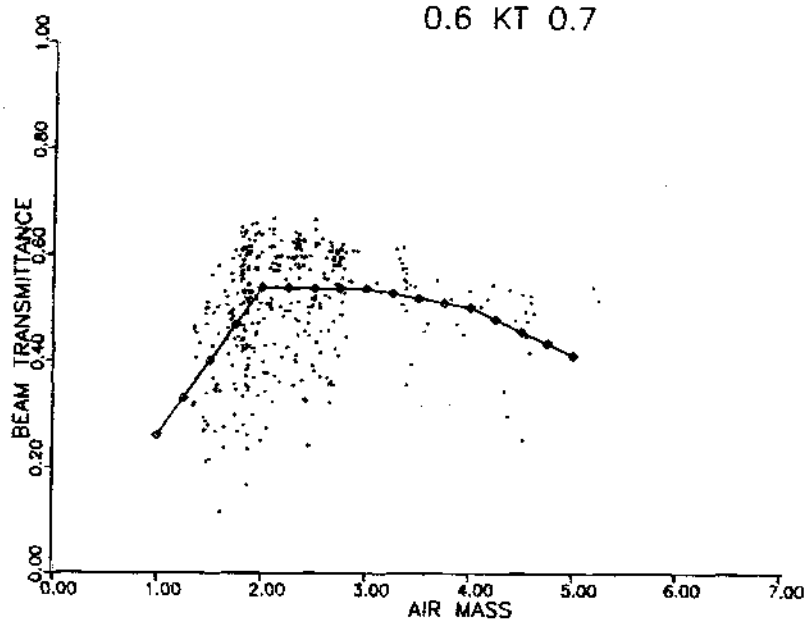

Figure 7.8 Scatter Plot of and Piecewise Regression on Shenandoah Data for a Clearness Index Range of 0.6 to 0.7 for Winter Seasons

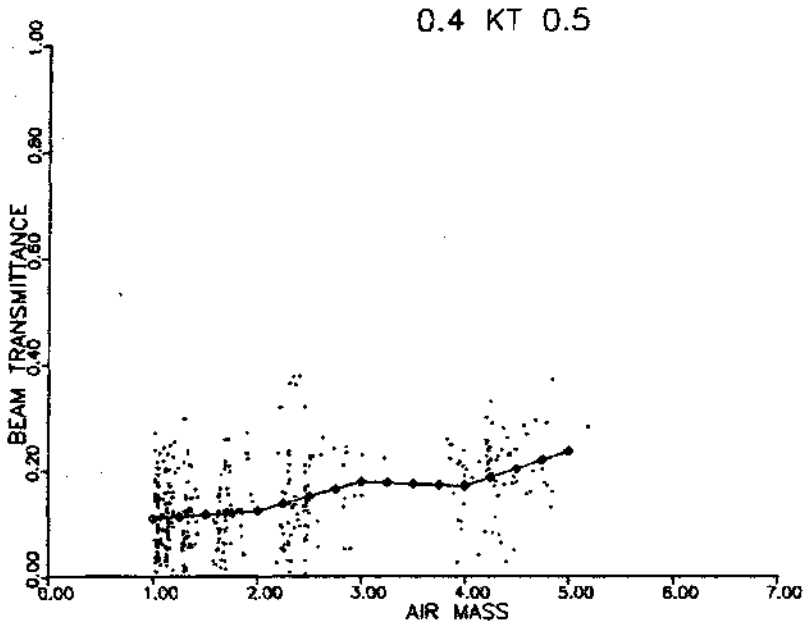

Figure 7.9 Scatter Plot of and Piecewise Regression on Shenandoah Data for a Clearness Index Range of 0.4 to 0.5 for Summer Seasons

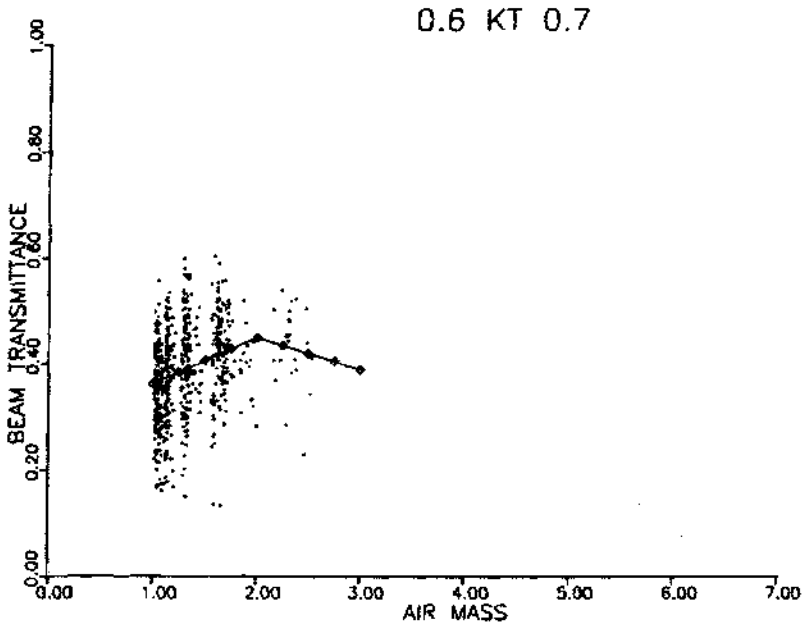

Figure 7.10 Scatter Plot of and Piecewise Regression on Shenandoah Data for a Clearness Index Range of 0.6 to 0.7 for Summer Seasonsm variations were not introduced by any seasonal effects.

Accordingly, we may conclude that there is no direct relationship of air-mass on beam transmittance even under clear skies. Although m should attenuate beam radiation the previous results do not support such a statement, but it rather seems that this is triggered by some other mechanism.

For example, we identified some of the data at low and high air-mass values, from Figures 7.7 and 7.9. According to these figures the regression exhibits a clear upward trend. For the summer seasons, Figure 7.7, data at low air mass and low beam transmittance represent hazy conditions (low τ_b for intermediate k_t). Data for high air-mass values and high beam transmittance occurred during partly cloudy conditions (high τ_b for intermediate k_t). Thus, the increasing trend of the beam transmittance data with air-mass is attributed to clearing sky conditions. The effects of air-mass were overcomed by increasing beam radiation due to clearing skies. Similar observations were made in relation to Figure 7.9.

For completeness, the next step taken was the study of (k_t-m) correlations for different τ_b cases. Representative results shown in Figures 7.11 to 7.14 indicate that for clear sky conditions (high τ_b cases) the global radiation decreases with increasing air-mass. The data do not exhibit much scatter and are mostly grouped at high clearness indices where m has a dominant effect on k_t. For overcast skies, low τ_b cases, the k_t values are considerably lower with a large

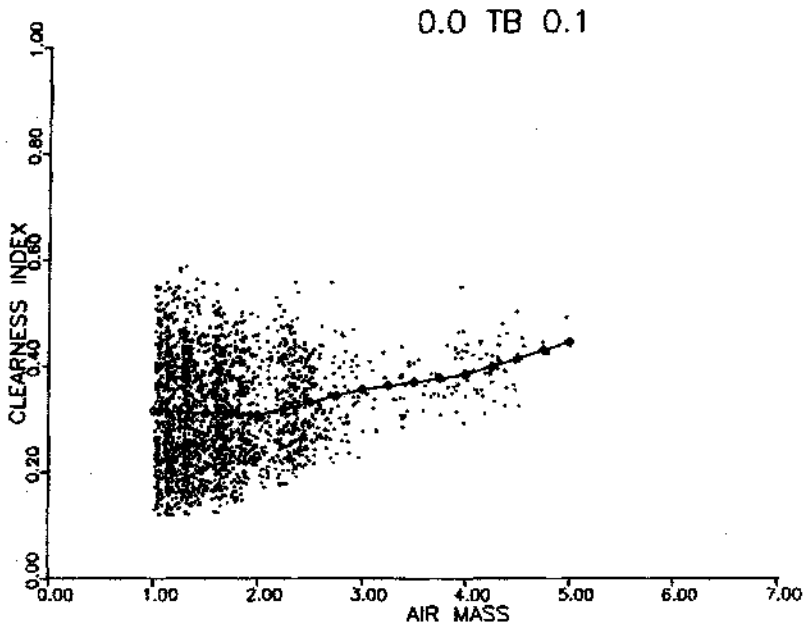

Figure 7.11 Scatter Plot of and Piecewise Regression on Shenandoah Data for a Clearness Index Range of 0.0 to 0.1

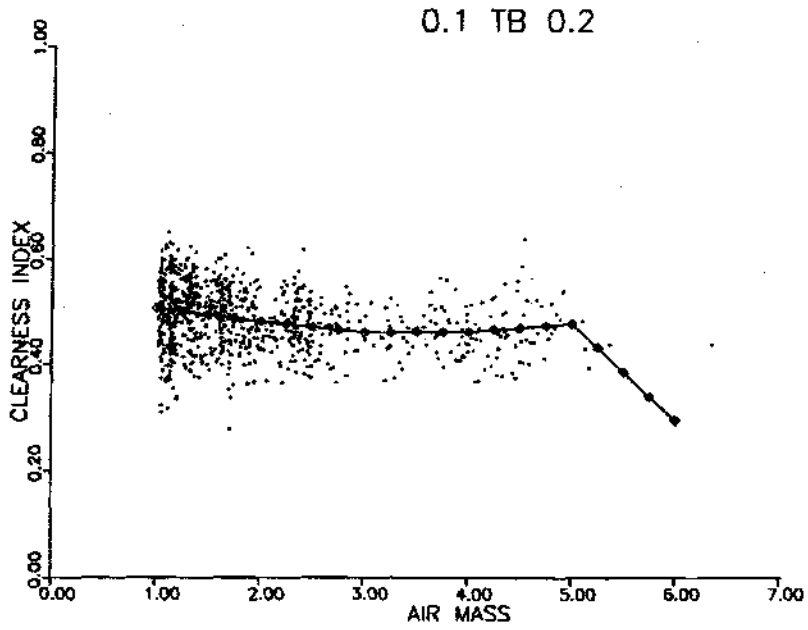

Figure 7.12 Scatter Plot of and Piecewise Regression on Shenandoah Data for a Clearness Index Range of 0.1 to 0.2

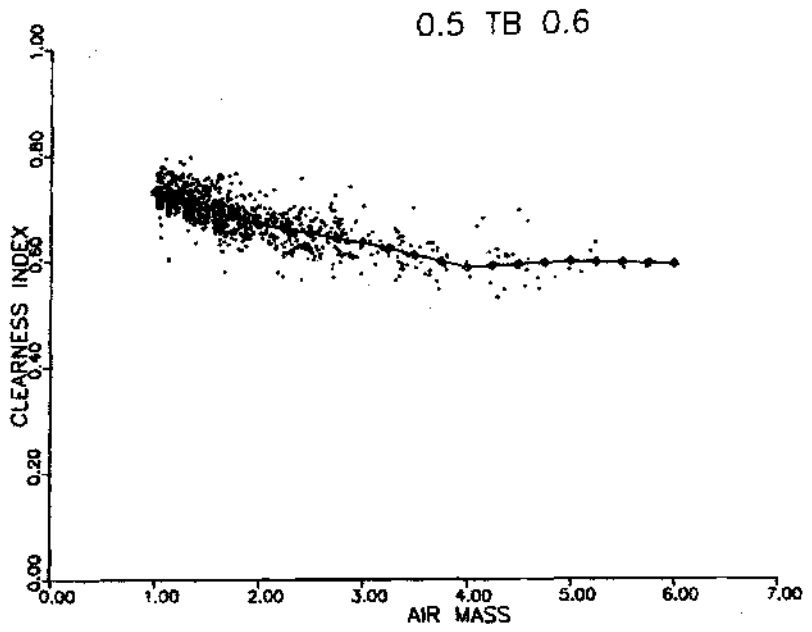

Figure 7.13 Scatter Plot of and Piecewise Regression on Shenandoah Data for a Clearness Index Range of 0.5 to 0.6

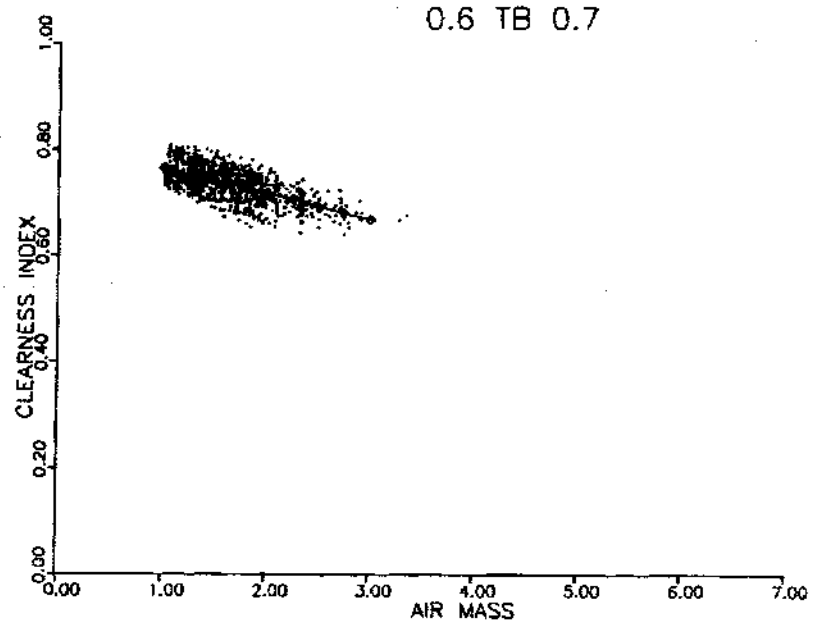

Figure 7.14 Scatter Plot of and Piecewise Regression on Shenandoah Data for a Clearness Index Range of 0.6 to 0.7

scatter. The effect of air-mass is limited under these conditions.

7.2.2 Model Validation

Maxwell (1987) also developed a correlation for the prediction of beam radiation. He investigated the relationship of beam transmittance and air-mass by studying instead the effects of m on $\Delta\tau_b$ for different ranges of clearness index. The latter variable, $\Delta\tau_b$, was defined as follows,

$$\Delta\tau_b = \tau_{bc} - \tau_b \qquad (7.8)$$

where τ_{bc} = limiting clear sky beam transmittance,

τ_b = measured beam transmittance values.

A least-squares regression analysis was used to fit each group of data (for different ranges of k_t) to the exponential form,

$$\Delta\tau_b = a + b * \exp(c * m) \qquad (7.9)$$

The resulting set of functions relating air-mass and $\Delta\tau_b$ are listed in Table 7.4. Maxwell finally proposed polynomial functions to calculate coefficients for Equation 7.9, and are determined using equations for two k_t ranges.

For $k_t < 0.6$

$$a = 0.512 - 1.56\ k_t + 2.286\ k_t^2 - 2.222\ k_t^3$$

$$b = 0.370 + 0.962\ k_t$$

$$c = -0.28 + 0.932\ k_t - 2.048\ k_t^2$$

Table 7.4

Functions Relating $\Delta\tau_b$ and Air-Mass, Maxwell (1987)

Clearness Index	Functions
0.25	0.230 + 0.6108 * EXP(-0.1817*m)
0.30	0.190 + 0.6558 * EXP(-0.1813*m)
0.35	0.150 + 0.7026 * EXP(-0.1987*m)
0.40	0.110 + 0.7641 * EXP(-0.2313*m)
0.45	0.070 + 0.7971 * EXP(-0.2739*m)
0.50	0.030 + 0.8590 * EXP(-0.3380*m)
0.55	-0.030 + 0.9013 * EXP(-0.3930*m)
0.60	-0.080 + 0.9411 * EXP(-0.4500*m)
0.65	-0.030 + 1.1815 * EXP(-0.8890*m)
0.70	-0.010 + 1.5504 * EXP(-1.4399*m)
0.75	-0.001 + 3.2996 * EXP(-2.6362*m)
0.80	-0.001 + 5.1625 * EXP(-3.9549*m)
0.85	-0.001 + 8.0000 * EXP(-5.5000*m)

For $k_t>0.6$

$$a=-5.743+21.77\ k_t-27.49\ k_t^2+11.56\ k_t^3$$

$$b=41.40-118.5\ k_t+66.05\ k_t^2+31.9\ k_t^3$$

$$c=-47.01+184.2\ k_t-222.0\ k_t^2+73.81\ k_t^3.$$

Equation 7.9 is the backbone of the so-called Direct Insolation Simulation Code (DISC). Maxwell validated his model using data from three stations - Brownsville, Texas, Albuquerque, New Mexico, and Bismarck, North Dakota - repre-

senting significantly different climate conditions.

The correlation developed by Maxwell was also expressed in terms of beam transmittance through Equation 7.8 using Equation 7.3 for τ_{bc}. The DISC model, expressed in terms of $\tau_{b'}$ was then compared to our correlation through algorithm CURVE2. Representative results are illustrated in Figures 7.15 to 7.16, for different clearness index ranges.

The two models are in very close agreement. Most importantly one should observe the similar trend both models exhibit. Clearly, we may conclude that there is no dominating effect of air mass on beam transmittance. The most it can be said is that under clear skies the relationship of beam radiation and air-mass exhibits a decrease of τ_b with increasing m. For partly cloudy and overcast skies there is no discrete variation of the τ_b with m.

Accordingly, Maxwell's claim that air-mass is the dominant parameter affecting the relationship between τ_b and k_t cannot be supported. The conclusions reached herein are valid for the considered range of air-mass, applicable to studies of beam radiation. Figure 7.17 illustrates the variation of k_t with m for the five year data. Observe though that data for high air-mass values at low clearness indices are not present. These data were excluded during the initial stages of data quality control processes.

The observed behavior of beam transmittance and air-mass might not necessarily be the same that one could obtain with

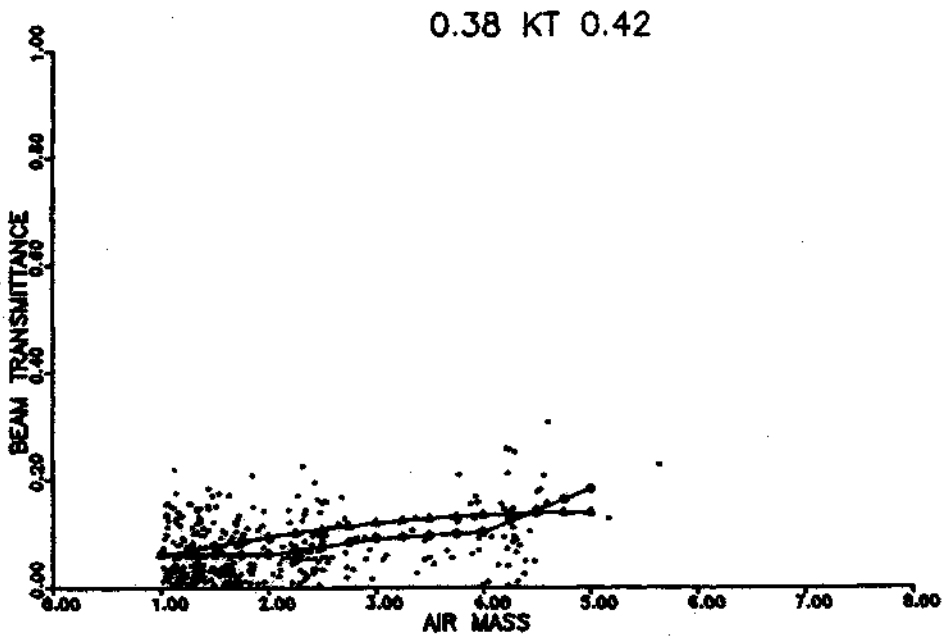

Figure 7.15 Variation of Beam Transmittance with Air-mass for a Clearness Index Range of 0.38 to 0.42 from Shenandoah. Rubi Indicate the Shenandoah (τ_b-m) model. Triangles Indicate the Maxwell Model

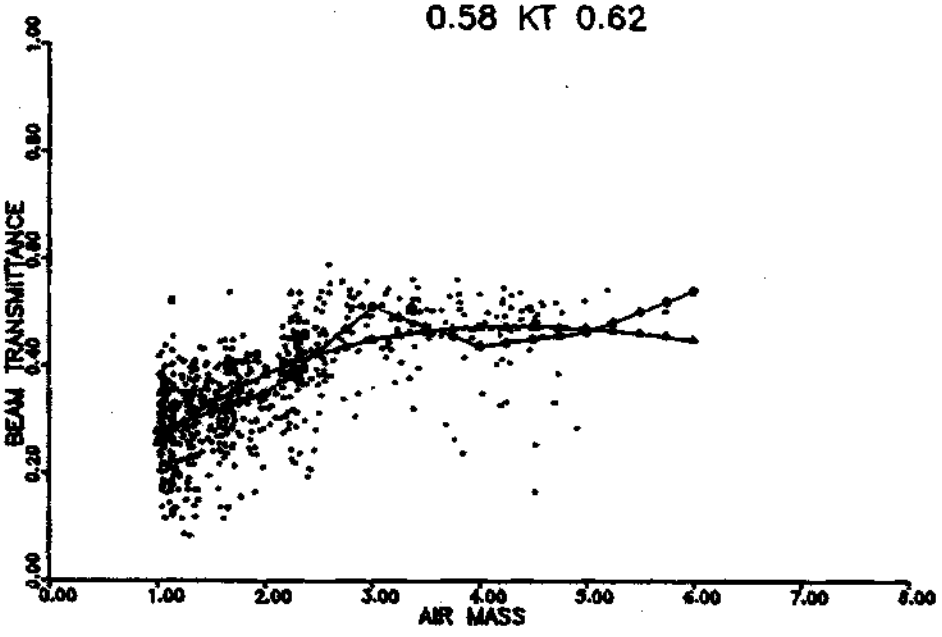

Figure 7.16 Variation of Beam Transmittance with Air-mass for a Clearness Index Range of 0.58 to 0.62 from Shenandoah. Rubi Indicate the Shenandoah (τ_b-m) model. Triangles Indicate the Maxwell Model

a larger range of m values. For our purposes, data at such low clearness indices are of little importance, and in general, of questionable quality. Thus, an independent variable is often kept within a small range to keep the dependent variable within acceptable limits. In the case of air-mass the "operability" region is the interval of $1<m<6$.

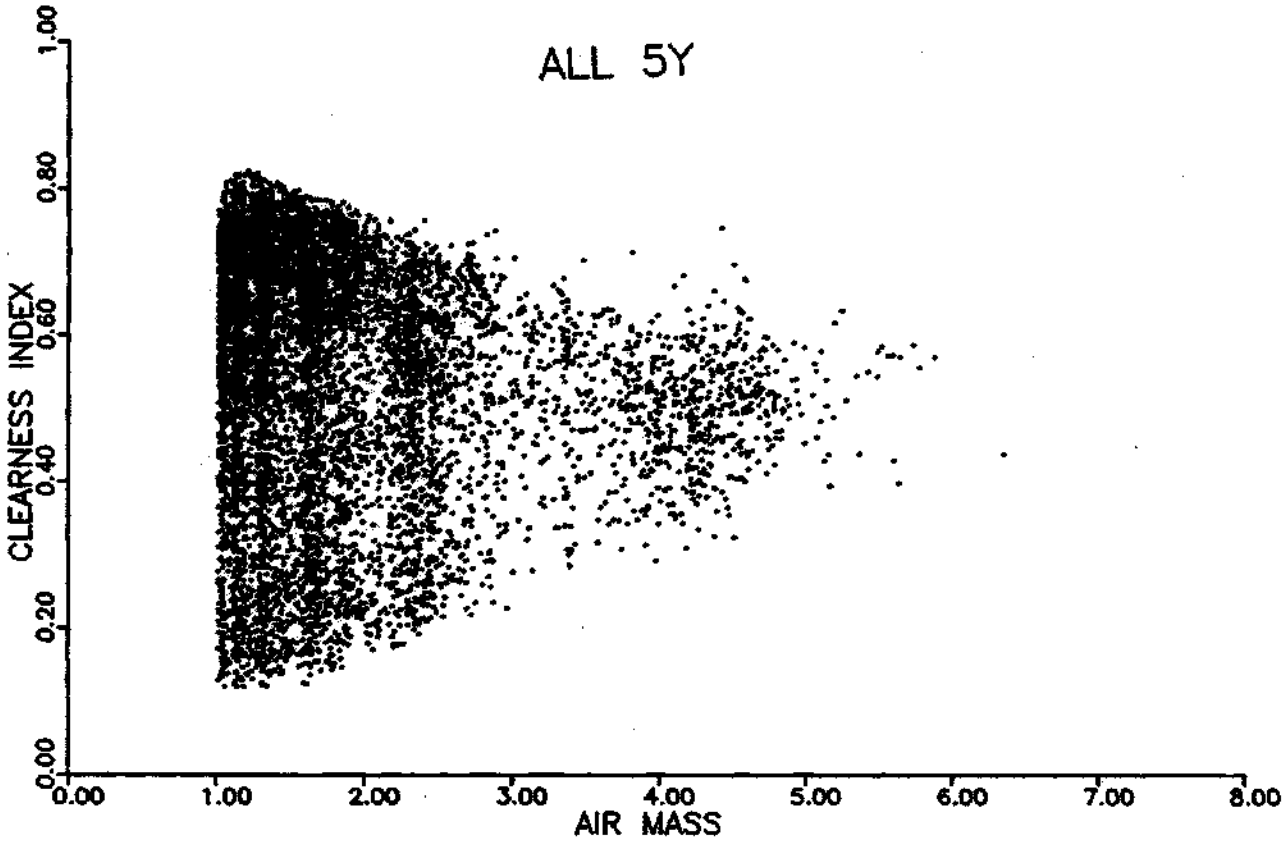

Figure 7.17 Variation of Clearness Index with Air-mass from the Shenandoah Five Year Data Base

The small operability region may cause the corresponding regression coefficients to be found "non-significant". Such a conclusion may, on a physical basis, be questionable, because it is "known" that air-mass is an effective variable. Both view points are of course, compatible. If an effective

independent variable is not varied much, it will show little or no effect.

Let there be no doubt to the reader that for our purposes high air-mass has no practical significance, due to high attenuation and the position of the sun. Hence, exclusion of such data was justifiable. For some applications, one may wish to explore the whole region of possible air-mass values, but this is of little interest for beam radiation studies. Instead, as done here, one would like to explore only a limited range of interest and would then arrive at similar conclusions.

Due to the large scatter of the data, a statistical analysis will not provide any additional information on the performance of the model. In addition, the (τ_b-m) linear regression model was not proposed here as a tool for the prediction of the beam radiation. Rather, it may be used as an indicator of the relationship between the beam transmittance and air-mass, which proved to be non-significant under most sky conditions.

CHAPTER VIII

IMPROVED BEAM RADIATION MODELS

Two improved models for the beam radiation are presented in this chapter. First, there is a correlation between the beam transmittance, clearness index, and air-mass. Second, there is a correlation between beam transmittance, clearness index, and a variable η, which accounts for the sky condition without the need of any meteorological observations.

The three variable correlations have significantly increased the predictive powers of the beam radiation model without compensating for additional input information. The correlations can predict different values of τ_b for a given day and, over the year, for the same value of k_t which is what is observed. As a general note, the surface fitting techniques used in the development of the three-dimensional model are applicable to similar response surface studies.

8.1 Surface Fitting Techniques

The basic and seasonal Shenandoah five-year models, described in previous chapters were of the form $\tau_b=f(k_t)$. Besides the single independent variable that is included in the model, it does not take into account any other variables.

The value of this equation lies in the fact that it shows how knowledge of a variable which can be reliably measured (as in the case of global radiation), may be used as an indication of a more important but less readily available quantity of the beam transmittance (or beam radiation).

It is, however, by no means an exact relationship. In reality, there is no one-to-one relationship of the beam transmittance to the clearness index. The reader should recall that a single regression function cannot be used to reproduce the observed variation of the data (Figure 4.2). The residual scatter of data about the regression line defined by the relationship of the two variables remains significant. For some practical applications, knowledge of global radiation alone could be a sufficient guide to the relative magnitude of beam radiation. It is possible however, that other easily obtainable information, in addition to knowledge of clearness index, might enable us to predict the beam transmittance with better accuracy.

In fact, we will attempt to relate the beam transmittance to more than one property that directly effects the intensity of the beam radiation. Such candidates include airmass, cloud cover, atmospheric composition, etc. A study of this nature would expose the effects of changes of the above variables on the beam radiation.

This work is exclusively based on available solar radiation measurements. Consequently, one is limited on the

choice of a third variable. Introducing the atmospheric air-mass in a (τ_b-k_t) correlation is appealing, since the calculation of m does not require any additional information. We recall from Chapter 4 that air-mass values can be accurately computed from knowledge of solar altitude alone.

Using the Shenandoah five year data of (k_t, m, τ_b), the following procedures can be used to establish empirically (by fitting some form of a mathematical model), the type of relationship that is present between the response variable, τ_b, and its influencing factors, k_t and m. The response variable, namely the beam transmittance, is the quantity whose value is assumed to be affected by changing the levels of the factors. The factors are the input variables, namely the clearness index and air-mass, whose values are readily available. Presumably, if one changes the values of the factors, the value of the response varies as well.

When there are two independent variables, it is possible to construct a three-dimensional scatter model by fitting a surface through the available data. Another possibility is to plot τ_b separately against each of the independent variables, as was done in Chapter 4 for (τ_b vs k_t) and in Chapter 7 for (τ_b vs m). This is a potentially misleading practice though, since we are interested in the partial relationship between the dependent variable and each independent variable, statistically holding the other independent variable constant.

Still, the choice of air-mass as the third variable may seem to be a bad option in light of the conclusions reached in Chapter 7. The reader should recall that m was found to have a small impact on τ_b. Let us though refer back to Figure 7.1 where the variation of τ_b and m is illustrated for the whole five year period.

Figure 7.1 shows no signs of a close relationship between the beam transmittance and air-mass. At first sight, it does not seem that the additional variable (m) will be of much value for purposes of prediction. Figure 7.1 does not, however, tell the whole story.

If we are to use air-mass to assist in the prediction of beam transmittance, we must relate the observed variations in m to the as yet unexplained variations in τ_b, i.e. to the variations of τ_b about the regression of τ_b upon k_t, rather than the overall variation. If we do this, we also eliminate any variations in air-mass which can themselves be associated with variations in k_t. Independent analyses of (τ_b-k_t) and (τ_b-m) cannot guarantee to give us the true relationship between the three variables.

In general, plotting the dependent variable (X_3) separately against each independent variable displays the simple relationship between the corresponding X_1 and X_2 variables. If the independent variables are correlated with each other, as in the case of k_t and m, these simple relationships may be different from the partial relationships.

The potential discrepancy between simple and partial relationships can be avoided by performing a three variable study that accounts for the significance of both independent variables (X_1, X_2) to predict the dependent variable (X_3). Accordingly, we may develop a model based on a surface fitting procedure for three variables. The procedure was first applied to the five year Shenandoah data base (clearness index, air-mass, and beam transmittance).

These techniques, though, can be applied for any surface fitting problem, with an objective to generate a response surface from scattered three dimensional data. This was illustrated by substitution of the air-mass by the sky condition variable, η, to be discussed later. Based on the (k_t,η,τ_b) data, we repeated the same procedures to develop a new three variable model. The principles used by the proposed algorithm and its application are described in the following sections.

8.1.1 Development of a Surface Fitting Algorithm

The method developed utilizes a discrete data set of three variables, (X_1, X_2, X_3), to fit through these data a continuous surface composed of quadrilateral planes. The method calls for an initial specification of some fairly large number of scattered data, lying in a bounded three dimensional space. Measured data usually has errors which have to be smoothed out. One way to reduce the noise inherent

in the raw data is to fit the approximating function by the method of the least squares.

To start, the three-dimensional data are broken down into X_1 and X_2 bands, of appropriate width each. This creates a number of working spaces shown in Figure 8.1. For every rectangular space that is created by the band partitioning of the (X_1, X_2) plane, the bounded data are identified and collected. These rectangular planes are called patches.

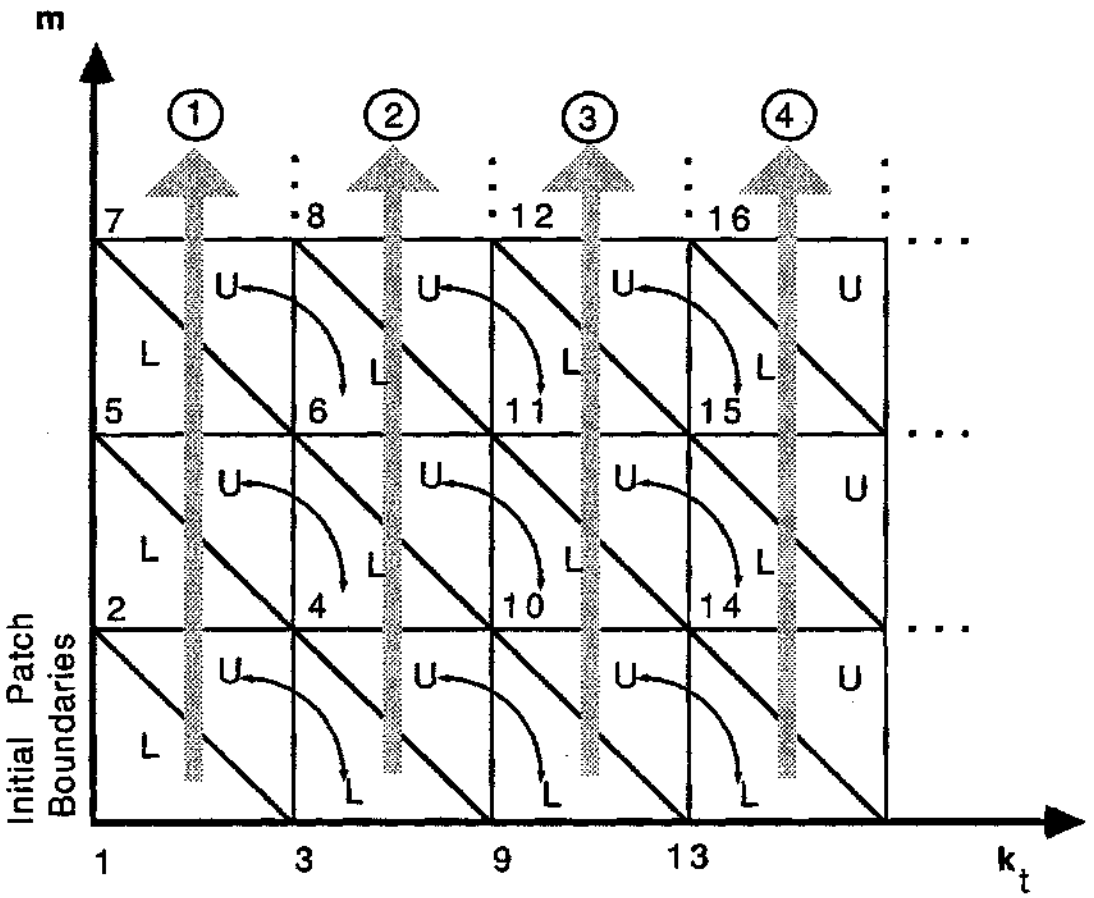

Figure 8.1 Band Wise Sweeping Process for Triangular Patch Generation on the (X_1-X_2) or (k_t-m) Plane

Each quadrilateral patch can be broken down to two triangular patches; an upper triangular patch (U-patch), and a lower triangular patch (L-patch). The numbered corner points marked in Figure 8.1 are called nodes, connecting the patch boundaries. These triangular patches may then be fitted to the appropriate data within the given patch boundaries in the least squares sense.

The resulting surface is composed of an assembly of patches. To ensure that adjacent patches are continuous across their contiguous boundaries, some boundary conditions have to be imposed. It becomes quit clear our method must not only fit surface patches to the corresponding data, but also blend fitted pre-defined patches together.

Every triangular patch has two known nodes (all three coordinates specified) and one unknown node (X_3 co-ordinate unspecified). The third node is fully defined by fitting a given triangular patch to the appropriate data in the least square sense. The existence though of lower and upper patches, suggests that for convenience a standard approach should be developed to perform the fitting procedures.

A solution to this problem is achieved by establishing a fixed co-ordinate system (x, y, z). This would require the development of a coordinate transformation procedure to relate for example the (k_t, m, τ_b) co-ordinates to an (x, y, z) co-ordinate system.

One such transformation is illustrated with the following example, based on our (k_t, m, τ_b) data. Consider three nodes: (k_{t1}, m_1, τ_{b1}), (k_{t2}, m_2, τ_{b2}), and (k_{t3}, m_3, τ_{b3}). The axes are rotated through an angle θ about the origin located at point 1, as shown in the two-dimensional representation in Figure 8.2.

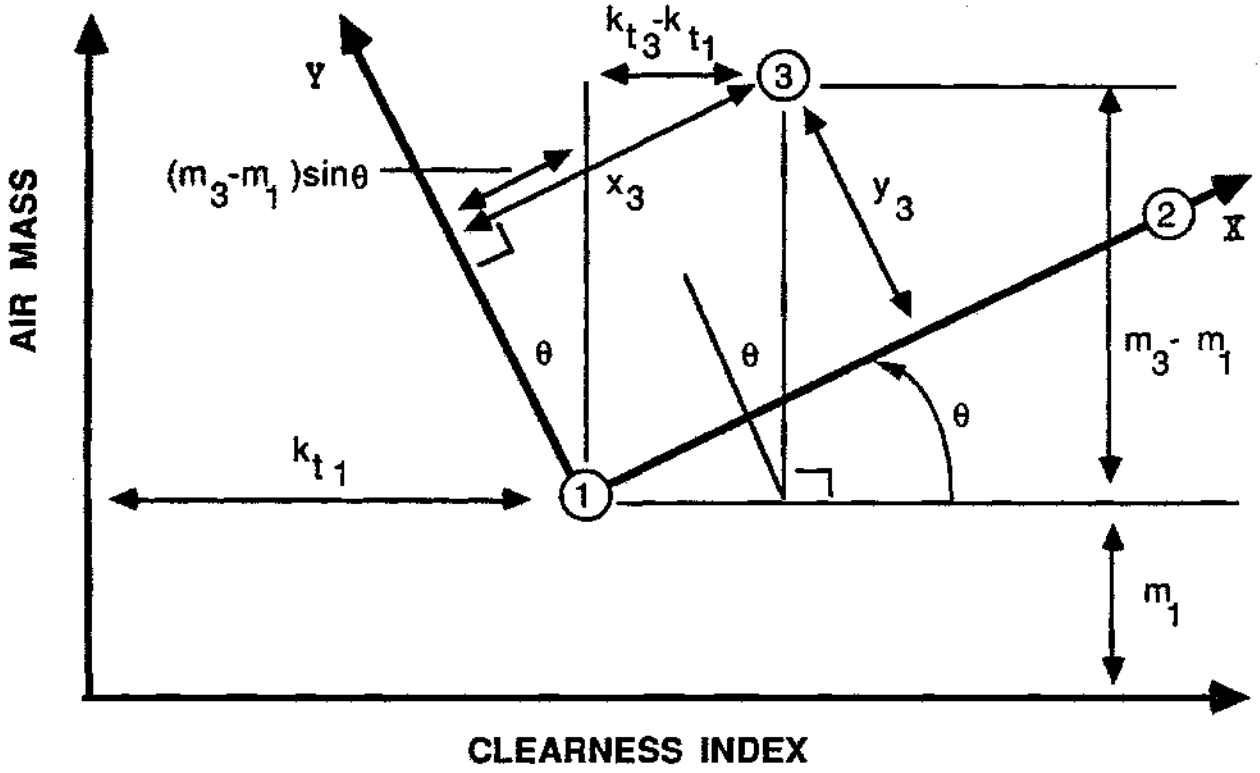

Figure 8.2 Mapping and Trigonometric Relations Between the Original (k_t, m, τ_b) Coordinate System and the Standard (x, y, z) Coordinate System

From basic trigonometry the following relations between the two co-ordinate systems were obtained,

$$y \cos\theta + x \sin\theta = m - m_1 = \delta m \qquad (8.1)$$

$$-y \sin\theta + x \cos\theta = k_t - k_{t1} = \delta k_t. \qquad (8.2)$$

Equations 8.1 and 8.2 can easily be expressed in a matrix form as

$$\begin{vmatrix} \sin\theta & \cos\theta \\ \cos\theta & -\sin\theta \end{vmatrix} \begin{vmatrix} x \\ y \end{vmatrix} = \begin{vmatrix} -\delta m \\ \delta k_t \end{vmatrix} \qquad (8.3)$$

and for the two equations system the solution becomes,

$$x = \frac{\begin{vmatrix} \delta m & \cos\theta \\ \delta k_t & -\sin\theta \end{vmatrix}}{D}, \quad y = \frac{\begin{vmatrix} -\sin\theta & -\delta m \\ -\cos\theta & -\delta k_t \end{vmatrix}}{D} \qquad (8.4)$$

where D is the determinant of the matrix in Equation 8.3 and is given by $D=-\sin^2\theta-\cos^2\theta=-1$. Equation 8.4 then becomes,

$$x = \delta m \sin\theta + \delta k_t \cos\theta \qquad (8.5)$$

$$y = \delta m \cos\theta - \delta k_t \sin\theta \qquad (8.6)$$

while for the z co-ordinate the relationship is simply,

$$z = \tau_b - \tau_{b1}. \qquad (8.7)$$

Thus, for a given triangular patch all the data and known nodes with coordinates (k_t, m, τ_b) can be mapped to the standard x-y-z co-ordinate system through Equations 8.5 to 8.7. The known vertices of the triangular patch are located at (0, 0, 0) and (x_2, 0, z_2) while the third node is located at (x_3, y_3, z_3), as shown in Figure 8.2.

The objective is to determine z_3 through a least square minimization. The fitting of a triangular plane can always be done on the standard (x,y,z) coordinate system and then transformed to any given coordinate system. The equation of a plane passing through these three points can be expressed as,

$$\begin{vmatrix} x & y & z & 1 \\ 0 & 0 & 0 & 1 \\ x_2 & 0 & z_2 & 1 \\ x_3 & y_3 & z_3 & 1 \end{vmatrix} = \begin{vmatrix} x & y & z \\ x_2 & 0 & z_2 \\ x_3 & y_3 & z_3 \end{vmatrix} = 0 \qquad (8.8)$$

Equation 8.8 can be reduced to,

$$z = \frac{(y_3 z_2)x + (x_2 z_3 - z_2 x_3)y}{x_2 y_3} \qquad (8.9)$$

The residual for a point is defined as the distance of a data point from (x_1, y_1, z_1), (x_2, y_2, z_2), (x_3, y_3, z_3) plane, and can be expressed as,

$$\varepsilon_i = d_i - z \quad \text{or} \quad \Sigma\varepsilon_i^2 = \Sigma(d_i - z)^2 \qquad (8.10)$$

where d_i = distance of (x_i, y_i, d_i) data from plane,

z = elevation of data on the plane according to Equation 8.9.

The least square minimization then requires that,

$$\frac{d\varepsilon_i^2}{dz_3} = 0 \qquad (8.11)$$

which results in an expression for z_3,

$$z_3 = \frac{\Sigma\, d_i y_i - \Sigma \dfrac{x_i z_2 y_i}{x_2} + \Sigma \dfrac{z_2 x_3 y_i^2}{x_2 y_3}}{\Sigma \dfrac{y_i^2}{y_3}} \qquad (8.12)$$

where x_i, y_i, d_i = data co-ordinates,

x_2, z_2 = co-ordinates of second node (y_2=0), and

x_3, y_3 = known co-ordinates of third node.

The next step would be to map the z_3 coordinate in the reverse direction, from the standard system onto the original coordinate system, according to Equation 8.7.

The three nodes (k_{t1}, m_1, τ_{b1}), (k_{t2}, m_2, τ_{b2}), and (k_{t3}, m_3, τ_{b3}) now completely define a triangular plane of the form,

$$\begin{vmatrix} k_t-k_{t1} & m-m_1 & \tau_b-\tau_{b1} \\ k_{t2}-k_{t1} & m_2-m_1 & \tau_{b2}-\tau_{b1} \\ k_{t3}-k_{t1} & m_3-m_1 & \tau_{b3}-\tau_{b1} \end{vmatrix} = 0 \qquad (8.13)$$

where k_t, m, τ_b = data co-ordinates bounded into the specified triangular plane between nodes 1,2, and 3.

Once an L-patch has been fixed, the common boundary nodes with the U-patch are used to repeat the process for the third unspecified node of the U-patch. The result is a fully specified rectangular patch. Blending is achieved through

successive patch generation. The newly generated patch must satisfy the boundary conditions of its previously defined neighbor. Once the first patch is generated, the next patch on the same k_t band may be generated, and so on. The same procedure is repeated for the following k_t bands.

8.1.2 Alternative Surface Fitting Methods

For completeness, one needs some other fitting techniques to which our method may be compared (a task undertaken in a later section). There are several software libraries that provide algorithms for surface fitting to three dimensional data. For example, the general purpose mathematical library, International Mathematical and Statistical Libraries, IMSL (1977), includes useful facilities for surface fitting.

The IMSL library provides a user-callable subroutine, IQHSCV, that performs smooth surface fitting to irregularly distributed data points. IQHSCV calculates an interpolating function which is a fifth-degree polynomial in each triangle of a triangulation of the (X_1, X_2) projection of the surface. The interpolation function is continuous and has continuous first-order partial derivatives. The reader may refer to IMSL (1977) and Akima (1978) for more details. The author found the implementation of IQHSCV quite difficult due to the large memory requirements of 31N (N total number of data).

An alternative surface fitting may be successfully performed with the use of DISSPLA (1981). The user must provide a double-dimensioned array containing the elevations (z values) that describe the surface to be fitted. Available routines may be used to generate an evenly spaced grid from irregular sets of x, y, z data.

The algorithm to prepare a regular matrix of z values is a mathematical weighting technique based on the distance from a grid node to the irregular spaced data points in its selected "search area". This technique is an inversely weighted fit which is simply stated by:

$$z_{jk} = \frac{\sum_{1}^{n} \frac{1}{D_i^w} z_i}{\sum_{1}^{n} \frac{1}{D_i^w}} \qquad (8.14)$$

where z_{jk} = value to be computed for node jk of the grid,

D_i = distance from the node jk to the irregular point z_i,

w = weighting factor, and

n = number of irregular points which fall in the "search area" for the irregular point z_i.

The selected "search area" is shown in Figure 8.3. The method first finds which cell the irregular point P_i lies in. It then looks two cells to the left (counting the cell it is

currently in, as one), two cells to the right, two cells below, and two cells above, for any irregular points (P_n) to consider in the weighting equation. This forms a nine cell search area bounded by ABCD. Caution has to be exercised when dealing with sparse data. DISSPLA provides algorithms that can handle such problems (surface smoothing).

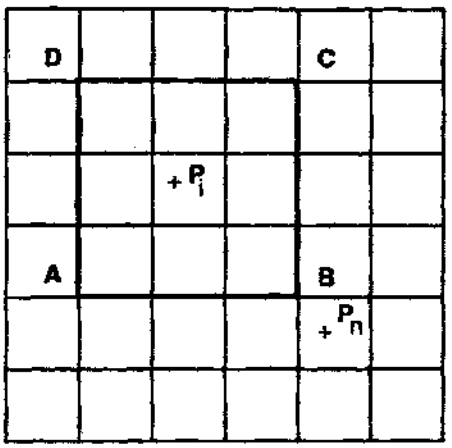

Figure 8.3 Search Area for an Irregular Point P_i, Used by DISSPLA (1981) for its Weighting Technique to Generate an Evenly Spaced Grid

Most of the traditional triangulation techniques do not easily lend themselves to applications in which high surface accuracy is not the main objective. For example, methods used for such applications as in the case of Computer Aided Geometric Design (CAGD), picture production, and geological applications, offer a high degree of intricacy but are of no interest to our study.

For reference though, let us list some of these methods. The principles of surface fitting presented by Lancaster and Salkauskas (1986) offers an excellent introductory overview on the subject. Farin (1986) developed an algorithm that uses triangular Bernstein-Bezier surfaces applicable for CAGD applications. Sloan (1987) has proposed an algorithm for conducting Delaunay triangulations in the plane, with improved run time.

Correc and Chapuis (1987) have also dealt with triangulation of scattered data in a Delaunay's sense suitable for digital terrain modelling. This method is primarily of interest to geologists and geographers for developing maps from geographical data bases. A survey of some surface fitting methods by Barnhill (1977) covers several modelling approaches to the detail design of bivariate surfaces.

8.2 A Correlation Between (k_t, m, τ_b)

In section 8.1.1 we introduced an approach for the development of a model with three-variables. However, the user must apply caution in using these methods, since in general linear models and least squares fitting are subject to a variety of difficulties. Collinearity is a prime example of such problems.

For the extreme case that the regressors are perfectly linearly related, the least squares regression coefficient is not uniquely defined. Less-than-perfect collinearity causes

regression estimates to be unstable. The correlation between the independent variables k_t and m (Figure 7.17) is slight, as indicated by the broad scatter of the data. Therefore, the least squares regression plane that would be fitted through a given data set, has a firm base support.

Collinearity was not a problem for the Shenandoah data. One should always, though, investigate the possibility of highly collinear regressors. In the event that collinearity is present, different strategies can be used. Fox (1984) treats collinearity in depth and provides methods for overcoming these problems.

8.2.1 Model Development

The objective of the algorithm described in Section 8.1 was to form a model of a surface by developing a mathematical expression that results from a best fit to irregularly spaced data. The algorithm consists of a series of sequential steps.

First, the three-dimensional data (k_{ti}, m_i, τ_{bi}) has to be grouped into appropriate working spaces. Accordingly, the data were broken down into eighteen clearness index bands of 0.05 width each, and five air-mass bands of 1.0 width each. Each patch is a 1.0 by 0.05 projection on the (k_t, m) plane of a surface-element. Each rectangular patch was then divided into a lower and an upper triangular patch, with their corresponding data grouped for latter use. These steps have been coded in algorithm TRGD found in Appendix E.

The initial boundary conditions are two nodes at the first patch located at zero clearness index. These boundary conditions are justifiable since at such low k_t one may assume that there would be practically no beam radiation. Thus, the corresponding τ_b value is zero. The coordinates of the two nodes of the first patch are then completely known.

The recurrent process is to fit in the least squares sense a triangular patch to the corresponding data, once two of the nodes are known. The cycle progresses along a given k_t band for all m bands and then continue with the next k_t band. The process was illustrated in Figure 8.1.

Let the initial boundary conditions be nodes 1 and 2. Through our best fit process, node 3 can be specified. What we mean by "specified" is the calculation of the elevation at node 3, given its other two coordinates. For the U-patch, based on nodes 2 and 3, node 4 was defined next. The same process continuous and sweeps the first k_t band, every time using two fixed nodes and estimate the third one.

Moving to the second k_t band, first we observe from Figure 8.1 that all nodes along the left side boundary have already been fixed from the previous sweep, while the right side boundary nodes are unspecified. Repeating the same procedure along the second k_t band, first one can specify nodes 9 and 10, in that order. The next lower triangular patch has already its three nodes (4, 10, and 6) fixed by our previous calculations.

As we proceed, the same problem arises with all remaining lower triangular patches. This of course means that the data bounded within these patches were not directly accounted for, or in a sense "lost". Thus, the method discussed up to this point may use only a fraction of the available data.

Applied to the Shenandoah five year data the method produced the least square error fit surface shown in Figure 8.4. The surface nodes were generated through FIT3D2B and plotted through PLOT3DB, for air-mass band widths of unity and for the whole available air-mass range (m<7). A listing of both codes may be found in Appendix E.

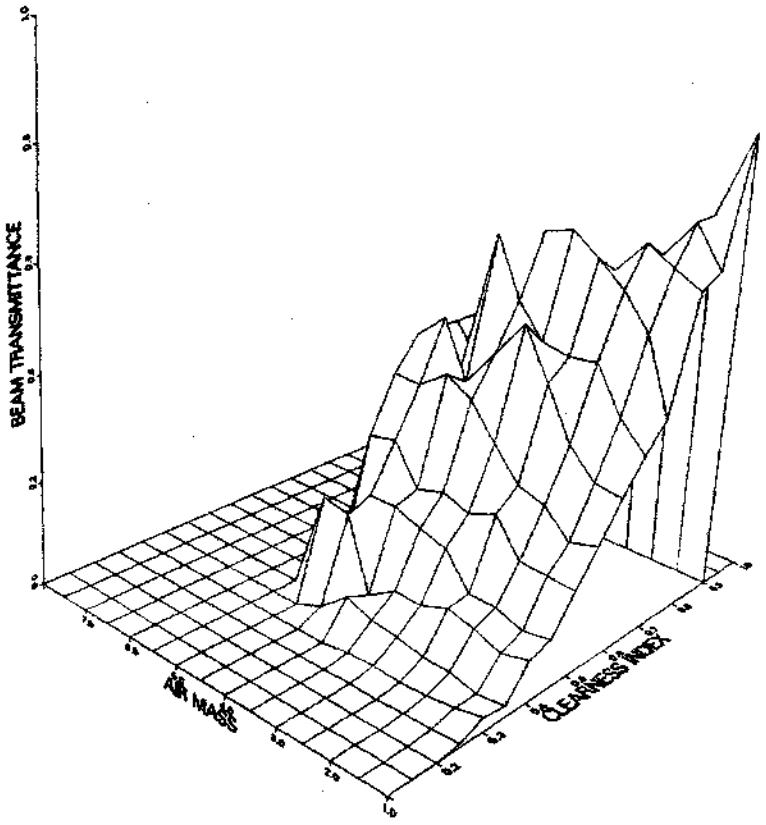

Figure 8.4 Locally Weighted Surface Using Part of the Shenandoah Five Year Data. Air-mass Band Width 0.05 and Clearness Index Band Width 0.05.

The next logical step was to alter the method developed thus far in such a way that all data are accounted for. Figure 8.1 may be used again here to help us visualize the new procedure. The upper triangular patches adjacent to fixed lower ones should attract our attention.

For example, consider the <4,5,6> U-patch. At this point nodes 4 and 5 are known. Previously node 6 was to be calculated based only on the data enclosed by <4,5,6>. This time, the data from the lower triangular patch <4,6,10>, of the adjacent k_t band, are also going to be incorporated in the calculations, weighted though as one half.

A similar least square minimization had to be performed to the grouped data, as it was done in section 8.1.1. The corresponding sum of squares of the residuals is now composed of two components. The first originates from the data enclosed in the upper triangular patch and is denoted by $\Sigma\varepsilon_U^2$. The second component originates from the appropriate data of the adjacent L-patch and is denoted by $\Sigma\varepsilon_L^2$.

A minimization was then performed on the sum of the sums, weighting each term accordingly, $\Sigma\varepsilon_U^2+1/2\Sigma\varepsilon_L^2$. Again we require that,

$$\frac{d\varepsilon_U^2}{dz_3} = 0 \quad \text{and} \quad \frac{d\varepsilon_L^2}{dz_3} = 0 \qquad (8.15)$$

which results to a new expression for z_3,

$$z_3 = \frac{1}{\Sigma\frac{y_{Ui}}{y_3} + \frac{1}{2}\Sigma\frac{y_{Li}}{y_3}} \left\{\Sigma(d_{Ui}\, y_{Ui}) + \frac{1}{2}\Sigma(d_{Li}\, y_{Li})\right.$$

$$- \Sigma\frac{z_2\, x_{Ui}\, y_{Ui}}{x_2} - \frac{1}{2}\Sigma\frac{z_2\, x_{Li}\, y_{Li}}{x_2}$$

$$\left. + \Sigma\frac{z_2\, x_3\, y_{Ui}^2}{x_2\, y_3} + \frac{1}{2}\Sigma\frac{z_2\, x_3\, y_{Li}^2}{x_2\, y_3}\right\} \qquad (8.16)$$

where (x_{Ui}, y_{Ui}, d_{Ui}) = data co-ordinates from U-patch, and

(x_{Li}, y_{Li}, d_{Li}) = data co-ordinates from L-patch.

The procedure is repeated for every U-patch of all m bands, except the first one, using the data from the L-patch of their adjacent k_t bands. The method is coded in FIT3DB, found in Appendix E.

Results of the least square error fit using all the Shenandoah five year data are shown in Table 8.1. A total of 102 nodes are required to fully describe the data. Data describing the surface includes the three dimensional co-ordinates of the nodes (clearness index, air-mass, and beam transmittance) followed by the number of data used in each patch (8077 in total). Some data had to be excluded from our initial data base simply because our surface fitting technique is sensitive to sparsely populated patches. This is for example the case at high air-mass bands (m>5).

TABLE 8.1

Coordinates of the Locally Weighted Least Square Error Fit Surface Using All the Shenandoah Five Year Data

Clearness Index	Air Mass	Beam Transmittance	No. Of Data
0.1	1.0	0.	0
0.1	2.0	0.	0
0.1	3.0	0.	0
0.1	4.0	0.	0
0.1	5.0	0.	0
0.15	1.0	0.0002	24
0.15	2.0	0.	0
0.15	3.0	0.	0
0.15	4.0	0.	0
0.15	5.0	0.	0
0.2	1.0	0.0008	122
0.2	2.0	0.	71
0.2	3.0	0.	4
0.2	4.0	0.	0
0.2	5.0	0.	0
0.25	1.0	0.0067	144
0.25	2.0	0.0031	121
0.25	3.0	0.	33
0.25	4.0	0.	0
0.25	5.0	0.	0
0.3	1.0	0.0228	133
0.3	2.0	0.0103	108
0.3	3.0	0.0172	36
0.3	4.0	0.0038	2
0.3	5.0	0.	0
0.35	1.0	0.0259	126
0.35	2.0	0.0293	97
0.35	3.0	0.0400	38
0.35	4.0	0.0604	13
0.35	5.0	0.	2
0.4	1.0	0.0632	140
0.4	2.0	0.0682	115
0.4	3.0	0.0937	37
0.4	4.0	0.0904	14
0.4	5.0	0.1982	8
0.45	1.0	0.1053	176
0.45	2.0	0.1152	129

Table 8.1 (...continue)

Clearness Index	Air Mass	Beam Transmittance	No. Of Data
0.45	3.0	0.1463	47
0.45	4.0	0.1975	25
0.45	5.0	0.0715	18
0.5	1.0	0.1483	170
0.5	2.0	0.1645	109
0.5	3.0	0.2457	57
0.5	4.0	0.2235	38
0.5	5.0	0.3504	36
0.55	1.0	0.2220	260
0.55	2.0	0.2562	139
0.55	3.0	0.3070	85
0.55	4.0	0.3826	37
0.55	5.0	0.3578	43
0.6	1.0	0.2715	284
0.6	2.0	0.3539	164
0.6	3.0	0.4885	66
0.6	4.0	0.4624	41
0.6	5.0	0.4753	31
0.65	1.0	0.3505	386
0.65	2.0	0.4724	299
0.65	3.0	0.5163	84
0.65	4.0	0.5417	21
0.65	5.0	0.0386	6
0.7	1.0	0.4266	469
0.7	2.0	0.6144	395
0.7	3.0	0.6253	92
0.7	4.0	0.5419	0
0.7	5.0	0.0399	0
0.75	1.0	0.6058	643
0.75	2.0	0.6661	356
0.75	3.0	0.4809	9
0.75	4.0	0.4063	2
0.75	5.0	0.0408	0
0.8	1.0	0.6845	359
0.8	2.0	0.7470	123
0.8	3.0	0.4816	0
0.8	4.0	0.4065	0
0.8	5.0	0.0417	0
0.85	1.0	0.7873	44
0.85	2.0	0.7471	0
0.85	3.0	0.4823	0
0.85	4.0	0.4067	0
0.85	5.0	0.0426	0

The resulted locally weighted surface is shown in Figure 8.5. Such a graphical representation of the data can be used to give immediate evaluation of the considered phenomenon. Easily, one may extract useful information about the relationship of the two variables under study with the response variable τ_b.

According to Figure 8.5, the air-mass dependency becomes dominant at high clearness indices while there is not much variation under mostly cloudy skies (low k_t values). The beam transmittance though exhibits the expected behavior; τ_b increases with increasing k_t values. The projection of the surface on the (τ_b-k_t) plane follows the trend of the relationship obtained by Balaras (1985) for the relationship between these two variables.

A technique used to help visualize the shape of the three-dimensional response surface is to plot contours of the response surface as it was done in Figure 8.6. In a contour plot, lines or curves of constant response values are drawn on a graph or plane whose coordinate axes represent the levels k_t and m of the two independent variables.

The lines (or curves) are known as contours of the surface. Each contour represents a specific value for the height of the surface above the plane defined for combinations of the levels of the factors. Geometrically, each contour in Figure 8.6 is a projection onto the (k_t-m) plane of a cross-section of the response surface made by a plane

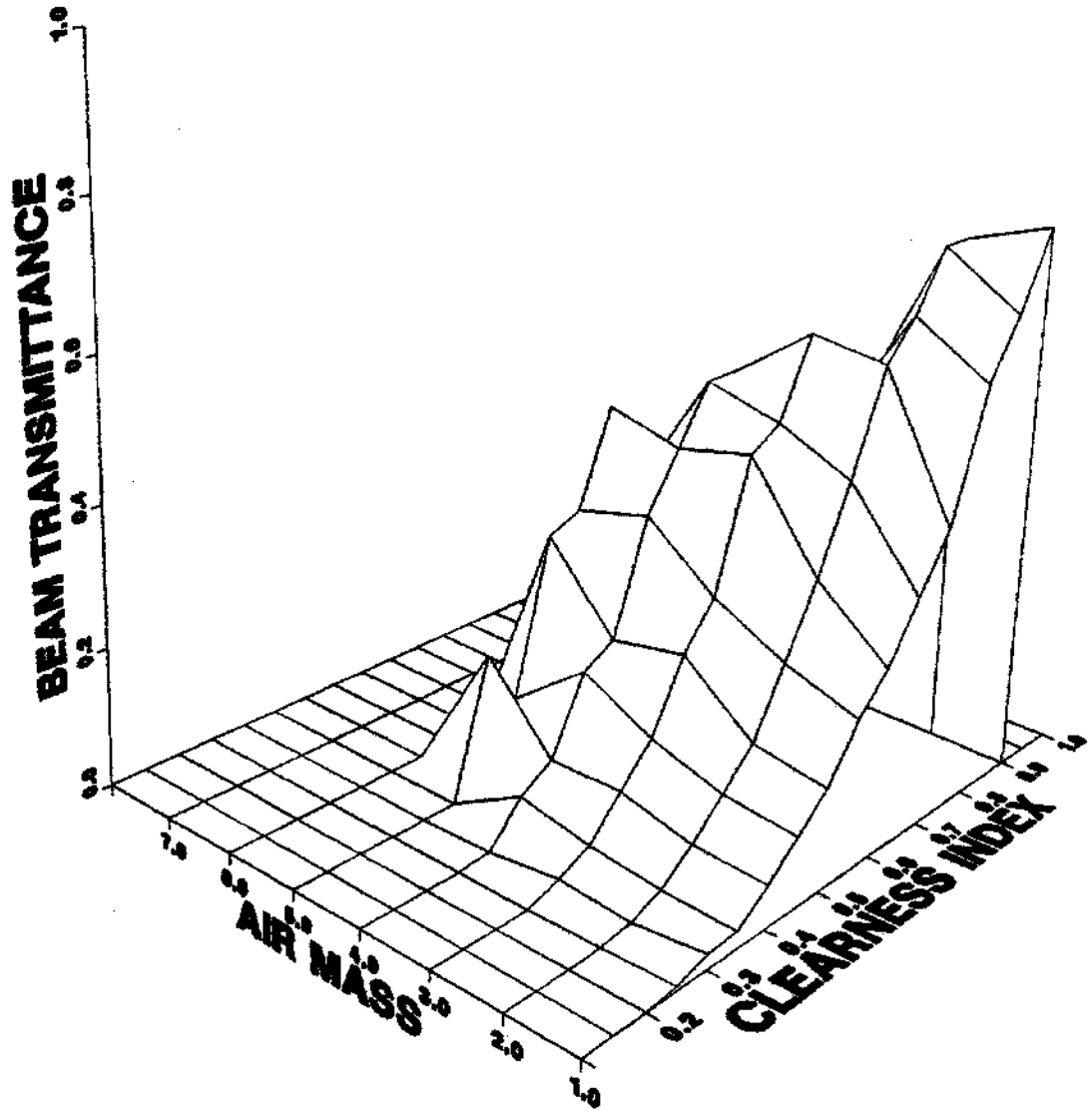

Figure 8.5 Locally Weighted Surface Using All the Shenandoah Five Year Data. Air-mass Band Width of 1, and Clearness Index Band Width of 0.05

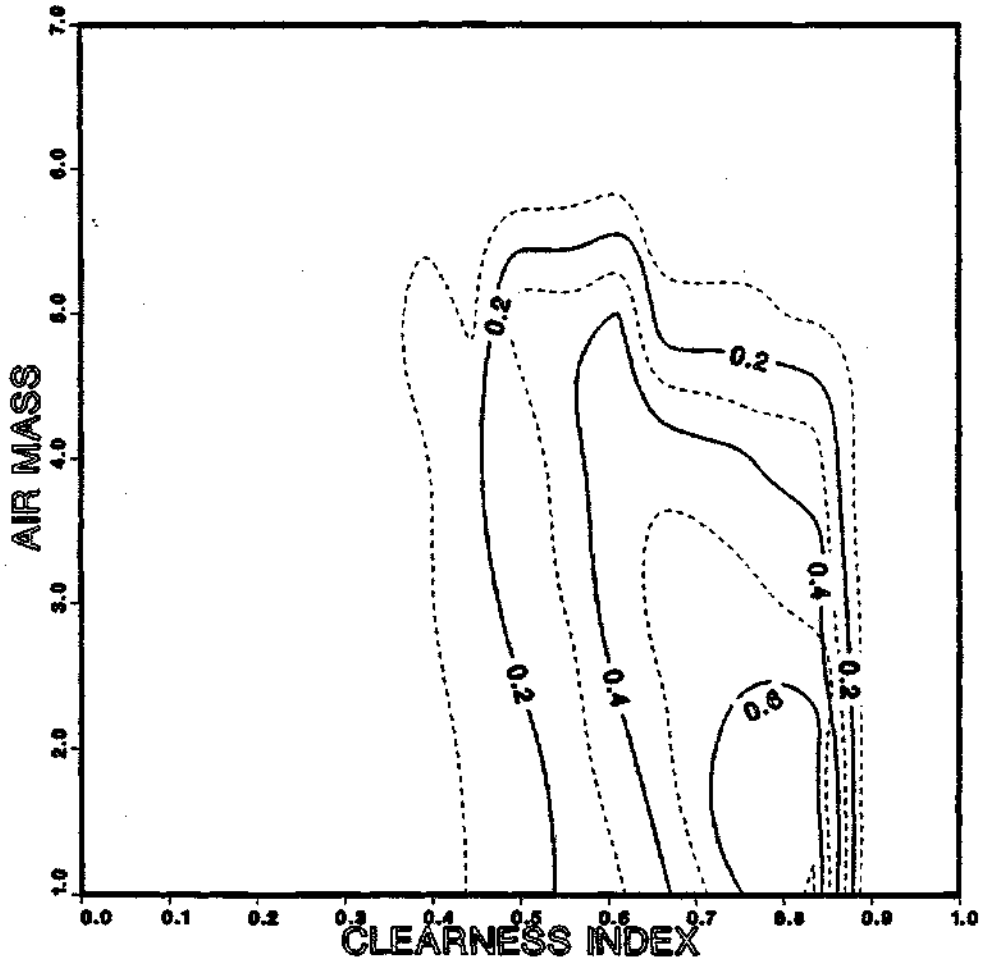

Figure 8.6 Response Contour Beam Transmittance for the Shenandoah Five-Year Data

parallel to the (k_t-m) plane, cutting through the surface. The plotting of different surface height values enables one to focus attention on the levels of the factors at which the changes occur in the surface shape.

The contour plot shown in Figure 8.6 was generated using DISSPLA's (1981) contouring option, as illustrated by the routine CONTOUR in Appendix E. The surface is described in a matrix form using the data from Table 8.1. The technique DISSPLA uses for generating contour lines, once a regular set of surface data are provided, is a linear interpolation of adjacent surface grid points in both the k_t and m directions.

One may observe from Figure 8.6 that there is very little variation of the beam transmittance with increasing air-mass values at low k_t values. Thus, both Figures 8.5 and 8.6 reveal that air-mass plays a dominant role in the attenuation of beam radiation only at high clearness indices.

The choice of the band widths for the clearness index and air-mass was arbitrary. Although, such a choice proved to be adequate and easy to implement (number of surface nodes was kept low), one should be aware that beyond practical limitations the band widths can be reduced to desired thickness. The developed algorithms FIT3DB, and PLOT3DB may be easily updated to undertake such a task.

For illustration purposes, we reconstructed the response surface with 30 k_t bands (0.025 thick each), and 20 m bands (0.2 thick each), Figure 8.7. One should note the disturb-

ances the surface exhibits due to the scarcity of the data at certain regions. A total of 858 nodes are now required to fully describe the surface between the intervals of $1<m<6$ and $0.1<k_t<0.9$ (the remaining nodes are on the k_t-m plane)..

Due to its high complexity, such a model may have low applicability. At the same time, though, one needs to examine its predictive powers. Better model performance might outweigh the disadvantages of increased complexity. These areas are investigated and discussed in the upcoming section of statistical analysis.

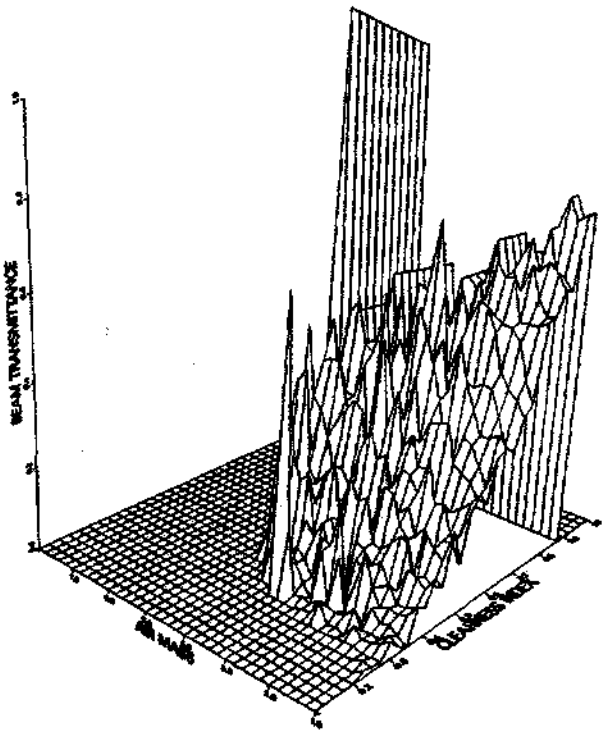

Figure 8.7 Locally Weighted Surface Using All the Shenandoah Five Year Data. Air-mass Band Width of 0.2, and Clearness Band Width of 0.025

At this point, let us also review the results of the response surfaces produced by the alternative surface fit methods discussed in section 8.1.2. The reader should recall that we were to consider two additional approaches using the surface fitting capabilities of IMSL and DISSPLA.

IMSL (1977) generated the response surface illustrated in Figure 8.8. One should use this method with sufficiently large working spaces to avoid excessive noise on the surface. We chose to use air-mass bands of unity (for the range of 1<m<5) and clearness index bands of 0.05 each, with a total of 8077 data. IMSLFIT algorithm in Appendix E illustrates the use of the IMSL routines.

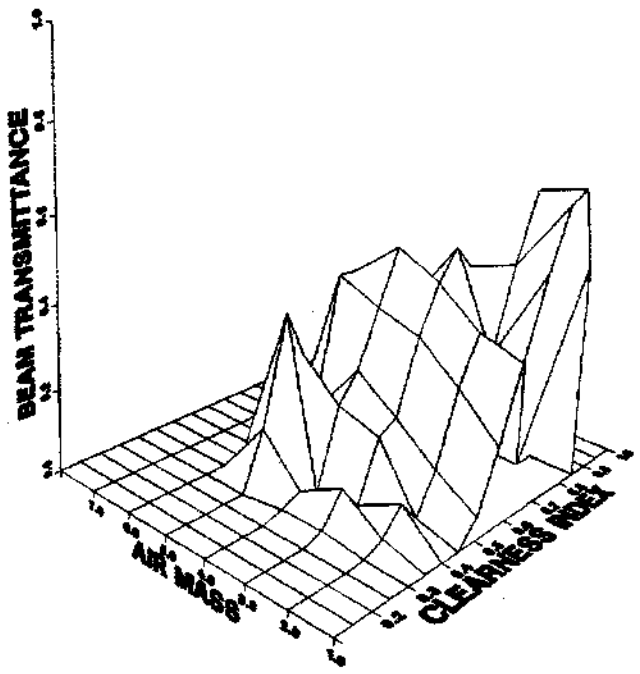

Figure 8.8 Surface Generated by IMSL (1977) Using All Shenandoah Five Year Data with (m) Less Than 5

DISSPLA (1981) generated both Figures 8.9 and 8.10. As before, the denser spaced surface of Figure 8.9 is only given here for illustrative purposes. The response surface shown in Figure 8.10 is analogous to our results from Figure 8.5. A total of 8077 data were used by DISSPLA, between $1<m<5$ with air-mass band thickness of unity and clearness index bands of 0.05. DISPLAS in Appendix E illustrates the use of the DISSPLA routines.

8.2.2 Model Validation

The surface fitting procedures used in Section 8.2.1 may be easily tested with data that we have extracted from a known surface. For this purpose we considered two kinds of surfaces; a plane surface, and a quadric one. Once these data were generated and separated into triangular patches, through TESTFIT listed in Appendix E, we applied the surface fitting algorithms in the usual manner to produce the corresponding response surfaces.

The plane surface was designed to extend between points (0.1,7,0), (0.7,1,0), and (0.7,7,1). A total number of 5001 points were generated from the surface and consisted our testing data base. The resulting fitted surface is illustrated in Figure 8.11, which indicates a perfect fit to the data. As a point of information, the coefficient of determination reached the value of 100 percent for this case.

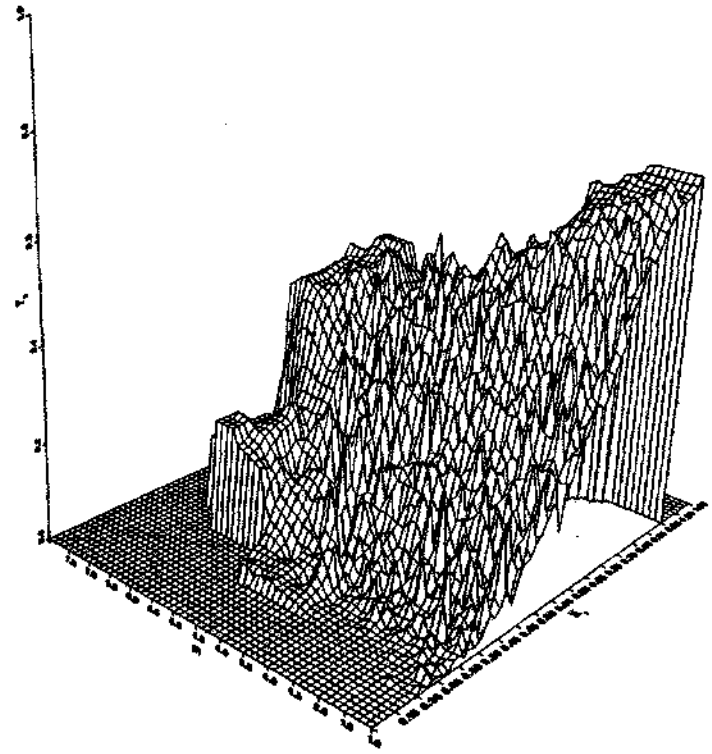

Figure 8.9 Surface Generated by DISSPLA (1981). Mesh Spacing (73,57) with Surface Smoothing on Shenandoah Data

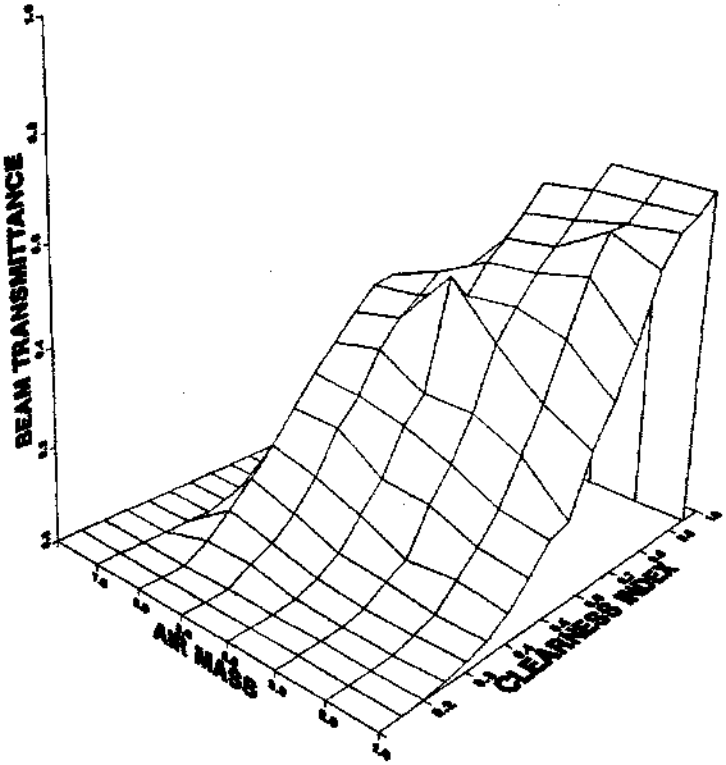

Figure 8.10 Surface Generated by DISSPLA (1981). Mesh Spacing (19,8) on Shenandoah Data.

In a similar manner, one may proceed using data from a quadric surface. We considered only the upper dome of the ellipsoid centered at (0.5,4,0). A total of 7001 surface points were used in our analysis. It is important to make sure that enough data are available so that the surface fitting procedures may result to a smooth surface.

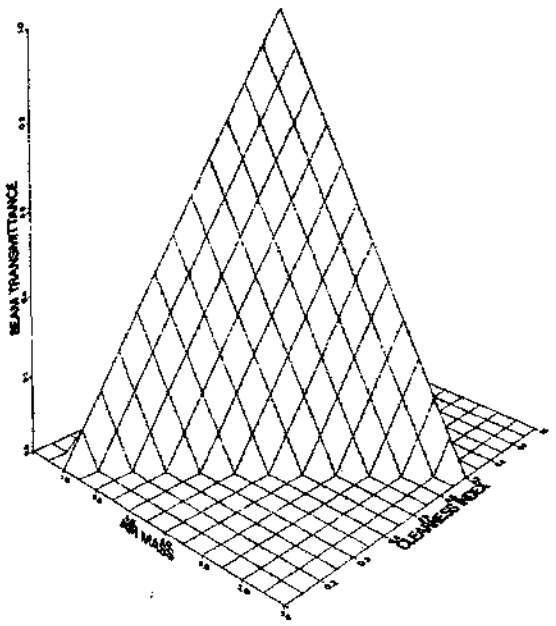

Figure 8.11 Surface Generated Using the Developed Surface Fitting Procedure on All Test Data from a Plane

The resulted response surface is shown in Figure 8.12. Our fitting method successfully handled the sharply changing slopes of the surface; either increasing or decreasing. Subsequently, our surface fitting techniques (in the cases of using all and part of the available data) were proven capable of recreating predefined surfaces, and may be used with

confidence in dealing with similar problems.

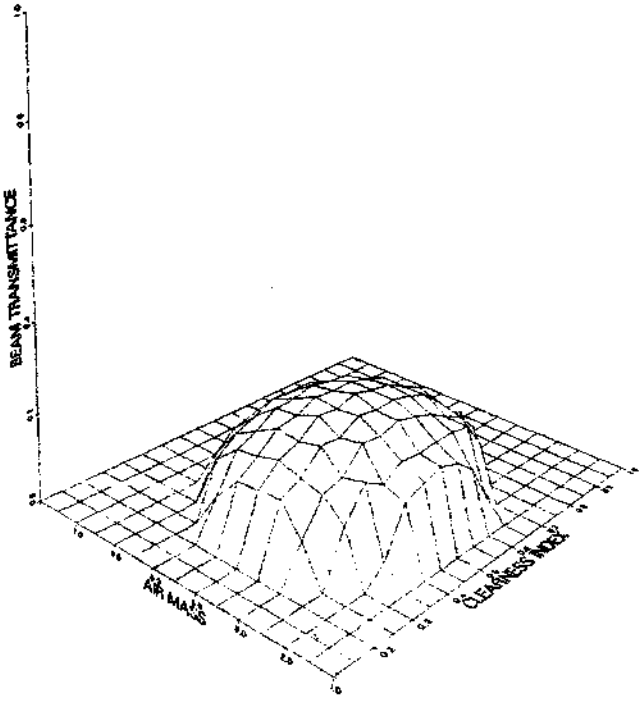

Figure 8.12 Surface Generated Using the Developed Surface Fitting Procedure on All Test Data from a Ellipsoid

8.2.3 Statistical Analysis

The incorporation of an additional variable in our correlation is expected to increase the models accuracy. One though is called upon to investigate the significance of such an improvement. Specifically, we would like to statistically examine the performance of both approaches for generating the response surfaces to the Shenandoah data, using part of or all available data, and their relative performance against the response surfaces from IMSL and DISSPLA.

The pertinent statistical results are summarized in Table 8.2, in accordance to the discussion in Chapter 5. According to Table 8.2 the coefficient of determination indicates that 98.24% of the variation of the beam transmittance is accounted for by the dependence on the clearness index and air-mass ratio when all the data were used. This is a considerable improvement over the single regression model by Balaras (1985), for which the corresponding value was 89%.

Table 8.2

Statistical Analysis for the (k_t-m-τ_b) Model Using All the Available Data, the (k_t-m-τ_b) Model Using Part of the Data, the Surface Generated by IMSL, and the Surface Generated by DISSPLA, Based on the Shenandoah Data Screened for Air-mass Values Less Than 5. Total Number of Data 8077

Statistical	(k_t-m-τ_b) Model Using δm=1 and δk_t=0.05			
Parameter	All Data	Part Data	IMSL	DISSPLA
Total Variation	417.64	417.64	417.64	417.64
Residual Sum of Squares	7.34	12.16	23.09	10.28
Explained Variation	410.30	405.48	394.55	407.36
Coef. of Determination	0.9824	0.9709	0.9447	0.9754

Our two approaches did not result to any substantial differences in performance for the developed response surface. The fit, according to the coefficient of determi-

nation values, was slightly better in the case when all the data were used. In fact, this is the procedure we are proposing for future work.

Let us now examine how our fitted surface performs compared to the alternative surface fitting methods reviewed in section 8.1.2. DISSPLA produced a response surface for the Shenandoah five year data, illustrated in Figure 8.9, with a coefficient of determination value equal to 95.54%. According to our calculations, IMSL exhibited the poorest performance with a value of r^2 equal to 92.25 percent.

We have previously presented several surfaces generated with different band thicknesses. Their complexity was not justified by a substantial increase in their predictive powers. For reference, consider that the model produced with an air-mass band thickness of $\delta m=0.5$ and clearness index band thickness of $\delta k_t=0.05$ resulted in an r^2 equal to 98.34%. For $\delta m=0.2$ and $\delta k_t=0.025$ a value of 98.72% was calculated for the coefficient of determination.

As one would expect, a more dense surface resulted in a slight improvement on the performance of the model as illustrated by the increase in the value of the coefficient of determination. The significance for such an improvement of the order of half of a percent on the value of r^2 for the case of $\delta m=0.2$ and $\delta k_t=0.025$ over the case of $\delta m=1$ and $\delta k_t=0.05$ is not justified considering the increased complexity of such a model. One just needs to recall that the more

dense surface requires 858 nodes, while the proposed model of (k_t-m-τ_b) with δm=1 and δk_t=0.05 bands and using all the data requires a total of 102 nodes.

The surface fitting technique we have developed and applied to our data, has proven to be successful. It has been a unique way to describe the variability of the beam radiation, in terms of two independent variables. As an alternative approach in developing the three variable correlation, we could have chosen to fit a polynomial to the (k_t,m,τ_b) data. This approach was not found appealing, since as it was illustrated by the use of the IMSL routine, the data variation and continuity constraints would have required a high degree polynomial. On the other hand, our technique allows us to describe the observed data variations with desirable accuracy, and may easily be used for any three variable study, as illustrated in the following sections.

8.3 A Correlation Between (k_t, η, τ_b)

Variations in the sky condition are expected to have a direct impact on the attenuation of incoming solar radiation. A variable accounting for such a variation is of course very attractive and a prime candidate to become an independent variable in our study. A problem arises though from the fact that traditionally such a candidate is chosen from variables such as cloud cover or percent sunshine, data which were not included in the Shenandoah five year data base.

Other means for describing the temporal variation of solar energy can be used. In the upcoming section we introduce a new variable, η, that accounts for the sky condition without the need of any additional information other than the already available solar radiation data. The surface fitting techniques presented in Section 8.1.1 were again employed to develop the correlations between (k_t, η, τ_b).

8.3.1 Model Development

An investigation of the temporal variation of global radiation was initiated under the following considerations. Let us first recall Figure 4.2, where we have illustrated the variation of beam and global radiation based on the Shenandoah data. We have already identified the scatter of the data and developed methods of accounting for it.

We observed that for the same intermediate values of clearness index there is a wide range of beam transmittance values. One may expect that beam radiation is high during partly cloudy skies while it is low during hazy skies. Thus, the region of data above the regression line (intermediate k_t values) represents partly cloudy skies, while the region below the regression line represents hazy conditions.

In extreme cases, under overcast skies there is practically no beam radiation component. As a result at low k_t values the τ_b values exhibit very small variation with values close to zero. Small data variations may be attributed

to instrumentation error or due to variations on the reflection of incoming solar radiation from the edges and sides of clouds.

Under clear skies, the clearness index may reach values up to 0.85. At such high k_t values again we observed from Figure 4.2 a limited amount of τ_b variation. Under clear sky conditions the radiation that reaches the surface of the earth is mainly composed of beam radiation. As a result the τ_b values reach their highest levels.

Under partly cloudy conditions we may have clearing conditions (clouds moving out) or conditions of increasing cloudiness (clouds moving in). One may identify enough variation in the recorded short period (15-minute) radiation data for a given hour, that may reflect such varying sky conditions.

In an extreme case, one small cloud in an otherwise predominantly clear sky could keep the sun obscured by slowly traveling the sky. On the other hand, it is also possible that a small break in a cloudy sky, could remain open to the sun for a long period. The value of η in itself does not directly give information as to which part of the sky is covered with clouds. In any event, though, that was not our intent. Rather we may use η to distinguish between clear skies, hazy conditions, and partly cloudy conditions, and account for some of the observed variations of τ_b with k_t.

Let us now move our attention to Figure 8.13, and consider an imaginary trace of an instantaneous radiative flux recorded by a pyranometer. The outermost curve represents a typical profile of the flux on a particularly clear day. Also shown are typical profiles of a flux on a hazy day, and on a partly cloudy day.

The global radiation, I_i, is the quantity obtained after integrating the collected irradiances over a 15-minute period in this case ($I_i=\int Gdt=k_t I_{oi}$). Hourly irradiation, I_h, values may then be calculated by summing up the four 15 minute radiation values ($I_h=I_1+I_2+I_3+I_4$). This actually the value included in our Shenandoah five year data base used thus far.

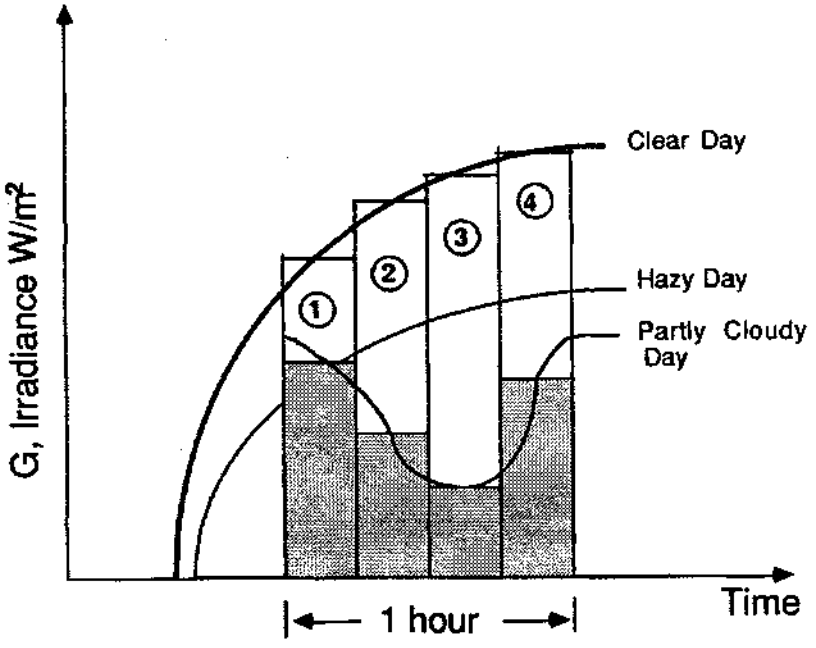

Figure 8.13 Variation of Solar Irradiance with Time During Clear, Hazy, and Partly Cloudy Sky Conditions

Within an hour though variations of the fifteen minute global radiation values are expected to be significant for partly cloudy conditions. This phenomenon is represented by the shaded areas in Figure 8.13. Temporal variations in the sky condition are expected to have an effect on the variations of global radiation. Increasing values of I_i signify clearing conditions, while decreasing values indicate that cloud conditions dominate the sky at that time. Clear sky or hazy conditions do not exhibit any significant short period variations.

To study the variations under partly cloudy conditions, we need to base our analysis on the Shenandoah fifteen minute data. The temporal variation factor must be defined in such a way that it accounts for the variation of the short period radiation. Clear and hazy conditions should be related to small η values.

Accordingly, we defined the temporal variation coefficient as follows. First, η was approximated by summing up, over an hour, the squares of the variation of short period radiation values from their corresponding average value, namely,

$$\eta_1 = \sqrt{\frac{\Sigma(I_i - k_t\, I_{io})^2}{I^2}} \qquad (8.17)$$

Second, η_2, was approximated by summing up over an hour the

squares of the variation of short period radiation values from their corresponding predicted values of a least square fit, namely,

$$\eta_2 = \sqrt{\frac{\Sigma(I_i - I_{est,i})^2}{I^2}} \qquad (8.18)$$

Third, η_3, was approximated by summing up over an hour the squares of the variation values from the corresponding hourly average irradiation value ($I_{avg}=\Sigma I_i/4$), namely,

$$\eta_3 = \sqrt{\frac{\Sigma(I_i - I_{avg})^2}{I^2}} \qquad (8.19)$$

The hourly global radiation was used everytime as a non-dimensionilizing factor.

Numerically the above calculations were performed through TEMPV algorithm listed in Appendix E. One must provide the annual 15 minute data (the so-called Qfiles) and the five year hourly data. Since the hourly data includes only valid data, the code was developed to use this data to identify the corresponding short periods that composed the hourly data. The data were processed sequentially starting from 1979, for the available five years.

The net result was the creation of a new data base that included the values of the temporal variation coefficients,

with the corresponding clearness index, air-mass and beam transmittance values for a given hourly period. This new data base was then easily manipulated to study the correlation of the new variable η with beam radiation.

The data were grouped for different clearness index cases to study the variation of beam transmittance with the temporal variation coefficient. Based on our initial results though we concluded that high air-mass values had to be screened out. This was justified on the basis that high air-mass values (greater than two) may create conditions analogous to a "gray" day, thus diminishing the partly cloudy conditions effects. Under such circumstances, we deviate from our main objective, that is to study these temporal variations under partly cloudy skies.

The total number of data that remained after the air-mass screening for values of m less than two (a zenith angle of 60°) was 5728. These data were used with our previously developed surface fitting techniques. Minor modifications were made in our programs, mainly to successfully import the (k_t,η,τ_b) data into these algorithms.

The data were first grouped into appropriate working areas, through TRDATA. The surface fitting program, FIT3DB, was then used to generate the locally weighted surfaces shown in Figures 8.14 to 8.16., that describe the variations of (k_t,η_1,τ_b), (k_t,η_2,τ_b), and (k_t,η_3,τ_b) respectively. The coordinates of the locally weighted least square error fit

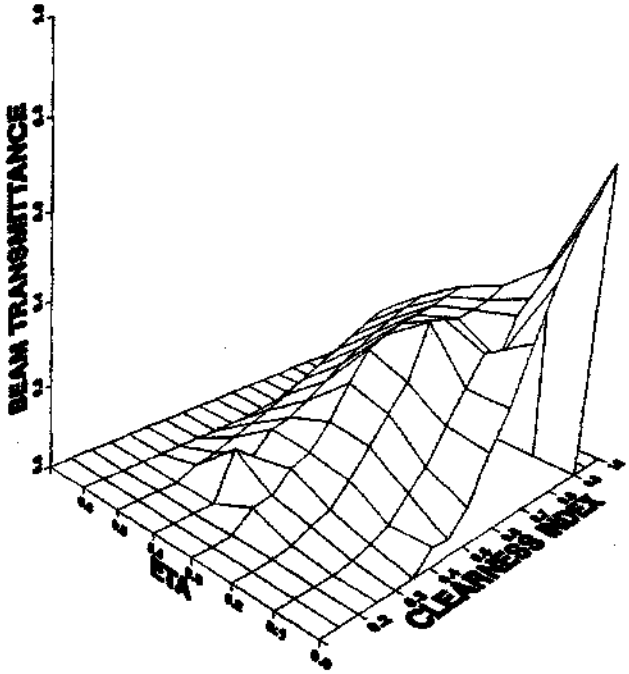

Figure 8.14 Locally Weighted Surface Using All the Available (k_t, η_1, τ_b) Data

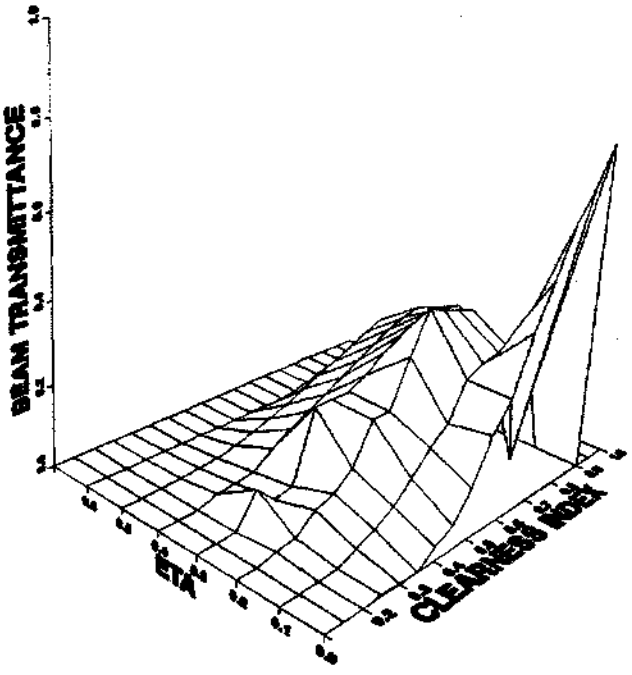

Figure 8.15 Locally Weighted Surface Using All the Available (k_t, η_2, τ_b) Data

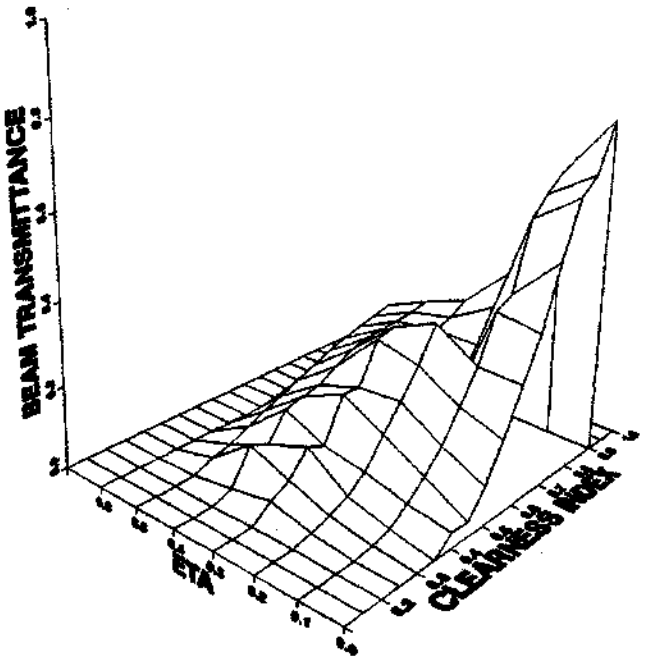

Figure 8.16 Locally Weighted Surface Using All the Available (k_t, η_3, τ_b) Data

surface (using all the data) for the three cases are listed in Appendix E (Tables E.1 to E.3).

At high clearness indices, one expects that τ_b attains high values while η approaches zero. For intermediate k_t values, the variation along the second variable has been reduced. A statistical analysis in the following section demonstrates that the proposed correlations can explain most of the observed variation.

The calculated values for the temporal variation may be verified by referring to the corresponding daily radiation charts. Let us examine first an extreme case when the value of η_1 equals 0.00026, that occurred on September 22, 1984, during the period of 1300 to 1400. The interpretation of such

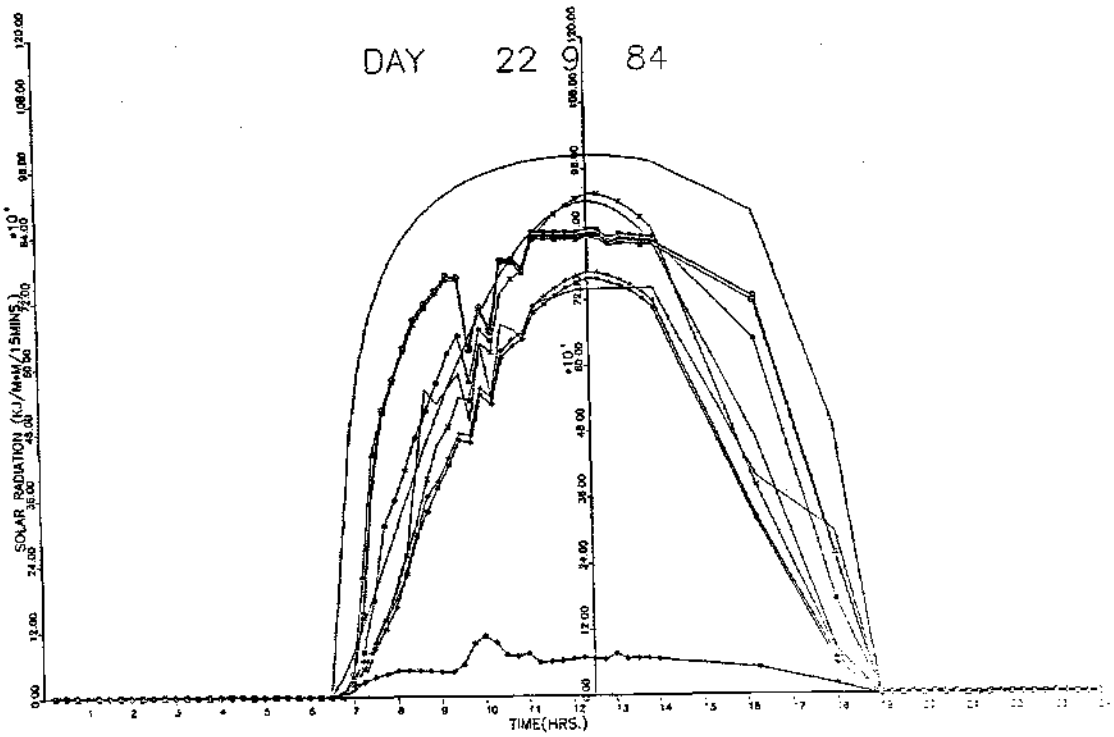

Figure 8.17 Daily Radiation Chart for September 22, 1984

a low value for the temporal variation leads us to believe that there was no major variation in the sky condition during this hour. This may be verified by examining Figure 8.17.

The pyranometer data (identified by a cross) remains steady for the duration of the period. The beam normal values (identified by circles and squares) did not experience any noticeable variation. Thus, all instruments were functioning properly and our observations are valid.

On August 4, 1980, during the hourly period ending at 1350 we have a case of partially cloudy conditions. The corresponding value for the temporal variation was estimated to equal 0.43947. We may expect then that this high value is

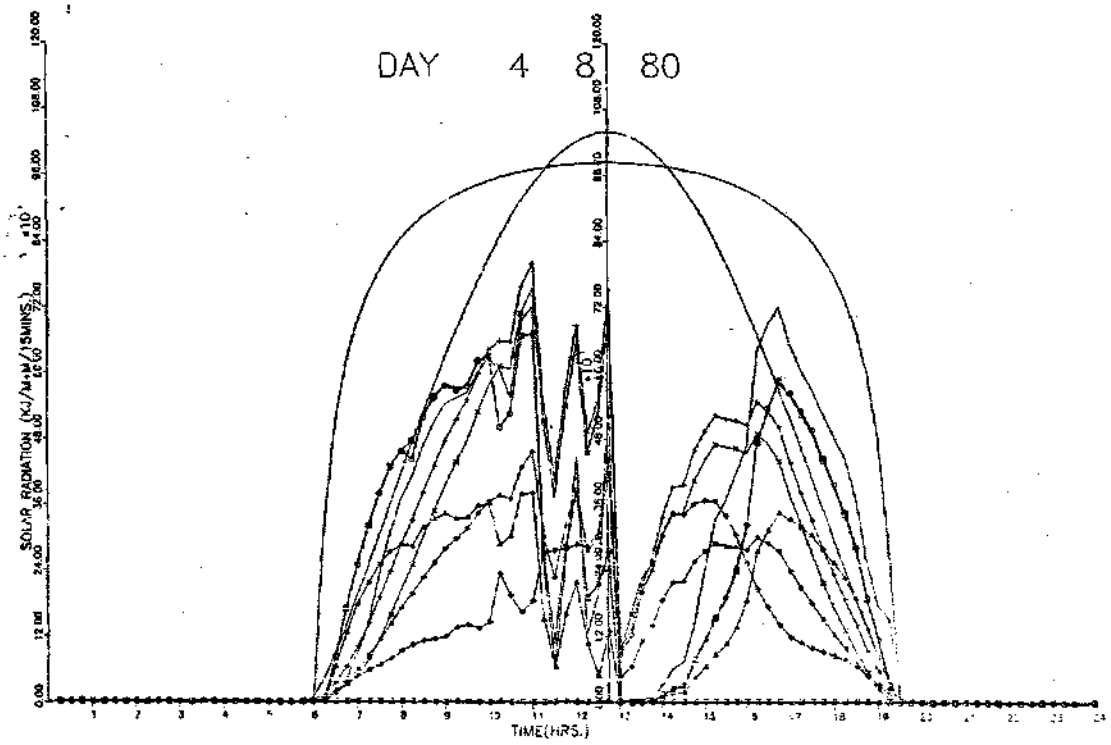

Figure 8.18 Daily Radiation Chart for August 4, 1980

reflected by a noticeable variation of the global radiation.

Referring to Figure 8.18 we observe that the pyranometer values experienced a dramatic drop, from approximately 720 KJ/m^2 to 10 KJ/m^2 for the first 15 minutes of the hour, and finally recorded 20 KJ/m^2 for the last 15 minute period. The overall variation during that day clearly indicates that the day started with clear sky conditions, and around noon to early afternoon partial cloudy conditions dominated. A typical summer day pattern for the southeast United States.

8.3.2 Statistical Analysis

The total number of data used for our (k_t,η,τ_b) study was 5728 hourly values. The pertinent statistical results are

summarized in Table 8.3, and are in accordance to the discussion in Chapter 5.

Table 8.3

Statistical Analysis for Testing the Temporal Variation Models Based on η_1, η_2, and η_3. Total Number of Data 5728.

Statistical	Temporal Variation Models (k_t,η,τ_b) Using		
	η_1	η_2	η_3
Total Variation	322.74	322.74	322.74
Residual Sum of Squares	3.67	4.38	4.73
Explained Variation	319.07	318.36	318.01
Coef. of Determination	0.9886	0.9864	0.9853

The coefficient of determination indicates that in either of the three cases almost 99 percent of the variability in the data is accounted for by the corresponding models. The "best" performance was obtained using η_1 in the first model.

8.4 Effects of Other Variables on Beam Radiation

The development of correlations that require knowledge of meteorological parameters is beyond the scope of this study. We may wish though to investigate the relative significance some of these variables have on the depletion of the

beam irradiation. In the process, we would also illustrate the use of the previously developed procedures when the air-mass is replaced, for example, by a meteorological parameter.

The atmosphere is not homogeneous but contains clouds of finite width and finite thickness. Therefore an intermittent cloud cover transmits less radiation at large than at small incidence angles, and high values of beam radiation can be reached only on very clear days. The water drops of which the clouds are composed strongly scatter the incoming solar radiation, while also absorbing some of it.

There is a direct correlation between the thickness and type of clouds, and the amount of solar radiation that arrives on the surface of the earth. In most cases, we may expect that clouds markedly reduce incoming radiation. However, reflections from sides of scattered and broken cumulus clouds often leads to larger than clear sky radiances at the surface at a given moment. Thus, Kaiser and Hill (1976) found that the irradiance increased on the approach of a cloud until the cloud obscured the sun.

The Shenandoah five year data base does not contain any information other than solar radiation values. To facilitate our study we used the Hourly Data Base (HDB) that was briefly described in Chapter 4, and which includes a variety of solar and meteorological observations. The measurements were made at the Georgia Tech campus (33.777° N, 84.398° W). These data were used in combination with some assumptions that were

necessary to be made in relation to the optical properties of clouds, since such dependable measurements are not available.

According to Stephens (1978), we assumed eight cloud model distributions to be used in our following calculations. These types of clouds correspond to some of the available observations on the type of clouds in the HDB. Their main important physical properties are summarized in Table 8.4.

Table 8.4

Cloud Model Droplet Distribution Parameters, Heights and Thickness, to be Used in the Present Study. Adapted from Stephens (1978)

Cloud Type	LWC g/m^3	Drop Radius μm	Height Km	Thickness Km
Stratus	0.22	3.5	0.5	0.5
Stratocumulus	0.14	3.5	2.0	0.5
Nimbostratus	0.5	3.5	1.0	2.5
Altostratus	0.28	4.5	3.5	0.5
Cumulus	1.0	5.5	1.0	0.5
Cumulonimbus	2.5	6.0	1.5	2.5

The Liquid Water Content (LWC) ranges from 0.05 g m^{-3} to 2.5 g m^{-3}, while the drop-size distributions range from 2.25 to 7.5 μm. The selected cloud positions and thickness shown in Table 8.4 are also according to Stephens. The clouds were assumed to be vertically and horizontally homogeneous, with

respect to drop-size distribution.

The cloud optical thickness (τ_c) is the most important parameter needed to describe the radiative properties of clouds, since it is directly related to the liquid water content of the cloud. The value of τ_c may vary considerably. A rough range is $5<\tau_c<500$, with typical values between 10 and 20. According to Twomey (1976), if the sun's disc is not visible through a cloud then τ_c must be about 10 or greater.

The optical thickness of a cloud is directly related to Liquid Water Path (LWP). In the second part of his work, Stephens (1978) presented a relationship for τ_c in terms of LWP and the effective radius of distribution, approximated as

$$\tau_c = \frac{3}{2}\frac{W}{r_e} = \frac{3}{2}\frac{w\, z\Big|_0^{\Delta z}}{r_e} \qquad (8.20)$$

where W = liquid water path, g m^{-2},

w = liquid water content, g m^{-3},

r_e = effective radius of cloud droplet, μm, and

Δz = cloud depth varying between 0 to Δz.

Based on the assumption that the cloud is vertically uniform with respect to drop-size distribution, the total vertical liquid water path becomes $W=w\,\Delta z$. The data for w and Δz were taken from Table 8.4. The above information combined with the observations of the cloud type included in HDB, enabled us to calculate the cloud optical depth related to

the measured values of beam and global irradiations.

A data base that includes hourly values of the clearness index, the cloud optical depth, and the beam transmittance were used with the procedures presented in Section 8.1. Representative results for 1983 are illustrated in Figure 8.19. A total of 1282 hourly data were used. Use of the data were limited to the available type of clouds from Table 8.4.

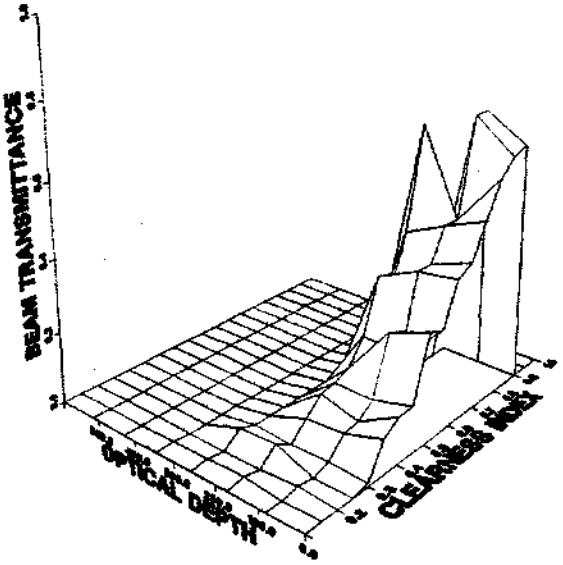

Figure 8.19 Locally Weighted Surface Using All the Available (k_t,τ_c,τ_b) Data from 1983 HDB

According to Figure 8.19 the beam transmittance tends to zero as τ_c increases. At low optical depths the variation of τ_b is the one we have already observed from our previous correlations, that is, higher values of beam transmittance for clearing skies (or increasing k_t values). High optical depth values quickly attenuate the beam radiation completely. The fitted surface explained 97.8% of the observed variation.

The cloud fraction (CF) was an additional parameter included in HDB. The percent of sky dome covered by opaque clouds is of course expected to be closely related to the variation of the beam and global radiation. The values used in HDB to describe the opaque cloud fraction ranged from 0 (no clouds) to 10 (overcast). These values were again collected together with the corresponding clearness index and beam transmittance values to produce the response surface relating (k_t, CF, τ_b), shown in Figure 8.20.

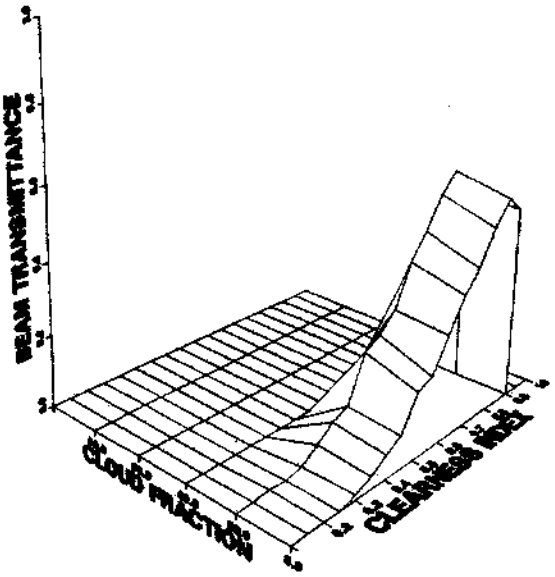

Figure 8.20 Locally Weighted Surface Using All the Available (k_t,CF,τ_b) Data from 1983 HDB

Figure 8.20 illustrates the high attenuation of beam radiation with increasing opaque cloud coverage of the sky. At zero cloud fraction (clear skies) we observe the familiar trend of increasing beam radiation with increasing K_t. The total number of data used were 2391. Given these data, 97.3%

of the variation was accounted for by the fitted correlation.

Relations between solar radiation and observations of the amount of sky covered by clouds are known to be less reliable than the corresponding insolation-sunshine correlations, Norris (1968). Figure 8.21 illustrates the relationship between beam transmittance, percent sunshine (SS), and clearness index based on data from 1983 HDB.

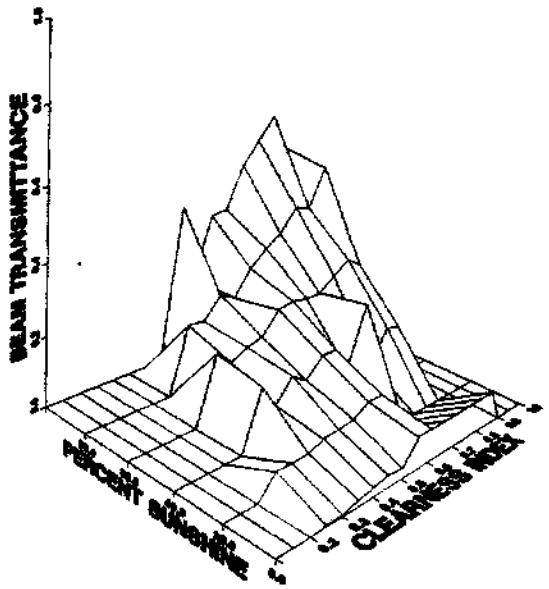

Figure 8.21 Locally Weighted Surface Using All the Available (k_t,SS,τ_b) Data from 1983 HDB

High values of beam transmittance are expected for the combination of high SS and k_t periods, since both of these variables describe the sky conditions. The surface exhibits a relatively smooth upward trend. Overcast conditions are related with no beam radiation, and as a result beam transmittance values tend to zero. For clear conditions, the beam transmittance peaks, and its values tend to unity. A

total of 2391 data were used, and the response surface explained 98.4% of the observed variation.

In conclusion, this section of our discussion was included for illustration purposes. Our goal was to demonstrate how the procedures developed in this chapter may easily be adapted for similar studies, when additional information become available. No further elaboration on these observations were prescribed. In the following and final chapter, the reader has the opportunity to review the candidates from the correlations we have developed in order to choose the "best" model.

CHAPTER IX

CONCLUSIONS AND RECOMMENDATIONS

The various models presented in the previous chapters were developed for determining the amount of beam normal irradiation when only global radiation data is available. These models were shown to be preferred over already existing correlations based on the Shenandoah data. Next, we present an overall statistical validation of the developed correlations, and a performance test of our "best" model with data other than the underlying data base upon which these empirical models were developed. The three variable models of (k_t, m, τ_b) and (k_t, η, τ_b) are found to be appropriate models that actually reflect the real life variations in the relationship of beam and global radiation. This work is finally completed with some recommendations for future work that may add some useful refinements to the models presented herein.

9.1 Model Comparisons

We are now at the point of our development where we embark on the problem of selecting the best model. In Chapter 4 we reviewed the techniques that can be used to assist us in our decision process and were applied as described in the

following discussion. The reader must always keep in mind that the choice of an appropriate model will very strongly depend on the particular problem. There are no universal answers here: The model chosen should depend on the nature of available data, and the needs of the user for the specific application.

9.1.1 Statistical Validation of Proposed Correlations

We recall that at the conclusion of each of our previous analyses, a basic statistical study proved some correlations less powerful (as in the case of monthly seasonal models and the beam transmittance air-mass correlations). Let us at this point summarize the remaining candidate correlations. We started with the basic Shenandoah five-year model, proceeded to the five-year seasonal model, and then finished with the three variable studies of (k_t, m, τ_b) and (k_t, η, τ_b).

A common criteria for comparing the performance of different correlations is the use of the coefficient of determination. Accordingly, we may examine the pattern of the corresponding r^2 values as a first step. Figure 9.1 summarizes the r^2 values for each of the models. Clearly, there is a consistent upward trend.

We have succeeded in explaining about 99 percent of the variation that the Shenandoah data exhibits with the correlation that involves the temporal variation coefficient. This correlation is also attractive due to the fact that one can

account for the sky condition without requiring any additional meteorological observations.

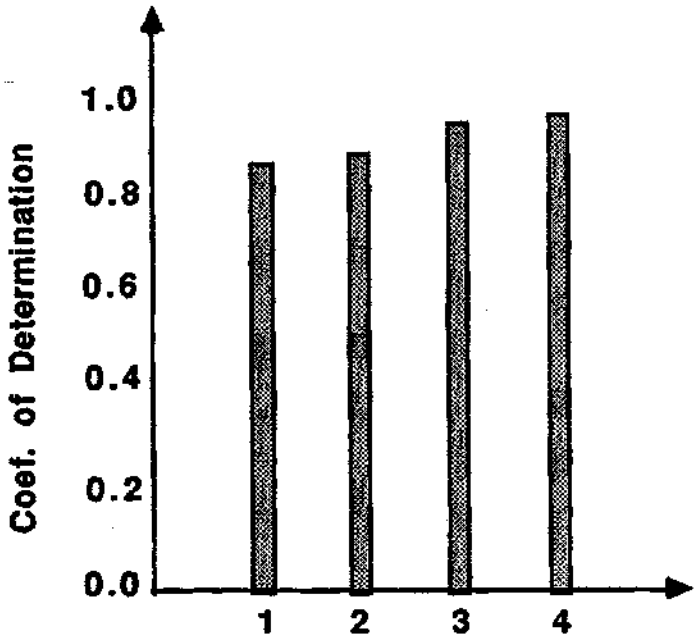

Figure 9.1 Plot of the Coefficient of Determination for the (1) Basic Shenandoah Five Year Model, (2) Five Year Seasonal Model, (3) (k_t,m,τ_b) Model, and (4) (k_t,η,τ_b) Model.

The final choice of a model though, should not be based on the absolute value of the r^2 statistic. As a matter of fact, models 3 and 4 in Figure 9.1 differ only by 0.6%, suggesting that the correlation of (k_t,m,τ_b) is also an excellent candidate, especially since it was developed from a wider range of air-mass values.

A second criterion we considered was the mean square error for the p-variable model, $MS_E(p)$. According to Figure 9.2, the $MS_E(p)$ decreases as the number of variables in the model increased to two. The knee of the curve is character-

istic of approaching a minimum MS_E value. Again, either model 3 or 4 is an appropriate choice.

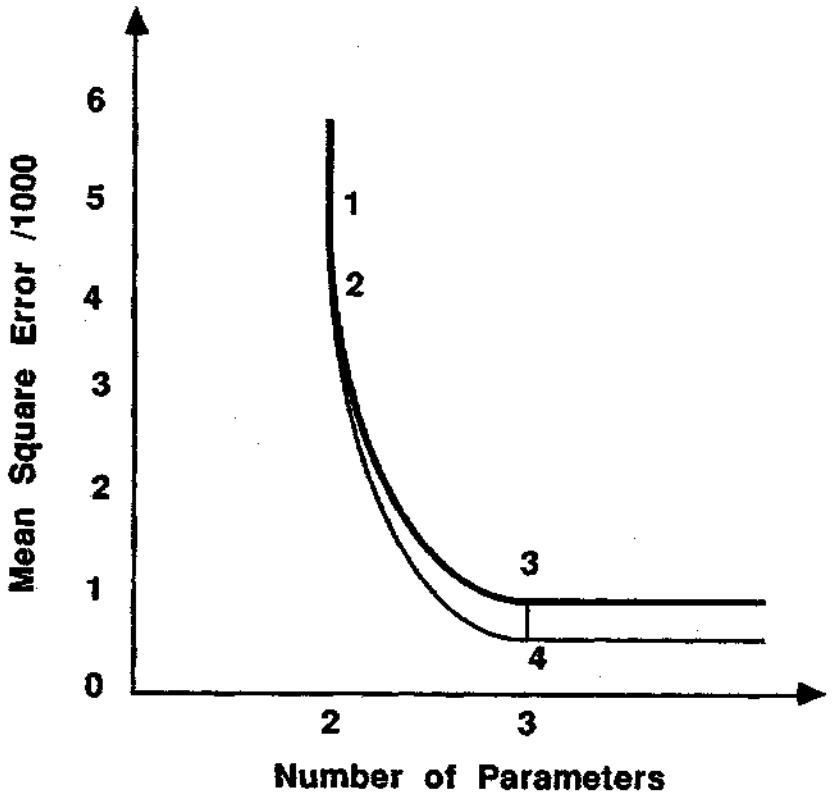

Figure 9.2 Plot of the Mean Square Error Against Number of Parameters in the (1) Basic Shenandoah Five Year Model, (2) Five Year Seasonal Model, (3) (k_t, m, τ_b) Model, and (4) (k_t, η, τ_b) Model.

Use of the adjusted coefficient of determination that accounts for the number of variables in the model also resulted to similar conclusions. The coefficient was calculated according to Equation 5.13. Again we choose the regression model that had the maximum value of r_a^2. According to Figure 9.3, models 3 and 4 achieve the highest r_a^2 values, with a small difference between their corresponding values.

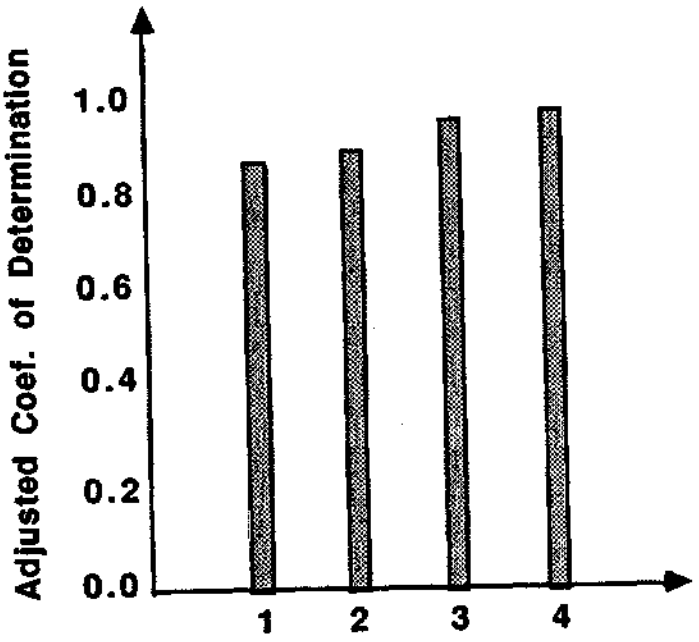

Figure 9.3 Plot of the Adjusted Coefficient of Determination for the (1) Basic Shenandoah Five Year Model, (2) Five Year Seasonal Model, (3) (k_t,m,τ_b) Model, and (4) (k_t,η,τ_b) Model.

For the step wise regression procedure we first considered a one independent variable, namely the clearness index, that is most highly correlated with the response τ_b. The degrees of freedom have been accordingly adjusted to account for the number of regression coefficients determined from the piecewise linear model of $\tau_b=f(k_t)$. Referring to Table 9.1 we may calculate the value of the F-statistic for the (τ_b-k_t) correlation, as the ratio of the corresponding means of the sum of squares for the regression and the residuals, to obtain $F(k_t)=1013.8$.

Using an $\alpha=0.01$, the reference F-statistic taken from the appropriate statistical tables was given by F(0.01, 8,

Table 9.1

Possible Regressions with Characteristic Statistical Variables

Variables in Model	$(df)_R$	$(df)_E$	Variables in Model	r^2	SSR	RSS	MS_E	MS_R
1	8	8112-9	k_t	0.8865	370.85	47.46	0.00586	5.93
1	5	8112-6	m	0.0023	0.9845	417.3	0.05148	0.197
2	80	8077-80	k_t,m	0.9824	417.64	7.34	0.00092	5.22
2	96	5729-96	k_t,η	0.9886	322.74	3.67	0.00065	3.362

$\infty)=F^{+}=2.51$. Because the value of the partial $F(k_t)$ greatly exceeds F^{+}, the k_t variable can be entered into the model. This was the first variable to enter the regression equation.

The second step begins by finding an additional variable, namely air-mass, to repeat the process. Regress τ_b on m, and the overall F-test shows that the regression equation is not significant. The value of the partial F(m) was calculated to be equal to F(m)=3.82, which must be compared to the reference value of $F(0.01, 5, \infty)=F^{-}=3.32$. Since F(m) approximately equals F^{-}, we reject m in a τ_b-m correlation. We reached the same conclusion in Chapter 7 by observation of the scatter plot of τ_b vs m. The wide variation of the data clearly indicated no direct use for such a correlation. The extremely low coefficient of determination, see Table 9.1, is an additional warning against the use of a direct relationship between the two variables under all sky conditions.

Consider now that we may incorporate the third variable m, given that k_t is in the model or $\tau_b=f(k_t,m)$. This correlation has an r^2 of 98.2% and is significant, since we have an overall F-statistic equal to $F(k_t,m)=5686.5$, which greatly exceeds $F(0.01,80,\infty)=F^{+}=1.0$. Thus, the addition of the m variable in a two variable correlation was significant, although the partial F-statistic for m was not significant.

This could have potentially lead us to exclude m from our development. Our previous discussion though, in Chapter 7, clearly indicated that one needs to explore the effect

that adding a variable would have on the whole relationship. Our decision process may not always be based on conclusions derived from partial F-tests.

A similar procedure can be repeated for η. The $\tau_b=f(k_t,\eta)$ correlation has an r^2 of 98.9% and is significant since we have an overall F-statistic equal to $F(k_t,\eta)=5160.2$, which greatly exceeds $F(0.01,96,\infty)=F^+=1.0$. Between the two correlations, $\tau_b=f(k_t,m)$ and $\tau_b=f(k_t,\eta)$, the selection of either one would result to a satisfactory performance.

Our selection criteria should not only be based on statistics, but rather should reflect one's specific needs. In the event, for example, that distinct weather patterns prevail at an area of interest with known patterns of sky variations, then the $\tau_b=f(k_t,\eta)$ correlation should be preferred. Otherwise, the $\tau_b=f(k_t,m)$ correlation may be used with confidence.

9.1.2 Observed and Modeled Variables

Modeled and observed values for the beam transmittance were compared based on the available Shenandoah five year data. The two "best" models, (k_t,m,τ_b) and (k_t,η,τ_b), were used to predict hourly values of τ_b. Because errors are mainly random, an increased averaging period would increase the model's accuracy. Therefore, for some applications it may be necessary to select an averaging period to ensure a required level of accuracy.

Figure 9.4 is a plot of observed versus predicted beam transmittance using the model with air-mass as the second independent variable. The deviations from the one-to-one regression line are substantially smaller for the higher τ_b range, which indicates that the model performs better for clear sky conditions. The main body of the data, though, closely follows a one-to-one correlation.

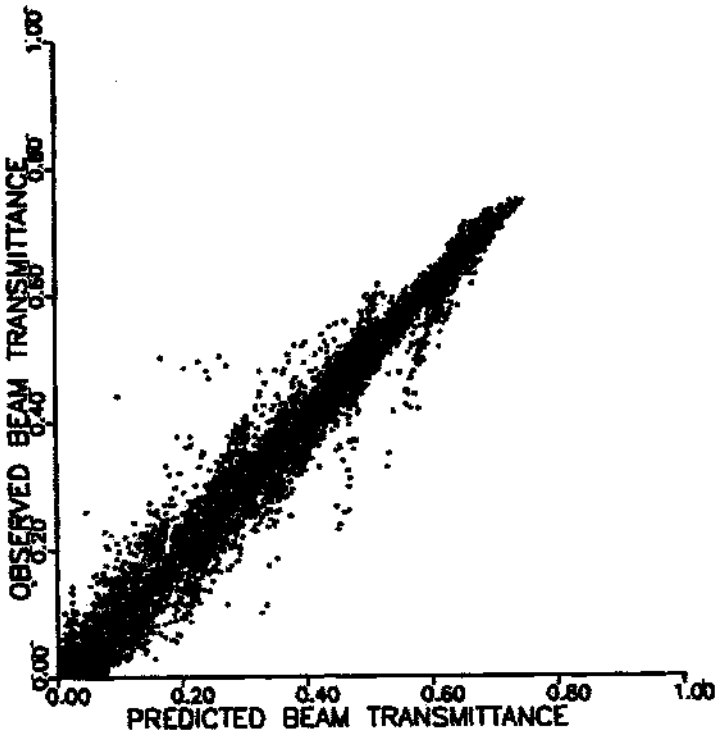

Figure 9.4 Observed vs. Modeled Beam Transmittance, from the Shenandoah Five Year Data and the (k_t, m, τ_b) Model

Figure 9.5 is a similar plot of observed versus predicted beam transmittance using the model with the temporal variation as the second independent variable. The variation of the data about the one-to-one regression has decreased.

One would expect a smaller variation since $1-r^2$, which is a measure of this variance, is smaller for this model than the corresponding value of the (k_t,m,τ_b) model.

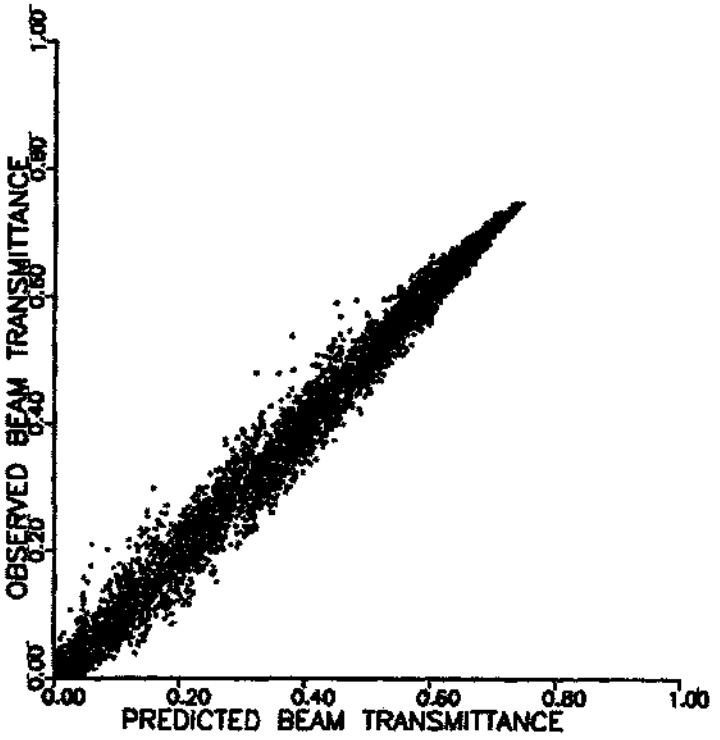

Figure 9.5 Observed vs. Modeled Beam Transmittance, from the Shenandoah Five Year Data and the (k_t,η,τ_b) Model

9.2 Model Validation with Independent Data

The models developed in the previous chapters were empirically derived from the five year Shenandoah data. Consequently, our models resulted in a better performance when other independently derived correlations were compared with them. Although the observed differences between these models were shown to be significant, at this stage one would

like to test the performance of the models with some independent data.

We are mostly interested in the performance of our two best correlations, namely $\tau_b=f(k_t,m)$ and $\tau_b=f(k_t,\eta)$. Good fit to an independent data base would be an encouraging sign that our regression models had a wide applicability, while lack of fit would indicate that the correlations were not valid for these sites. For this purpose, we used three years of global and diffuse data (from which the beam component was estimated) obtained from the National Observatory of Athens (NOA), Greece (37.5° N, 23.5° E).

The raw data from NOA were not free of erroneous measurements. Accordingly, we imposed some validity tests in an attempt to exclude data that were verified to be outliers. Finally, a total of 5439 hourly values were used in our analysis. Some questionable data had to remain though because no basis was found on which to exclude them. Figure 9.6 illustrates the wide scatter of the data at high k_t values which is a clear indicator of the questionable quality of these data points.

The least amount of observations was recorded during the winter months, with mostly uniform distribution of low τ_b values for intermediate cases of k_t. This is primarily the behavior one would expect for winter months in a Mediterranean climate, during which, mostly cloudy skies prevail. For the remaining months the opposite is true. There is a

persistently high concentration of data taken at high clearness indices. This is directly related to the predominance of clear skies during these months.

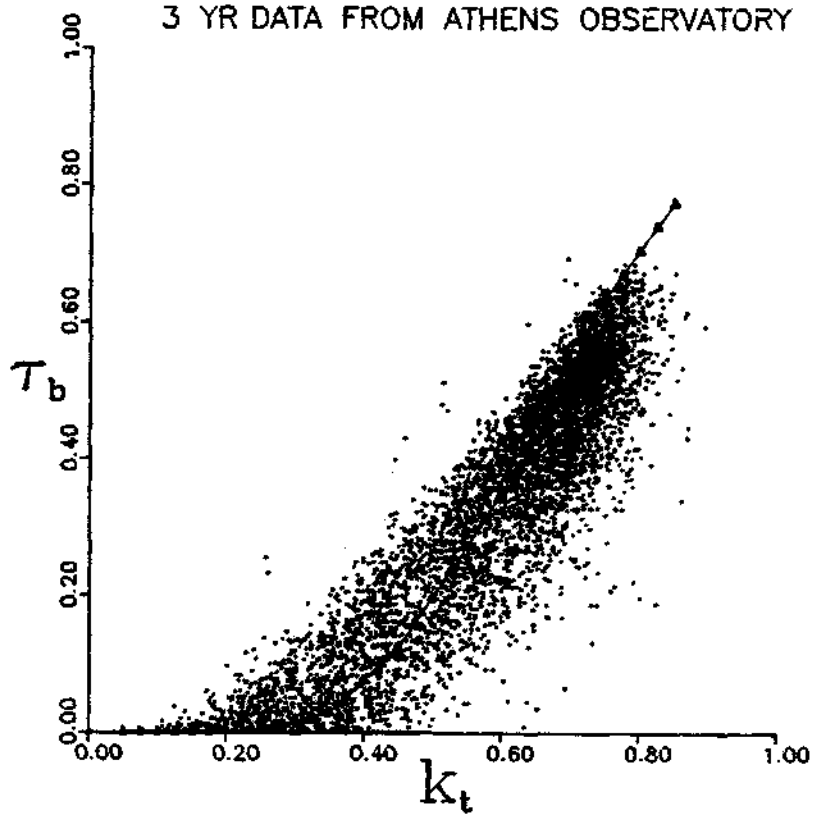

Figure 9.6 Scatter Plot of the Three Year Data from NOA. The Basic Shenandoah Five Year Model is Shown by the Plain Line

For the area of Athens, though, the summer months exhibit another distinct characteristic - unusually low values of the beam transmittance at high clearness indices. This is probably due to the existence of atmospheric pollution that prevails during the summer months in the city of Athens. That of course would result in an unusually high

value for the diffuse irradiation, and thus a low I_{bn} for high values of global irradiation. These observations were also made by Lalas et al. (1987).

Using the available 5439 hourly values, we first applied our procedures to these data in order to develop a correlation of the form (k_t, m, τ_b) for the area of Athens. The proposed correlation is shown in Figure 9.7. The surface is described in Appendix F. The calculated coefficient of determination was found equal to 95.7%.

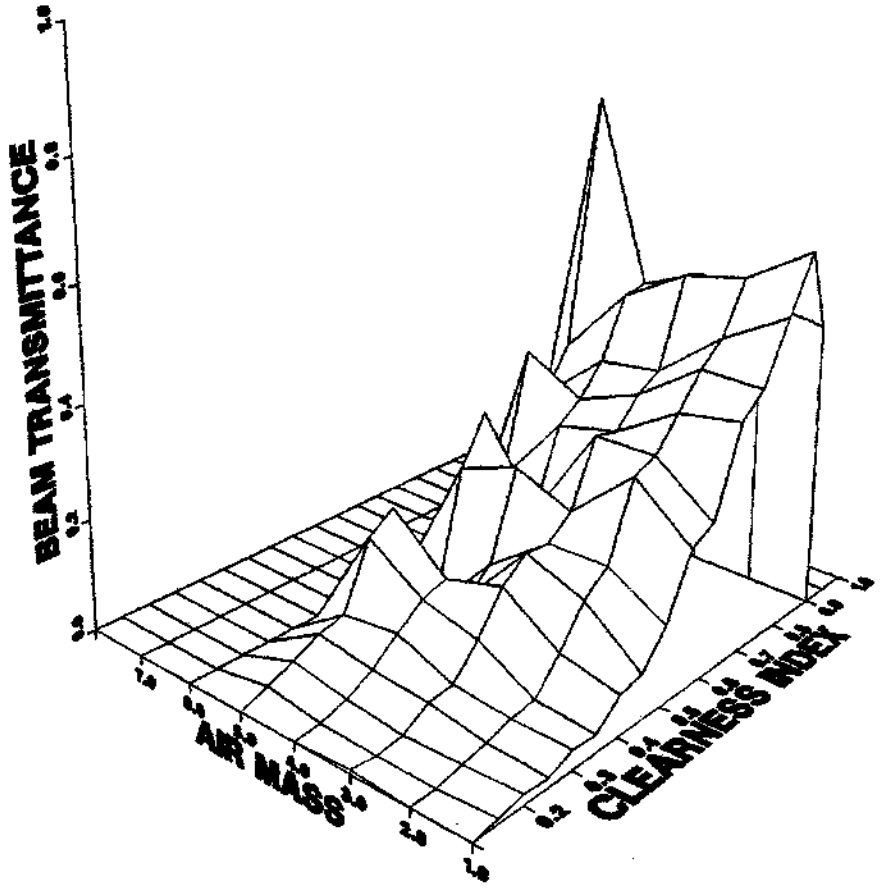

Figure 9.7 Locally Weighted Surface Using All the Available (k_t, m, τ_b) Data from the National Observatory of Athens, Greece

The proposed (k_t,m,τ_b) model developed from the Shenandoah data base was successfully applied to the NOA data. The model produced an r^2 statistic of 90.45%, and a root-mean-square error of 0.04. An observed τ_b versus predicted τ_b plot using our three variable model and the NOA data is shown in Figure 9.8. The variation of the data points from the one-to-one regression line may look alarming at first sight.

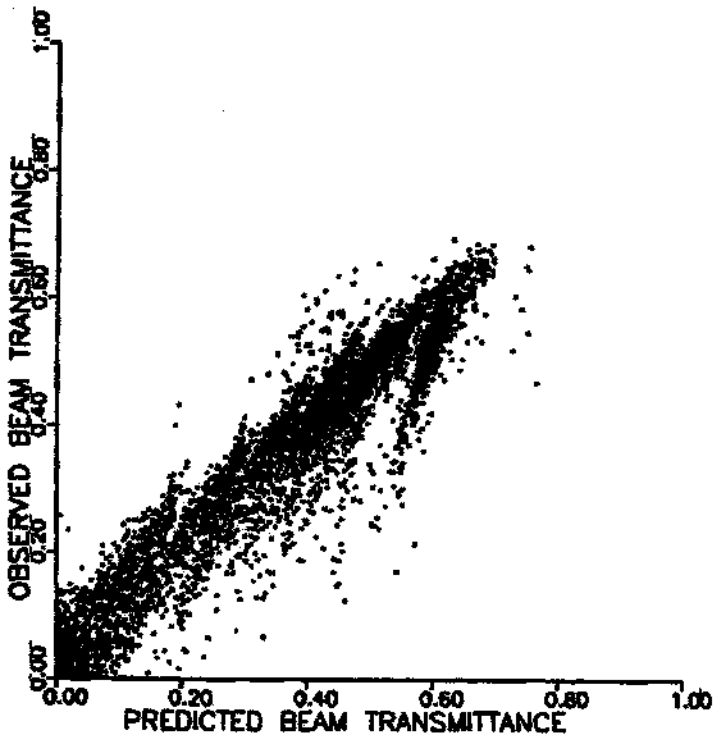

Figure 9.8 Observed vs. Modeled Beam Transmittance, from the NOA Data and the Shenandoah (k_t,m,τ_b) Model

Considering though that many data that remained in the data base were highly questionable especially at intermediate

clearness indices, one should be more concerned with the general trend of the correlation. The observed differences may, for example, originate from measurement errors, transformed now to appear as discrepancies between observed and predicted values. In fact, we believe that our model performed very well, and it is evident that its applicability may be extended outside the southeast region of the United States. Further testing of course is required with a more dependable and validated data base.

A similar plot was obtained using the three variable (k_t,m,τ_b) model developed for the area of Athens. The variance about the one-to-one line has decreased in comparison to Figure 9.8. We expected a better performance from the Athens model based on the NOA data. However, the model exhibits a lower accuracy at intermediate k_t values due to the large variation of the observed data for this clearness index range.

9.3 Residual Analysis

Formal tests using the residuals provide a natural means of validating models. If we wish to test our fitted regression models, with normal errors, based on the independent data, we may write

$$y_i = y_{i,est} + e_i \qquad (9.1)$$

where $y_{i,est}$ = fitted value corresponding to actual data y_i,

e_i = residuals, random variables with zero mean, constant variance, and normal distribution.

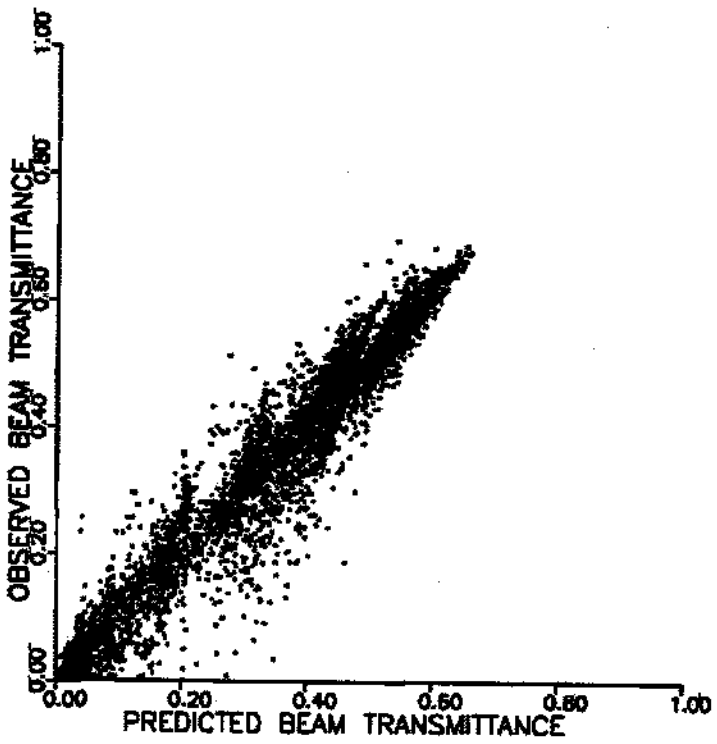

Figure 9.9 Observed vs. Modeled Beam Transmittance, from the NOA Data and the Athens (k_t,m,τ_b) Model

In the event that the residuals do not show the properties described, then the model is not as good as we thought it was. Usually plots of the residuals indicate where the inadequacies of the model lie. The residuals should be examined in all possible ways in order to check for any discernible patterns. There are many helpful ways of plotting the residuals, the following being the most common:

a. Residuals against the fitted value y_{est} (the modeled value of τ_b in our case). Such a plot will indicate any systematic deviation of the underlying structure from the model when the deviation varies with the magnitude of y_{est}. Figures 9.10 and 9.11 reveal no such alarming signs. The residuals were generated using the (k_t, m, τ_b) model with the Shenandoah and NOA data respectively. One should notice how the residual variation is decreased at high τ_b values (clear skies) for the case of the Shenandoah data.

b. Residuals against the observed values y_i (the value of the τ_b in our case). This plot is similar in interpretation to case (a). It has the advantage of allowing more random features to appear, in that y_i includes the effect of ε_i more strongly than $y_{i,est}$. However, it compares the residuals with the real situation and not the assumed model which would be important if the assumed model was not a close fit. Figures 9.12 and 9.13 again correspond to the Shenandoah and NOA data respectively. Notice the increased residual variation compared to the previous two figures, more evident in the case of the NOA data. However, there is no distinct pattern of the residual variation to suggest any problems with the model.

c. Residuals against regressor variables, (k_t in our case). The objective of such plots is to illustrate any problems with the way the regressor influences the dependent variable. Then the error produced will be contained in the

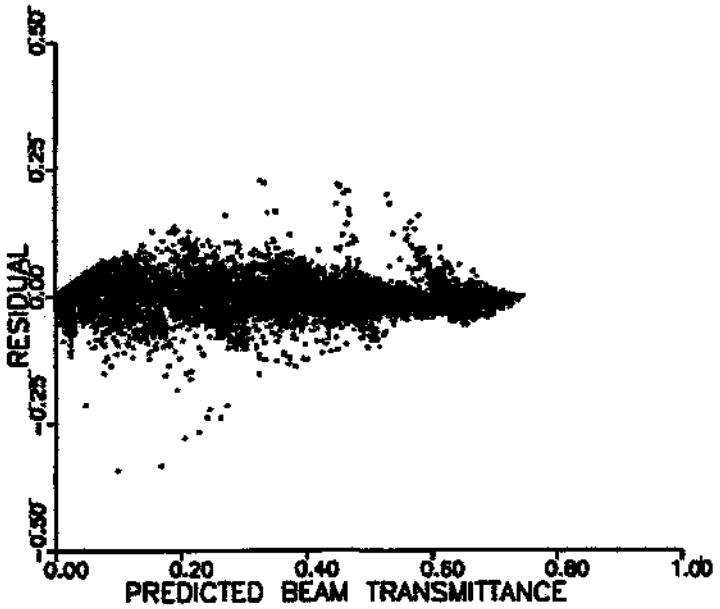

Figure 9.10 Residuals vs Predicted Beam Transmittance Value, Using the (k_t,m,τ_b) Model and Shenandoah Data

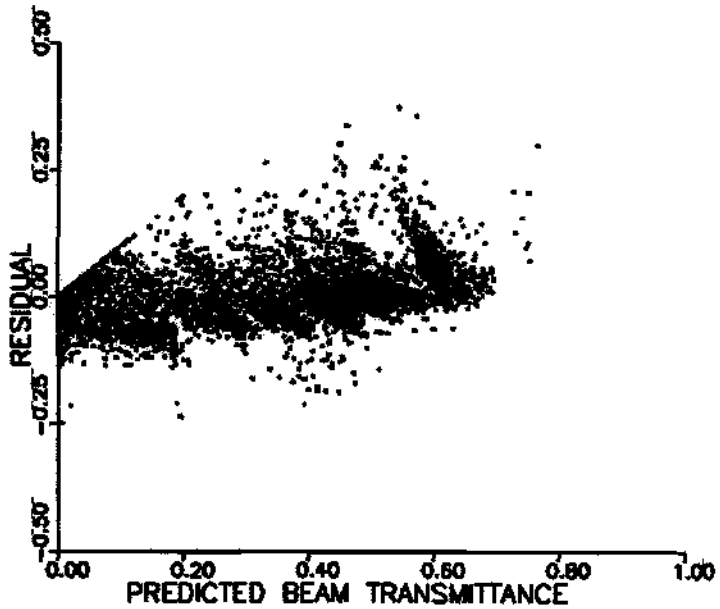

Figure 9.11 Residuals vs Predicted Beam Transmittance Value, Using the (k_t,m,τ_b) Model and NOA Data

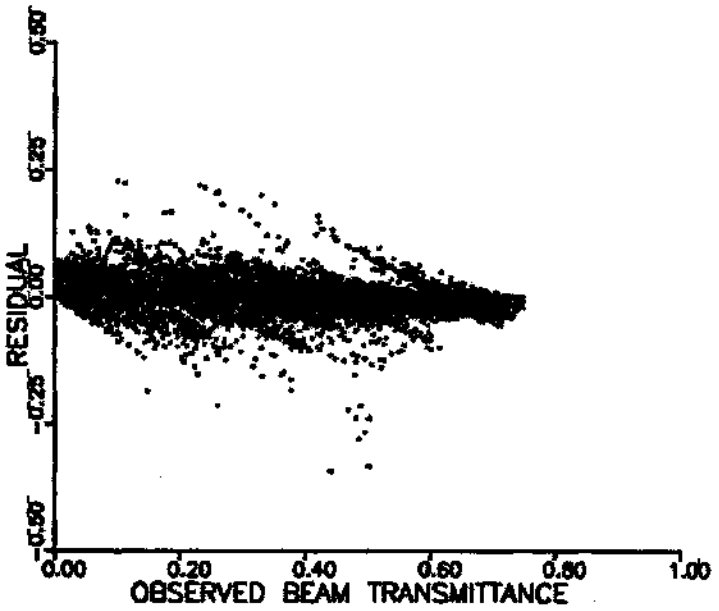

Figure 9.12 Residuals vs Observed Beam Transmittance Value, Using the (k_t,m,τ_b) Model and Shenandoah Data

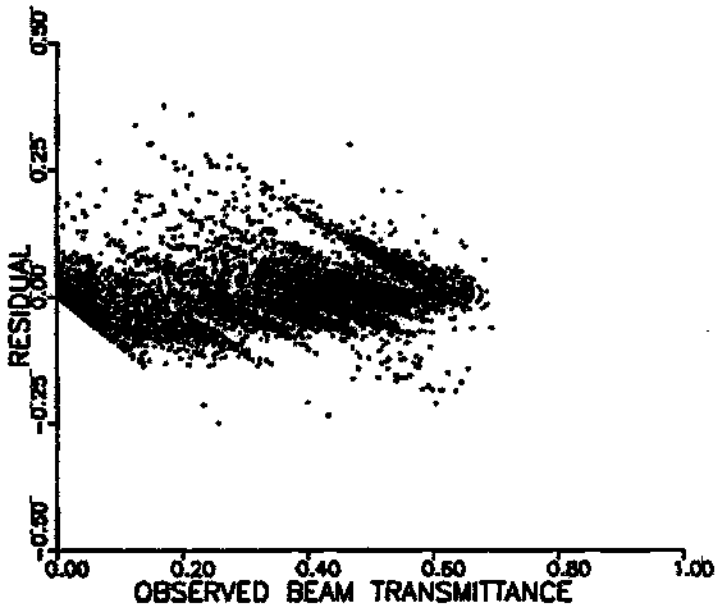

Figure 9.13 Residuals vs Observed Beam Transmittance Value, Using the (k_t,m,τ_b) Model and NOA Data

residual. In this situation, a plot of the residuals against the regressor variable would then show a systematic variation. Figures 9.14 and 9.15 show no systematic variation, while they exhibit a substantial randomness in both cases of the two data bases.

Overall, the study of the residuals displayed no problematic areas. The width of the residuals band showed that the quality of the fit, in either case of the two data bases, was good. The relatively small and fairly constant width indicates that we do well in predicting the observed variations with our proposed correlation even for regions outside the southeastern United States.

The developed beam radiation models provide us with a dependable means for obtaining the pattern of beam solar radiation received at a particular locality with only required input the corresponding global radiation. They also provide a means by which knowledge of solar radiation data can be passed from collectors to users of such information.

From the user's point of view, the proposed models satisfy his needs since they successfully and accurately describe past behavior of the beam solar radiation at the measuring station, they are easy to understand and use, and the developed procedures may easily be updated to account for newly gathered information.

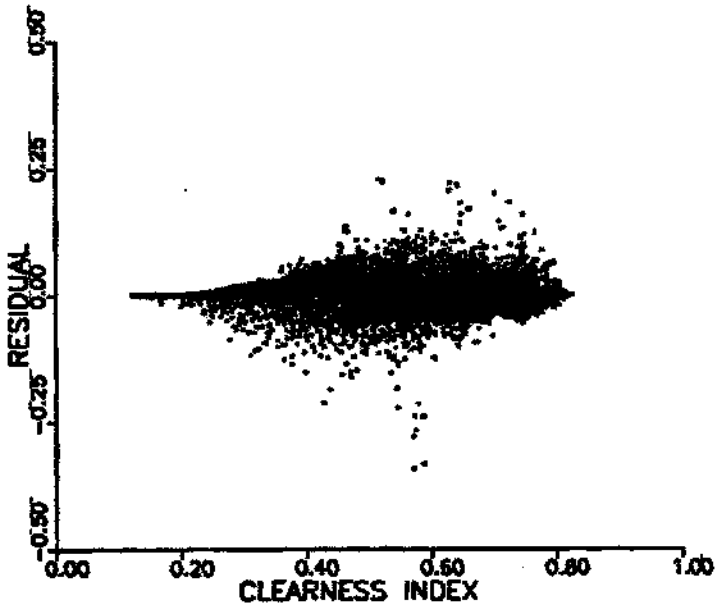

Figure 9.14 Residuals vs Clearness Index Value, Using the (k_t, m, τ_b) Model and Shenandoah Data

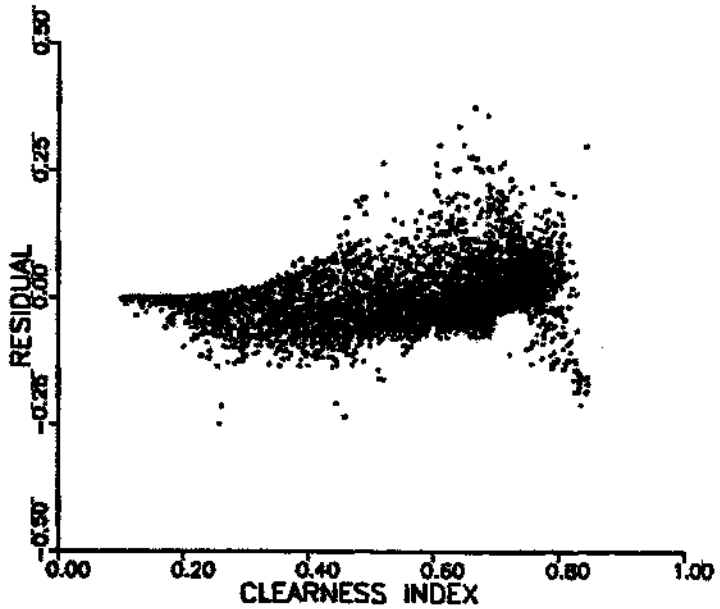

Figure 9.15 Residuals vs Clearness Index Value, Using the (k_t, m, τ_b) Model and NOA Data

9.4 Future Work

Our work has been concluded successfully. As a result we have obtained two powerful correlations that satisfy our initial goals; simplicity of the model, and required input information limited to global solar radiation, to accurately predict beam radiation and account for its real life variability. In the process we have presented a method that may easily incorporate a number of different combinations of independent variables, in order to study their effects on τ_b.

Empirical correlations, though, have a drawback. Interested third parties some times express severe conservation on employing such correlations that may have been developed from data of questionable quality. In principle, such a conservative approach is recommended. In our case, though, we have made every effort to employ a mostly dependable data base for our model development. After four years of continuous use of the Shenandoah data by the author and repeated checks and validation procedures, we have every reason to feel very comfortable with its accuracy.

However, it is to our advantage to have additional sources of data that may be used to validate our proposed models. Use of data from different climatic regions is of course needed in order to establish the model's wider applicability outside the southeastern United States. For our region, it is doubtful that the proposed models would become

absolute in the near future due to large climatic variability.

Once we have dependable numerical models to accurately predict the components of local solar radiation, we may combine this information with orographic maps of a given area. Tilt and orientation of the ground may be used to calculate solar radiation values of appropriate time length and represent them on maps.

Once the beam radiation has been accurately predicted for a horizontal surface, one may predict its value on an arbitrarily oriented surface. The contribution of the sky radiation then becomes of particular importance to that surface, which is a function of the uniformity of the radiant intensity of the sky. As an approximation, it is common to assume that the sky is diffuse or uniformly luminous.

In reality, the sky is to some degree anisotropic with an especially bright region around the sun, called the "far circumsolar" component, and a brightening near the horizon, the "planetary limb" effect. Various methods exist that determine the magnitude of the sky radiation received by an arbitrarily oriented surface and the distribution of its origin over the sky hemisphere, from available data of beam and sky radiation on a horizontal plane. An empirical approximation may then be developed to complement our present calculations. Several models have been reviewed and compared based on the Shenandoah data by Jeter and Balaras (1986).

The output of solar thermal systems is sensitive to variations in the solar energy input. One may recognize fluctuations, for example, on the amount of cloudiness that follows a specific trend. Separating such effects may be achieved with a time series analysis. Sequential characteristics of radiation can then be represented in some numerical terms derived from the autocorrelation functions of a stochastic model.

The current state of knowledge thus indicates that the most fruitful avenue of research are likely to be refined characterization of the anisotropy of the sky radiation and the temporal patterns in beam and global radiation.

APPENDIX A

HELGO	Subroutine to Calculate the Position of the Sun
GAST	Function to Calculate the Greenwich Actual Siderial Time
JDAY	Subroutine to Calculate the Standard Julian Date
EXTRAD	Subroutine to Calculate Extraterrestrial Normal and Global Radiation

```
      SUBROUTINE HELGO(IYEAR,MONTH,IDAY,CVLT,ALONGD,ALATD,ALONST,ZONE,
     &ALTR,DECL,EOT,HANG,RADIUS)
C
C
C                        SUBROUTINE HELGO
C                    C. BALARAS     1-31-85
C
C
C...THIS IS THE LATEST VERSION OF THE SUBROUTINE USED IN PROGRAMS
C   (DY104) AND (HOUR5). THE INPUTS IN THIS SUBROUTINE ARE INTEGER
C   VALUES UNDER THE FOLLOWING VARIABLE NAMES:
C                                   IYEAR (CURRENT YEAR, MONTH I.E. 83)
C                                   MONTH (CURRENT MONTH, I.E. 3 )
C                                   IDAY  (CURRENT DAY IN THE MONTH)
C                                   CVLT  (THE CIVIL LOCAL TIME)
C                                   ALONGD (LONGITUDE IN DEGREES)
C                                   ALATD  (LATITUDE IN DEGREES)
C                                   ALONST (STD. LONG. IN DEGREES)
C                                   ZONE   (TIME ZONE OF THE LOCALITY
C                                          E-W OF GREENWICH)
C   THE OUTPUTS ARE: ALTR  (ALTITUDE UNITS ARE RADIANS)
C                    DECL  (DECLINATION UNITS ARE RADIANS)
C                    EOT   (EQUATION OF TIME UNITS ARE MINUTES)
C                    HANG  (HOUR ANGLE UNITS ARE RADDIANS)
C                    RADIUS (RADIUS OF EARTH'S ORBIT IN
C                           ASTRONOMICAL UNITS R/RAVE )
C   FOR OTHER POSSIBLE OUTPUTS COULD CONSIDER THE CALCULATED HOUR
C   ANGLE, THE ALTITUDE AND AZIMUTH ANGLES (IN RADIANS).
C   FOR SOME OF THE FOLLOWING CALCULATIONS, LOW PRECISION EQUATIONS
C   ARE USED  (TAKEN FROM THE ALMANAC FOR COMPUTERS 1984) AS
C   PRESENTED BY R.L. JOHNSON OF MCDONNELL DOUGLAS
C
C   THIS SUBROUTINE WAS TESTED BY COMPARING ITS COMPUTED VALUES
C   WITH THE ALMANAC OF COMPUTERS (PROGRAM (MCDON) FOR THE YEAR OF
C   AND THE LOCALITY OF GREENWICH).
C
C...DEFINITIONS OF VARIABLES
C     ANGCR  : MEAN ANOMALY
C     AZIM   : AZIMUTH, UNITS ARE RADIANS
C     ALONGH : LONGITUDE IN HOURS
C     ALONST : STANDARD LONGITUDE IN DEGREES
C     ALATR  : LATITUDE, UNITS ARE RADIANS
C     ALT    : ALTITUDE, UNITS ARE DEGREES
C     CVLT   : LOCAL TIME, UNITS ARE HOURS
C     DECL   : DECLINATION, UNITS ARE RADIANS
C     DRCONV : DEGREES TO RADIANS CONVERSION
C     ECLL   : ECLIPTIC LONGITUDE OR TRUE GEOCENTRIC LONGITUDE,
C              UNITS ARE RADIANS
C     ECLO   : OBLIQUITY OF THE ECLIPTIC, UNITS ARE RADIANS
C     GAST   : GREENWICH ACTUAL SIDERAL TIME, UNITS ARE HOURS
C     HANG   : LOCAL HOUR ANGLE OF THE SUN, UNITS ARE RADIANS
C     RADIUS : THE DISTANCE OF SUN TO EARTH IN ASTRONOMICAL UNITS
C     RTAS   : RIGHT ASCENSION, UNITS ARE RADIANS
C     SMALAL : SMALLEST ALTITUDE ALLOWED
```

```
C      TREF    : STANDARD EPOCH JANUARY 2000.0
C                WHICH IS 12 UT, 1 JANUARY 2000.0
C      UT      : UNIVERSAL TIME, LOCAL TIME FROM GRENWICH
C                MIDNIGHT IN HOURS
C      XCON    : STANDARD EPOCH 0 UT, 0JANUARY 1984
C                WHICH IS MIDNIGHT UT STARTING 31 DECEMBER 1983
C      XD      : DAYS SINCE STANDARD EPOCH TREF
C      XL1     : MEAN LONGITUDE
C      XN      : DAYS SINCE STANDARD EPOCH XCON
C
C...CONSTANTS
C...CONSTANTS FOR LOW PRECISION EQUATIONS FOR ECLL AND ECLO
       DATA  A1,A2,A3,A4,A5,A6,A7,A8,A9,TREF,XCON/6.2400408,
     &1.720197E-2,4.8934184,1.7202536E-2,3.3479055E-2,
     &2.2936565E-9,3.7606585E-4,4.0911372E-1,6.21199E-9,
     &2451545.0,2445699.5/
C...CONSTANTS FOR ATMOSPHERIC REFRACTION EQUATION
       DATA  B1,B2,B3,B4,B5/-9.036938093E-5,-1.600076095E-5,
     &2.948314656E-4,-3.278909E-6,-1.234081940E-8/
       PI=4.0*ATAN(1.0)
       TWOPI=2.0*PI
       DRCONV=PI/180.0
       ALONGH=ALONGD/15.
       ALATR=ALATD*DRCONV
       CLAT=COS(ALATR)
       SLAT=SIN(ALATR)
       SMALAL=0.008
       HRCONV=15.0*DRCONV
       IYEAR2=1900+IYEAR
C
       CALL JDAY(XJUDAT,IYEAR2,MONTH,IDAY)
C
C...CALCULATE THE UNIVERSAL TIME FOR THE LOCATION (EAST US: 5)
       UT=CVLT+ZONE
C...CALCULATE THE MEAN ANOMALY
       TD=XJUDAT-TREF+UT/24.0
       ANGCR=A1+A2*TD
       ANGCR=(ANGCR/TWOPI-AINT(ANGCR/TWOPI))*TWOPI
C...CALCULATE THE DISTANCE OF SUN FROM EARTH IN ASTRONOMICAL UNITS
       RADIUS=1.00014-0.01671*COS(ANGCR)-0.00014*COS(ANGCR)
C...CALCULATE THE MEAN LONGITUDE
       XL1=A3+A4*TD
C...CALCULATE THE TRUE LONGITUDE
       ECLL=XL1+(A5-A6*TD)*SIN(ANGCR)+A7*SIN(2.0*ANGCR)
       ECLL=(ECLL/TWOPI-AINT(ECLL/TWOPI))*TWOPI
C...CALCULATE THE OBLIQUITY
       ECLO=A8-A9*TD
C...CONVERT TO RT ASCENSION AND DECINATION
       RTAS=ATAN2(SIN(ECLL)*COS(ECLO),COS(ECLL))
       SLSE=SIN(ECLL)*SIN(ECLO)
       DECL=ATAN2(SLSE,SQRT(1.0-SLSE**2.0))
C...CALCULATE THE HOUR ANGLE
       XN=XJUDAT-XCON
       DAY=XN+UT/24.0
```

```
      HANG=HRCONV*(GAST(XN,UT,DAY)-ALONGH)-RTAS
      HANG=AMOD(HANG,TWOPI)
      IF (HANG.GT.PI.AND.HANG.LT.TWOPI) HANG=HANG-TWOPI
      IF (HANG.LT.-PI) HANG=HANG+TWOPI
C...CONVERT TO ELEVATION AND AZIMUTH
      ALT=ASIN(SLAT*SIN(DECL)+COS(DECL)*COS(HANG)*CLAT)
      IF (ALT.LT.SMALAL) ALT=SMALAL
      AZIM=-ATAN2(SIN(HANG),(COS(HANG)*SLAT-TAN(DECL)*CLAT))
C...REFRACTION, RC=0.0, IF ALT<=5 DEGREES=0.08727 RADIANS
C   NO CORRECTION FOR REFRACTION IS MADE FOR ALTITUDES LESS THAN
C   5 DEGREES
      RC=0.0
      IF (ALT.GT.0.08727)
     &RC=B1*(ALT)+B2+B3*(1/ALT)+B4*((1/ALT)**2.0)+B5*((1/ALT)**3)
      ALTR=ALT+RC
C...CALCULATE THE HOUR ANGLE IN DEGREES
      HANGDE=HANG/DRCONV
      HANGDE=AMOD(HANGDE,360.)
      IF (HANGDE.GT.180.0.AND.HANGDE.LT.360.0) HANGDE=HANGDE-360.
      IF (HANGDE.LT.-180.0.AND.HANGDE.GT.-360.0) HANGDE=HANGDE+360.
C...CALCULATE THE APARENT SOLAR TIME
      AST=HANGDE/15.+12.
C...CALCULATE THE MEAN SOLAR TIME
      AMST=CVLT+(ALONST-ALONGD)/15.0
C...CALCULATE THE EQUATION OF TIME
      EOT=(AST-AMST)*60.
      IF (HANGDE.GT.180) EOT=-EOT
      EOT=AMOD(EOT,1440.)
      IF (EOT.GT.1000.0.AND.EOT.LT.1440.0) EOT=EOT-1440.
      RETURN
      END
```

```
      FUNCTION GAST(XN,UT,DAY)
C
C
C           FUNCTION GAST
C
C
C...CALCULATE THE GREENWICH ACTUAL SIDERAL TIME
C   BASED ON EQUATIONS IN ALMANAC FOR COMPUTERS 1984
C
C...DEFINITIONS
C     DAY    : XN+UT/24.0
C     DRCONV : CONVERSION FROM DEGREES TO RADIANS
C     E      : EQUATION OF THE EQUINOXES, IN HOURS
C     GAST   : GREENWICH ACTUAL SIDERAL TIME, IN HOURS
C     GMST   : GREENWICH MEAN SIDERAL TIME(VERNAL EQUINOX ANGLE
C              FROM GREENWICH), IN HOURS.
C     UT     : LOCAL TIME (FROM GREENWICH MIDNIGHT), UNITS IN HOURS
C     XN     : DAYS SINCE STANDARD EPOCH XCON
C     XOMEGA : MEAN LONGITUDE OF ASCENDING NODE OF THE MOON'S ORBIT,
C    &         IN RADIANS
C
      DATA  G1,G2,G3,G4,G5,G6/6.5905966,0.0657098242,
     &      1.00273791,74.5658,-0.0529539,-0.00029/
      PI=4.0*ATAN(1.0)
      DRCONV=PI/180.
      GMST=G1+G2*XN+G3*UT
      GMST=24.0*(GMST/24.0-AINT(GMST/24.0))
      XOMEGA=DRCONV*(G4+G5*DAY)
      E=G6*SIN(XOMEGA)
C...IN THE NEXT STATEMENT GMST IS CORRECTED
C   FOR PERTUBATIONS INDUCED BY MOTION OF THE MOON TO
C   YIELD AN ACCURATE VALUE FOR GAST
      GAST=GMST+E
      RETURN
      END
```

```
      SUBROUTINE JDAY(XJUDAT,IYEAR2,MONTH,IDAY)
C
C
C                  SUBROUTINE JDAY
C
C
C...SUBROUTINE JDAY CALCULATES THE STANDARD JULIAN DATE
C   NOTE: VARIOUS STANDARD EPOCHS ARE USED IN APPLICATIONS
      JD=IDAY+1461*(IYEAR2+4800+(MONTH-14)/12)/4
     &   +367*(MONTH-2-(MONTH-14)/12*12)/12
      JD=JD-32075-3*((IYEAR2+4900+(MONTH-14)/12)/100)/4
      XJUDAT=JD-0.5D0
      RETURN
      END
```

```
      SUBROUTINE EXTRAD(DECL,HANG,RADIUS,HBNIO,HGIO,AZCOS,AHANG,DLO2)
C
C
C                SUBROUTINE EXTRAD
C
C
C...GIVEN DECLINATION AND HOUR ANGLE
C...COMPUTES EXTRATERRESTRIAL NORMAL AND GLOBAL
C...COMMONS
      COMMON /CNSTS/ ALATR,DELOMO2,GSCF,HRCONV
C
C...BEGIN COMPUTATIONS
      W1=HANG-DELOMO2
      W2=HANG+DELOMO2
C...DETERMINE SUNSET HOUR ANGLE
      SSHA=ACOS(-TAN(ALATR)*TAN(DECL) )
      DLO2=SSHA*HRCONV
C...ZERO OUTPUTS WHEN SUN HAS SET
      IF( (W1.GT.SSHA).OR.(W2.LT.-SSHA) ) THEN
C     SUN HAS SET
        HBNIO=HGIO=0.0
        AZCOS=-99.
        RETURN
      ENDIF
C...ADJUST INTERVAL AS NECESSARY
      IF(W1.LT.-SSHA) THEN
        W1=-SSHA
      ENDIF
      IF(W2.GT.SSHA) THEN
        W2=SSHA
      ENDIF
C...CALCULATE AVERAGE HOUR ANGLE
      AHANG=(W2+W1)/2.0
C...COMPLETE THE CALCULATIONS
      GONF=GSCF/RADIUS**2
      HBNIO=GONF*(W2-W1)
      HGIO =GONF*( COS(DECL)*COS(ALATR)*(SIN(W2)-SIN(W1) )+
     &       (W2-W1)*SIN(DECL)*SIN(ALATR) )
C...CALCULATE AVERAGE ZENITH COSINE
      IF((HGIO.LE.0.0).OR.(HBNIO.LE.0.0)) THEN
         AZCOS=-99.
         RETURN
      ENDIF
      AZCOS=HGIO/HBNIO
      RETURN
      END
```

APPENDIX B

SUBI	Subroutine to Calculate k_t and τ_b
AMASS	Function to Calculate Atmospheric Air Mass
TBLU1	Function for Lookup and Table Interpolation
TERP1	Function for Langragian Interpolation

```
      SUBROUTINE SUBI(OMEGA,ALATD,DELTA,BADPER,GSC,IFRST,R,HRZTOT,DIR,
     &KT,TB)
C
C                    SUBROUTINE SUBI
C                 C. BALARAS     5-31-85
C
C
C...SUBROUTINE TO CALCULATE KT AND TB AT THE MIDPOINT OF EACH PERIOD
C   INPUTS:
C          OMEGA   : HOUR ANGLE IN RADIANS (FROM HELGO)
C          ALATD   : LATITUDE OF LOCALITY IN DEGREES
C          DELTA   : DECLINATION IN RADIANS (FROM HELGO)
C          BADPER  : 15-MINUTE PERIOD MISSING FROM HOURLY DATA
C          GSC     : SOLAR CONSTANT, 1367 W/M/M
C          IFRST   : TO PREVENT REPETITION OF CALCULATIONS
C          R       : EARTH-SUN DISTANCE IN AU (FROM HELGO)
C          HRZTOT  : HOURLY HORIZONTAL IRRADIATION
C          DIR     : DIRECT BEAM IRRADIATION
C   OUTPUTS:
C          KT      : HOURLY CLEARNESS INDEX
C          TB      : HOURLY BEAM TRANSMITTANCE
C
      INTEGER BADPER
      REAL KT,ION,IO,IO2,ION2
      IF (IFRST.LT.1) GO TO 333
      PI=4.0*ATAN(1.0)
      DRCONV=PI/180.0
      ALAT=ALATD*DRCONV
      F1=GSC*12.0*3600.0/PI/1000.0
      FA1=3.6*GSC*180.0/PI/15.0
      IFRST=0
 333  CONTINUE
C...SUBROUTINE INITIALIZATIONS
      F2=F1/R**2
      FA2=FA1/R**2
      IO2=0.0
      ION2=0.0
      OMEG1A=0.0
      OMEG2A=0.0
      OMEG3A=0.0
      OMEG4A=0.0
C...CALCULATE THE HOUR ANGLES AT THE START END OF THE PERIOD
      OMEGA1=OMEGA-15.0/2.*DRCONV
      OMEGA2=OMEGA+15.0/2.*DRCONV
C...CORRECT HOUR ANGLES FOR FIRST AND LAST PERIODS OF DAY
      WSS=ACOS(-TAN(ALAT)*TAN(DELTA))
      IF(OMEGA2.GT.WSS) OMEGA2=WSS
      IF(OMEGA1.LT.-WSS) OMEGA1=-WSS
C
C...DETERMINE MISSING PERIOD
       IPD=IFIX(AMOD(FLOAT(BADPER),10.))
C...DETERMINE HOUR ANGLES
C   IF FIRST PERIOD IS MISSING
       IF (IPD.EQ.1) OMEGA1=OMEGA1+15./4.*DRCONV
```

```
C    IF LAST PERIOD IS MISSING
        IF (IPD.EQ.4) OMEGA2=OMEGA2-15./4.*DRCONV
C    IF SECOND PERIOD IS MISSING
        IF (IPD.EQ.2) THEN
        OMEG1A=OMEGA1+15./4.*DRCONV
        OMEG2A=OMEG1A+15./4.*DRCONV
C    CALCULATE THE EXTRATER. HORIZONTAL IRRADIATION
C    FOR THE MISSING PERIOD
         IO2=F2*((COS(DELTA)*COS(ALAT)*(SIN(OMEG2A)-SIN(OMEG1A)))
     &+((OMEG2A-OMEG1A)*SIN(DELTA)*SIN(ALAT)))
C    CALCULATE THE EXTRATTER. NORMAL IRRADIATION
C    FOR THE MISSING PERIOD
       ION2=FA2*(OMEG2A-OMEG1A)
        END IF
C    IF THIRD PERIOD IS MISSING
         IF (IPD.EQ.3) THEN
        OMEG3A=OMEGA1+15./2.*DRCONV
         OMEG4A=OMEG3A+15./4.*DRCONV
C    CALCULATE THE EXTRATER. HORIZONTAL IRRADIATION
C    FOR THE MISSING PERIOD
         IO2=F2*((COS(DELTA)*COS(ALAT)*(SIN(OMEG4A)-SIN(OMEG3A)))
     &+((OMEG4A-OMEG3A)*SIN(DELTA)*SIN(ALAT)))
C    CALCULATE EXTRATTER. NORMAL IRRADIATION
       ION2=FA2*(OMEG4A-OMEG3A)
        END IF
C
C...CALCULATE EXTRATERRESTRIAL NORMAL RADIATION
       GON=GSC/R**2
C
C...CALCULATE EXTRATERRESTRIAL NORMAL IRRADIATION
       ION=FA2*(OMEGA2-OMEGA1)
C...ACCOUNT FOR A MISSING PERIOD
       ION=ION-ION2
C
C...CALCULATE EXTRATERRESTRIAL HORIZONTAL IRRADIATION
       IO=F2*((COS(DELTA)*COS(ALAT)*(SIN(OMEGA2)-SIN(OMEGA1)))
     &+((OMEGA2-OMEGA1)*SIN(DELTA)*SIN(ALAT)))
C...ACCOUNT FOR A MISSING PERIOD
        IO=IO-IO2
C
C...CALCULATE CLEARNESS INDEX
       KT=HRZTOT/IO
C
C...CALCULATE BEAM NORMAL TRANSMITTANCE
       TB=DIR/ION
       RETURN
       END
```

```
      FUNCTION AMASS(ALT)
C
C
C...FUNCTION AMASS
C
C
C...CALCULATES STD AIR MASS RATIO AS FUNCTION OF SOLAR ALTITUDE
C...DECLARATIONS
      DIMENSION ALARR(9),AMARR(9)
C...INITIALIZATIONS
      DATA ALARR/0.,.017,.035,.052,.070,.087,.105,.122,.140/
      DATA AMARR/22.0,20.0,18.0,15.6,12.5,10.4,9.0,8.0,7.185/
C...BEGIN EVALUATION
      IF(ALT.LT.0.0) THEN
C       FOR NEGATIVE ALTITUDE
        AMASS=1.0E50
        RETURN
      ELSE
        IF(ALT.GE. 0.140) THEN
C         COSECANT FOR LARGER ALTITUDES
          AMASS=1.0/SIN(ALT)
          RETURN
        ELSE
C         TABULATION FOR SMALLER ALTITUDES
          AMASS=TBLU1(ALT,ALARR,AMARR,2,9,9)
          RETURN
        ENDIF
      ENDIF
      WRITE(6,*) 'AMASS SHOULD NOT REACH THIS LINE'
      RETURN
      END
```

```
C
      FUNCTION TBLU1(XX,X,Y,MD,N)
C
C
C                     FUNCTION TBLU1
C
C
C...TABLE LOOKUP AND INTERPOLATION

      DIMENSION Y(1)
      INTEGER SEARCH
C
C     X ALWAYS INCREASING (OR DECREASING)
      ND = MD
      IF(SEARCH(XX,X,ND,N,I) .EQ. 0)GO TO 43
C     RETURN EXACT VALUE
      TBLU1 = Y(I)
      GO TO 51
C      INTERPOLATE
   43 TBLU1 = TERP1(XX,X,Y,ND,I)
   51 RETURN
      END
C
      INTEGER FUNCTION SEARCH(Z,X,ND,M,IS)
C                              BINARY SEARCH
C
      DIMENSION X(1)
C     FUNCTION TO HALVE INDEX DURING BINARY SEARCH
      IHALF(I) = (I + 1)/2
C
      N = IABS(M)
      SEARCH = 1
      I = 1
      IF(N .LE. 1)GO TO 24
C     INPUT PARAMETER ND MAY BE CHANGED BECAUSE DEG. IS TOO LARGE
      ND = MINO(ND,N-1)
      IF(M .GE. 0)GO TO 445
C     TEST TO PREVENT EXTRAPOLATION WHEN N IS NEGATIVE
      IF(ABS(Z+Z-X(1)-X(N)) .LE. ABS(X(1)-X(N)))GO TO 445
      IF  (X(N).GT.X(1).AND.Z.GT.X(N))   I=N
      IF(X(N).LT.X(1).AND.Z.LT.X(N))   I=N
      GO TO 24
  445 IGO = 1
      IF(X(1) .GT. X(2))IGO = 0
C     DESCENDING X ARRAY

C     BINARY SEARCH TO BRACKET Z BETWEEN X(I) AND X(I+1)

      I = IHALF(N)
      IDLT = I

C     MAIN SEARCH LOOP

    5 IDLT = IHALF(IDLT)
```

```
      DIF = X(I) - Z
      IF(IGO .EQ. 0)DIF = -DIF
      IF(DIF)30,24,20

C     X(I) IS EXACT VALUE
   24 IS = I
      GO TO 52

C     I TOO LARGE (UNLESS I = 1)
   20 IF(I - 1)40,40,21
   21 IF(I - IDLT)22,22,23
C     IDLT TOO LARGE (BECAUSE N NOT POWER OF 2)
   22 IDLT = IHALF(IDLT)
   23 I = I - IDLT
      I=MAXO(I,1)
      GO TO 5

C     I OK OR TOO SMALL (UNLESS I = N)
   30 IF(I - N)31,40,40
C     Z NOT OUTSIDE RIGHT END OF TABLE
   31 DIF = X(I+1) - Z
      IF(IGO .EQ. 0)DIF = -DIF
      IF(DIF)34,36,40

C     X(I+1) IS EXACT VALUE
   36 IS = I + 1
      GO TO 52

C     I TOO SMALL
   34 I = I + IDLT
      IF(I - N)5,5,35

C     IDLT WAS TOO LARGE (BECAUSE N NOT POWER OF 2)
   35 I = I - IDLT
      IDLT = IHALF(IDLT)
      GO TO 34

C     Z BRACKETED BY X(I), X(I+1)
   40 IF(ND)44,44,43
C     ND .LE. 0 - - RETURN NEAREST POINT IN TABLE
   44 IF(I .EQ. N)GO TO 24
      IF(ABS(Z - X(I)) .LE. ABS(Z - X(I+1)))GO TO 24
      GO TO 36
C     FIND ND + 1 POINTS CENTERED (IF POSSIBLE) AROUND Z
   43 I = MINO(MAXO(1, I - (ND - 1)/2), N - ND)
      IS = I
      SEARCH = 0

   52 RETURN
      END
```

```
C
      FUNCTION TERP1(Z,X,Y,ND,I)
C                              LAGRANGIAN INTERPOLATION
      DIMENSION X(1), Y(1)
      N = I + ND
C     INTERPOLATE FOR Y(Z)
      TERP1 = 0.
      DO 50 J = I, N
      PX = 1.
      DO 42 K = I, N
      IF(K .EQ. J) GO TO 42
      PX = (PX/(X(J) - X(K)))*(Z - X(K))
   42 CONTINUE
   50 TERP1 = TERP1 + PX*Y(J)
   51 RETURN
      END
```

APPENDIX C

BCALCL	Calculations for Daily Annual Seasonal Factors
SEARCH	Function for Binary Search
BEAMNI	Calculations for Beam Normal Irradiation and Comparison of Basic and Seasonal Shenandoah Five Year Models
SYR	Subroutine to Calculate Day of Year
SUBIR	Subroutine to Calculate Extraterrestrial Irradiation and Clearness Index
SUBTB	Subroutine to Calculate Beam Transmittance for Basic and Seasonal Models
CRAD	Subroutine to Calculate Clear Day Beam Normal and Diffuse Horizontal Irradiation
SUBPLOT	Subroutine to Plot Monthly Average Daily Irradiation vs. Month of the Year

```
      PROGRAM BCALCL(INPUT,OUTPUT,TAPE5=INPUT,TAPE6=OUTPUT,TAPE2,
     &TAPE36,TAPE37,TAPE38,TAPE39,TAPE40,TAPE41)
C
C      C. BALARAS      7-30-85
C
C...THIS PROGRAM USES INTERPOLATION SUBROUTINES IN ORDER TO DETERMINE
C   THE SEASONAL FACTORS FOR EVERY DAY OF THE YEAR. THE DATA IS GIVEN
C   AT THE MID-POINT OF EVERY MONTH FOR ALL THE ANNUAL MODELS AND
C   ALSO THE 5-YR.
C...TO GET A PLOT OF THE SEASONAL FACTORS AGAINST THE DAY OF THE
C   YEAR HAVE TO CHANGE THE DO LOOP IN ORDER TO PLOT EVERY OTHER
C   FIFTH POINT.
C
C   TO RUN BCALCL DO AS FOLLOWS:
C          AT,CALCOMP,PLOTR/UN=LIBRARY
C          X,LIBRARY,CALCOMP
C          FTN5,I=BCALCL,L=0
C          LGO
C
C...DIMENSIONS
      DIMENSION DARR(16),FARR(16),IBUF(512)
      DIMENSION DARR79(16),FARR79(16),DARR80(15),FARR80(15)
      DIMENSION DARR81(14),FARR81(14),DARR83(13),FARR83(13)
      DIMENSION DARR84(12),FARR84(12)
C
C...DATA FOR THE 5-YEAR MODEL
      DATA DARR/-46.,-15.5,15.5,45.,74.5,105.,135.5,166.,196.5,227.5,
     &        258.,288.5,319.,349.5,380.5,410./
      DATA FARR/1.112819430513,1.150584021146,
     &1.090280732204,1.032839889323,0.9994031925052,
     &0.9893924379533,0.8858780740504,0.9668638483537,
     &0.8981737462856,0.8750437397945,0.9510854382403,
     &1.075994300622,1.112819430513,1.150584021146,
     &1.090280732204,1.032839889323/
C
C...DATA FOR THE 1979 MODEL
      DATA DARR79/-46.,-15.5,15.5,45.,74.5,105.,135.5,166.,196.5,227.5,
     &        258.,288.5,319.,349.5,380.5,410./
      DATA FARR79/1.092787424479,1.084911142215,
     &1.032139579574,0.991917118241,0.963483532136,
     &0.9181302224242,0.7245407972914,0.8594481112892,
     &0.8853363843749,0.884710801937,0.783950228733,
     &1.046071551677,1.092787424479,1.084911142215,
     &1.032139579574,0.991917118241/
C
C...DATA FOR THE 1980 MODEL (DECEMBER IS MISSING)
      DATA DARR80/-76.5,-46.,15.5,45.,74.5,105.,135.5,166.,196.5,227.5,
     &        258.,288.5,319.,380.5,410./
      DATA FARR80/1.042244358951,
     &1.085864383893,1.059509046709,0.9961142364608,
     &0.9628604949356,0.9900239277385,0.8080860939143,
     &0.9003335388831,0.7848468282467,0.8574302460837,
     &0.8490471351617,1.042244358951,1.085864383893,
     &1.059509046709,0.9961142364608/
```

```
C
C...DATA FOR THE 1981 MODEL (MAY AND NOVEMBER ARE MISSING)
      DATA DARR81/-76.5,-15.5,15.5,45.,74.5,105.,166.,196.5,227.5,258.,
     &        288.5,349.5,380.5,410./
      DATA FARR81/1.127652272685,
     &1.227356492727,1.172972439337,1.123864103601,
     &1.061209296254,1.003169956122,0.9885802713705,
     &0.9131805638459,0.8489704186377,1.055424867906,
     &1.127652272685,1.227356492727,1.172972439337,
     &1.123864103601/
C
C...DATA FOR THE 1983 MODEL (JAN, AUGUST, SEPT, ARE MISSING)
      DATA DARR83/-46.,-15.5,45.,74.5,105.,135.5,166.,196.5,
     &        288.5,319.,349.5,410.,439.5/
      DATA FARR83/1.158839320263,1.359432317192,1.089944293619,
     &0.9882797294025,1.025492037989,0.9818527100992,
     &1.011531702683,1.013243020432,1.205804750524,
     &1.158839320263,1.359432317192,1.089944293619,
     &0.9882797294025/
C
C...DATA FOR THE 1984 MODEL (FEB, MARCH, APRIL,JUNE ARE MISSING)
      DATA DARR84/-46.,-15.5,15.5,135.5,196.5,227.5,258.,
     &        288.5,319.,349.5,380.5,500.5/
      DATA FARR84/1.157031509529,1.163610381837,1.287810018201,
     &0.9924953248904,0.8177878908015,0.9038915498049,
     &1.003255627719,1.046434065597,1.157031509529,
     &1.163610381837,1.287810018201,0.9924953248904/
C
C...OPEN PLOT FILES
      CALL PLOTS(IBUF,512,2,40)
      CALL PLOTMX(18.5)
      CALL PLOT(3.0,1.0,-3)
C...DRAW X-AXIS
      CALL AXIS(0.0,0.0,'DAY OF YEAR',-11,13.0,0.0,0.0,30.0)
C...DRAW Y-AXIS
      CALL AXIS(0.0,0.0,'SEASONAL FACTOR',15,8.0,90.0,0.6,0.1)
      CALL AXIS(12.16667,0.0,'SEASONAL FACTOR',-15,8.0,90.0,0.6,0.1)
C...TITLE GRAPH
      CALL SYMBOL(5.5,8.0,0.07,0,0.0,-1)
      CALL SYMBOL(5.75,8.0,0.07,0,0.0,-1)
      CALL SYMBOL(6.0,8.0,0.07,0,0.0,-1)
      CALL SYMBOL(6.15,8.0,0.14,4H1979,0.0,4)
      CALL SYMBOL(5.5,7.75,0.07,1,0.0,-1)
      CALL SYMBOL(5.75,7.75,0.07,1,0.0,-1)
      CALL SYMBOL(6.0,7.75,0.07,1,0.0,-1)
      CALL SYMBOL(6.15,7.75,0.14,4H1980,0.0,4)
      CALL SYMBOL(5.5,7.50,0.085,2,0.0,-1)
      CALL SYMBOL(5.75,7.50,0.085,2,0.0,-1)
      CALL SYMBOL(6.0,7.50,0.085,2,0.0,-1)
      CALL SYMBOL(6.15,7.50,0.14,4H1981,0.0,4)
      CALL SYMBOL(5.5,7.25,0.07,4,0.0,-1)
      CALL SYMBOL(5.75,7.25,0.07,4,0.0,-1)
      CALL SYMBOL(6.0,7.25,0.07,4,0.0,-1)
      CALL SYMBOL(6.15,7.25,0.14,4H1983,0.0,4)
```

```
      CALL SYMBOL(5.5,7.0,0.085,14,0.0,-1)
      CALL SYMBOL(5.75,7.0,0.085,14,0.0,-1)
      CALL SYMBOL(6.0,7.0,0.085,14,0.0,-1)
      CALL SYMBOL(6.15,7.0,0.14,4H1984,0.0,4)
      AINCR=0.0
C
      DO 77 IK=1,11
      CALL SYMBOL(5.5+AINCR,6.75,0.05,19,0.0,-1)
      AINCR=AINCR+0.05
 77   CONTINUE
C
      CALL SYMBOL(6.15,6.75,0.14,4H5-YR,0.0,4)
C
C...PLOT THE FIRST POINTS AT 0 DAY
      B79=TBLU1(0.0,DARR79,FARR79,3,16,16)
      BE79=(B79/0.1)-6.0
      CALL SYMBOL(0.0,BE79,0.07,0,0.0,-1)
      B80=TBLU1(0.0,DARR80,FARR80,3,15,15)
      BE80=(B80/0.1)-6.0
      CALL SYMBOL(0.0,BE80,0.07,1,0.0,-1)
      B81=TBLU1(0.0,DARR81,FARR81,3,14,14)
      BE81=(B81/0.1)-6.0
      CALL SYMBOL(0.0,BE81,0.085,2,0.0,-1)
      B83=TBLU1(0.0,DARR83,FARR83,2,13,13)
      BE83=(B83/0.1)-6.0
      CALL SYMBOL(0.0,BE83,0.07,4,0.0,-1)
      B84=TBLU1(0.0,DARR84,FARR84,2,12,12)
      BE84=(B84/0.1)-6.0
      CALL SYMBOL(0.0,BE84,0.085,14,0.0,-1)
      B=TBLU1(0.0,DARR,FARR,3,16,16)
      BE=(B/0.1)-6.0
      CALL SYMBOL(0.0,BE,0.07,19,0.0,-1)
C     WRITE(37,9001) B79
C     WRITE(38,9001) B80
C     WRITE(39,9001) B81
C     WRITE(40,9001) B83
C     WRITE(41,9001) B84
C     WRITE(36,9001) B
C9001 FORMAT(4X,F10.8)
C
C...IN ORDER TO CREATE THE PLOT USE : DO 10 I=5,365,5
      DO 10 I=1,365
            XD=FLOAT(I)
            B79=TBLU1(XD,DARR79,FARR79,3,16,16)
            B80=TBLU1(XD,DARR80,FARR80,3,15,15)
            B81=TBLU1(XD,DARR81,FARR81,3,14,14)
            B83=TBLU1(XD,DARR83,FARR83,2,13,13)
            IF (I.GT.45.AND.I.LE.349) THEN
            B83=TBLU1(XD,DARR83,FARR83,3,13,13)
            END IF
            B84=TBLU1(XD,DARR84,FARR84,2,12,12)
            IF (I.GT.136.5.AND.I.LT.320) THEN
            B84=TBLU1(XD,DARR84,FARR84,3,12,12)
            END IF
```

```
C             PLOT THIS DATUM
C             SCALES
              XDAY=XD/30.
C             FOR 1979
              BE79=(B79/0.1)-6.
              CALL SYMBOL(XDAY,BE79,0.07,0,0.0,-1)
              WRITE(37,9000) I,B79
C             FOR 1980
              BE80=(B80/0.1)-6.
              CALL SYMBOL(XDAY,BE80,0.07,1,0.0,-1)
              WRITE(38,9000) I,B80
C             FOR 1981
              BE81=(B81/0.1)-6.
              CALL SYMBOL(XDAY,BE81,0.08,2,0.0,-1)
              WRITE(39,9000) I,B81
C             FOR 1983
              BE83=(B83/0.1)-6.
              CALL SYMBOL(XDAY,BE83,0.07,4,0.0,-1)
              WRITE(40,9000) I,B83
C             FOR 1984
              BE84=(B84/0.1)-6.
              CALL SYMBOL(XDAY,BE84,0.08,14,0.0,-1)
              WRITE(41,9000) I,B84
C
9000   FORMAT(I3,1X,F10.8)
C
10     CONTINUE
C
C...REPEAT CALCULATIONS FOR 5-YEAR
       DO 11 I=1,365
              XD=FLOAT(I)
              B=TBLU1(XD,DARR,FARR,3,16,16)
              XDAY=XD/30
              BE=(B/0.1)-6.
              CALL SYMBOL(XDAY,BE,0.07,19,0.0,-1)
              WRITE(36,9000) I,B
 11    CONTINUE
C
C...CLOSE PLOTTING FILE
       CALL PLOT(7.0,0.0,3)
       CALL PLOT(7.0,0.0,999)
C
       STOP
       END
```

```
      INTEGER FUNCTION SEARCH(Z,X,ND,M,IS)
C                              BINARY SEARCH
C
      DIMENSION X(1)
C     FUNCTION TO HALVE INDEX DURING BINARY SEARCH
      IHALF(I) = (I + 1)/2
C
      N = IABS(M)
      SEARCH = 1
      I = 1
      IF(N .LE. 1)GO TO 24
C     INPUT PARAMETER ND MAY BE CHANGED BECAUSE DEG. IS TOO LARGE
      ND = MINO(ND,N-1)
      IF(M .GE. 0)GO TO 445
C     TEST TO PREVENT EXTRAPOLATION WHEN N IS NEGATIVE
      IF(ABS(Z+Z-X(1)-X(N)) .LE. ABS(X(1)-X(N)))GO TO 445
      IF  (X(N).GT.X(1).AND.Z.GT.X(N))   I=N
      IF(X(N).LT.X(1).AND.Z.LT.X(N))   I=N
      GO TO 24
  445 IGO = 1
      IF(X(1) .GT. X(2))IGO = 0
C     DESCENDING X ARRAY

C     BINARY SEARCH TO BRACKET Z BETWEEN X(I) AND X(I+1)

      I = IHALF(N)
      IDLT = I

C     MAIN SEARCH LOOP

    5 IDLT = IHALF(IDLT)
      DIF = X(I) - Z
      IF(IGO .EQ. 0)DIF = -DIF
      IF(DIF)30,24,20

C     X(I) IS EXACT VALUE
   24 IS = I
      GO TO 52

C     I TOO LARGE (UNLESS I = 1)
   20 IF(I - 1)40,40,21
   21 IF(I - IDLT)22,22,23
C     IDLT TOO LARGE (BECAUSE N NOT POWER OF 2)
   22 IDLT = IHALF(IDLT)
   23 I = I - IDLT
      I=MAXO(I,1)
      GO TO 5

C     I OK OR TOO SMALL (UNLESS I = N)
   30 IF(I - N)31,40,40
C     Z NOT OUTSIDE RIGHT END OF TABLE
   31 DIF = X(I+1) - Z
      IF(IGO .EQ. 0)DIF = -DIF
      IF(DIF)34,36,40
```

```
C       X(I+1) IS EXACT VALUE
   36   IS = I + 1
        GO TO 52

C       I TOO SMALL
   34   I = I + IDLT
        IF(I - N)5,5,35

C       IDLT WAS TOO LARGE (BECAUSE N NOT POWER OF 2)
   35   I = I - IDLT
        IDLT = IHALF(IDLT)
        GO TO 34

C       Z BRACKETED BY X(I), X(I+1)
   40   IF(ND)44,44,43
C       ND .LE. 0 - - RETURN NEAREST POINT IN TABLE
   44   IF(I .EQ. N)GO TO 24
        IF(ABS(Z - X(I)) .LE. ABS(Z - X(I+1)))GO TO 24
        GO TO 36
C       FIND ND + 1 POINTS CENTERED (IF POSSIBLE) AROUND Z
   43   I = MINO(MAXO(1, I - (ND - 1)/2), N - ND)
        IS = I
        SEARCH = 0

   52   RETURN
        END
```

```
      PROGRAM BEAMNI(INPUT,OUTPUT,TAPE5=INPUT,TAPE6=OUTPUT,TAPE12,
     &               TAPE36,TAPE2,TAPE7)
C
C     C. BALARAS      8-2-85
C     C. BALARAS      8-12-85
C
C...THIS PROGRAM CAN BE USED TO COMPARE TWO MODELS: THE 5-YRF MODEL
C   AND THE 5-YEAR SEASONAL FACTOR (B)*5-YRF MODEL. THE COMPARISON
C   IS BASED ON HOW WELL THEY PREDICT THE BEAM NORMAL IRRADIATION,
C   WHEN ONLY THE GLOBAL IRRADIATION IS AVAILABLE. THESE CALCUALTIONS
C   WILL BE PERFORMED BASED ON THE DATA COLLECTED IN ATLANTA, GA.
C   THE DATA (IN TX3 FROM UN=MEFACBL) IS IN AN HOURLY FORMAT.
C   IT INCLUDES THE DAY OF THE YEAR, SOLAR TIME,
C   STD TIME, AND THE IRRADIATION VALUES RECORDED AT THE END
C   OF THE HOURLY PERIOD. THE DATA FOR EACH MONTH IS A COLLECTION
C   FROM DIFFERENT REPRESENTATIVE YEARS:
C   JAN-1953, FEB-1971, MAR-1969, APR-1965, MAY-1957, JUN-1957,
C   JUL-1957, AUG-1959, SEP-1963, OCT-1967, NOV-1967, DEC-1970
C   THE PREDICTED VALUES ARE FINALLY COMPARED WITH THE AVAILABLE
C   MEASURED VALUE OF BEAM NORMAL IRRADIATION. A PLOT IS PRODUCED
C   WITH THE AVERAGE VALUE OF BEAM NORMAL IRRADIATION FOR EACH MONTH,
C   OF THIS TYPICAL YEAR.
C
C   TO RUN BEAMNI DO AS FOLLOWS:
C         AT, CALCOMP,PLOTR/UN=LIBRARY
C         X,LIBRARY,CALCOMP
C         G,BCALCL            (PROGRAM TO CREATE THE 5-YR B'S)
C         FTN5,I=BCALCL,L=0
C         LGO                  (CREATE TAPE36: (5-YR) B'S)
C            AT,TX3/UN=MEFACBL           (DATA FILE)
C            C,TX3,TAPE12
C         FTN5,I=BEAMNI,L=0
C         LGO
C
C...DIMENSIONS
      DIMENSION AMOLN(12),H(12),H1(12),H2(12)
      DIMENSION HAV(12),H1AV(12),H2AV(12)
C...DECLARATIONS
      REAL AMOP
      COMMON /SUBTB/ BAR(365)
C...INITIALIZATIONS
      ALATD=33.65
      ALONGD=84.43
      ALONST=75.0
      ZONE=5.0
      GSC=1367.0
      IFRST=1
      MOC=1
      H(1)=0.0
      H1(1)=0.0
      H2(1)=0.0
      HYR=0.0
      HYR1=0.0
      HYR2=0.0
```

```
C
C...READ THE 5-YR SEASONAL FACTORS (B)
C   FOR EVERY DAY OF THE YEAR
      DO 10 I=1,365
      READ(36,11) B
 11   FORMAT(4X,F10.8)
C...PLACE DATA IN ARRAYS
      BAR(I)=B
 10   CONTINUE
C
      DO 100 IJ=1,8760
C
C...READ THE HOURLY DATA FOR A YEAR
C   IHR, MIN : STANDARD TIME
C   GLOBI    : GLOBAL IRRADIANCE IN (KJ/M/M)
C   BNI      : BEAM NORMAL IRRADIANCE IN KJ/M/M
      READ(12,101) MO,IDAY,IHR,MIN,BNI,GLOBI
 101  FORMAT(I2,I2,4X,I2,I2,4X,F4.0,4X,F4.0)
C
C...CALL SUBROUTINE (SYR) TO CALCULATE FROM THE MONTH
C   THE YEAR ,THE DAY OF THE YEAR AND THE LENGTH OF THE MONTH IN DAYS
      CALL SYR(MO,IDAY,IYEAR,IDAYYR,AMOLN)
C
C...CALL SUBROUTINE HELGO FOR TIME-0.5 HOURS
      CVLT=(IHR+MIN/60.0)-0.5
      IYR=IYEAR-1900
      CALL HELGO(IYR,MO,IDAY,CVLT,ALONGD,ALATD,ALONST,ZONE,
     &ALTR,DELTAR,EOT,OMEGAR,RADIUS)
C
C...CALL SUBROUTINE IRRADIATION TO CALCULATE CLRIND, AND ION
      CALL SUBIR(OMEGAR,ALATD,DELTAR,GSC,RADIUS,GLOBI,IFRST,CLRIND,
     &           EXTRBN,EXTRG,ICALC)
C
C...IF THE PERIOD IS BEFORE SUNRISE SKIP FOLLOWING CALCULATIONS
C   ICALC: CONTINUE CALCULATIONS 0=YES 1=NO
      IF (ICALC.EQ.1) GO TO 200
C
C...CALL SUBROUTINE BEAM TRANSMITTANCE
      CALL SUBTB(CLRIND,IDAYYR,TB1,TB2)
C
C...CALCULATE THE BEAM NORMAL IRRADIATION USING
C   THE 5-YR MODEL TO PREDICT TB1
      BNI1=TB1*EXTRBN
C   THE B*5-YR MODEL TO PREDICT TB2
      BNI2=TB2*EXTRBN
C
C...CALCULATE THE AVERAGE ALTITUDE (ALTAV) VALUE
      ALTAV=ASIN(EXTRG/EXTRBN)
C
C...CORRECT BEAM NORMAL IRADIATION FOR LOW ALTITUDES
C   ALTAV<=6 DEGREES = 0.10472 RADIANS
C   WITH THE CLEAR DAY BEAM NORMAL VALUES
      IF (ALTAV.LT.0.10472) THEN
```

```
C...CALL SUBROUTINE (CRAD) TO CALCULATE CLEAR DAY IRRADIATION VALUES
C   DAY OF THE YEAR AS A REAL
      ANYR=FLOAT(IDAYYR)
      CALL CRAD(IDAYYR,ALTAV,EXTRBN,CBNI,CDHI,CGLOB)
      IF (BNI1.GT.CBNI) BNI1=CBNI
      IF (BNI2.GT.CBNI) BNI2=CBNI
      END IF
C
C...CALCULATE THE BEAM NORMAL IRRADIATION FOR EACH MONTH
      IF (MOC.EQ.MO) THEN
          H(MO)=H(MO)+BNI
          H1(MO)=H1(MO)+BNI1
          H2(MO)=H2(MO)+BNI2
      ELSE
C         A MONTH HAS BEEN COMPLETED
C         RESET TOTAL MONTHLY IRRADIATION VALUES TO ZERO
C         FOR THE FOLLOWING MONTH
          H(MO)=0.0
          H1(MO)=0.0
          H2(MO)=0.0
C         INCREMENT COUNTER
          MOC=MOC+1
      END IF
 200  ICALC=0
C
 100  CONTINUE
C
C...CALCULATE THE CORRESPONDING MONTHLY AVERAGE DAILY IRRADIATION
      DO 336 II=1,12
            HAV(II)=H(II)/AMOLN(II)
            H1AV(II)=H1(II)/AMOLN(II)
            H2AV(II)=H2(II)/AMOLN(II)
            WRITE(7,*) 'HAV=',HAV(II),'H1AV=',H1AV(II),'H2AV=',H2AV(II)
 336  CONTINUE
C
C...PLOT THE DATA
      CALL SUBPLOT(HAV,H1AV,H2AV)
C
C...CALCLULATE TOTAL ANNUAL IRRADIATION
      DO 335 IL=1,12
        HYR=HYR+H(IL)
        HYR1=HYR1+H1(IL)
        HYR2=HYR2+H2(IL)
 335  CONTINUE
      WRITE(7,*) 'HYR=',HYR,'HYR1=',HYR1,'HYR2=',HYR2
C
C...CALCULATE ANNUAL AVERAGE DAILY IRRADIATION
      HYRAV=HYR/365.0
      HYRAV1=HYR1/365.0
      HYRAV2=HYR2/365.0
      WRITE(7,*) 'HYRAV=',HYRAV,'HYRAV1=',HYRAV1,'HYRAV2=',HYRAV2
C
      STOP
      END
```

```
      SUBROUTINE SYR(MO,IDAY,IYEAR,IDAYYR,AMOLN)
C
C
C                  SUBROUTINE SYR
C              C. BALARAS     8-8-85
C
C
C...SUBROUTINE TO CALCULATE THE YEAR THAT THE MONTHLY DATA
C   WAS TAKEN FROM, AND THE DAY OF THE YEAR
C   INPUTS:
C           MO       : MONTH THE DATA IS GIVEN FOR
C           IDAY     : DAY OF THE MONTH
C   OUTPUTS:
C           IYEAR    : THE YEAR THE MONTHLY DATA WAS TAKEN FROM
C           IDAYYR   : DAY OF THE YEAR
C
      DIMENSION AMOLN(12)
      IF (MO.EQ.1) THEN
           IYEAR=1953
           IDAYYR=IDAY
           AMOLN(1)=31
      ELSE IF (MO.EQ.2) THEN
           IYEAR=1971
           IDAYYR=IDAY+31
           AMOLN(2)=28
      ELSE IF (MO.EQ.3) THEN
           IYEAR=1969
           IDAYYR=IDAY+59
           AMOLN(3)=31
      ELSE IF (MO.EQ.4) THEN
           IYEAR=1965
           IDAYYR=IDAY+90
           AMOLN(4)=30
      ELSE IF (MO.EQ.5) THEN
           IYEAR=1957
           IDAYYR=IDAY+120
           AMOLN(5)=31
      ELSE IF (MO.EQ.6) THEN
           IYEAR=1957
           IDAYYR=IDAY+151
           AMOLN(6)=30
      ELSE IF (MO.EQ.7) THEN
           IYEAR=1970
           IDAYYR=IDAY+181
           AMOLN(7)=31
      ELSE IF (MO.EQ.8) THEN
           IYEAR=1959
           IDAYYR=IDAY+211
           AMOLN(8)=31
      ELSE IF (MO.EQ.9) THEN
           IYEAR=1963
           IDAYYR=IDAY+242
           AMOLN(9)=30
      ELSE IF (MO.EQ.10) THEN
```

```
      IYEAR=1967
      IDAYYR=IDAY+272
      AMOLN(10)=31
ELSE IF (MO.EQ.11) THEN
      IYEAR=1967
      IDAYYR=IDAY+303
      AMOLN(11)=30
ELSE
      IYEAR=1970
      IDAYYR=IDAY+334
      AMOLN(12)=31
END IF
RETURN
END
```

```
      SUBROUTINE SUBIR(OMEGAR,ALATD,DELTAR,GSC,R,GLOBI,IFRST,CLRIND,
     &                 EXTRBN,EXTRG,ICALC)
C
C     C. BALARAS    8-2-85
C
C...SUBROUTINE TO CALCULATE IRRADIATION VALUES AND CLRIND
C   AT THE MID POINT OF THE HOURLY PERIOD
C   INPUTS:
C          OMEGAR  : HOUR ANGLE IN RADIANS (FROM HELGO)
C          ALATD   : LATITUDE OF LOCALITY IN DEGREES
C          DELTAR  : DECLINATION IN RADIANS (FROM HELGO)
C          GSC     : SOLAR CONSTANT, 1367 W/M/M
C          GLOBI   : GLOBAL IRRADIATION IN KJ/M/M
C          IFRST   : TO PREVENT REPETITION OF CALCULATIONS
C          R       : EARTH-SUN DISTANCE (FROM HELGO)
C   OUTPUTS:
C          CLRIND  : HOURLY CLEARNESS INDEX
C          EXTRBN  : HOURLY EXTRATTERESTRIAL NORMAL IRRADIATION
C          EXTRG   : HOURLY EXTRATERRESTRIAL GLOBAL IRRADIATION
C
C
      IF (IFRST.LT.1) GO TO 300
C...CONSTANTS
      PI=4.0*ATAN(1.0)
      DRCONV=PI/180.0
      ALATR=ALATD*DRCONV
      F1=GSC*12.0*3600.0/PI/1000.0
      IFRST=0
  300 CONTINUE
C
C...SUBROUTINE INITIALIZATIONS
      F2=F1/R/R
C
C...CALCULATE THE HOUR ANGLES AT THE START-END OF
C   EACH HOURLY PERIOD
      OMEGA1=OMEGAR-15.0/2.*DRCONV
      OMEGA2=OMEGAR+15.0/2.*DRCONV
C
C...CORRECT HOUR ANGLES FOR FIRST AND LAST PERIODS OF A DAY
C   BASED ON SUNSET HOUR ANGLE
      WSS=ACOS(-TAN(ALATR)*TAN(DELTAR))
      IF (OMEGA2.GT.WSS) OMEGA2=WSS
      IF (OMEGA1.LT.-WSS) OMEGA1=-WSS
C
C...CALCULATE EXTRATERRESTRIAL HORIZONTAL IRRADIATION
      EXTRG=F2*((COS(DELTAR)*COS(ALATR)*(SIN(OMEGA2)-SIN(OMEGA1)))+
     &((OMEGA2-OMEGA1)*SIN(DELTAR)*SIN(ALATR)))
C
C...CALCULATE EXTRATERRESTRIAL NORMAL IRRADIATION
      EXTRBN=F2*(OMEGA2-OMEGA1)
C
C...CALCULATE HOURLY CLEARNESS INDEX
      CLRIND=GLOBI/EXTRG
C
```

```
C...FOR WHOLE PERIODS BEFORE SUNRISE AND AFTER SUNSET
C   SET IRRADIATION VALUES EQUAL TO ZERO AND
C   SKIP ANY FOLLOWING CALCULATIONS (SET ICALC=1)
      IF (OMEGA2.LT.-WSS.OR.OMEGA1.GT.WSS) THEN
         EXTRG=0.0
         EXTRBN=0.0
         CLRIND=0.0
         ICALC=1
      END IF
C
      RETURN
      END
```

```
      SUBROUTINE SUBTB(CLRIND,IDAYYR,TB1,TB2)
C
C
C                SUBROUTINE SUBTB
C              C. BALARAS     8-2-85
C
C
C...SUBROUTINE TO CALCULATE THE BEAM TRANSMITTANCE FROM CLRIND
C   THERE ARE TWO AVAILABLE WAYS:
C   FIRST, USE A DIRECT RELATIONSHIP OF TB AND CLRIND, BASED ON
C   THE 5-YR MODEL, TB1=YO+(CLRIND-XO)*BETA(5-YR)
C   SECONDLY, USE THE RELATIONSHIP TB2=B*(YO+(CLRIND-XO)*BETA(5-YR))
C   WHERE B: SEASONAL FACTOR
C   INPUTS:
C          CLRIND : HOURLY CLEARNESS INDEX
C          BAR    : 5-YR SEASONAL FACTOR (B) VALUES FOR
C                   EACH DAY OF THE YEAR
C          IDAYYR : DAY OF THE YEAR
C   OUTPUTS:
C          TB1    : HOURLY BEAM TRANSMITTANCE CALCULATED USING THE
C                   5-YR MODEL REGRESSION COEFFICIENTS
C                   TB1=YO+(CLRIND-XO)*BETA(5YR)
C          TB2    : HOURLY BEAM TRANSMITTANCE CALCULATED USING THE
C                   5-YR SEASONAL FACTORS AND 5-YR MODEL REGRESSION
C                   COEFFICIENTS TB2=B*TB1
C
C...DIMENSION
      DIMENSION BETA(9),BAR(365),XO(10),YO(9)
C...DECLARATIONS
C
      COMMON /SUBTB/ BAR
      DATA IFRST2/1/
C
      IF (IFRST2.LT.1) GO TO 333
C
C...5-YR MODEL REGRESSION COEFFICIENTS
      BETA(1)=0.0
      BETA(2)=0.00071780490389l6
      BETA(3)=0.02972517920018
      BETA(4)=0.2490303701482
      BETA(5)=0.9466134865964
      BETA(6)=1.477191594315
      BETA(7)=1.56801154
      BETA(8)=2.077319493401
      BETA(9)=1.377810138749
C
C...DEFINE THE XO,YO COORDINATES FOR EACH
C   BAND OF THE 5-YR MODEL
      XO(1)=0.0
      XO(2)=0.05
      XO(3)=0.15
      XO(4)=0.25
      XO(5)=0.35
      XO(6)=0.45
```

```
      XO(7)=0.55
      XO(8)=0.65
      XO(9)=0.75
      XO(10)=0.85
      YO(1)=0.0
      DO 334 IK=2,9
      YO(IK)=YO(IK-1)+BETA(IK-1)*(XO(IK)-XO(IK-1))
 334  CONTINUE
      IFRST2=0
 333  CONTINUE
C
C   ******** 5-YR MODEL TB=YO+(CLRIND-XO)*BETA ********
C...FIRST CALCULATE TB1
C   DEPENDING ON CLRIND CHOOSE THE CORRESPONDING BETA
C...SECONDLY CALCULATE TB2
C   DEPENDING ALSO ON THE DAY OF THE YEAR TO CHOOSE THE
C   CORRESPONDING SEASONAL FACTOR
      IF (CLRIND.LE.0.05) THEN
           TB1=YO(1)+(CLRIND-XO(1))*BETA(1)
           TB2=BAR(IDAYYR)*TB1
      ELSE IF (CLRIND.LE.0.15) THEN
           TB1=YO(2)+(CLRIND-XO(2))*BETA(2)
           TB2=BAR(IDAYYR)*TB1
      ELSE IF (CLRIND.LE.0.25) THEN
           TB1=YO(3)+(CLRIND-XO(3))*BETA(3)
           TB2=BAR(IDAYYR)*TB1
      ELSE IF (CLRIND.LE.0.35) THEN
           TB1=YO(4)+(CLRIND-XO(4))*BETA(4)
           TB2=BAR(IDAYYR)*TB1
      ELSE IF (CLRIND.LE.0.45) THEN
           TB1=YO(5)+(CLRIND-XO(5))*BETA(5)
           TB2=BAR(IDAYYR)*TB1
      ELSE IF (CLRIND.LE.0.55) THEN
           TB1=YO(6)+(CLRIND-XO(6))*BETA(6)
           TB2=BAR(IDAYYR)*TB1
      ELSE IF (CLRIND.LE.0.65) THEN
           TB1=YO(7)+(CLRIND-XO(7))*BETA(7)
           TB2=BAR(IDAYYR)*TB1
      ELSE IF (CLRIND.LE.0.75) THEN
           TB1=YO(8)+(CLRIND-XO(8))*BETA(8)
           TB2=BAR(IDAYYR)*TB1
      ELSE
           TB1=YO(9)+(CLRIND-XO(9))*BETA(9)
           TB2=BAR(IDAYYR)*TB1
      END IF
C
      RETURN
      END
```

```
      SUBROUTINE CRAD(ANYR,ALT,BNIO,CBNI,CDHI,CGLOB)
C
C
C                     SUBROUTINE CRAD
C
C
C...COMPUTES CLEAR-DAY BEAM-NORMAL AND DIF-HORIZONTAL
C...FROM SIMPLE MODELS
C...OUTPUT
C   CBNI  : CLEAR DAY HOURLY BEAM-NORMAL IRRADIATION
C   CDHI  : CLEAR DAY HOURLY DIFFUSE-HORIZONTAL IRRADIATION
C   CGLOB : CLEAR DAY GLOBAL IRRADIATION
C
C...INPUT
C   ANYR : DAY SINCE 0 JAN CURRENT YEAR (REAL)
C   ALT  : SOLAR ALTITUDE (RADIANS)
C   BNIO : EXTRATERRESTRIAL BEAM NORMAL IRRADIATION (KJ/(SQ-METER) )
C
C...DECLARATIONS
      DIMENSION DARR(25),ECARR(25)
C
C...INITIALIZATIONS
      DATA ECARR/.1976,.1974,.2012,.2077,.2168,.2184,.2388,.2526,
     &.2631,.2744,.2855,.2962,.3009,.3048,.3073,.3047,.2978,.2862
     &,.2708,.2536,.2353,.219,.2057,.1971,.1930/
      DATA DARR/1.,16.,31.,46.,61.,76.,91.,106.,121.,136.,151.,
     &166.,181.,196.,211.,226.,241.,256.,271.,286.,301.,316.,331.,
     &346.,365./
C
C...BEGIN COMPUTATIONS
      IF(ALT.LT. 0.0) THEN
        CBNI=0.0
        CDHI=0.0
        RETURN
      ENDIF
C
C...CALCULATE EXTINCTION COEFFICIENT
      EXTC=TBLUI(ANYR,DARR,ECARR,2,25,25)
C
C...CALCULATE BEAM IRRADIATION
      AM=AMASS(ALT)
      TAUB=EXP(-EXTC*AM)
      CBNI=BNIO*TAUB
C
C...CLACULATE CLEAR DAY DIFFUSE
      CDHI=121.11*SQRT(ALT)-22.918*ALT
      CDHI=3.6*CDHI
C
C...CALCULATE CLEAR DAY GLOBAL
      CGLOB=CDHI+(CBNI*SIN(ALT))
C
      RETURN
      END
```

```
      SUBROUTINE SUBPLOT(HAV,H1AV,H2AV)
C
C
C              SUBROUTINE SUBPLOT
C             C. BALARAS   8-12-85
C
C
C...PLOTTING SUBROUTINE
C   MONTHLY AVERAGE DAILY IRRADIATION VS. MONTH OF THE YEAR
C
C...DIMENSIONS
      DIMENSION HAV(12),H1AV(12),H2AV(12),IBUF(512)
C
C...SUBROUTINE INITIALIZATIONS
      AMOP=1.0
C
C...OPEN PLOT FILES
      CALL PLOTS(IBUF,512,2,40)
      CALL PLOTMX(18.5)
      CALL PLOT(3.0,1.0,-3)
C...DRAW X-AXIS (MONTH OF THE YEAR)
      CALL AXIS(0.0,0.0,'MONTH',-5,12.0,0.0,0.0,1.0)
C...DRAW Y-AXIS (IRRADIATION)
      CALL AXIS(0.0,0.0,'MONTHLY AVERAGE DAILY IRRADIATION, (KJ/M/M)',
     &43,8.0,90.0,8000.0,2000.0)
C...TITLE GRAPH
C     CALL SYMBOL(5.0,8.5,0.1,0,0.0,-1)
C     CALL SYMBOL(5.2,8.5,0.18,14HREFERENCE DATA,0.0,14)
      CALL SYMBOL(5.0,8.2,0.1,1,0.0,-1)
      CALL SYMBOL(5.2,8.2,0.18,10H5-YR MODEL,0.0,10)
      CALL SYMBOL(5.0,7.9,0.1,4,0.0,-1)
      CALL SYMBOL(5.2,7.9,0.18,12HB*5-YR MODEL,0.0,12)
C
      DO 339 IIL=1,12
C             SET SCALES
              HAVP=(HAV(IIL)/2000.0)-4.0
              H1AVP=(H1AV(IIL)/2000.0)-4.0
              H2AVP=(H2AV(IIL)/2000.0)-4.0
C             PLOT REFERENCE DATA
C             CALL SYMBOL(AMOP,HAVP,0.1,0,0.0,-1)
C             PLOT DATA FROM 5-YR MODEL
              CALL SYMBOL(AMOP,H1AVP,0.1,1,0.0,-1)
C             PLOT DATA FROM B*5-YR MODEL
              CALL SYMBOL(AMOP,H2AVP,0.1,4,0.0,-1)
C             INCREMENT MONTHLY COUNTER
              AMOP=AMOP+1.0
 339  CONTINUE
C
C...CLOSE PLOTTING FILE
      CALL PLOT(7.0,0.0,3)
      CALL PLOT(7.0,0.0,999)
C
      RETURN
      END
```

APPENDIX D

AIRMAS3	Plotting of Air-mass vs. Beam Transmittance with Limiting Clear Sky Models
PLOTXY	Calculates Regression Coefficients
CSMSTAT	Calculates Clear Sky Conditions for a Given Air-mass Range, and Performs a Statistical Analysis for the Goodness of Fit for Three Clear Sky Models
IBN	Calculates Clear Sky Beam Radiation Using the CSBT Model and Compares Measured and Modelled Data for a Given Day of the Year
P3SUB	Subroutine to Plot Hourly Beam Normal Irradiation for a Given Day
CURVE2	Calculates Continuous Piecewise Linear Correlations Between Beam Transmittance and Air-Mass for a Given Clearness Index Range

```
      PROGRAM AIRMAS3(INPUT,OUTPUT,TAPE5=INPUT,TAPE6=OUTPUT,TAPE2,
     &                TAPE7,TAPE8)
C
C       C. BALARAS                  8-27-85
C       C. BALARAS                 11-6-85
C       C. BALARAS                 4-21-86
C       C. BALARAS                 5-27-86
C
C
C...THIS PROGRAM INVESTIGATES THE AIRMASS DEPENDENCY OF
C   BEAM TRANSMITTANCE. THE RESULT IS A BEAM TRANSMITTANCE
C   VS. AIRMASS GRAPH. THE RADIATION DATA IN TAPE7, IS ACTUALLY
C   THE 5-YR DATA. THERE IS AN OPTION TO MAKE THE ANALYSIS FOR
C   ALL 5-YRS OR FOR EACH ANNUAL YEAR.
C...THIS VERSION INCLUDES THE ADDITION OF THE CALCULATIONS
C   FOR THE LIMITING CURVE. THE DATA BETWEEN 1.0<AM<2.0 IS
C   BROKEN DOWN TO 12 BANDS. FOR EACH BAND ONLY THE HIGHEST
C   DATA ARE KEPT AND USING THESE POINTS THEN FIT THROUGH
C   AN EQUATION OF THE FORM TB=EXP(-K*AM) IN ORDER TO DETERMINE K.
C
C...THIS VERSION ALSO PLOTS THE LIMITING CURVES ON THE 5-YEAR PLOT
C   OF TB VS AIRMASS, ACCORDING TO THE R-W MODEL (TB=0.8847*EXP(-0.106*M)
C   THE MAXWELL MODEL (TB=0.886-0.122*M+.01211*M*M-0.000653*M**3+
C   0.000014*M**4) AND THE CSBT MODEL (TB=.84257*EXP(-0.0939*M)).
C   TO RUN THIS PROGRAM:
C                          AT,GD2H5Y              (DATA FILE)
C                          C,GD2H5Y,TAPE7
C                          AT,CALCOMP/UN=LIBRARY
C                          AT,IMSLIB5/UN=LIBRARY
C                          X,LIBRARY,CALCOMP,IMSLIB5
C                          FTN5,I=AIRMAS3,L=0
C                          LGO
C
C...DECLARATIONS
      DIMENSION IBUF(512)
C
      INTEGER BADPER
      REAL KT
C
      COMMON /CNSTS/ ALATR,DELOMO2,GSCF,HRCONV
C
      WRITE(6,*) 'WHAT IS THE TITLE (ALL 5Y)'
      READ(5,22) TITLE
 22   FORMAT(A6)
C...INITIALIZATIONS
      ALATD=33.4046
      ALONGD=84.7478
      ALONST=75.0
      ZONE=5.0
      GSC=1367.0
      PI=4.0*ATAN(1.0)
      GSCF=3.6*GSC*12.0/PI
      HRCONV=12.0/PI
      DRCONV=PI/180.0
```

```
      ALATR=ALATD*DRCONV
C     INTERVAL IN TERMS OF RADIANS
      DLOMEGA=15.0*DRCONV
      DELOMO2=DLOMEGA/2.0
      IFRST=1
      ICOUNT=0
      N=1
      NSIG=3
      MAXFN=500
      IOPT=0
C
C...OPEN PLOT FILES
      CALL PLOTS(IBUF,512,2,40)
      CALL PLOTMX(8.0)
      CALL PLOT(2.0,2.0,-3)
      CALL SYMBOL(-1.0,2.5,0.3,'&<#S;B',0.0,6)
      CALL SYMBOL(2.5,-0.6,0.3,'&AIRMASS',0.0,8)
C...DRAW X-AXIS (AIRMASS)
      CALL AXIS(0.0,0.0,'      ',-5,7.0,0.0,0.0,1.0)
C...DRAW Y-AXIS (BEAM TRANSMITTANCE)
      CALL AXIS(0.0,0.0,'  ',3,5.0,90.0,0.0,0.2)
C...TITLE GRAPH
      CALL SYMBOL(3.0,4.5,0.2,TITLE,0.0,6)
      DO 10 I=1,8112
C...RAEAD DATA (TIME, RADIATION VALUES, AND BADPERIOD)
      READ(7,101) IYR,MO,IDAY,IHR,MIN,HRZTOT,BNI,BADPER
 101  FORMAT(1X,I2,4(2X,I2),4X,2(F7.1,2X),46X,I2)
C
C...CALL SUBROUTINE HELGO FOR TIME - 0.5 HOURS
      CVLT=(IHR+MIN/60.0)-0.5
      CALL HELGO(IYR,MO,IDAY,CVLT,ALONGD,ALATD,ALONST,ZONE,
     &ALTR,DELTAR,EOT,OMEGAR,RADIUS)
C
C...CALL SUBROUTINE IRRADIATION
      CALL SUBI(OMEGAR,ALATD,DELTAR,BADPER,GSC,IFRST,RADIUS,
     &HRZTOT,BNI,KT,TB)
C
C...CALCULATE AVERAGE INCIDENT ANGLE
      CALL EXTRAD(DELTAR,OMEGAR,RADIUS,HBNIO,HGIO,AZCOS,AHANG,DLO2)
C
C...CALCULATE THE SOLAR ALTITUDE
      SINALT=AZCOS
      IF (SINALT.GE.0.0) THEN
         ALTAVE=ASIN(SINALT)
      ELSE
         ALTAVE=-99.0
      END IF
C...CALCULATE AIRMASS
      AM=AMASS(ALTAVE)
C...TEST FOR VALIDITY OF RESULTS
C...FOR NEGATIVE ALTITUDE, AM=1.0E50, SKIP CALCULATIONS
      IF (AM.GT.100.0) GO TO 10
C...PLOT THE PAIR OF DATA (IBN AND AIRMASS)
C       SET SCALES
```

```
      AMP=AM
      TBP=TB/0.2
      CALL SYMBOL(AMP,TBP,0.035,19,0.0,-1)
C
 10   CONTINUE
C
C...PLOT LIMITING CURVES
C
      AMM=1.0
      DO 20 J=1,25
C...BY R-W MODEL
      TBRW=0.8847*EXP(-0.106*AMM)
C...BY MAXWELL MODEL
      TBM=0.886-0.122*AMM+0.0121*AMM*AMM-
     &    0.000653*AMM**3.0+0.000014*AMM**4.0
C...BY CSBT MODEL
      TBC=0.84257*EXP(-0.0939*AMM)
C
      CALL SYMBOL(AMM,TBRW/0.2,0.105,0,0.0,-1)
      CALL SYMBOL(AMM,TBM/0.2,0.105,1,0.0,-1)
      CALL SYMBOL(AMM,TBC/0.2,0.105,2,0.0,-1)
      AMM=AMM+0.25
 20   CONTINUE
C
C...CLOSE PLOT FILE
      CALL PLOT(7.0,0.0,3)
      CALL PLOT(7.0,0.0,999)
C
      STOP
      END
```

```
      PROGRAM PLOTXY(INPUT,OUTPUT,TAPE5=INPUT,TAPE6=OUTPUT,TAPE10,
                     TAPE2)
C...PROGRAM:PLOTXY....FILE:PLOTXY
C...PROGRAM TO PLOT POINTS IN CARTESIAN COORDINATES
C...USAGE
C    /MNF,B=BF1,I=PLOTXY,L=0
C    /AT,CALCOMP/UN=LIBRARY
C    /X,LIBRARY,CALCOMP
C    /C,DATA,TAPE10
C    /RWF
C    /BF1
C    ...
C    /AT,PLOTR/UN=LIBRARY
C    /PLOTR,TAPE2
C    ...
C    /PLOTCV,TAPE2
      DIMENSION FY(4),FX(4),IBUF(512),XA(100),YA(100)
C...OBTAIN DATA AND PARAMETERS
      CALL PLOTS(IBUF,512,2,00)
      CALL PLOTMX(7.5)
      WRITE(6,*)'NUMBER OF DATA POINTS?'
      READ(5,*) N
      IF(N.GT.98) WRITE(6,*)'NOT ENOUGH ARRAY SPACE, STOP1'
      DO 10 I=1,N
      READ(10,9001) PN2,PN1
        XA(I)=PN1
        YA(I)=PN2
10    WRITE(6,*) XA(I),YA(I)
C...PRELIMINARIES
      CALL PLOT(0.0,0.0,3)
      WRITE(6,*)'MAGNIFICATION?'
      READ(5,*) XM
      CALL FACTOR(XM)
      WRITE(6,*)'HEIGHT AND WIDTH OF GRAPH?'
      READ(5,*)YH,XW
C...TO FORCE THE "SCALE" ROUTINE TO RETURN USEFUL RESULTS
C...IT IS OFTEN DESIRABLE TO FAKE A DATA PT AT THE ORIGIN
C...TEMPORARILY BEFORE THE ACTUAL DATA ARE PLOTTED
      DV=XA(1)
      DV2=YA(1)
      XA(1)=0.0
      YA(1)=0.0
      CALL SCALE(XA,XW,N,1)
      CALL SCALE(YA,YH,N,1)
      XA(1)=DV
      YA(1)=DV2
      CALL AXIS(0.,0.,0,0,YH,90.,YA(N+1),YA(N+2))
      CALL AXIS(0.,0.,0,0,XW,0.  ,XA(N+1),XA(N+2))
      CALL LINE(XA,YA,N,1,-1,1)
C...COMPUTE AND PLOT AN RMS LINE
      WRITE(6,*)'WANT AN RMS LINE (YES-POSITIVE)?'
      READ(5,*) YPOS
      IF(YPOS.LE.0.) GO TO 999
C...CALCULATE THE STATISTICS OF THE DATA
```

```
      SX=SXY=SY=SXSQ=0.0
      DO 20 I=1,N
      SXY=SXY+XA(I)*YA(I)
      SX=SX+XA(I)
      SY=SY+YA(I)
      SXSQ=SXSQ+XA(I)*XA(I)
20    CONTINUE
      WRITE(6,*) 'HOMOGENEOUS OR GENERAL (GENERAL-POSITIVE)?'
      READ(5,*) POSGEN
      IF(POSGEN.GE.0.0) GO TO 30
C...CALCULATE THE COEFFICIENTS (HOMOGENEOUS CASE)
      B0=0.0
      B1=SXY/SXSQ
      GO TO 40
30    CONTINUE
C...CALCULATE THE COEFFICIENTS (GENERAL LINEAR EXPRESSION)
      B1=(N*SXY-SX*SY)/(N*SXSQ-SX*SX)
      B0=(SY-B1*SX)/N
40    CONTINUE
C...REPORT RESULTS
      WRITE(6,9000) B0,B1
C...CALCULATE EXTREMA OF THE FITTED LINE
      FY(1)=B0
      EXX=XA(N+1)+XA(N+2)*XW
      FY(2)=B0+B1*EXX
      FY(3)=YA(N+1)
      FY(4)=YA(N+2)
      FX(1)=0.0
      FX(2)=EXX
      FX(3)=XA(N+1)
      FX(4)=XA(N+2)
      CALL LINE(FX,FY,2,1,0,0)
C...IDENTIFY  THE RESULTS
      CALL SYMBOL(0.5,0.5,0.25,4HY = ,0.0,4)
      CALL NUMBER(999.,999.,0.25,B0,0.0,3)
      IPN=3H +
      IF(B1.LT.0.0)  IPN=3H -
      IF(B1.LT.0.0)  B1=-B1
      CALL SYMBOL(999.,999.,0.25,IPN  ,0.0,3)
      CALL NUMBER(999.,999.,0.25,B1,0.0,3)
      CALL SYMBOL(999.,999.,0.25,3H* X,0.0,3)
999    CONTINUE
      CALL PLOT(7.,0.,3)
      CALL PLOT(0.,0.,999)
9000  FORMAT ( 10X," B0 = ",F8.4,/,10X," B1 = ",F8.4)
9001  FORMAT(F7.4,2X,F6.4)
      STOP
      END
```

```
      PROGRAM CSMSTAT (INPUT,OUTPUT,TAPE5=INPUT,TAPE6=OUTPUT,TAPE8)
C
C
C     C. BALARAS      8-13-86
C     C. BALARAS      4-13-88
C
C...USING THE MAX TB VS. AM DATA, THREE MODELS ARE TO BE FITTED
C
C   FIRST, OUR CLEAR SKY MODEL TB=0.84257*EXP(-0.0939*AM)
C   SECOND, THE R-W MODEL TB=0.8847*EXP(-0.106*AM)
C   THIRD, THE MAXWELL MODEL TB=.886-.122*AM+.01211*AM2+
C                              +.000653*AM3+.000014*AM4
C   VARIOUS STATISTICAL PARAMETERS ARE CALCULATED TO DETERMINE
C   WHICH MODEL HAS THE BEST FIT.
C
C   TAPE8 = OUTPUT OF STATISTICAL RESULTS
C
C         AT,CALCOMP,IMSLIB5/UN=LIBRARY
C         X,LIBRARY,CALCOMP,IMSLIB5
C         FTN5,I=CSMSTAT,L=0
C         LGO
C
C...DECLARATIONS
      DIMENSION TB(22),AM(22)
C
C...INITIALIZATIONS
      DATA TB/0.7473,0.7476,0.7478,0.7397,0.7450,0.7331,0.7229,
     & 0.7237,0.7082,0.6973,0.7015,0.6808,0.6803,0.6692,0.6503,
     & 0.6266,0.6478,0.6365,0.6095,0.6138,0.6169,0.5424/
      DATA AM /1.1245,1.2127,1.3264,1.4441,1.5533,1.6026,1.7775,
     & 1.8946,1.9068,2.0722,2.1760,2.2911,2.3449,2.4968,2.5018,
     &2.6507,2.7037,2.8971,2.9102,3.2826,3.3519,5.0728/
      SUMTB=0.0
      RSST1=0.0
      RSST2=0.0
      RSST3=0.
      SYY=0.0
C
C...CALCULATE THE SUM OF TB
      DO 100 I=1,22
      SUMTB=SUMTB+TB(I)
  100 CONTINUE
C...CALCULATE THE AVERAGE TB
      TBAVE=SUMTB/22.0
C
      DO 200 II=1,22
      YEST1=0.8426*EXP(-0.0939*AM(II))
      YEST2=0.8847*EXP(-0.106*AM(II))
      YEST3=0.886-0.122*AM(II)+0.01211*AM(II)**2-
     &      0.000653*AM(II)**3+0.000014*AM(II)**4
C...TOTAL RESIDUAL SUM OF SQUARES
      RSST1=RSST1+(TB(II)-YEST1)**2
      RSST2=RSST2+(TB(II)-YEST2)**2
      RSST3=RSST3+(TB(II)-YEST3)**2
```

```
C...TOTAL VARIATION
      SYY=SYY+(TB(I1)-TBAVE)**2
 200  CONTINUE
C
C...EXPLAINED VARIATION
      SSREG1=SYY-RSST1
      SSREG2=SYY-RSST2
      SSREG3=SYY-RSST3
C...COEFFICIENT OF CORRELATION
      AR1=SQRT(SSREG1/SYY)
      AR2=SQRT(SSREG2/SYY)
      AR3=SQRT(SSREG3/SYY)
C...COEFFICIENT OF DETERMINATION
      AR1SQ=AR1*AR1
      AR2SQ=AR2*AR2
      AR3SQ=AR3*AR3
C...F-TEST BETWEEN OUR MODEL AND R-W
C...RSST1 = RESIDUAL VARIATION FOR THE ALTERNATIVE MODEL
C...RSST2 = RESIDUAL VARIATION FOR THE HYPOTHESIZED MODEL
C           THE R-W MODEL OR THE MAXWELL MODEL
C...DFH   = DEGREES OF FREEDOM FOR THE HYPOTHESIZED MODEL, N
C...DFA   = DEGREES OF FREEDOM FOR THE ALTERNATIVE MODEL, N-P
C...N     = NUMBER OF DATA POINTS, 22
C...P     = NUMBER OF PARAMETERS, 2
      DFH=22.0
      DFA=22.0-2.0
      F1=((RSST2-RSST1)/(DFH-DFA))/(RSST1/DFA)
      F2=((RSST3-RSST1)/(DFH-DFA))/(RSST1/DFA)
C...CALCULATE CONFIDENCE AND ALPHA
      NRW=22
      N=22-2
      CALL MDFD(F1,NRW,N,P1,IER)
      ALPHA1=1.0-P1
      CALL MDFD(F2,NRW,N,P2,IER)
      ALPHA2=1.0-P2
C
C...REPORT RESULTS
      WRITE(8,*) '   CSBT ','    ','R-W MODEL','    ','MAXWELL MODEL'
      WRITE(8,*) ' '
      WRITE(8,*) 'SYY=',SYY
      WRITE(8,*) '  RSS=',RSST1,'        ',RSST2,'            ',RSST3
      WRITE(8,*) 'SSREG=',SSREG1,'    ',SSREG2,'          ',SSREG3
      WRITE(8,*)  'R=    ',AR1,'        ',AR2,'            ',AR3
      WRITE(8,*)'R2=     ',AR1SQ,'      ',AR2SQ,'          ',AR3SQ
      WRITE(8,*) 'F1= ',F1,'ALPHA1= ',ALPHA1,'P1= ',P1
      WRITE(8,*) 'F2= ',F2,'ALPHA2= ',ALPHA2,'P2= ',P2
C
      END
```

```
      PROGRAM IBN(INPUT,OUTPUT,TAPE5=INPUT,TAPE6=OUTPUT,
     &           TAPE8,TAPE3,TAPE9,TAPE10)
C
C       C. BALARAS                12-12-85
C       C. BALARAS                5-28-86
C
C...THE CLEAR DAY MODEL TO BE USED IS IBNC=ION*0.8426*EXP(-0.0939*AM)
C...THIS PROGRAM "IBN" READS HOURLY DATA FROM M19XXA IN TAPE9
C   (UN=MEFACBL) AND CREATES A PLOT OF IBN VS TIME (IN TAPE3) FOR
C   A GIVEN DAY OF YEAR.
C...A CLEAR DAY MODEL IS USED TO CALCULATE THE BEAM NORMAL IRRAD.
C   IBNC=ION*EXP(-K*AM). THE EXTINCTION COEFFICIENT HAS BEEN
C   PRECALCULATED (K=0.196). THE REASON FOR DOING THIS ANALYSIS
C   IS TO FIND OUT HOW GOOD THIS 0.196 VALUE IS.
C   FINALLY THE MODELED DATA IS PLOTTED WITH THE DATA FROM
C   THE TAPES FOR COMPARISON REASONS.
C
C   TO RUN THIS PROGRAM:
C                         AT,M19XXA/UN=MEFACBL
C                         C,M19XXA,TAPE9
C                         AT,CALCOMP,PLOTR/UN=LIBRARY
C                         X,LIBRARY,CALCOMP
C                         FTN5,I=IBN,L=0
C                         LGO
C
C...DECLARATIONS
      CHARACTER*12 TITLE1
      DIMENSION TIME(24),HBN1(24)
      DIMENSION ERROR(24),DIF(24)
      DIMENSION AIBN(24),AAM(24)
C
C
      COMMON /CNSTS/ ALATR,DELOM02,GSCF,HRCONV
C
      WRITE(6,*) 'WHAT IS THE MONTH DAY AND YEAR (030579) ?'
      READ(5,21) MO,IDAY,IYR
 21   FORMAT(I2,I2,I2)
      WRITE(6,*) 'WHAT IS THE DAY OF THE YEAR (XXX)?'
      READ(5,23) IDAYR
 23   FORMAT(I3)
      WRITE(6,*) 'WHAT IS THE IBN-TIME PLOTS TITLE (MAR 5, 1979)'
      READ(5,22) TITLE1
 22   FORMAT(A12)
C...INITIALIZATIONS
      ALATD=33.4046
      ALONGD=84.7478
      ALONST=75.0
      ZONE=5.0
      GSC=1367.0
      PI=4.0*ATAN(1.0)
C...SOLAR CONSTANT FACTOR IN HRS/RAD
      GSCF=3.6*GSC*12.0/PI
      HRCONV=12.0/PI
      DRCONV=PI/180.0
```

```
      ALATR=ALATD*DRCONV
C     INTERVAL IN TERMS OF RADIANS (1HR*15 DEGR/HR * DEGR TO RAD CONV FACTOR)
      DLOMEGA=15.0*DRCONV
      DELOMO2=DLOMEGA/2.0
      IFRST=1
      ICOUNT=0
C...INITIALIZE TIME
      IHR=0
C...SET PRECALCULATED EXTICTION COEFFICIENT TO BE TESTED
      EXTINC=0.196
C
      DO 10 I=1,24
C...CALCULATE TIME AT THE END
C   OF HOURLY PERIOD
      IHR=IHR+1
C
C...CALL SUBROUTINE HELGO FOR TIME - 0.5 HOURS
      CVLT=IHR-0.5
      CALL HELGO(IYR,MO,IDAY,CVLT,ALONGD,ALATD,ALONST,ZONE,
     &ALTR,DELTAR,EOT,OMEGAR,RADIUS)
C
C...CALCULATE AVERAGE INCIDENT ANGLE AND EXTRAT BEAM NORMAL IN KJ/M*M
C   INPUT TO THE SUBROUTINE IS THE LENGTH OF PERIOD USING
C   COMMON BLOCK. CORRECT "DLOMEGA" AS NEEDED IF DIFFERENT FROM 1HR
      CALL EXTRAD(DELTAR,OMEGAR,RADIUS,HBNIO,HGIO,AZCOS,AHANG,DLO2)
C
C...CALCULATE THE SOLAR ALTITUDE
      SINALT=AZCOS
      IF (SINALT.GE.0.0) THEN
         ALTAVE=ASIN(SINALT)
      ELSE
         ALTAVE=-99.0
      END IF
C...CALCULATE AIRMASS
      AM=AMASS(ALTAVE)
C...TEST FOR VALIDITY OF RESULTS
C...FOR NEGATIVE ALTITUDE, AM=1.0E50, SKIP CALCULATIONS
      IF (AM.GT.100.0) GO TO 10
C...CLEAR DAY MODEL
C   CALCULATE BEAM NORMAL IRRADIATION
C     AIBN(I)=HBNIO*EXP(-(EXTINC*AM))
      AIBN(I)=HBNIO*0.8426*EXP(-0.0939*AM)
C.............AIR MASS
      AAM(I)=AM
 10   CONTINUE
C
C...READ THE RADIATION DATA FROM M19XXA
C   LOCATE REQUESTED DAY OF YEAR
 80   READ(9,60) IYR,IDOY,HR,BNI
 60   FORMAT(I2,I3,F2.0,1X,F5.0)
      IF (IDOY.EQ.IDAYR-1.AND.HR.EQ.23.) THEN
      GO TO 90
      ELSE
      GO TO 80
```

```
      END IF
 90   DO 70 I=1,24
C     THE REQUESTED DAY HAS BEEN LOCATED
      READ(9,60) IYR,IDOY,HR,HBNI(I)
C...THE TIME ON M19XXA DATA IS AT THE
C   BEGINNING OF THE PERIOD
C...CONVERT TO CONVENTIONAL PERIOD ENDING IRRADIATION
C   ADD ONE HOUR
      TIME(I)=HR+1.0
C...RESET NEGATIVE BEAM DATA TO ZERO
      IF (HBNI(I).LT. 0.0) HBNI(I)=0.0
 70   CONTINUE
C...CALL PLOTTING SUBROUTINE FOR IBN AND TIME
C   PLOT TAPE DATA IBN AND CALCULATED DATA AIBN
C   AT THEIR CORRESPONDING TIME PERIODS
      CALL P3SUB(HBNI,TIME,AIBN,TITLE1)
C
C...CALCULATE THE DIFFERENCE BETWEEN
C   TAPE AND MODELED DATA
      WRITE(10,*) TITLE1
      DO 30 II=1,24
      DIF(II)=AIBN(II)-HBNI(II)
C...AVOID CALCULATIONS IF AIBN=0
      IF (AIBN(II).EQ.0.0) GO TO 30
C...PERCENT ERROR
      ERROR(II)=(AIBN(II)-HBNI(II))/AIBN(II)*100.
      WRITE(10,*) 'TIME=',TIME(II),'IBN=',AIBN(II),'HBNI=',HBNI(II),
     &'ERROR=',ERROR(II),'AMC=',AAM(II)
 30   CONTINUE
C
      STOP
      END
```

```
      SUBROUTINE P3SUB(HBNI,TIME,AIBN,TITLE1)
C
C       C. BALARAS            12-10-85
C
C...SUBROUTINE TO PLOT HOURLY BEAM NORMAL IRRADIATION AND TIME
C
      CHARACTER*12 TITLE1
      DIMENSION IBUF(512)
      DIMENSION TIME(24),HBNI(24),AIBN(24)
C
C...OPEN PLOT FILES
      CALL PLOTS(IBUF,512,3,40)
      CALL PLOTMX(8.0)
      CALL PLOT(2.0,2.0,-3)
C...DRAW AND LABEL X-AXIS (TIME)
      CALL AXIS(0.0,0.0,'TIME',-4,6.0,0.0,0.0,4.0)
C...DRAW AND LABEL Y-AXIS (HOURLY BEAM NORMAL IRRAD.)
      CALL SYMBOL(-1.0,3.5,0.3,'&I;[<B;[<N',0.0,10)
      CALL AXIS(0.0,0.0,' ',1,7.0,90.0,0.0,0.7)
C...TITLE GRAPH
      CALL SYMBOL(0.5,7.2,0.15,TITLE1,0.0,12)
C...SET SCALES AND PLOT TAPE DATA  RADIATION VALUES IN KJ/M*M
      DO 20 II=1,24
      TIMEP2=TIME(II)/4.0
      HBNIP=HBNI(II)/1000.0/0.7
      CALL SYMBOL (TIMEP2,HBNIP,0.08,0,0.0,-1)
 20   CONTINUE
C...SET SCALES AND PLOT MODELED DATA  RADIATION VALUES IN KJ/M*M
      DO 10 I=1,24
      AIBNP=AIBN(I)/1000.0/0.7
      TIMEP=TIME(I)/4.
      CALL SYMBOL(TIMEP,AIBNP,0.08,2,0.0,-2)
 10   CONTINUE
C...CLOSE PLOT FILE
      CALL PLOT(7.0,0.0,3)
      CALL PLOT(7.0,0.0,999)
      RETURN
      END
```

```
      PROGRAM CURVE2(INPUT,OUTPUT,TAPE5=INPUT,TAPE6=OUTPUT,TAPE2,TAPE7,
     &               TAPE8,TAPE9)
C
C
C       C. BALARAS          10-14-87
C       C. BALARAS          11-10-87
C       C. BALARAS          11-16-87
C       C. BALARAS          12-7-87
C       C. BALARAS           3-17-88
C
C
C...CURVE GENERATION FOR TB .VS. AM FOR A GIVEN KT BAND
C   FOR THE 5YR DATA, 5YR WINTER DATA, OR 5YR SUMMER DATA
C...THERE IS AN OPTION TO USE THE DISC MODEL BY MAXWELL FOR CASES
C   OF KT FROM 0.23 TO 0.87
C   SEPARATE DATA IN AM BANDS OF UNIT WIDTH
C   FOR THE FIRST BAND HAVE A LEAST SQUARE REGRESSION LINE (2 D.F.)
C   OF THE FORM TB=C1+C2*AM
C   FOR THE REMAINING BANDS A CONTINUOUS LINEAR REGRESSION (1 D.F.)
C   OF THE FORM TB=YO+B(AM-XO)
C   IN THE EVENT THAT THERE ARE ONLY UP TO TWO DATA POINTS IN THE
C   LAST BAND, THERE ARE NOT ENOUGH DATA AND THEY ARE IGNORED
C   FOR EACH CASE THE GOODNESS OF FIT IS CALCULATED AND A PLOT OF
C   THE SCATTERED DATA WITH THE REGRESSION LINES IS PREPARED
C   THE APPROPRIATE NUMBER OF BANDS FOR EACH CASE IS DETERMINED BY
C   IDENTIFYING THE MAXIMUM VALUE FOR AIR-MASS
C   NOTE THAT THE DATA ARRAYS CAN NOT HANDLE A STUDY OF ALL KT BANDS
C   AT ONCE.
C...ASSUME THAT THERE ARE NO DATA DISCONTINUITIES
C
C...INPUTS :
C          KTARR, AMARR, TBARR = CORRESPONDING DATA (TAPE8)
C          A1, A2 = UPPER LOWER LIMIT FOR KT BAND
C
C...TO RUN THIS PROGRAM:
C                        AT,TAPE8     (5YR DATA FILE)
C                        OR G,WKMT    C,WKMT,TAPE8     (FOR WINTER DATA)
C                        AT,IMSLIB5/UN=LIBRARY
C                        AT,CALCOMP/UN=LIBRARY
C                        X,LIBRARY,IMSLIB5,CALCOMP
C
C...TAPE DIRECTORY:
C                    TAPE2 = PLOTTING OUTPUT FILE
C                    TAPE7 = OUTPUT FILE
C                    TAPE8 = INPUT DATA FILE
C                    TAPE9 = AVAILABLE
C
      CHARACTER*4 TITLE(3)
C...DIMENSIONS
      DIMENSION IRVS(8112),IRVS1(8112),WK(1),IBUF(512)
      DIMENSION X(7),Y(7),Y2(7),NPTS(2100),I2(8)
      DIMENSION DKT(2100),DTB(2100),DAM(2100),XO(8),YO(8),BETA(8)
      DIMENSION COEF(3)
      REAL KTARR(8112),AMARR(8112),TBARR(8112)
```

```
      REAL KT
C
      DATA XO/1.0,2.0,3.0,4.0,5.0,6.0,7.0,8.0/
C
C...SPECIFY ANALYSIS
      WRITE(6,*) 'SPECIFY ANALYSIS 1-5YR, 2-WKMT, 3-SKMT'
      READ(5,*) ISD
C
C...OPTION TO USE DISC MODEL
      WRITE(6,*) 'OPTION TO USE DISC MODEL  YES-1 NO-0'
      READ(5,*) IOPT
C
C...INPUT TITLE
      WRITE(6,*) 'CLEARNESS INDEX BAND I.E. 0.23 KT 0.27'
      READ(5,10) (TITLE(I),I=1,3)
 10   FORMAT(3(A4))
C
C...KT BAND WIDTH
      WRITE(6,*) 'CLEARNESS INDEX BAND BETWEEN A1, A2'
      READ(5,*) A1,A2
C
C...CASE NO. FOR KT TO BE STUDIED
      WRITE(6,*) 'CASE NO. FOR KT ? (I.E. 1) '
      READ(5,*) ICASE
C...SHOW DATA ON OUTPUT PLOT?
      WRITE(6,*) 'SHOW DATA ON OUTPUT PLOT? Y-0, N-1 '
      READ(5,*) ISHOW
C
C...INITIALIZATIONS
      NPTST=0
      IBC=1
      IBCR=1
      IBND=1
      SUMY=SUMX=SUMXY=SUMXSQ=0.0
      SUMT=SUMM=SUMTM=SUMMSQ=0.0
      AMAX=0.0
      ISP=0
C
C...READ INPUT DATA
C...5YR DATA
      IF (ISD.EQ.1) THEN
         NPAIRS=8112
         DO 100 I=1,NPAIRS
            READ(8,20) KTARR(I),AMARR(I),TBARR(I)
 20         FORMAT(12X,3(2X,F16.14))
 100     CONTINUE
      END IF
C...WINTER DATA
      IF (ISD.EQ.2) THEN
         NPAIRS=1413
         DO 110 I=1,NPAIRS
            READ(8,*) KTARR(I),AMARR(I),TBARR(I)
 110     CONTINUE
      END IF
```

```
C...SUMMER DATA
      IF (ISD.EQ.3) THEN
         NPAIRS=2349
         DO 120 I=1,NPAIRS
                READ(8,*) KTARR(I),AMARR(I),TBARR(I)
 120     CONTINUE
      END IF
C
C...REARRANGE DATA IN ASCENDING KT VALUES
      DO 200 IA=1,NPAIRS
            IRVS(IA)=IA
 200  CONTINUE
C
      CALL VSRTP(KTARR,NPAIRS,IRVS)
C
      DO 300 IB=1,NPAIRS
            IRVS1(IB)=IRVS(IB)
 300  CONTINUE
C
      CALL VSRTU(AMARR,NPAIRS,NPAIRS,1,1,IRVS,WK)
      CALL VSRTU(TBARR,NPAIRS,NPAIRS,1,1,IRVS1,WK)
C
C...GROUP DATA ACCORDING TO KT
      ICOUNT=0
      AMIN=AMARR(1)
      DO 400 IC=1,NPAIRS
            IF (KTARR(IC).GE.A1.AND.KTARR(IC).LT.A2) THEN
               ICOUNT=ICOUNT+1
               DTB(ICOUNT)=TBARR(IC)
               DAM(ICOUNT)=AMARR(IC)
               DKT(ICOUNT)=KTARR(IC)
C              IDENTIFY MAX, MIN VALUE OF AM FOR THIS KT INTERVAL
               AMAX1=DAM(ICOUNT)
               AMIN1=DAM(ICOUNT)
               IF (AMAX1.GT.AMAX) AMAX=AMAX1
               IF (AMIN1.LT.AMIN) AMIN=AMIN1
            END IF
 400  CONTINUE
C
C...CHECK NUMBER OF DATA, IF NO DATA AVAILABLE
C   REPORT AND TERMINATE
      IF (ICOUNT.EQ.0) THEN
      WRITE(7,12) (TITLE(I),I=1,3)
      WRITE(6,12) (TITLE(I),I=1,3)
 12   FORMAT('NO DATA PRESENT FOR THIS KT INTERVAL ',3(A4))
      END IF
      IF (ICOUNT.EQ.0) GOTO 1000
C
C...THE DATA FOR GIVEN KT INTERVAL IS NOW AVAILABLE
C   REARRANGE DATA IN AM ASCENDING ORDER
      DO 310 JA=1,ICOUNT
 310  IRVS(JA)=JA
C
      CALL VSRTP(DAM,ICOUNT,IRVS)
```

```
C
      DO 315 JB=1,ICOUNT
 315  IRVS1(JB)=IRVS(JB)
C
      CALL VSRTU(DTB,ICOUNT,ICOUNT,1,1,IRVS,WK)
      CALL VSRTU(DKT,ICOUNT,ICOUNT,1,1,IRVS1,WK)
C
C...APPROPRIATE NUMBER OF AIR-MASS BANDS (NOB)
C   FOR EACH KT CASE
      IF (AMAX.GT.1.0.AND.AMAX.LE.2.0) NOB=1
      IF (AMAX.GT.2.0.AND.AMAX.LE.3.0) NOB=2
      IF (AMAX.GT.3.0.AND.AMAX.LE.4.0) NOB=3
      IF (AMAX.GT.4.0.AND.AMAX.LE.5.0) NOB=4
      IF (AMAX.GT.5.0.AND.AMAX.LE.6.0) NOB=5
      IF (AMAX.GT.6.0.AND.AMAX.LE.7.0) NOB=6
      IF (AMAX.GT.7.0.AND.AMAX.LE.8.0) NOB=7
C
C...INITIALIZE
      NOBR=NOB
C
C...MOVE TO THE FIRST BAND WITH DATA
      IF (DAM(1).GT.XO(IBC+1)) THEN
         IBC=2
         NOBR=NOB-1
         IBCR=2
      END IF
      IF (DAM(1).GT.XO(IBC+1)) THEN
         IBC=3
         NOBR=NOB-1
         IBCR=3
      END IF
      IF (DAM(1).GT.XO(IBC+1)) THEN
         IBC=4
         NOBR=NOB-1
         IBCR=4
      END IF
C
C...INITIALIZE DATA COUNTER FOR FIRST BAND
      NPTS(IBC)=0
C
C...START REGRESSION ANALYSIS FOR EACH BAND
      DO 320 JB=1,ICOUNT
            AM=DAM(JB)
            TB=DTB(JB)
C
            IF (AM.GT.XO(IBC+1).OR.JB.EQ.ICOUNT) THEN
C
C               PICKUP LAST POINT
                IF (JB.EQ.ICOUNT.AND.AM.LE.XO(IBC+1)) THEN
C               NOTE THAT IF THERE ARE UPTO TWO POINTS IN THE LAST BAND
C               THEN THIS BAND IS LEFT UNTREATED
                    SUMT=SUMT+TB
                    XBND=AM-XO(IBC)
                    YBND=TB-YO(IBC)
```

```
                    SUMX=SUMX+XBND
                    SUMY=SUMY+YBND
                    SUMXY=SUMXY+XBND*YBND
                    SUMXSQ=SUMXSQ+XBND*XBND
                    NPTS(IBC)=NPTS(IBC)+1
                END IF
C
                IF (IBCR.EQ.IBC) THEN
                    C1=((SUMT*SUMMSQ)-(SUMM*SUMTM))/
     &                  ((NPTS(IBC)*SUMMSQ)-(SUMM*SUMM))
                    C2=((NPTS(IBC)*SUMTM)-(SUMM*SUMT))/
     &                  ((NPTS(IBC)*SUMMSQ)-(SUMM*SUMM))
                    YO(IBCR)=C1+C2*XO(IBCR)
                    YO(IBCR+1)=C1+C2*XO(IBCR+1)
                    NPTST=NPTST+NPTS(IBC)
                END IF
C
                IF (IBC.GT.IBCR) THEN
                    BETA(IBC)=SUMXY/SUMXSQ
                    YO(IBC+1)=YO(IBC)+BETA(IBC)*(XO(IBC+1)-XO(IBC))
                    NPTST=NPTST+NPTS(IBC)
                END IF
C
C                   REINITIALIZE FOR NEXT BAND
                    IBC=IBC+1
                    SUMY=SUMX=SUMXY=SUMXSQ=0.0
                    NPTS(IBC)=0
            END IF
C
            NPTS(IBC)=NPTS(IBC)+1
C
C           IF LAST BAND HAS LESS THAN 2 POINTS THEN
C           EXCLUDE THESE DATA FROM 'SUMT'
            ILP=0
            IF (JB.EQ.ICOUNT.AND.NPTS(IBC-1).LE.2) THEN
               DO 325 ICO=1,NPTS(IBC-1)
                      SUMT=SUMT-DTB(NPTST-ILP)
                      ILP=ILP+1
 325           CONTINUE
            END IF
            IF (ILP.GT.0) GOTO 320
C
C           ANALYSIS FOR BAND COUNTER 'IBC'
            SUMT=SUMT+DTB(JB)
            SUMM=SUMM+DAM(JB)
            SUMTM=SUMTM+DTB(JB)*DAM(JB)
            SUMMSQ=SUMMSQ+DAM(JB)*DAM(JB)
            IF (IBC.GT.IBCR) THEN
               XBND=AM-XO(IBC)
               YBND=TB-YO(IBC)
               SUMX=SUMX+XBND
               SUMY=SUMY+YBND
               SUMXY=SUMXY+XBND*YBND
               SUMXSQ=SUMXSQ+XBND*XBND
```

```
            END IF
C
 320  CONTINUE
C
C
C...TOTAL NO. OF POINTS USED IN ANALYSIS
      NPTST=NPTST-ILP
C
C...STATISTICAL ANALYSIS
      RSST=0.0
      SYY=0.0
      RSST2=0.
C
      TAVE=SUMT/FLOAT(NPTST)
C
C...FIRST BAND
      I1=0
      DO 600 JC=1,NPTST
            AM=DAM(JC)
            TB=DTB(JC)
            KT=DKT(JC)
            IF (AM.GE.XO(IBCR).AND.AM.LT.XO(IBCR+1)) THEN
               YEST=C1+C2*AM
               RSST=RSST+(TB-YEST)*(TB-YEST)
               SYY=SYY+(TB-TAVE)**2
               IF (IOPT.EQ.1) THEN
               CALL DISC(A1,A2,KT,AM,COEF,TBEST)
               RSST2=RSST2+(TB-TBEST)*(TB-TBEST)
               END IF
               I1=I1+1
            END IF
 600  CONTINUE
      I2(IBCR)=I1
C
C...REMAINING BANDS
      IBC=IBCR+1
      IX=0
      DO 700 JD=1,NPTST
            AM=DAM(JD)
            TB=DTB(JD)
            IF (AM.LT.XO(IBCR+1)) GOTO 700
            IF (AM.GE.XO(IBC+1)) THEN
               YO(IBC+1)=YO(IBC)+BETA(IBC)*(XO(IBC+1)-XO(IBC))
               I2(IBC)=IX
               IBC=IBC+1
               IX=0
            END IF
            YEST=YO(IBC)+BETA(IBC)*(AM-XO(IBC))
            RSST=RSST+(TB-YEST)*(TB-YEST)
            SYY=SYY+(TB-TAVE)*(TB-TAVE)
               IF (IOPT.EQ.1) THEN
               CALL DISC(A1,A2,KT,AM,COEF,TBEST)
               RSST2=RSST2+(TB-TBEST)*(TB-TBEST)
               END IF
```

```
            IX=IX+1
            IF (JD.EQ.NPTST) I2(IBC)=IX
 700  CONTINUE
C
C...EXPLAINED VARIATION
      SSREG=SYY-RSST
C...COEF. OF CORRELATION
      AR=SQRT(SSREG/SYY)
C...COEF. OF DETERMINATION
      AR2=AR*AR
C
C...STATISTICS FOR DISC MODEL
      IF (IOPT.EQ.1) THEN
         SSREG2=SYY-RSST2
         IF (SSREG2.GT.0.) THEN
            ARS=SQRT(SSREG2/SYY)
            AR2S=ARS*ARS
         ELSE
            AR2S=9999.9
         END IF
      END IF
C
C...REPORT RESULTS
      WRITE(7,11) (TITLE(I),I=1,3)
 11   FORMAT('FOR THE CLEARNESS INDEX INTERVAL OF ',3(A4))
      WRITE(7,*) ' '
      WRITE(7,*) 'TOTAL NO. OF DATA =',ICOUNT,'     NO. OF DATA USED =',
     &NPTST
      DO 750 ITR=1,NOB
      WRITE(7,*) 'AM BAND NO. ',ITR,' WITH ',I2(ITR),' POINTS'
 750  CONTINUE
      WRITE(7,*) ' '
      WRITE(7,*) 'TOTAL VARIATION= ',SYY
      WRITE(7,*) 'RESIDUAL VARIATION= ',RSST
      WRITE(7,*) 'EXPLAINED VARIATION= ', SSREG
      WRITE(7,*) 'COEF. OF DETERMINATION= ',AR2
      WRITE(7,*) ' '
      WRITE(7,*) 'FIRST BAND TB=',C1,'+',C2,'*AM'
      WRITE(7,*) 'REMAINING BANDS OF THE FORM TB=YO+B*(AM-XO)'
      BETA(IBCR)=999.9
      WRITE(7,*) (BETA(I),I=1,7)
      WRITE(7,751)
 751  FORMAT(/,/,'*** RESULTS FOR THE DISC MODEL ***',/)
      WRITE(7,*) 'TB= ',COEF(1),' + (',COEF(2),' * EXP(',COEF(3),
     &' * AM)'
      WRITE(7,*) 'TOTAL VARIATION = ',SYY
      WRITE(7,*) 'RESIDUAL VARIATION = ',RSST2
      WRITE(7,*) 'EXPLAINED VARIATION = ',SSREG2
      WRITE(7,*) 'COEF. OF DETERMINATION = ',AR2S
C
C...PLOTTING ROUTINE
C
C...OPEN PLOT FILES
      CALL PLOTS(IBUF,512,2,50)
```

```
      CALL PLOTMX(18.5)
      CALL FACTOR(0.55)
      CALL PLOT(3.0,1.0,-3)
C
C
C...PLOT REGRESSION LINES
C   SET SCALLING FOR 'CALL LINE'
      X(6)=0.0
      X(7)=1.0
      Y(6)=0.0
      Y(7)=0.2
      Y2(6)=0.0
      Y2(7)=0.2
C
      DO 800 I=IBCR,IBC
            W=XO(I+1)-XO(I)
C
            DO 900 J=1,5
                  IF (I.EQ.IBCR) THEN
                     X(J)=XO(I)+W*(J-1)/4.0
                     Y(J)=(C1+C2*X(J))
                  ELSE
                     X(J)=XO(I)+W*(J-1)/4.0
                     Y(J)=(YO(I)+(X(J)-XO(I))*BETA(I))
                  END IF
                  IF (IOPT.EQ.1) THEN
                     CALL DISC2(ICASE,X(J),Y2(J))
                  END IF
 900        CONTINUE
      CALL LINE(X,Y,5,1,1,5)
      CALL LINE(X,Y2,5,1,1,2)
 800  CONTINUE
C
C...DRAW X AXIS
      CALL AXIS(0.0,0.,'AIR MASS',-8,8.0,0.0,0.0,1.0)
C...DRAW Y AXIS
      CALL AXIS(0.0,0.0,'BEAM TRANSMITTANCE',18,5.0,90.0,0.0,0.2)
C...DRAW TITLE
      CALL SYMBOL(3.5,5.15,0.2,TITLE,0.0,12)
C
C...DRAW DATA
      IF (ISHOW.EQ.0) THEN
      DO 500 ID=1,ICOUNT
            CALL SYMBOL(DAM(ID),DTB(ID)/0.2,0.035,19,0.0,-1)
 500  CONTINUE
      END IF
C
C...TERMINATE PLOT JOB
      CALL PLOT(7.0,0.0,3)
      CALL PLOT(7.0,0.0,999)
C
 1000 STOP
      END
```

APPENDIX E

CRTAPE9	Rearrange Five Year Data in Descending Clearness Index Order
DATA	Subroutine to Collect k_t,m,τ_b Data
TRGD	Separate Three Dimensional Scatter Data into Triangular Working Areas and Store them with Identifying Information on the Band Counter and L or U Patch
VSRTP	IMSL Routine for Sorting of Arrays by Absolute Value
VSRTU	IMSL Routine for Interchange the Rows or Columns of a Matrix
TRG	Subroutine to Separate Three Dimensional Data into Upper and Lower Patches
FIT3D2B	Surface Fitting Algorithm Using Part of the Three Dimensional Data
COORDCH	Subroutine to Transform Three Dimensional Data into a Fixed Three Dimensional Co-ordinate System
CORDCH	Subroutine to Estimate the Elevation of the Third Node at the Fixed Three Dimensional Co-ordinate System
TRGFIT	Subroutine to Perform a Least Square Fit of a Triangular Patch to Three Dimensional Data at a Fixed Co-ordinate System When Part of the Data are Used
PLANEQ	Subroutine to Define the Equation of a Plane Passing Through Three Points
PLOT3DB	Plots a Response Surface Given the Elevations at the Intersections of the Base Grid Using DISSPLA
FIT3DB	Surface Fitting Algorithm Using All Available Three Dimensional Data

```
      PROGRAM CRTAPE9(INPUT,OUTPUT,TAPE5=INPUT,TAPE6=OUTPUT,TAPE9,
     1                TAPE8)
C
C
C     C. BALARAS        6-19-87
C
C
C...READ DATA FROM GD2H5Y
C   REARRANGE DATA AND RECORD IN TAPE9 IN DESCENDING KT ORDER
C   OUTPUT TAPE9 TO BE USED BY "TRGD"
C
C...TO RUN THIS PROGRAM:
C                       AT,GD2H5Y
C                       C,GD2H5Y,TAPE8
C                       AT,IMSLIB5/UN=LIBRARY
C                       X,LIBRARY,IMSLIB5
C
C...TAPE DIRECTORY:
C                   TAPE9 : 5YR DATA SORTED IN DESCENDING KT ORDER
C                   TAPE8 : INPUT ARRAY OF KNOWN DATA KT,AM,TB FROM
C                           GD2H5Y
C
C...COMMONS
      COMMON /CNSTS/ ALATR,DELOMO2,GSCF,HRCONV
C
      DIMENSION IRVS(8112),IRVS4(8112),WK(1)
      REAL KTAR(8112),AMAR(8112),TBAR(8112)
      REAL KTARR(8112),AMARR(8112),TBARR(8112)
      REAL KT,K,KT1,TB1,TB,ION,IO,IO2,ION2
      INTEGER BADPER,YR,DAY,MO,HR,MIN
C
C...NO. OF DATA FROM GD2H5Y (TAPE8)
      NPAIRS=8112
C
C
C...CONSTANTS
      ALATD=33.4046
      ALONGD=84.7478
      ALONST=75.0
      ZONE=5.0
      GSC=1367.0
      PI=4.0*ATAN(1.0)
      DRCONV=PI/180.0
      HRCONV=12.0/PI
      ALATR=ALATD*DRCONV
      DLOMEGA=15.0*DRCONV
      DELOMO2=DLOMEGA/2.0
      GSCF=3.6*GSC*12.0/PI
C
C...READ HOURLY DATA FROM GD2H5Y (TAPE8)
C   IN CALL STATEMENT NPAIRS=8112
C   NPRS IS THE VALUE OF THE NO OF DATA THAT PASSED THE TEST
C   (NPRS.LE.NPAIRS)
      CALL DATA(KTARR,AMARR,TBARR,NPAIRS,NPRS)
```

```
C
C...SORT DATA IN KT ASCENDING ORDER
C   CALL IMSL SORTING SUBROUTINES
      DO 300 IBA=1,NPRS
            IRVS(IBA)=IBA
 300  CONTINUE
C
      CALL VSRTP(KTARR,NPRS,IRVS)
C
      DO 400 IS=1,NPRS
 400  IRVS4(IS)=IRVS(IS)
C
      CALL VSRTU(AMARR,NPRS,NPRS,1,1,IRVS,WK)
C
      CALL VSRTU(TBARR,NPRS,NPRS,1,1,IRVS4,WK)
C
C...SORT DATA IN KT DESCENDING ORDER
      IDE=1
      DO 500 IE=NPRS,1,-1
            KTAR(IDE)=KTARR(IE)
            AMAR(IDE)=AMARR(IE)
            TBAR(IDE)=TBARR(IE)
            IDE=IDE+1
 500  CONTINUE
C
C...RECORD DATA IN TAPE9
      DO 600 IR=1,NPRS
            WRITE(9,601) KTAR(IR),AMAR(IR),TBAR(IR)
 601        FORMAT(3(2X,F16.14))
 600  CONTINUE
C
      STOP
      END
```

```
      SUBROUTINE DATA(KTARR,AMARR,TBARR,NPAIRS,NPRS)
C
C
C              SUBROUTINE DATA
C           C. BALARAS   1-25-87
C
C
C...SUBROUTINE TO READ DATA FROM GD2H5Y (TAPE9) FILE AND COLLECT
C   THE DATA FOR KT,AM,TB
C
C...INPUTS : NPAIRS = NO OF POINTS (8112 FOR THE 5YR DATA)
C...OUTPUTS : KTARR,AMARR,TBARR : CALC. VARIABLE ARRAYS
C             NPRS = NO OF GOOD DATA (.LE. 8112)
C
C...DIMENSION
      REAL KTARR(NPRS),AMARR(NPRS),TBARR(NPRS)
          REAL KT,K,KT1,TB1,TB,ION,IO,IO2,ION2
          INTEGER BADPER,YR,DAY,MO,HR,MIN
C
C...CONSTANTS
          ALATD=33.4046
          ALONGD=84.7478
          ALONST=75.0
          ZONE=5.0
          GSC=1367.0
          PI=4.0*ATAN(1.0)
          DRCONV=PI/180.0
          HRCONV=12.0/PI
          ALATR=ALATD*DRCONV
          DLOMEGA=15.0*DRCONV
          DELOMO2=DLOMEGA/2.0
          GSCF=3.6*GSC*12.0/PI
          NPRS=0
          IFRST=1
C
      DO 200 II=1,NPAIRS
C...READ ONE HOURS DATA
      READ(9,20) YR,MO,DAY,HR,MIN,HRZTOT,DIR,KT1,
     &KT,TB1,TB,PCT,BADPER
 20   FORMAT(1X,I2,4(2X,I2),4X,2(F7.1,2X),4X,2(F5.3,2X),
     &4X,2(F5.3,2X),4X,F4.2,2X,I2)
C...CALL SUBROUTINE HELGO FOR TIME-0.5 HOURS
      CVLT=(HR+MIN/60.)-0.5
      CALL HELGO(YR,MO,DAY,CVLT,ALONGD,ALATD,ALONST,ZONE,ALPHA,
     &DELTA,EOT,OMEGA,R)
C
C...CALL SUBROUTINE IRRADIATION
      CALL SUBI(OMEGA,ALATD,DELTA,BADPER,GSC,IFRST,R,HRZTOT,DIR,
     &KT,TB)
C
C...CALCULATE EXTRAT. NORMAL AND GLOBAL AND AVERAGE ZENITH COS.
      CALL EXTRAD(DELTA,OMEGA,R,HBNIO,HGIO,AZCOS,AHANG,DLO2)
C
C...CALCULATE THE SOLAR ALTITUDE
```

```
      SINALT=AZCOS
      IF (SINALT.GE.0.0) THEN
         ALTAVE=ASIN(SINALT)
      ELSE
         ALTAVE=-99.0
      END IF
C...CALCULATE AIRMASS
      AM=AMASS(ALTAVE)
C...TEST FOR VALIDITY OF RESULTS
C...FOR NEGATIVE ALTITUDE, AM=1.0E50, SKIP CALCULATIONS
      IF (AM.GT.100.0) GO TO 200
C
C..PLACE DATA IN ARRAYS
      NPRS=NPRS+1
      KTARR(NPRS)=KT
      TBARR(NPRS)=TB
      AMARR(NPRS)=AM
C
200   CONTINUE
C
      RETURN
      END
```

```
      PROGRAM TRGD(INPUT,OUTPUT,TAPE5=INPUT,TAPE6=OUTPUT,TAPE9,
     &             TAPE8,TAPE16)
C
C
C     C. BALARAS        6-18-87
C
C
C...SEPERATE DATA IN TRIANGULAR AREAS AND STORE THEM IN TAPE8
C   IN DESCENDING KT AND AM ORDER
C   OUTPUT DATA INCLUDES THE FOLLOWING INFORMATION:
C   NA : KT BAND COUNTER
C   NB : AM BAND COUNTER
C   IU : 0 LOWER TRIANGLE'S DATA
C        1 UPPER TRIANGLE'S DATA
C   KT, AM, TB : CORRESPONDING DATA
C   DATA ARE RECORDED FOR A GIVEN KT BAND, IN AM & KT DESCENDING
C   ORDER FOR A GIVEN TRIANGULAR AREA
C
C...TO RUN THIS PROGRAM:
C                       RUN "CRTAPE9" TO OBTAIN DATA
C                       GD2H5Y IN DESCENDING KT ORDER
C                       DATA WILL THEN BE RECORDED IN TAPE9
C                       AT,IMSLIB5/UN=LIBRARY
C                       X,LIBRARY,IMSLIB5
C
C...TAPE DIRECTORY:
C                   TAPE8 : 5YR DATA SORTED IN TRIANGULAR AREAS
C                   TAPE9 : INPUT ARRAY OF KNOWN DATA KT,AM,TB FROM
C                           "CRTAPE9" (5YR DATA IN DESCENDING KT)
C
C...COMMONS
      COMMON /CNSTS/ ALATR,DELOMO2,GSCF,HRCONV
C
      DIMENSION XO(16),YO(7)
      DIMENSION IRVS(8112),IRVS4(8112),WK(1)
      DIMENSION AKT(1500),AAM(1500),ATB(1500)
      DIMENSION AKILT(1000),AMILT(1000),ATBILT(1000)
      DIMENSION AKIUT(1000),AMIUT(1000),ATBIUT(1000)
      DIMENSION AKI(8112),AMI(8112),ATBI(8112)
      REAL KTARR(8112),AMARR(8112),TBARR(8112)
      REAL KT,K,KT1,TB1,TB,ION,IO,IO2,ION2
      INTEGER BADPER,YR,DAY,MO,HR,MIN
      DATA XO/0.85,0.8,0.75,0.7,0.65,0.6,0.55,0.5,0.45,0.4,0.35,
     &0.3,0.25,0.2,0.15,0.1/
      DATA YO/7.0,6.0,5.0,4.0,3.0,2.0,1.0/
C
C...NO. OF DATA FROM GD2H5Y (TAPE9)
      NPAIRS=8112
C
C...INITIALIZATIONS
      NAC=15
      NBC=6
      IH=0
      IRE=1
```

```
      IDE=1
      IDU=1
      IPTSX=IPTSY=ITPTS=0
      IPTC=1
      ILOC=1
      IA=IB=2
C
C
C...CONSTANTS
      ALATD=33.4046
      ALONGD=84.7478
      ALONST=75.0
      ZONE=5.0
      GSC=1367.0
      PI=4.0*ATAN(1.0)
      DRCONV=PI/180.0
      HRCONV=12.0/PI
      ALATR=ALATD*DRCONV
      DLOMEGA=15.0*DRCONV
      DELOM02=DLOMEGA/2.0
      GSCF=3.6*GSC*12.0/PI
C
C...READ HOURLY DATA FROM TAPE9
C   DATA ARE SORTED IN DESCENDING KT ORDER
      DO 12 IE=1,NPAIRS
            READ(9,13) KTARR(IE),AMARR(IE),TBARR(IE)
 13         FORMAT(3(2X,F16.14))
 12   CONTINUE
C
C
C             **** BEGIN TRIANGULATION OF DATA ****
C
      DO 400 IK=1,NPAIRS
C.....SEPARATE DATA IN KT BANDS START FROM 0.85
C     DOWN WITH 0.05 INCREMENTS
      IF (KTARR(IK).LT.XO(IA).OR.IK.EQ.NPAIRS) THEN
          IF (IK.EQ.NPAIRS) ITPTS=ITPTS+1
C           SORT DATA IN INCREASING AM
C           CALL IMSL SORTING SUBROUTINES
C           WE HAVE DETERMINED A NUMBER OF POINTS
C           WITHIN A KT BAND
C         WRITE(16,*) 'DESCENDING KT ORDER'
            DO 223 IBC=IK-IPTSX,ITPTS
                  KTARR(IDU)=KTARR(IBC)
                  AMARR(IDU)=AMARR(IBC)
                  TBARR(IDU)=TBARR(IBC)
C         WRITE(16,13) KTARR(IDU),AMARR(IDU),TBARR(IDU)
                  IDU=IDU+1
 223        CONTINUE
            DO 222 IBA=1,IDU-1
                  IRVS(IBA)=IBA
 222        CONTINUE
            CALL VSRTP(AMARR,IDU-1,IRVS)
            DO 555 IS=1,IDU-1
```

```
 555          IRVS4(IS)=IRVS(IS)
              CALL VSRTU(KTARR,IDU-1,IDU-1,1,1,IRVS,WK)
              CALL VSRTU(TBARR,IDU-1,IDU-1,1,1,IRVS4,WK)
C...RECORD DATA IN DESCENDING AM ORDER
C   CALL SUBR. REVM TO REVERSE THE ORDER OF KT,AM,TB ARRAYS
C   IN CALLING KT,AM,TB ARE IN AM ASCENDING ORDER
C   ON OUTPUT KT,AM,TB ARE IN DESCENDING ORDER
      CALL REVM(KTARR,AMARR,TBARR,IDU-1,AKT,AAM,ATB)
C          WRITE(16,*) 'AM DESCENDING ORDER'
C          DO 1 IPSA=1,IDU-1
C          WRITE(16,13) KTARR(IPSA),AMARR(IPSA),TBARR(IPSA)
C1    CONTINUE
C
           IFL=0
              DO 401 IL=1,IDU-1
C.............SEPARATE DATA IN AM BANDS START FROM 7.0 WITH
C               1.0 INCREMENTS DOWN TO 1.0
           IF (IFL.EQ.0) THEN
                 DO 2 ICHD=1,6
            IF (AMARR(IL).LT.YO(IB-1).AND.AMARR(IL).LT.YO(IB)) THEN
C          WRITE(16,*) 'AMARR(IL)=',AMARR(IL),YO(IB-1),YO(IB)
                    IB=IB+1
C          WRITE(16,*) 'IB=',IB
                  END IF
 2         CONTINUE
           IFL=1
           END IF
              IF (AMARR(IL).LT.YO(IB).OR.
     &              IL.EQ.IDU-1) THEN
C          WRITE(16,*) 'YO(',IB,')=',YO(IB)
C            POINTS IN AM BAND
             IF (IL.LT.IDU-1) IPTY=IPTC-1
C             HAVE EXHAUSTED THE POINTS, THE IPTC COUNTER WAS NOT
C             INCREMENTED YET. THEREFORE HAVE TO ACCOUNT FOR THAT
C             LOST POINT
             IF (IL.EQ.IDU-1) IPTY=IPTC
                    DO 402 IM=1,IPTY
                          IH=IH+1
                          AKI(IM)=KTARR(IH)
                          AMI(IM)=AMARR(IH)
                          ATBI(IM)=TBARR(IH)
 402                CONTINUE
C
C...DEFINE A QUADRILATERAL PLANE
C   WITH COORDINATES KT, AM
      AKI1=XO(IA-1)
      AMI1=YO(IB)
      AKI2=XO(IA-1)
      AMI2=YO(IB-1)
      AKI3=XO(IA)
      AMI3=YO(IB-1)
      AKI4=XO(IA)
      AMI4=YO(IB)
C
```

```
C...DEFINE A LOWER AND UPPER TRIANGLE
C    CALL SUBR. TRG TO SEPARATE DATA
       CALL TRG(AKI,AMI,ATBI,AKI1,AMI1,AKI3,AMI3,IPTY,
     & AKILT,AMILT,ATBILT,AKIUT,AMIUT,ATBIUT,NPTSLT,NPTSUT)
C
C...CREATE A DATA BASE WITH THE FOLLOWING INFORMATION:
C    NA : KT BAND COUNTER
C    NB : AM BAND COUNTER
C    IU : 0  LOWER TRIANGLE'S DATA
C         1  UPPER TRIANGLE'S DATA
C    KT,AM,TB CORRESPONDING DATA
       IF (NPTSLT.GT.0) THEN
       DO 100 I=1,NPTSLT
              ILOC=ILOC+1
                  NA=ABS(NAC-16)
           NB=IB-1
              IU=0
              AKI(ILOC)=AKILT(I)
              AMI(ILOC)=AMILT(I)
              ATBI(ILOC)=ATBILT(I)
              WRITE(8,101) NA,NB,IU,AKI(ILOC),
     &         AMI(ILOC),ATBI(ILOC)
 101          FORMAT(3(2X,I2),3(2X,F16.14))
 100   CONTINUE
       END IF
C
       IF (NPTSUT.GT.0) THEN
       DO 200 II=1,NPTSUT
              ILOC=ILOC+1
              NA=ABS(NAC-16)
           NB=IB-1
              IU=1
              AKI(ILOC)=AKIUT(II)
              AMI(ILOC)=AMIUT(II)
              ATBI(ILOC)=ATBIUT(II)
              WRITE(8,101) NA,NB,IU,AKI(ILOC),
     &         AMI(ILOC),ATBI(ILOC)
 200   CONTINUE
       END IF
C
C...INCREMENT AM BAND COUNTER
           IB=IB+1
           NBC=NBC-1
           IFL=0
C...RESET POINT COUNTER
       IPTC=1
C
       END IF
C
C...TOTAL NUMBER OF POINTS IN ALL AM BANDS
       IPTSY=IPTSY+1
C...POINTS IN EACH AM BAND
       IPTC=IPTC+1
 401   CONTINUE
```

```
C          REINITIALIZE VARIABLES FOR NEXT KT BAND
           IPTSX=IPTSY=0
             IPTC=1
C          INCREMENT COUNTERS
           IA=IA+1
           NAC=NAC-1
C          REINITIALIZE THE AM BAND COUNTER
           IB=2
           NBC=6
           IDU=1
           IH=0
           IRE=1
       END IF
C          NUMBER OF POINTS IN KT BANDS
           IPTSX=IPTSX+1
C          TOTAL NUMBER OF POINTS
           ITPTS=ITPTS+1
  400  CONTINUE
       STOP
       END
```

```
      SUBROUTINE TRG(AKI,AMI,ATBI,AKI2,AMI2,AKI3,AMI3,IPTY,
     &          AKILT,AMILT,ATBILT,AKIUT,AMIUT,ATBIUT,NPTSLT,NPTSUT)
C
C
C                    SUBROUTINE TRG
C                 C. BALARAS   10-15-86
C
C
C...SUBROUTINE TO SEPARATE THE GIVEN DATA AKI,AMI,ATBI, INTO AN
C   UPPER AND LOWER TRIANGLE OF THE DEFINED QUADRILATERAL PLANE
C
C...INPUTS:
C   AKI,AMI,ATBI : COORDINATES OF DATA
C   IPTY         : NUMBER OF POINTS IN QUADRILATERAL PLANE
C...OUTPUTS:
C   AKILT,AMILT,ATBILT : COORDINATES OF DATA FOR LOWER TRIANGLE
C   AKIUT,AMIUT,ATBIUT  : COORDINATES OF DATA FOR UPPER TRIANGLE
C   NPTSLT, NPTSUT   : NUMBER OF POINTS IN LOWER AND UPPER TRIANGLE
C
C...DIMENSIONS
           DIMENSION AKI(IPTY),AMI(IPTY),ATBI(IPTY)
           DIMENSION AKILT(IPTY),AMILT(IPTY),ATBILT(IPTY)
           DIMENSION AKIUT(IPTY),AMIUT(IPTY),ATBIUT(IPTY)
C
C...INITIALIZE
           NPTSLT=NPTSUT=0
C
       DO 10 I=1,IPTY
C      VALUE OF AIRMASS ON THE COMMON LINE BETWEEN THE TWO TRIANGLES
              DMLINE=(AKI(I)-AKI2)*((AMI2-AMI3)/(AKI2-AKI3))+AMI2
C
C...DATA FOR LOWER TRIANGLE
       IF (DMLINE.GT.AMI(I)) THEN
          NPTSLT=NPTSLT+1
          AKILT(NPTSLT)=AKI(I)
          AMILT(NPTSLT)=AMI(I)
          ATBILT(NPTSLT)=ATBI(I)
       ELSE
C...DATA FOR UPPER TRIANGLE
          NPTSUT=NPTSUT+1
          AKIUT(NPTSUT)=AKI(I)
          AMIUT(NPTSUT)=AMI(I)
          ATBIUT(NPTSUT)=ATBI(I)
       END IF
 10    CONTINUE
       RETURN
       END
```

```
      PROGRAM FIT3D2B(INPUT,OUTPUT,TAPE5=INPUT,TAPE6=OUTPUT,TAPE9,TAPE8,
     &               TAPE16)
C
C
C     C. BALARAS        3-27-87
C
C
C...READ 5YR DATA FROM TAPE8
C   THE DATA INCLUDES THE FOLLOWING INFORMATION
C   NA : KT BAND COUNTER
C   NB : AM BAND COUNTER
C   IU : 0 LOWER TRIANGLE'S DATA
C        1 UPPER TRIANGLE'S DATA
C   KT,AM,TB : CORRESPONDING DATA
C   THE 8112 HOURLY DATA ARE RECORDED FOR A GIVEN KT BAND,
C   IN ASCENDING ORDER BASED ON AIRMASS
C...THE OUTPUT ARE VALUES OF TB FOR THE BEST FITTED PLANE
C   THROUGH TRIANGULATED REGIONS OF THE DATA
C...THE RESULTS SHOULD AGREE WITH THE ONES OBTAINED USING "TEST8"
C   AGAIN IN THIS PROGRAM LOWER PREDEFINED TRIANGLES ARE LOST
C   "FIT3D" ACCOUNTS FOR ALL DATA
C
C...TO RUN THIS PROGRAM:
C                       AT,TAPE8
C                       AT,IMSLIB5/UN=LIBRARY
C                       X,LIBRARY,IMSLIB5
C
C...TAPE DIRECTORY:
C                   TAPE8 : INPUT 5YR DATA
C                   TAPE9 : AVAILABLE
C                   TAPE16 : OUTPUT CORNER COORDINATES OF TRIANGULAR PLANES
C                            TO BE USED BY PLOT3D2
C
C...COMMONS
      COMMON /CNSTS/ ALATR,DELOMO2,GSCF,HRCONV
C
      DIMENSION XO(16),YO(7)
      DIMENSION Z3(208,208)
      DIMENSION NA(8112),NB(8112),IU(8112)
      DIMENSION AKI(1000),AMI(1000),ATBI(1000)
      DIMENSION X(1000),Y(1000),Z(1000)
      REAL KTARR(8112),AMARR(8112),TBARR(8112)
      REAL KT,K,KT1,TB1,TB,ION,IO,IO2,ION2
      INTEGER BADPER,YR,DAY,MO,HR,MIN
      DATA XO/0.1,0.15,0.2,0.25,0.3,0.35,0.4,0.45,0.5,0.55,0.6,0.65,0.7,
     &0.75,0.8,0.85/
      DATA YO/1.0,2.0,3.0,4.0,5.0,6.0,7.0/
C
C...NO. OF DATA FROM GD2H5Y (TAPE9)
      NPAIRS=8112
C
C
C
C...READ 5YR HOURLY DATA (TAPE8)
```

```
      DO 100 I=1,NPAIRS
            READ(8,101) NA(I),NB(I),IU(I),KTARR(I),AMARR(I),TBARR(I)
 101        FORMAT(3(2X,I2),3(2X,F16.14))
 100  CONTINUE
C
C...INITIALIZE Z COORDINATE FOR FIRST TWO POINTS Z3(IA,IB)
      Z3(1,1)=Z3(1,2)=0.0
      IH=0
      IDU=1
      IPO=0
      IPTSX=IPTSY=ITPTS=0
      IPTC=1
      IA=IB=2
      SUMT=0.0
      RSST=0.0
      SYYT=0.0
C
C...START RECORDING COORDINATES OF KT,AM,Z3
C   FIRST TWO KNOWN CORNER POINTS
      WRITE(16,*) XO(1),YO(1),Z3(1,1),IA-1,IB-1
      WRITE(16,*) XO(1),YO(2),Z3(1,2),IA-1,IB
C
C      **** BEGIN CALCULATIONS ****
C
C...ANALYZE A KT BAND
      DO 400 IKT=1,15
C
C...ANALYZE AM BANDS FOR THE IKT BAND
      DO 401 IAM=1,6
C
C             FOR THE FIRST AM BAND (1<AM<1.5)
            IF (IAM.EQ.1) THEN
C             DEFINE CORNER POINTS OF QUADRILATERAL PLANE
C             KNOWN POINTS ARE 1 AND 2
C             POINT 1
            AKI1=XO(IKT)
            AMI1=YO(IAM+1)
            ATBI1=Z3(IKT,IAM+1)
C             POINT 2
            AKI2=XO(IKT)
            AMI2=YO(IAM)
            ATBI2=Z3(IKT,IAM)
C             POINT 3
            AKI3=XO(IKT+1)
            AMI3=YO(IAM)
C             POINT 4
            AKI4=XO(IKT+1)
            AMI4=YO(IAM+1)
C
C             FOR THE DEFINED QUADRIALTERAL PLANE
C             COLLECT DATA FOR LOWER TRIANGLE
            ICHECK=0
            DO 402 IBR=1,NPAIRS
            IF (ICHECK.EQ.1) GOTO 402
```

```
                    IF (NA(IBR).EQ.IKT.AND.NB(IBR).EQ.IAM.AND.
     &               IU(IBR).EQ.0) THEN
                       IM=IBR
                       NPTSLT=0
                    ICHECK=1
                    END IF
 402          CONTINUE
C              COLLECT DATA OF LOWER TRIANGLE
C              FOR THAT AM BAND
             IF (ICHECK.EQ.1) THEN
             IEND=1
             DO 403 ILOC=IM,NPAIRS
             IF (IEND.EQ.0) GOTO 403
                    IF (IU(ILOC).EQ.1.OR.NB(ILOC).GT.IAM.OR.
     &                NA(ILOC).GT.IKT) THEN
C                      STOP COLLECTING DATA
                  IEND=0
                       GO TO 403
                    END IF
C
                    NPTSLT=NPTSLT+1
                    AKI(NPTSLT)=KTARR(ILOC)
                    AMI(NPTSLT)=AMARR(ILOC)
                    ATBI(NPTSLT)=TBARR(ILOC)
          IPO=IPO+1
 403          CONTINUE
                    ELSE
C                     THERE ARE NO DATA AVAILABLE
C                     SET VALUE OF Z3 AND SKIP FOLLOWING CALCS.
                     PHI=ATAN2((AMI2-AMI1),(AKI2-AKI1))
                     CALL CORDCH(AKI1,AMI1,ATBI1,AKI2,AMI2,ATBI2,
     &                          AKI3,AMI3,PHI,Z3(IKT+1,IAM))
                     Z3(IKT+1,IAM)=Z3(IKT+1,IAM)+ATBI1
                       GO TO 799
                    END IF
C
C...CHANGE TO NEW COORDINATES FOR LOWER TRG POINTS
C   CALCUALTE ANGLE OF ROTATION
      PHI=ATAN2((AMI2-AMI1),(AKI2-AKI1))
      CALL COORDCH(AKI,AMI,ATBI,AKI1,AMI1,ATBI1,
     &AKI2,AMI2,ATBI2,AKI3,AMI3,PHI,NPTSLT,X,Y,Z,X2,Y2,Z2,X3,Y3)
C...FOR THE TRG SPACE, FIT THE BEST TRG PLANE TO MIN ERROR
      CALL TRGFIT(X,Y,Z,X2,Y2,Z2,X3,Y3,NPTSLT,Z3(IKT+1,IAM))
C...CHANGE Z3 TO OLD COORDINATES
      Z3(IKT+1,IAM)=Z3(IKT+1,IAM)+ATBI1
      IF (Z3(IKT+1,IAM).LT.0.0) Z3(IKT+1,IAM)=0.0
C...CALCULATE EQ. OF PLANEA1X+A2Y+A3Z+D=0
      CALL PLANEQ(AKI1,AMI1,ATBI1,AKI2,AMI2,ATBI2,AKI3,AMI3,
     &Z3(IKT+1,IAM),A1,A2,A3,D)
C...UNEXPLAINED VARIATION
      DO 800 IDIS=1,NPTSLT
C   DISTANCE OF A DATA POINT FROM PLANE, H
      H=ABS(A1*AKI(IDIS)+A2*AMI(IDIS)+A3*ATBI(IDIS)+D)/
     &SQRT(A1*A1+A2*A2+A3*A3)
```

```
      RSST=RSST+H*H
 800  CONTINUE
C   RECORD POINT COORDINATES
 799  WRITE(16,*) XO(IKT+1),YO(IAM),Z3(IKT+1,IAM),IKT+1,IAM
C
C...FOR THE UPPER TRIANGLES
C   FIRST KT BAND
      IF (IKT.EQ.1) THEN
C...LOCATE STARTING POINT
      ICHECK=0
      DO 404 IBR=1,NPAIRS
            IF (ICHECK.EQ.1) GOTO 404
            IF (NA(IBR).EQ.IKT.AND.NB(IBR).EQ.IAM.AND.
     &        IU(IBR).EQ.1) THEN
              IM=IBR
              NPTSUT=0
            ICHECK=1
            END IF
 404  CONTINUE
C
C...IF THERE ARE NO DATA
      IF (ICHECK.EQ.0) THEN
         PHI=ATAN2((AMI3-AMI1),(AKI3-AKI1))
         CALL CORDCH(AKI1,AMI1,ATBI1,AKI3,AMI3,Z3(IKT+1,IAM),
     &             AKI4,AMI4,PHI,Z3(IKT+1,IAM+1))
         Z3(IKT+1,IAM+1)=Z3(IKT+1,IAM+1)+ATBI1
         GO TO 798
      END IF
C
C...COLLECT DATA
            IEND=1
      DO 405 ILOC=IM,NPAIRS
            IF(IEND.EQ.0) GOTO 405
            IF (NB(ILOC).GT.1.OR.NA(ILOC).GT.1) THEN
            IEND=0
               GO TO 405
            END IF
            NPTSUT=NPTSUT+1
            AKI(NPTSUT)=KTARR(ILOC)
            AMI(NPTSUT)=AMARR(ILOC)
            ATBI(NPTSUT)=TBARR(ILOC)
             IPO=IPO+1
 405  CONTINUE
      END IF
C
C...FOR UPPER TRIANGLES
C   REMAINING KT BANDS
      IF (IKT.GT.1) THEN
C...LOCATE STARTING POINT
      ICHECK=0
      DO 331 IBR=1,NPAIRS
            IF (ICHECK.EQ.1) GOTO 331
            IF (NA(IBR).EQ.IKT.AND.NB(IBR).EQ.IAM.AND.
     &        IU(IBR).EQ.1) THEN
```

```
                IM=IBR
                NPTSUT=0
              ICHECK=1
              END IF
 331  CONTINUE
C
C...IF THERE ARE NO DATA
      IF (ICHECK.EQ.0) THEN
         PHI=ATAN2((AMI3-AMI1),(AKI3-AKI1))
         CALL CORDCH(AKI1,AMI1,ATBI1,AKI3,AMI3,Z3(IKT+1,IAM),
     &              AKI4,AMI4,PHI,Z3(IKT+1,IAM+1))
         Z3(IKT+1,IAM+1)=Z3(IKT+1,IAM+1)+ATBI1
         GO TO 798
      END IF
C
C...COLLECT DATA
              IEND=1
      DO 332 ILOC=IM,NPAIRS
              IF(IEND.EQ.0) GOTO 332
              IF (NB(ILOC).GT.1.OR.NA(ILOC).GT.IKT) THEN
              IEND=0
                 GO TO 332
              END IF
              NPTSUT=NPTSUT+1
              AKI(NPTSUT)=KTARR(ILOC)
              AMI(NPTSUT)=AMARR(ILOC)
              ATBI(NPTSUT)=TBARR(ILOC)
                   IPO=IPO+1
 332  CONTINUE
      END IF
C
C...CHANGE TO NEW COORDINATES FOR UPPER TRG POINTS
C   CALCULATE ANGLE OF ROTATION
      PHI=ATAN2((AMI3-AMI1),(AKI3-AKI1))
      CALL COORDCH(AKI,AMI,ATBI,AKI1,AMI1,ATBI1,
     &AKI3,AMI3,Z3(IKT+1,IAM),AKI4,AMI4,PHI,NPTSUT,
     &X,Y,Z,X3,Y3,ZP3,X4,Y4)
C   FIT THE BEST TRG PLANE TO MINIMIZE ERROR
      CALL TRGFIT(X,Y,Z,X3,Y3,ZP3,X4,Y4,NPTSUT,
     &Z3(IKT+1,IAM+1))
C   CHANGE TO OLD COORD
      Z3(IKT+1,IAM+1)=Z3(IKT+1,IAM+1)+ATBI1
      IF (Z3(IKT+1,IAM+1).LT.0.0) Z3(IKT+1,IAM+1)=0.0
C...CALCULATE EQ. OF PLANE A1X+A2Y+A3Z+D=0
      CALL PLANEQ(AKI1,AMI1,ATBI1,AKI3,AMI3,Z3(IKT+1,IAM),
     &AKI4,AMI4,Z3(IKT+1,IAM+1),A1,A2,A3,D)
C...FOR THE DATA IN THE PLANE CALC.
C   UNEXPLAINED VARIATION
      DO 801 IDIS=1,NPTSUT
C   DISTANCE OF A DATA POINT FROM PLANE, H
      H=ABS(A1*AKI(IDIS)+A2*AMI(IDIS)+A3*ATBI(IDIS)+D)/
     &SQRT(A1*A1+A2*A2+A3*A3)
      RSST=RSST+H*H
 801  CONTINUE
```

```
C...RECORD POINT COORD
 798  WRITE(16,*) XO(IKT+1),YO(IAM+1),Z3(IKT+1,IAM+1),IKT+1,IAM+1
      END IF
C
C
C...REMAINING AM BANDS
      IF (IAM.GT.1) THEN
C
C...DEFINE CORNER POINT OF QUADRILATERAL PLANE
C   KNOWN POINTS ARE 1 AND 2
C   POINT 1
      AKI1=XO(IKT)
      AMI1=YO(IAM)
      ATBI1=Z3(IKT,IAM)
C   POINT 2
      AKI2=XO(IKT+1)
      AMI2=YO(IAM)
      ATBI2=Z3(IKT+1,IAM)
C   POINT 3
      AKI3=XO(IKT)
      AMI3=YO(IAM+1)
C   POINT 4
      AKI4=XO(IKT+1)
      AMI4=YO(IAM+1)
C
C...FOR THE DEFINED QUADRILATERAL PLANE COLLECT
C   DATA FOR LOWER TRIANGLE
C...FOR THE FIRST KT BAND
      IF (IKT.EQ.1) THEN
      ICHECK=0
      DO 410 IBR=1,NPAIRS
            IF (ICHECK.EQ.1) GOTO 410
            IF (NA(IBR).EQ.IKT.AND.NB(IBR).EQ.IAM.AND.
     &       IU(IBR).EQ.0) THEN
              IM=IBR
              NPTSLT=0
               ICHECK=1
            END IF
 410  CONTINUE
C
C...IF THERE ARE NO DATA SET Z3=0.
      IF (ICHECK.EQ.0) THEN
         PHI=ATAN2((AMI2-AMI1),(AKI2-AKI1))
         CALL CORDCH(AKI1,AMI1,ATBI1,AKI2,AMI2,ATBI2,
     &          AKI3,AMI3,PHI,Z3(IKT,IAM+1))
         Z3(IKT,IAM+1)=Z3(IKT,IAM+1)+ATBI1
         GO TO 797
      END IF
C
C...COLLECT DATA OF LOWER TRIANGLE
C   FOR THAT AM BAND
            IEND=1
      DO 411 ILOC=IM,NPAIRS
            IF (IEND.EQ.0) GOTO 411
```

```
            IF (IU(ILOC).EQ.1.OR.NB(ILOC).GT.IAM.OR.
     &NA(ILOC).GT.IKT) THEN
            IEND=0
               GO TO 411
            END IF
C
            NPTSLT=NPTSLT+1
            AKI(NPTSLT)=KTARR(ILOC)
            AMI(NPTSLT)=AMARR(ILOC)
            ATBI(NPTSLT)=TBARR(ILOC)
                 IPO=IPO+1
 411  CONTINUE
C
C...CHANGE TO NEW COORDINATES FOR LOWER TRG POINTS
C    CALCULATE ANGLE OF ROTATION
       PHI=ATAN2((AMI2-AMI1),(AKI2-AKI1))
       CALL COORDCH(AKI,AMI,ATBI,AKI1,AMI1,ATBI1,
     &AKI2,AMI2,ATBI2,AKI3,AMI3,PHI,NPTSLT,
     &X,Y,Z,X2,Y2,Z2,X3,Y3)
C    FIT THE BEST TRG PLANE TO MINIMIZE ERROR
       CALL TRGFIT(X,Y,Z,X2,Y2,Z2,X3,Y3,NPTSLT,
     &Z3(IKT,IAM+1))
C    CHANGE TO OLD COORD
       Z3(IKT,IAM+1)=Z3(IKT,IAM+1)+ATBI1
       IF (Z3(IKT,IAM+1).LT.0.0) Z3(IKT,IAM+1)=0.0
C...CALCULATE EQ. OF PLANE A1X+A2Y+A3Z+D=0
       CALL PLANEQ(AKI1,AMI1,ATBI1,AKI2,AMI2,Z3(IKT+1,IAM),
     &AKI3,AMI3,Z3(IKT,IAM+1),A1,A2,A3,D)
C...FOR THE DATA IN THE PLANE CALC.
C    UNEXPLAINED VARIATION
       DO 802 IDIS=1,NPTSLT
C    DISTANCE OF A DATA POINT FROM PLANE, H
       H=ABS(A1*AKI(IDIS)+A2*AMI(IDIS)+A3*ATBI(IDIS)+D)/
     &SQRT(A1*A1+A2*A2+A3*A3)
       RSST=RSST+H*H
 802  CONTINUE
C...RECORD POINT COORD
 797  WRITE(16,*) XO(IKT),YO(IAM+1),Z3(IKT,IAM+1),IKT,IAM+1
C
C...FOR THE UPPER TRIANGLE OF THE FIRST KT BAND
       ICHECK=0
       DO 412 IBR=1,NPAIRS
            IF (ICHECK.EQ.1) GOTO 412
            IF (NA(IBR).EQ.IKT.AND.NB(IBR).EQ.IAM.AND.
     &       IU(IBR).EQ.1) THEN
               IM=IBR
               NPTSUT=0
                ICHECK=1
            END IF
 412   CONTINUE
C
C...IF THERE ARE NO DATA IN UPPER TRG
       IF (ICHECK.EQ.0) THEN
          PHI=ATAN2((AMI2-AMI3),(AKI2-AKI3))
```

```
          CALL CORDCH(AKI3,AMI3,Z3(IKT,IAM+1),AKI2,AMI2,ATBI2,
     &          AKI4,AMI4,PHI,Z3(IKT+1,IAM+1))
          Z3(IKT+1,IAM+1)=Z3(IKT+1,IAM+1)+Z3(IKT,IAM+1)
          GO TO 796
        END IF
C
C...COLLECT DATA FOR UPPER TRG FOR THAT AM BAND
              IEND=1
        DO 413 ILOC=IM,NPAIRS
              IF (IEND.EQ.0) GOTO 413
           IF (IU(ILOC).EQ.0.OR.NB(ILOC).GT.IAM.OR.NA(ILOC).GT.IKT) THEN
              IEND=0
                 GO TO 413
              END IF
C
              NPTSUT=NPTSUT+1
              AKI(NPTSUT)=KTARR(ILOC)
              AMI(NPTSUT)=AMARR(ILOC)
              ATBI(NPTSUT)=TBARR(ILOC)
                  IPO=IPO+1
 413  CONTINUE
C
C...CHANGE TO NEW COORDINATES FOR UPPER TRG POINTS
C    CALCULATE ANGLE OF ROTATION
 635  PHI=ATAN2((AMI2-AMI3),(AKI2-AKI3))
        CALL COORDCH(AKI,AMI,ATBI,AKI3,AMI3,Z3(IKT,IAM+1),
      &AKI2,AMI2,ATBI2,AKI4,AMI4,PHI,NPTSUT,
      &X,Y,Z,X2,Y2,Z2,X4,Y4)
C    FIT THE BEST TRG PLANE TO MINIMIZE ERROR
        CALL TRGFIT(X,Y,Z,X2,Y2,Z2,X4,Y4,NPTSUT,
      &Z3(IKT+1,IAM+1))
C    CHANGE TO OLD COORD
        Z3(IKT+1,IAM+1)=Z3(IKT+1,IAM+1)+Z3(IKT,IAM+1)
        IF (Z3(IKT+1,IAM+1).LT.0.0) Z3(IKT+1,IAM+1)=0.0
C...CALCULATE EQ. OF PLANE A1X+A2Y+A3Z+D=0
        CALL PLANEQ(AKI3,AMI3,Z3(IKT,IAM+1),AKI2,AMI2,ATBI2,
      &AKI4,AMI4,Z3(IKT+1,IAM+1),A1,A2,A3,D)
C...FOR THE DATA IN THE PLANE CALC.
C    UNEXPLAINED VARIATION
        DO 803 IDIS=1,NPTSUT
C    DISTANCE OF A DATA POINT FROM PLANE, H
        H=ABS(A1*AKI(IDIS)+A2*AMI(IDIS)+A3*ATBI(IDIS)+D)/
      &SQRT(A1*A1+A2*A2+A3*A3)
        RSST=RSST+H*H
 803  CONTINUE
C...RECORD POINT COORD
 796  WRITE(16,*) XO(IKT+1),YO(IAM+1),Z3(IKT+1,IAM+1),IKT+1,IAM+1
        END IF
C
C...FOR KT BANDS .NE. 1 AND AM .NE. 1
C    WORK ON UPPER TRG ONLY
        IF (IKT.GT.1) THEN
           ICHECK=0
           DO 416 IBR=1,NPAIRS
```

```
            IF (ICHECK.EQ.1) GOTO 416
            IF (NA(IBR).EQ.IKT.AND.NB(IBR).EQ.IAM.AND.
     &       IU(IBR).EQ.1) THEN
               IM=IBR
               NPTSUT=0
                ICHECK=1
            END IF
 416  CONTINUE
C
C...IF THERE ARE NO DATA IN UPPER TRG
      IF (ICHECK.EQ.0) THEN
         PHI=ATAN2((AMI2-AMI3),(AKI2-AKI3))
         CALL CORDCH(AKI3,AMI3,Z3(IKT,IAM+1),AKI2,AMI2,ATBI2,
     &          AKI4,AMI4,PHI,Z3(IKT+1,IAM+1))
         Z3(IKT+1,IAM+1)=Z3(IKT+1,IAM+1)+Z3(IKT,IAM+1)
         GO TO 795
      END IF
C
C...COLLECT DATA
            IEND=1
      DO 417 ILOC=IM,NPAIRS
            IF (IEND.EQ.0) GOTO 417
         IF (IU(ILOC).EQ.0.OR.NB(ILOC).GT.IAM.OR.NA(ILOC).GT.IKT) THEN
            IEND=0
               GO TO 417
            END IF
            NPTSUT=NPTSUT+1
            AKI(NPTSUT)=KTARR(ILOC)
            AMI(NPTSUT)=AMARR(ILOC)
            ATBI(NPTSUT)=TBARR(ILOC)
                IPO=IPO+1
 417  CONTINUE
C
C...CHANGE TO NEW COORDINATES FOR UPPER TRG POINTS
C    CALCULATE ANGLE OF ROTATION
      PHI=ATAN2((AMI2-AMI3),(AKI2-AKI3))
      CALL COORDCH(AKI,AMI,ATBI,AKI3,AMI3,Z3(IKT,IAM+1),
     &AKI2,AMI2,ATBI2,AKI4,AMI4,PHI,NPTSUT,
     &X,Y,Z,X2,Y2,Z2,X4,Y4)
C    FIT THE BEST TRG PLANE TO MINIMIZE ERROR
      CALL TRGFIT(X,Y,Z,X2,Y2,Z2,X4,Y4,NPTSUT,
     &Z3(IKT+1,IAM+1))
C    CHANGE TO OLD COORD
      Z3(IKT+1,IAM+1)=Z3(IKT+1,IAM+1)+Z3(IKT,IAM+1)
      IF (Z3(IKT+1,IAM+1).LT.0.0) Z3(IKT+1,IAM+1)=0.0
C...CALCULATE EQ. OF PLANE A1X+A2Y+A3Z+D=0
      CALL PLANEQ(AKI3,AMI3,Z3(IKT,IAM+1),AKI2,AMI2,ATBI2,
     &AKI4,AMI4,Z3(IKT+1,IAM+1),A1,A2,A3,D)
C...FOR THE DATA IN THE PLANE CALC.
C    UNEXPLAINED VARIATION
      DO 804 IDIS=1,NPTSUT
C    DISTANCE OF A DATA POINT FROM PLANE, H
      H=ABS(A1*AKI(IDIS)+A2*AMI(IDIS)+A3*ATBI(IDIS)+D)/
     &SQRT(A1*A1+A2*A2+A3*A3)
```

```
      RSST=RSST+H*H
 804  CONTINUE
C...RECORD POINT COORD
 795  WRITE(16,*) XO(IKT+1),YO(IAM+1),Z3(IKT+1,IAM+1),IKT+1,IAM+1
      END IF
         END IF
 401  CONTINUE
 400  CONTINUE
C...STATISTICAL ANALYSIS
C...SUMMATION OF BEAM TRANSMITTANCES
      DO 776 IP=1,NPAIRS
            SUMT=SUMT+TBARR(IP)
 776  CONTINUE
      TAVE=SUMT/NPAIRS
C...CALCULATE TOTAL VARIATION
      DO 777 IS=1,NPAIRS
            SYYT=SYYT+(TBARR(IS)-TAVE)**2
 777  CONTINUE
C...EXPLAINED VARIATION
      SSREG=SYYT-RSST
      WRITE(16,*) 'RSST=',RSST,'  SYYT=',SYYT,'  SSREG=',SSREG
C...COEFFICIENT OF CORRELATION
      AR=SQRT(SSREG/SYYT)
C...COEFFICIENT OF DETERMINATION
      AR2=AR*AR
      WRITE(16,*) ' '
      WRITE(16,*) 'R=',AR,'  R2=',AR2
      WRITE(16,*) 'NUMBER OF POINTS USED: ',IPO
      STOP
      END
```

```
      SUBROUTINE COORDCH(DKI,DMI,DTBI,PKT1,PAM1,PTB1,PKT2,PAM2,PTB2,
     &                   PKT3,PAM3,PHI,NPNTS,
     &                   X,Y,Z,X2,Y2,Z2,X3,Y3)
C
C
C                    SUBROUTINE COORDCH
C                  C. BALARAS   10-20-86
C
C
C...THIS SUBROUTINE TRANSFORMS THE KT,AM,TB COORDINATES INTO X,Y,Z
C   COORDINATES (THE CORD. SYSTEM STILL REMAINS RIGHT HANDED)
C   THE ORIGIN OF THE NEW COORD IS SET AT THE FIRST KNOWN POINT OF
C   THE TRIANGULAR PLANE (XO=YO=ZO=0 AT KT1,AM1,TB1)
C   THE SECOND KNOWN POINT IS ON THE X AXIS (WITH Y2=0)
C   THE OLD COORDINATE SYSTEM IS SHIFTED BY AN ANGLE OF PHI
C...INPUTS :
C   DKI,DMI,DTBI COORDINATES OF DATA IN KT,AM,TB SYSTEM
C   PKT1,PAM1,PTB1 COORDINATES OF FIRST KNOWN POINT IN OLD SYSTEM
C                  IN NEW COORDINATES THEY ARE THE ORIGIN
C   PKT2,PAM2,PTB2 COORDINATES OF SECOND KNOWN POINT IN OLD SYSTEM
C   PKT3,PAM3 X,Y COORDINATES OF TOP CORNER POINT
C...OUTPUTS :
C   X,Y,Z NEW COORDINATES OF DATA POINTS
C   X2,Y2,Z2 NEW COORDINATES OF SECOND KNOWN POINT
C   X3,Y3 NEW COORDINATES OF TOP CORNER POINT
C...DEPENDING ON THE CALL STATEMENT- FOR LOWER OR UPPER TRIANGLES
C   THESE POINTS REPRESENT POINTS 2 AND 1 (LOWER) OR 2 AND 3 (UPPER)
C   IN THE ORIGINAL COORD. SYSTEM
C
C...DIMENSION
      DIMENSION DKI(NPNTS),DMI(NPNTS),DTBI(NPNTS),X(NPNTS),Y(NPNTS),
     &          Z(NPNTS)
C
C
C...COORDINATE TRANSFORMATION FOR DATA POINTS
      DO 10 I=1,NPNTS
            X(I)=(DMI(I)-PAM1)*SIN(PHI)+(DKI(I)-PKT1)*COS(PHI)
            Y(I)=(DMI(I)-PAM1)*COS(PHI)-(DKI(I)-PKT1)*SIN(PHI)
            Z(I)=DTBI(I)-PTB1
 10   CONTINUE
C...COORDINATE TRANSFORMATION FOR CORNER POINTS 2 & 3
      X2=(PAM2-PAM1)*SIN(PHI)+(PKT2-PKT1)*COS(PHI)
      Y2=(PAM2-PAM1)*COS(PHI)-(PKT2-PKT1)*SIN(PHI)
      Z2=PTB2-PTB1
      X3=(PAM3-PAM1)*SIN(PHI)+(PKT3-PKT1)*COS(PHI)
      Y3=(PAM3-PAM1)*COS(PHI)-(PKT3-PKT1)*SIN(PHI)
      RETURN
      END
```

```
      SUBROUTINE CORDCH(PKT1,PAM1,PTB1,PKT2,PAM2,PTB2,
     &                  PKT3,PAM3,PHI,Z3)
C
C
C                    SUBROUTINE CORDCH
C                  C. BALARAS   6-2-86
C
C
C...THIS SUBROUTINE ESTIMATES THE COORD. Z3 WHEN DATA ARE NOT
C   AVAILABLE. THE ORIGIN OF THE NEW COORD IS SET AT THE FIRST
C   KNOWN POINT OF THE TRIANGULAR PLANE (XO=YO=ZO=0 AT KT1,AM1,TB1)
C   THE SECOND KNOWN POINT IS ON THE X AXIS (WITH Y2=0)
C   THE OLD COORDINATE SYSTEM IS SHIFTED BY AN ANGLE OF PHI
C...INPUTS :
C   PKT1,PAM1,PTB1 COORDINATES OF FIRST KNOWN POINT IN OLD SYSTEM
C                  IN NEW COORDINATES THEY ARE THE ORIGIN
C   PKT2,PAM2,PTB2 COORDINATES OF SECOND KNOWN POINT IN OLD SYSTEM
C   PKT3,PAM3 X,Y COORDINATES OF TOP CORNER POINT
C...OUTPUTS :
C   Z3 ESTIMATED NEW COORDINATE
C...DEPENDING ON THE CALL STATEMENT- FOR LOWER OR UPPER TRIANGLES
C   THESE POINTS REPRESENT POINTS 2 AND 1 (LOWER) OR 2 AND 3 (UPPER)
C   IN THE ORIGINAL COORD. SYSTEM
C
C
C...COORDINATE TRANSFORMATION FOR CORNER POINTS 2 & 3
      X2=(PAM2-PAM1)*SIN(PHI)+(PKT2-PKT1)*COS(PHI)
      Y2=(PAM2-PAM1)*COS(PHI)-(PKT2-PKT1)*SIN(PHI)
      Z2=PTB2-PTB1
      X3=(PAM3-PAM1)*SIN(PHI)+(PKT3-PKT1)*COS(PHI)
      Y3=(PAM3-PAM1)*COS(PHI)-(PKT3-PKT1)*SIN(PHI)
      Z3=(X3/X2)*Z2
      RETURN
      END
```

```
      SUBROUTINE TRGFIT(X,Y,Z,X2,Y2,Z2,X3,Y3,NPNTS,Z3)
C
C
C                       SUBROUTINE TRGFIT
C                    C. BALARAS   10-10-86
C
C
C...SUBROUTINE TO CALCULATE THE Z COORDINATE OF THE UPPER CORNER
C   OF THE TRIANGULAR PLANE TO MINIMIZE ERROR
C   INPUTS:
C           X,Y,Z : COORD. OF DATA POINTS
C           X2,Y2,Z2 : COORD. OF SECOND KNOWN POINT. FIRST KNOWN POINT
C                      IS LOCATED AT THE ORIGIN (0,0,0) OF THIS COORD.
C                      SYSTEM
C           X3,Y3    : KNOWN COORD. OF THE THIRD (TOP) POINT
C           NPNTS    : NUMBER OF DATA POINTS
C   OUTPUT:
C           Z3 : Z COORD. OF THIRD POINT TO MINIMIZE ERROR
C
C
C...DIMENSIONS
          DIMENSION X(NPNTS),Y(NPNTS),Z(NPNTS)
C
C
C...INITIALIZATIONS
          S1=S2=S3=S4=0.0
C
C...FIRST POINT IS THE ORIGIN
       DO 10 I=1,NPNTS
             S1=S1+Z(I)*Y(I)
             S2=S2+(Z2*X(I)*Y(I)/X2)
             S3=S3+((Y(I)*Y(I)*X3*Z2)/(Y3*X2))
             S4=S4+(Y(I)*Y(I)/Y3)
  10   CONTINUE
C
       Z3=(S1+S3-S2)/S4
          IF (Z3.LT.0.0) Z3=0.0
C
       RETURN
       END
```

```
      SUBROUTINE PLANEQ(X1,Y1,Z1,X2,Y2,Z2,X3,Y3,Z3,A1,A2,A3,D)
C
C
C                          SUBROUTINE PLANEQ
C                        C. BALARAS  2-25-87
C
C
C...GIVEN THREE POINTS DEFINE THE EQUATION OF THE PLANE PASSING
C   THROUGH (X1,Y1,Z1)  (X2,Y2,Z2)  (X3,Y3,Z3)
C   THE FORM OF THE EQUATION IS A1*X+A2*Y+A3*Z+D=0
C...INPUTS:
C           X1,Y1,Z1: X,Y,Z COORD. OF FIRST POINT
C           X2,Y2,Z2: X,Y,Z COORD. OF SECOND POINT
C           X3,Y3,Z3: X,Y,Z COORD. OF THIRD POINT
C...OUTPUTS:
C           A1,A2,A3,D: COEF. OF THE EQ. OF PLANE
C
      A1=((Z3-Z1)*(Y2-Y1))-((Z2-Z1)*(Y3-Y1))
      A2=((Z2-Z1)*(X3-X1))-((X2-X1)*(Z3-Z1))
      A3=((X2-X1)*(Y3-Y1))-((Y2-Y1)*(X3-X1))
      D=-(A1*X1)-(A2*Y1)-(A3*Z1)
      RETURN
      END
```

```
      PROGRAM PLOT3DB(INPUT,OUTPUT,TAPE5=INPUT,TAPE6=OUTPUT,TAPE16,
     &                TAPE2,TAPE8)
C
C   C. BALARAS    6-8-87
C
C...PLOTTING OF A 3-D SURFACE DEFINED BY A MATRIX [Z(X,Y)]
C   A 2-D MATRIX IS SUPPLIED WHOSE VALUES CORRESPOND
C   TO THE Z VALUES AT THE INTERSECTIONS OF THE BASE GRID
C   (REFER TO SECTION 3.2 OF THE DISSPLA MANUAL)
C...CAN ALSO PLOT THE SOLAR DATA
C   TAPE16 = DATA TAPE OF AN X,Y,Z ARRAY
C   TAPE8 = SOLAR DATA (OUTPUT OF TRGDATA)
C   TAPE2 = OUTPUT PLOT FILE
C
C...TO RUN THIS PROGRAM -
C                        C,GD2H5Y,TAPE26
C                        AT,CALCOMP,IMSLIB5/UN=LIBRARY
C                        X,LIBRARY,CALCOMP,IMSLIB5
C                        FTN5,I=TEST6,L=0       (TO CREATE TAPE16)
C                        AT,DISSPLA/UN=LIBRARY
C                        X,LIBRARY,DISSPLA
C                        FTN5,I=PLOT3D2,L=0,REW
C...TO SUBMIT PLOTTING JOBTO CALCOMP-
C        PLOTQ,TAPE2,PN=5,PA=0,FC=50
C   WHERE  PN - PEN CODE
C          PA - PAPER CODE
C          FC - SCALLING FACTOR
C...TO SUBMIT A JOB TO XEROX PRINTER - EPIC,TAPE2
C
C...DIMENSIONS
      DIMENSION TBMAT(19,8),IBUF(512)
C...DECLARATIONS
      REAL KT
C...SHOULD SOLAR DATA APPEAR ON THE PLOT?
      WRITE(6,*) 'SHOULD SOLAR DATA APPEAR ON THE PLOT (Y=1, N=0)'
      READ(5,*) ISHOW
C...DECLARE OUTPUT PLOTTING FILE AND PLOTTER (VRSTEC)
C     CALL PVRSTC
C     CALL VRSTEC(IBUF,512,2)
C...USING CALCOMP
C     CALL PCLCMP
C     CALL CALCMP(IBUF,512,2)
C...USING XEROX PRINTER
C   TO PLOT USE, EPIC,TAPE2
      CALL PEPIC
      CALL EPIC(300.,0,7.0,7.0,2)
C...SELECT PLOT REDUCTION OR ENLARGEMENT FACTOR
      CALL BLOWUP(1.0)
C...CALL FOR SWISS-LIGHT LETTERING STYLE
      CALL SWISSL
C...PLOTTING OF A 3-D SURFACE
C...PAGE SIZE BORDER
      CALL PAGE(12.0,15.0)
```

```
C...DEFINE SUBPLOT AREA
      CALL AREA2D(11.5,14.5)
C...DEFINE X,Y,Z WORKBOX IN INCHES
      CALL VOLM3D(5.0,4.0,5.0)
C...DEFINE 3-D AXIS LABELS
      CALL MIXALF('INSTRU')
      CALL X3NAME('(H-1.5)CLEARNESS INDEX$',100)
      CALL Y3NAME('(H-1.5)AIR MASS$',100)
      CALL Z3NAME('(H-1.5)BEAM TRANSMITTANCE$',100)
C...DEFINE THE VIEW POINT
      CALL VUABS(-7.5,-6.0,7.5)
C...3-D GRAPH SETUP ROUTINES
      CALL GRAF3D(0.1,0.1,1.0,1.0,1.0,8.0,0.0,0.2,1.0)
C...READ DATA
      DO 100 I=1,80
         READ(16,*) KT,AM,TB,IX,IY
         TBMAT(IX,IY)=TB
 100  CONTINUE
C...DRAW DATA
      IF (ISHOW.EQ.1) THEN
      DO 200 I=1,8112
            READ(8,300) XF,YF,ZT
 300        FORMAT(12X,3(2X,F16.14))
            CALL RLVEC3(XF,YF,0.0,XF,YF,ZT,0)
 200  CONTINUE
      END IF
C...3-D SURFACE DRAWING
      CALL SURMAT(TBMAT,1,19,1,8,0)
C...PLOT TERMINATION
      CALL ENDPL(1)
      CALL DONEPL
      CALL EXIT
         STOP
         END
```

```
      PROGRAM FIT3DB(INPUT,OUTPUT,TAPE5=INPUT,TAPE6=OUTPUT,TAPE9,TAPE8,
     &               TAPE16)
C
C
C     C. BALARAS        5-19-87
C
C
C...READ 5YR DATA FROM TAPE8C
C...FOR AM 1<M<5 AND DM=1
C   THE DATA INCLUDES THE FOLLOWING INFORMATION
C   NA : KT BAND COUNTER
C   NB : AM BAND COUNTER
C   IU : 0 LOWER TRIANGLE'S DATA
C        1 UPPER TRIANGLE'S DATA
C   KT,AM,TB : CORRESPONDING DATA
C   THE 8112 HOURLY DATA ARE RECORDED FOR A GIVEN KT BAND,
C   IN ASCENDING ORDER BASED ON AIRMASS
C...THE OUTPUT ARE VALUES OF TB FOR THE BEST FITTED PLANE
C   THROUGH TRIANGULATED REGIONS OF THE DATA
C   ALL DATA ARE USED BUT FOR SOME CALCULATIONS ARE WEIGHTED AS 1/2
C
C...TO RUN THIS PROGRAM:
C                       AT,TAPE8C    (C,TAPE8C,TAPE8)
C                       TOTAL # 8079 (UPTO AM<5)
C                       AT,IMSLIB5/UN=LIBRARY
C                       X,LIBRARY,IMSLIB5
C
C...TAPE DIRECTORY:
C                   TAPE8 : INPUT 5YR DATA
C                   TAPE9 : AVAILABLE
C                   TAPE16: OUTPUT CORNER COORDINATES OF
C                           TRIANGULAR PLANES (KT,AM,Z3) TO
C                           BE USED BY PLOT3D2
C
C...COMMONS
      COMMON /CNSTS/ ALATR,DELOMO2,GSCF,HRCONV
C
      DIMENSION XO(16),YO(5)
      DIMENSION Z3(208,208)
      DIMENSION NA(8112),NB(8112),IU(8112)
      DIMENSION AKIP1(1000),AMIP1(1000),ATBIP1(1000)
      DIMENSION AKIP2(1000),AMIP2(1000),ATBIP2(1000)
      DIMENSION XP1(1000),YP1(1000),ZP1(1000)
      DIMENSION XP2(1000),YP2(1000),ZP2(1000)
      REAL KTARR(8112),AMARR(8112),TBARR(8112)
      REAL KT,K,KT1,TB1,TB,ION,IO,IO2,ION2
      INTEGER BADPER,YR,DAY,MO,HR,MIN
      DATA XO/0.1,0.15,0.2,0.25,0.3,0.35,0.4,0.45,0.5,0.55,0.6,0.65,0.7,
     &0.75,0.8,0.85/
      DATA YO/1.0,2.0,3.0,4.0,5.0/
C
C...NO. OF DATA FROM GD2H5Y (TAPE9)
      NPAIRS=8079
C
```

```
C
C
C...READ 5YR HOURLY DATA (TAPE8)
      DO 100 I=1,NPAIRS
           READ(8,101) NA(I),NB(I),IU(I),KTARR(I),AMARR(I),TBARR(I)
 101       FORMAT(3(2X,I2),3(2X,F16.14))
 100  CONTINUE
C
C...INITIALIZE Z COORDINATE FOR FIRST TWO POINTS Z3(IA,IB)
      Z3(1,1)=Z3(1,2)=0.0
      IH=0
      IDU=1
      IPTSX=IPTSY=ITPTS=0
      IPTC=1
      IPO=IPO+1
      IA=IB=2
      SUMT=0.0
      RSST=0.0
      SYYT=0.0
C
C...START RECORDING COORDINATES OF KT,AM,Z3
C   FIRST TWO KNOWN CORNER POINTS
      WRITE(16,*) XO(1),YO(1),Z3(1,1),IA-1,IB-1
      WRITE(16,*) XO(1),YO(2),Z3(1,2),IA-1,IB
C
C      **** BEGIN CALCULATIONS ****
C
C...ANALYZE A KT BAND
      DO 400 IKT=1,15
C
C...ANALYZE AM BANDS FOR THE IKT BAND
      DO 401 IAM=1,4
C
C             FOR THE FIRST AM BAND (1<AM<1.5)
            IF (IAM.EQ.1) THEN
C             DEFINE CORNER POINTS OF QUADRILATERAL PLANE
C             KNOWN POINTS ARE 1 AND 2
C             POINT 1
            AKI1=XO(IKT)
            AMI1=YO(IAM+1)
            ATBI1=Z3(IKT,IAM+1)
C             POINT 2
            AKI2=XO(IKT)
            AMI2=YO(IAM)
            ATBI2=Z3(IKT,IAM)
C             POINT 3
            AKI3=XO(IKT+1)
            AMI3=YO(IAM)
C             POINT 4
            AKI4=XO(IKT+1)
            AMI4=YO(IAM+1)
C
C             FOR THE DEFINED QUADRIALTERAL PLANE
C             COLLECT DATA FOR LOWER TRIANGLE
```

```
            ICHECK=0
          NPTSLT=0
            DO 402 IBR=1,NPAIRS
            IF (ICHECK.EQ.1) GOTO 402
                  IF (NA(IBR).EQ.IKT.AND.NB(IBR).EQ.IAM.AND.
     &                IU(IBR).EQ.0) THEN
                     IM=IBR
                  ICHECK=1
                  END IF
 402        CONTINUE
C             COLLECT DATA OF LOWER TRIANGLE
C             FOR THAT AM BAND
            IF (ICHECK.EQ.1) THEN
            IEND=1
            DO 403 ILOC=IM,NPAIRS
 !          IF (IEND.EQ.0) GOTO 403
                  IF (IU(ILOC).EQ.1.OR.NB(ILOC).GT.IAM.OR.
     &                NA(ILOC).GT.IKT) THEN
C                    STOP COLLECTING DATA
                IEND=0
                    GO TO 403
                  END IF
C
                  NPTSLT=NPTSLT+1
                  AKIP1(NPTSLT)=KTARR(ILOC)
                  AMIP1(NPTSLT)=AMARR(ILOC)
                  ATBIP1(NPTSLT)=TBARR(ILOC)
                 IPO=IPO+1
 403         CONTINUE
                  ELSE
C                   THERE ARE NO DATA AVAILABLE
C                   SET VALUE OF Z3 AND SKIP FOLLOWING CALCS.
                   PHI=ATAN2((AMI2-AMI1),(AKI2-AKI1))
                   CALL CORDCH(AKI1,AMI1,ATBI1,AKI2,AMI2,ATBI2,
     &                 AKI3,AMI3,PHI,Z3(IKT+1,IAM))
                   Z3(IKT+1,IAM)=Z3(IKT+1,IAM)+ATBI1
                     GO TO 799
                  END IF
C
C...CHANGE TO NEW COORDINATES FOR LOWER TRG POINTS
C   CALCUALTE ANGLE OF ROTATION
      PHI=ATAN2((AMI2-AMI1),(AKI2-AKI1))
      CALL COORDCH(AKIP1,AMIP1,ATBIP1,AKI1,AMI1,ATBI1,
     &AKI2,AMI2,ATBI2,AKI3,AMI3,PHI,NPTSLT,XP1,YP1,ZP1,X2,Y2,Z2,X3,Y3)
C...FOR THE TRG SPACE, FIT THE BEST TRG PLANE TO MIN ERROR
      CALL TRGFIT(XP1,YP1,ZP1,X2,Y2,Z2,X3,Y3,NPTSLT,Z3(IKT+1,IAM))
C...CHANGE Z3 TO OLD COORDINATES
      Z3(IKT+1,IAM)=Z3(IKT+1,IAM)+ATBI1
      IF (Z3(IKT+1,IAM).LT.0.0) Z3(IKT+1,IAM)=0.0
C...CALCULATE EQ. OF PLANEA1X+A2Y+A3Z+D=0
      CALL PLANEQ(AKI1,AMI1,ATBI1,AKI2,AMI2,ATBI2,AKI3,AMI3,
     &Z3(IKT+1,IAM),A1,A2,A3,D)
```

```
C...UNEXPLAINED VARIATION
      DO 800 IDIS=1,NPTSLT
C   DISTANCE OF A DATA POINT FROM PLANE, H
      H=ABS(A1*AKIP1(IDIS)+A2*AMIP1(IDIS)+A3*ATBIP1(IDIS)+D)/
     &SQRT(A1*A1+A2*A2+A3*A3)
      RSST=RSST+H*H
 800  CONTINUE
C   RECORD POINT COORDINATES
 799  WRITE(16,*) XO(IKT+1),YO(IAM),Z3(IKT+1,IAM),IKT+1,IAM,NPTSLT
C
C...FOR THE UPPER TRIANGLES
C   FIRST KT BAND
      IF (IKT.EQ.1) THEN
C...LOCATE STARTING POINT
      ICHECK=0
               NPTSUT=0
      DO 404 IBR=1,NPAIRS
             IF (ICHECK.EQ.1) GOTO 404
             IF (NA(IBR).EQ.IKT.AND.NB(IBR).EQ.IAM.AND.
     &         IU(IBR).EQ.1) THEN
               IM=IBR
             ICHECK=1
             END IF
 404  CONTINUE
C
C...IF THERE ARE NO DATA
      IF (ICHECK.EQ.0) THEN
         PHI=ATAN2((AMI3-AMI1),(AKI3-AKI1))
         CALL CORDCH(AKI1,AMI1,ATBI1,AKI3,AMI3,Z3(IKT+1,IAM),
     &        AKI4,AMI4,PHI,Z3(IKT+1,IAM+1))
         Z3(IKT+1,IAM+1)=Z3(IKT+1,IAM+1)+ATBI1
         GO TO 798
      END IF
C
C...COLLECT DATA
             IEND=1
      DO 405 ILOC=IM,NPAIRS
            IF(IEND.EQ.0) GOTO 405
            IF (NB(ILOC).GT.1.OR.NA(ILOC).GT.1) THEN
            IEND=0
               GO TO 405
            END IF
            NPTSUT=NPTSUT+1
            AKIP1(NPTSUT)=KTARR(ILOC)
            AMIP1(NPTSUT)=AMARR(ILOC)
            ATBIP1(NPTSUT)=TBARR(ILOC)
               IPO=IPO+1
 405  CONTINUE
      END IF
C
C...FOR UPPER TRIANGLES
C   REMAINING KT BANDS
      IF (IKT.GT.1) THEN
```

```
C...LOCATE STARTING POINT
      ICHECK=0
                NPTSUT=0
      DO 331 IBR=1,NPAIRS
             IF (ICHECK.EQ.1) GOTO 331
             IF (NA(IBR).EQ.IKT.AND.NB(IBR).EQ.IAM.AND.
     &         IU(IBR).EQ.1) THEN
             IM=IBR
             ICHECK=1
             END IF
 331  CONTINUE
C
C...IF THERE ARE NO DATA
      IF (ICHECK.EQ.0) THEN
         PHI=ATAN2((AMI3-AMI1),(AKI3-AKI1))
         CALL CORDCH(AKI1,AMI1,ATBI1,AKI3,AMI3,Z3(IKT+1,IAM),
     &        AKI4,AMI4,PHI,Z3(IKT+1,IAM+1))
         Z3(IKT+1,IAM+1)=Z3(IKT+1,IAM+1)+ATBI1
         GO TO 798
      END IF
C
C...COLLECT DATA
             IEND=1
      DO 332 ILOC=IM,NPAIRS
             IF(IEND.EQ.0) GOTO 332
             IF (NB(ILOC).GT.1.OR.NA(ILOC).GT.IKT) THEN
             IEND=0
                GO TO 332
             END IF
             NPTSUT=NPTSUT+1
             AKIP1(NPTSUT)=KTARR(ILOC)
             AMIP1(NPTSUT)=AMARR(ILOC)
             ATBIP1(NPTSUT)=TBARR(ILOC)
                  IPO=IPO+1
 332  CONTINUE
C
C...INCLUDE DATA FROM LOWER TRG OF NEXT AM BAND
      ICHECK=0
         NPTSUT2=0
      DO 408 IBR=1,NPAIRS
             IF (ICHECK.EQ.1) GO TO 408
             IF (NA(IBR).EQ.IKT.AND.NB(IBR).EQ.IAM+1.AND.
     &    IU(IBR).EQ.0) THEN
         IM=IBR
         ICHECK=1
      END IF
 408  CONTINUE
C
C...IF THERE ARE NO POINTS, SKIP FOLLOWING CALCS
      IF (ICHECK.EQ.0) GO TO 634
C
C...COLLECT DATA FROM LOWER TRG OF NEXT AM BAND
      IEND=1
```

```
      DO 409 ILOC=IM,NPAIRS
             IF (IEND.EQ.0) GO TO 409
             IF (IU(ILOC).EQ.1.OR.NB(ILOC).GT.IAM+1.OR.
     &           NA(ILOC).GT.IKT) THEN
                IEND=0
                GO TO 409
             END IF
             NPTSUT2=NPTSUT2+1
             AKIP2(NPTSUT2)=KTARR(ILOC)
             AMIP2(NPTSUT2)=AMARR(ILOC)
             ATBIP2(NPTSUT2)=TBARR(ILOC)
                  IPO=IPO+1
 409  CONTINUE
C
 634  END IF
C
C...CHANGE TO NEW COORDINATES FOR UPPER TRG POINTS
C    CALCULATE ANGLE OF ROTATION
       PHI=ATAN2((AMI3-AMI1),(AKI3-AKI1))
C...CHANGE COORD. FOR MAIN DATA
       CALL COORDCH(AKIP1,AMIP1,ATBIP1,AKI1,AMI1,ATBI1,
     &AKI3,AMI3,Z3(IKT+1,IAM),AKI4,AMI4,PHI,NPTSUT,
     &XP1,YP1,ZP1,X3,Y3,ZP3,X4,Y4)
C...CHANGE COORD FOR ADDITIONAL DATA, IF AVAILABLE
       IF (ICHECK.EQ.1) THEN
       CALL COORDCH(AKIP2,AMIP2,ATBIP2,AKI1,AMI1,ATBI1,
     &AKI3,AMI3,Z3(IKT+1,IAM),AKI4,AMI4,PHI,NPTSUT2,
     &XP2,YP2,ZP2,X3,Y3,ZP3,X4,Y4)
C    FIT THE BEST TRG PLANE TO MINIMIZE ERROR
       CALL TRGFIT2(XP1,YP1,ZP1,XP2,YP2,ZP2,X3,Y3,ZP3,
     &X4,Y4,NPTSUT,NPTSUT2,Z3(IKT+1,IAM+1))
       GO TO 234
       END IF
C...FIT THE BEST TRG PLANE TO MIN ERROR
C    WHEN ADDITIONAL DATA ARE NOT AVAILABLE
       CALL TRGFIT(XP1,YP1,ZP1,X3,Y3,ZP3,X4,Y4,NPTSUT,
     &Z3(IKT+1,IAM+1))
C    CHANGE TO OLD COORD
 234  Z3(IKT+1,IAM+1)=Z3(IKT+1,IAM+1)+ATBI1
       IF (Z3(IKT+1,IAM+1).LT.0.0) Z3(IKT+1,IAM+1)=0.0
C...CALCULATE EQ. OF PLANE A1X+A2Y+A3Z+D=0
       CALL PLANEQ(AKI1,AMI1,ATBI1,AKI3,AMI3,Z3(IKT+1,IAM),
     &AKI4,AMI4,Z3(IKT+1,IAM+1),A1,A2,A3,D)
C...FOR THE DATA IN THE PLANE CALC.
C    UNEXPLAINED VARIATION
       DO 801 IDIS=1,NPTSUT
C    DISTANCE OF A DATA POINT FROM PLANE, H
       H=ABS(A1*AKIP1(IDIS)+A2*AMIP1(IDIS)+A3*ATBIP1(IDIS)+D)/
     &SQRT(A1*A1+A2*A2+A3*A3)
       RSST=RSST+H*H
 801  CONTINUE
C...RECORD POINT COORD
 798  WRITE(16,*) XO(IKT+1),YO(IAM+1),Z3(IKT+1,IAM+1),IKT+1,IAM+1,NPTSUT
       END IF
```

```
C
C
C...REMAINING AM BANDS
      IF (IAM.GT.1) THEN
C
C...DEFINE CORNER POINT OF QUADRILATERAL PLANE
C   KNOWN POINTS ARE 1 AND 2
C   POINT 1
      AKI1=XO(IKT)
      AMI1=YO(IAM)
      ATBI1=Z3(IKT,IAM)
C   POINT 2
      AKI2=XO(IKT+1)
      AMI2=YO(IAM)
      ATBI2=Z3(IKT+1,IAM)
C   POINT 3
      AKI3=XO(IKT)
      AMI3=YO(IAM+1)
C   POINT 4
      AKI4=XO(IKT+1)
      AMI4=YO(IAM+1)
C
C...FOR THE DEFINED QUADRILATERAL PLANE COLLECT
C   DATA FOR LOWER TRIANGLE
C...FOR THE FIRST KT BAND
      IF (IKT.EQ.1) THEN
      ICHECK=0
                NPTSLT=0
      DO 410 IBR=1,NPAIRS
             IF (ICHECK.EQ.1) GOTO 410
             IF (NA(IBR).EQ.IKT.AND.NB(IBR).EQ.IAM.AND.
     &          IU(IBR).EQ.0) THEN
                IM=IBR
                 ICHECK=1
             END IF
 410  CONTINUE
C
C...IF THERE ARE NO DATA SET Z3=0.
      IF (ICHECK.EQ.0) THEN
      PHI=ATAN2((AMI2-AMI1),(AKI2-AKI1))
      CALL CORDCH(AKI1,AMI1,ATBI1,AKI2,AMI2,ATBI2,
     &     AKI3,AMI3,PHI,Z3(IKT,IAM+1))
      Z3(IKT,IAM+1)=Z3(IKT,IAM+1)+ATBI1
         GO TO 797
      END IF
C
C...COLLECT DATA OF LOWER TRIANGLE
C   FOR THAT AM BAND
             IEND=1
      DO 411 ILOC=IM,NPAIRS
             IF (IEND.EQ.0) GOTO 411
             IF (IU(ILOC).EQ.1.OR.NB(ILOC).GT.IAM.OR.
     &NA(ILOC).GT.IKT) THEN
             IEND=0
```

```
                GO TO 411
              END IF
C
              NPTSLT=NPTSLT+1
              AKIP1(NPTSLT)=KTARR(ILOC)
              AMIP1(NPTSLT)=AMARR(ILOC)
              ATBIP1(NPTSLT)=TBARR(ILOC)
                IPO=IPO+1
 411  CONTINUE
C
C...CHANGE TO NEW COORDINATES FOR LOWER TRG POINTS
C    CALCULATE ANGLE OF ROTATION
       PHI=ATAN2((AMI2-AMI1),(AKI2-AKI1))
       CALL COORDCH(AKIP1,AMIP1,ATBIP1,AKI1,AMI1,ATBI1,
      &AKI2,AMI2,ATBI2,AKI3,AMI3,PHI,NPTSLT,
      &XP1,YP1,ZP1,X2,Y2,Z2,X3,Y3)
C    FIT THE BEST TRG PLANE TO MINIMIZE ERROR
       CALL TRGFIT(XP1,YP1,ZP1,X2,Y2,Z2,X3,Y3,NPTSLT,
      &Z3(IKT,IAM+1))
C    CHANGE TO OLD COORD
       Z3(IKT,IAM+1)=Z3(IKT,IAM+1)+ATBI1
       IF (Z3(IKT,IAM+1).LT.0.0) Z3(IKT,IAM+1)=0.0
C...CALCULATE EQ. OF PLANE A1X+A2Y+A3Z+D=0
       CALL PLANEQ(AKI1,AMI1,ATBI1,AKI2,AMI2,Z3(IKT+1,IAM),
      &AKI3,AMI3,Z3(IKT,IAM+1),A1,A2,A3,D)
C...FOR THE DATA IN THE PLANE CALC.
C    UNEXPLAINED VARIATION
       DO 802 IDIS=1,NPTSLT
C    DISTANCE OF A DATA POINT FROM PLANE, H
       H=ABS(A1*AKIP1(IDIS)+A2*AMIP1(IDIS)+A3*ATBIP1(IDIS)+D)/
      &SQRT(A1*A1+A2*A2+A3*A3)
       RSST=RSST+H*H
 802  CONTINUE
C...RECORD POINT COORD
 797  WRITE(16,*) XO(IKT),YO(IAM+1),Z3(IKT,IAM+1),IKT,IAM+1,NPTSLT
C
C...FOR THE UPPER TRIANGLE OF THE FIRST KT BAND
       ICHECK=0
                NPTSUT=0
       DO 412 IBR=1,NPAIRS
              IF (ICHECK.EQ.1) GOTO 412
              IF (NA(IBR).EQ.IKT.AND.NB(IBR).EQ.IAM.AND.
     &         IU(IBR).EQ.1) THEN
                IM=IBR
                 ICHECK=1
              END IF
 412   CONTINUE
C
C...IF THERE ARE NO DATA IN UPPER TRG
       IF (ICHECK.EQ.0) THEN
          PHI=ATAN2((AMI2-AMI3),(AKI2-AKI3))
          CALL CORDCH(AKI3,AMI3,Z3(IKT,IAM+1),AKI2,AMI2,ATBI2,
     &         AKI4,AMI4,PHI,Z3(IKT+1,IAM+1))
          Z3(IKT+1,IAM+1)=Z3(IKT+1,IAM+1)+Z3(IKT,IAM+1)
```

```
         GO TO 796
      END IF
C
C...COLLECT DATA FOR UPPER TRG FOR THAT AM BAND
            IEND=1
      DO 413 ILOC=IM,NPAIRS
            IF (IEND.EQ.0) GOTO 413
         IF (IU(ILOC).EQ.0.OR.NB(ILOC).GT.IAM.OR.NA(ILOC).GT.IKT) THEN
            IEND=0
               GO TO 413
            END IF
C
            NPTSUT=NPTSUT+1
            AKIP1(NPTSUT)=KTARR(ILOC)
            AMIP1(NPTSUT)=AMARR(ILOC)
            ATBIP1(NPTSUT)=TBARR(ILOC)
                IPO=IPO+1
 413  CONTINUE
C
C...INCLUDE DATA OF NEXT KT BAND SAME AM BAND LOWER TRG
      ICHECK=0
                NPTSUT2=0
      DO 414 IBR=1,NPAIRS
            IF (ICHECK.EQ.1) GOTO 414
            IF (NA(IBR).EQ.IKT+1.AND.NB(IBR).EQ.IAM.AND.
     &      IU(IBR).EQ.0) THEN
               IM=IBR
               ICHECK=1
            END IF
 414  CONTINUE
C
C...IF THERE ARE NO DATA SKIP FOLLOWING CALCS.
      IF (ICHECK.EQ.0) GO TO 635
C
C...COLLECT DATA
      IEND=1
      DO 415 ILOC=IM,NPAIRS
            IF (IEND.EQ.0) GOTO 415
            IF (IU(ILOC).EQ.1.OR.NB(ILOC).GT.IAM.OR.
     &         NA(ILOC).GT.IKT+1) THEN
               IEND=0
               GOTO 415
            END IF
            NPTSUT2=NPTSUT2+1
            AKIP2(NPTSUT2)=KTARR(ILOC)
            AMIP2(NPTSUT2)=AMARR(ILOC)
            ATBIP2(NPTSUT2)=TBARR(ILOC)
 415  CONTINUE
C
C...CHANGE TO NEW COORDINATES FOR UPPER TRG POINTS
C   CALCULATE ANGLE OF ROTATION
 635  PHI=ATAN2((AMI2-AMI3),(AKI2-AKI3))
C...CHANGE COORD FOR MAIN DATA
      CALL COORDCH(AKIP1,AMIP1,ATBIP1,AKI3,AMI3,Z3(IKT,IAM+1),
```

```
     &AKI2,AMI2,ATBI2,AKI4,AMI4,PHI,NPTSUT,
     &XP1,YP1,ZP1,X2,Y2,Z2,X4,Y4)
C...CHANGE COORD FOR ADDITIONAL DATA, IF AVAILABLE
      IF (ICHECK.EQ.1) THEN
      CALL COORDCH(AKIP2,AMIP2,ATBIP2,AKI3,AMI3,Z3(IKT,IAM+1),
     &AKI2,AMI2,ATBI2,AKI4,AMI4,PHI,NPTSUT2,
     &XP2,YP2,ZP2,X2,Y2,Z2,X4,Y4)
C   FIT THE BEST TRG PLANE TO MINIMIZE ERROR
      CALL TRGFIT2(XP1,YP1,ZP1,XP2,YP2,ZP2,X2,Y2,Z2,
     &X4,Y4,NPTSUT,NPTSUT2,Z3(IKT+1,IAM+1))
      GO TO 235
      END IF
C...IF NO ADDITIONAL DATA ARE AVAILABLE
      CALL TRGFIT(XP1,YP1,ZP1,X2,Y2,Z2,X4,Y4,NPTSUT,
     &Z3(IKT+1,IAM+1))
C   CHANGE TO OLD COORD
 235  Z3(IKT+1,IAM+1)=Z3(IKT+1,IAM+1)+Z3(IKT,IAM+1)
      IF (Z3(IKT+1,IAM+1).LT.0.0) Z3(IKT+1,IAM+1)=0.0
C...CALCULATE EQ. OF PLANE A1X+A2Y+A3Z+D=0
      CALL PLANEQ(AKI3,AMI3,Z3(IKT,IAM+1),AKI2,AMI2,ATBI2,
     &AKI4,AMI4,Z3(IKT+1,IAM+1),A1,A2,A3,D)
C...FOR THE DATA IN THE PLANE CALC.
C   UNEXPLAINED VARIATION
      DO 803 IDIS=1,NPTSUT
C   DISTANCE OF A DATA POINT FROM PLANE, H
      H=ABS(A1*AKIP1(IDIS)+A2*AMIP1(IDIS)+A3*ATBIP1(IDIS)+D)/
     &SQRT(A1*A1+A2*A2+A3*A3)
      RSST=RSST+H*H
 803  CONTINUE
C...RECORD POINT COORD
 796  WRITE(16,*) XO(IKT+1),YO(IAM+1),Z3(IKT+1,IAM+1),IKT+1,IAM+1,NPTSUT
      END IF
C
C...FOR KT BANDS .NE. 1 AND AM .NE. 1
C   WORK ON UPPER TRG ONLY
      IF (IKT.GT.1) THEN
         ICHECK=0
                NPTSUT=0
         DO 416 IBR=1,NPAIRS
             IF (ICHECK.EQ.1) GOTO 416
             IF (NA(IBR).EQ.IKT.AND.NB(IBR).EQ.IAM.AND.
     &        IU(IBR).EQ.1) THEN
                IM=IBR
                 ICHECK=1
             END IF
 416  CONTINUE
C
C...IF THERE ARE NO DATA IN UPPER TRG
      IF (ICHECK.EQ.0) THEN
         PHI=ATAN2((AMI2-AMI3),(AKI2-AKI3))
         CALL CORDCH(AKI3,AMI3,Z3(IKT,IAM+1),AKI2,AMI2,ATBI2,
     &         AKI4,AMI4,PHI,Z3(IKT+1,IAM+1))
         Z3(IKT+1,IAM+1)=Z3(IKT+1,IAM+1)+Z3(IKT,IAM+1)
         GO TO 795
```

```
      END IF
C
C...COLLECT DATA
            IEND=1
      DO 417 ILOC=IM,NPAIRS
            IF (IEND.EQ.0) GOTO 417
         IF (IU(ILOC).EQ.0.OR.NB(ILOC).GT.IAM.OR.NA(ILOC).GT.IKT) THEN
            IEND=0
               GO TO 417
            END IF
            NPTSUT=NPTSUT+1
            AKIP1(NPTSUT)=KTARR(ILOC)
            AMIP1(NPTSUT)=AMARR(ILOC)
            ATBIP1(NPTSUT)=TBARR(ILOC)
               IPO=IPO+1
 417  CONTINUE
C
C...INCLUDE ADDITIONAL DATA OF NEXT AM BAND LOWER TRG
      ICHECK=0
               NPTSUT2=0
      DO 418 IBR=1,NPAIRS
            IF (ICHECK.EQ.1) GO TO 418
            IF (NA(IBR).EQ.IKT.AND.NB(IBR).EQ.IAM+1.AND.
     &          IU(IBR).EQ.0) THEN
               IM=IBR
               ICHECK=1
            END IF
 418  CONTINUE
C
C...IF THERE ARE NO DATA IN LOWER TRG OF NEXT AM BAND
      IF (ICHECK.EQ.0) GO TO 636
C
      IEND=1
      DO 419 ILOC=IM,NPAIRS
            IF (IEND.EQ.0) GOTO 419
            IF (IU(ILOC).EQ.1.OR.NB(ILOC).GT.IAM+1.OR.
     &         NA(ILOC).GT.IKT) THEN
               IEND=0
               GOTO 419
            END IF
            NPTSUT2=NPTSUT2+1
            AKIP2(NPTSUT2)=KTARR(ILOC)
            AMIP2(NPTSUT2)=AMARR(ILOC)
            ATBIP2(NPTSUT2)=TBARR(ILOC)
                  IPO=IPO+1
 419  CONTINUE
C
 636  IF (ICHECK.EQ.0) THEN
C     NO DATA IN LOWER TRG OF NEXT AM BAND
C     GO THROUGH DATA AND CHECK IF THERE ARE
C     ANY DATA IN THIS KT BAND
C     IF SO THEN SKIP FOLLOWING CALCS
      IFLAG=1
      DO 422 IBR=1,NPAIRS
```

```
            IF (IFLAG.EQ.0) GOTO 422
            IF (NA(IBR).EQ.IKT.AND.NB(IBR).GT.IAM) THEN
               IFLAG=0
            END IF
 422  CONTINUE
C
C     IF IFLAG=0 THERE ARE DATA LEFT IN THIS KT BAND
      IF (IFLAG.EQ.0) GOTO 637
C
C...IF THIS IS THE LAST AM BAND FOR A GIVEN KT BAND
C   THEN CONSIDER IF DATA ARE AVAILABLE FROM LOWER TRG
C   NEXT KT BAND SAME AM BAND
C   OTHERWISE DO NOTHING (FIT TRG TO ITS OWN DATA)
C      LOCATE STARTING POINT  FOR
C     DATA IN NEXT KT BAND, SAME AM BAND
      ICHECK=0
               NPTSUT2=0
      DO 420 IBR=1,NPAIRS
            IF (ICHECK.EQ.1) GOTO 420
            IF (NA(IBR).EQ.IKT+1.AND.NB(IBR).EQ.IAM.AND.
     &           IU(IBR).EQ.0) THEN
               IM=IBR
               ICHECK=1
            END IF
 420  CONTINUE
C
      IF (ICHECK.EQ.1) THEN
C     COLLECT DATA
      IEND=1
      DO 421 ILOC=IM,NPAIRS
            IF (IEND.EQ.0) GOTO 421
            IF (IU(ILOC).EQ.1.OR.NB(ILOC).GT.IAM+1.OR.
     &           NA(ILOC).GT.IKT) THEN
               IEND=0
               GO TO 421
            END IF
            NPTSUT2=NPTSUT2+1
            AKIP2(NPTSUT2)=KTARR(ILOC)
            AMIP2(NPTSUT2)=AMARR(ILOC)
            ATBIP2(NPTSUT2)=TBARR(ILOC)
 421  CONTINUE
      END IF
 637  END IF
C
C...CHANGE TO NEW COORDINATES FOR UPPER TRG POINTS
C   CALCULATE ANGLE OF ROTATION
      PHI=ATAN2((AMI2-AMI3),(AKI2-AKI3))
      CALL COORDCH(AKIP1,AMIP1,ATBIP1,AKI3,AMI3,Z3(IKT,IAM+1),
     &AKI2,AMI2,ATBI2,AKI4,AMI4,PHI,NPTSUT,
     &XP1,YP1,ZP1,X2,Y2,Z2,X4,Y4)
      IF (ICHECK.EQ.1) THEN
      CALL COORDCH(AKIP2,AMIP2,ATBIP2,AKI3,AMI3,Z3(IKT,IAM+1),
     &AKI2,AMI2,ATBI2,AKI4,AMI4,PHI,NPTSUT2,
     &XP2,YP2,ZP2.X2,Y2,Z2,X4,Y4)
```

```
C    FIT THE BEST TRG PLANE TO MINIMIZE ERROR
       CALL TRGFIT2(XP1,YP1,ZP1,XP2,YP2,ZP2,X2,Y2,Z2,
      &X4,Y4,NPTSUT,NPTSUT2,Z3(IKT+1,IAM+1))
       GO TO 236
       END IF
C...IF THERE ARE NO ADDITIONAL DATA
C    FIT THE BEST TRG PALNE TO MINIMIZE ERROR
       CALL TRGFIT(XP1,YP1,ZP1,X2,Y2,Z2,X4,Y4,NPTSUT,
      &Z3(IKT+1,IAM+1))
C    CHANGE TO OLD COORD
 236   Z3(IKT+1,IAM+1)=Z3(IKT+1,IAM+1)+Z3(IKT,IAM+1)
       IF (Z3(IKT+1,IAM+1).LT.0.0) Z3(IKT+1,IAM+1)=0.0
C...CALCULATE EQ. OF PLANE A1X+A2Y+A3Z+D=0
       CALL PLANEQ(AKI3,AMI3,Z3(IKT,IAM+1),AKI2,AMI2,ATBI2,
      &AKI4,AMI4,Z3(IKT+1,IAM+1),A1,A2,A3,D)
C...FOR THE DATA IN THE PLANE CALC.
C    UNEXPLAINED VARIATION
       DO 804 IDIS=1,NPTSUT
C    DISTANCE OF A DATA POINT FROM PLANE, H
       H=ABS(A1*AKIP1(IDIS)+A2*AMIP1(IDIS)+A3*ATBIP1(IDIS)+D)/
      &SQRT(A1*A1+A2*A2+A3*A3)
       RSST=RSST+H*H
 804   CONTINUE
C...RECORD POINT COORD
 795   WRITE(16,*) XO(IKT+1),YO(IAM+1),Z3(IKT+1,IAM+1),IKT+1,IAM+1,NPTSUT
       END IF
           END IF
 401   CONTINUE
 400   CONTINUE
C...STATISTICAL ANALYSIS
C...SUMMATION OF BEAM TRANSMITTANCES
       DO 776 IP=1,NPAIRS
             SUMT=SUMT+TBARR(IP)
 776   CONTINUE
       TAVE=SUMT/NPAIRS
C...CALCULATE TOTAL VARIATION
       DO 777 IS=1,NPAIRS
             SYYT=SYYT+(TBARR(IS)-TAVE)**2
 777   CONTINUE
C...EXPLAINED VARIATION
       SSREG=SYYT-RSST
       WRITE(16,*) 'RSST=',RSST,'  SYYT=',SYYT,'  SSREG=',SSREG
C...COEFFICIENT OF CORRELATION
       AR=SQRT(SSREG/SYYT)
C...COEFFICIENT OF DETERMINATION
       AR2=AR*AR
       WRITE(16,*) ' '
       WRITE(16,*) 'R=',AR,'  R2=',AR2
       WRITE(16,*) 'NUMBER OF DATA USED: ',IPO
       STOP
       END
```

```
      SUBROUTINE TRGFIT2(XP1,YP1,ZP1,XP2,YP2,ZP2,X2,Y2,Z2,
     &             X3,Y3,NPNTS,NPNTS2,Z3)
C
C
C                  SUBROUTINE TRGFIT2
C               C. BALARAS     5-19-87
C
C
C...SUBROUTINE TO CALCULATE THE Z COORDINATE OF THE UPPER CORNER
C   OF THE TRIANGULAR PLANE TO MINIMIZE ERROR, WHEN ADDITIONAL
C   DATA ARE USED (ANALOGOUS TO "TRGFIT")
C
C...INPUTS:
C          XP1, YP1, ZP1 : COORD OF DATA POINTS IN MAIN TRIANGULAR PLANE
C          XP2, YP2, ZP2 : COORD OF DATA POINTS IN ADDITIONAL TRG PLANE
C          X2, Y2, Z2    : COORD OF SECOND KNOWN POINT
C                          FIRST KNOWN POINT IS LOCATED AT THE ORIGIN
C                          (0,0,0) OF THIS COORD. SYSTEM
C          X3, Y3        : KNOWN COORD OF THE THIRD (TOP) POINT
C          NPNTS         : NUMBER OF MAIN DATA
C          NPNTS2        : NUMBER OF ADDITIONAL DATA
C...OUTPUT:
C          Z3 : Z COORD OF THIRD POINT TO MINIMIZE ERROR
C
C...DIMENSIONS
      DIMENSION XP1(NPNTS),YP1(NPNTS),ZP1(NPNTS)
      DIMENSION XP2(NPNTS2),YP2(NPNTS2),ZP2(NPNTS2)
C
C...INITIALIZATIONS
      S1=S2=S3=S4=0.0
      S5=S6=S7=S8=0.0
C
C...FIRST POINT IS THE ORIGIN
C
C...CALCULATIONS FOR MAIN DATA
      DO 10 I=1,NPNTS
            S1=S1+(ZP1(I)*YP1(I))
            S2=S2+(Z2*XP1(I)*YP1(I)/X2)
            S3=S3+((Z2*X3*YP1(I)*YP1(I))/(X2*Y3))
            S4=S4+(YP1(I)*YP1(I)/Y3)
 10   CONTINUE
C
C...CALCULATIONS FOR ADDITIONAL DATA
      DO 100 I=1,NPNTS2
            S5=S5+(ZP2(I)*YP2(I))
            S6=S6+(Z2*XP2(I)*YP2(I)/X2)
            S7=S7+((Z2*X3*YP2(I)*YP2(I))/(X2*Y3))
            S8=S8+(YP2(I)*YP2(I)/Y3)
 100  CONTINUE
C
      Z3=(S1+(S5/2.)+S3+(S7/2.)-S2-(S6/2.))/(S4+(S8/2.))
C
      IF (Z3.LT.0.0) Z3=0.0
C
```

```
RETURN
END
```

```
      PROGRAM CONTOUR(INPUT,OUTPUT,TAPE5=INPUT,TAPE6=OUTPUT,TAPE9,
     &TAPE2,TAPE10)
C
C
C       C. BALARAS       1-19-88
C       C. BALARAS       4-22-88
C
C
C...PLOT CONTOUR LINES FOR THE (KT,AM,TB) DATA
C   USING DISSPLA
C
C...TO RUN THIS PROGRAM:
C                          AT,DISSPLA/UN=LIBRARY
C                          AT,CALCOMP/UN=LIBRARY
C                          X,LIBRARY,CALCOMP,DISSPLA
C                          G,TAPE9
C
C...TO SUBMIT A JOB TO CALCOMP
C             PLOTQ,TAPE2,PN=5,PA=0,FC=50
C             PN-PEN CODE, PA-PAPER CODE, FC-SCALLING
C...TO SUBMIT A JOB TO XEROX PRINTER
C             EPIC,TAPE2
C
      DIMENSION TBMAT(19,7),IBUF(512)
      COMMON WORK(5000)
      REAL KT
C
C...CHOOSE OUTPUT PLOTTING DEVICE
C     VESRATEC
C     CALL PVRSTC
C     CALL VRSTEC(IBUF,512,2)
C     CALCOMP
C     CALL PCLCMP
C     CALL CALCMP(IBUF,512,2)
C     XEROX PRINTER
      CALL PEPIC
      CALL EPIC(300.0,0,7.0,7.0,2)
C...SELECT PLOT REDUCTION/ENLARGEMENT FACTOR
      CALL BLOWUP(1.0)
C...SWISS-MEDIUM LETTERING
      CALL SWISSM
C
C...CREATE CONTOURS
      CALL AREA2D(7.,7.)
      CALL MIXALF('INSTRU')
      CALL XNAME('(H-1.5)CLEARNESS INDEX$',100)
      CALL YNAME('(H-1.5)AIR MASS$',100)
      CALL HEADIN('CONTOUR PLOT$',100,1.5,2)
      CALL HEADIN('OF THE 3-D SURFACE$',100,1.5,2)
      CALL GRAF(0.,0.1,1.0,1.0,1.0,7.0)
      CALL FRAME
      CALL BCOMON(5000)
C   DISSPLA CONSTRUCTS A REGULAR MATRIX FROM
C   A COLLECTION OF POINTS TO BE USED BY CONMAK
```

```
      CALL BGNMAT(19,7)
      DO 1000 I=1,126
         READ(9,*) KT,AM,TB
         CALL GETMAT(KT,AM,TB,1,0)
 1000 CONTINUE
      CALL ENDMAT(TBMAT,0)
C...GENERATE CONTOUR LINES
      CALL CONMAK(TBMAT,19,7,0.1)
C...PLOT CONTOUR LINES
      CALL CONLIN(0,'SOLID','LABELS',2,10)
      CALL CONLIN(1,'DASH','NOLABELS',1,3)
      CALL CONANG(90.)
      CALL RASPLN(0.25)
      CALL CONTUR(2,'LABELS','DRAW')
C...PLOT TERMINATION (OUTPUT DESIGNATED AS PLOT '1')
      CALL ENDPL(1)
      CALL DONEPL
      STOP
      END
```

```
      PROGRAM TESTFIT(INPUT,OUTPUT,TAPE5=INPUT,TAPE6=OUTPUT,TAPE9,TAPE8,
     &               TAPE16)
C
C
C     C. BALARAS        5-25-87
C
C
C...CREATE A DATA BASE FOR TESTING PURPOCES
C   THERE WILL BE 1000 POINTS ON A PLANE PASSING THROUGH (X,Y,Z) OR (KT,M,TB)-
C   (0.1,7,0)  (0.7,1.0,0)  (0.7,7,1.0)
C   THE SAME PROGRAM CAN BE USED TO CREATE DATA FOR AN
C   ELLIPTIC PARABOLOID WITH ITS CENTER AT (0.425,3.5,0)
C   THE DATA ARE THEN SEPERATED IN TRIANGULAR AREAS AND STORED IN TAPE8
C   OUTPUT DATA INCLUDES THE FOLLOWING INFORMATION-
C   NA - KT BAND COUNTER
C   NB - AM BAND COUNTER
C   IU - 0 LOWER TRIANGLE'S DATA
C        1 UPPER TRIANGLE'S DATA
C   KT, AM, TB - CORRESPONDING DATA
C   DATA ARE RECORDED FOR A GIVEN KT BAND, IN AM ASCENDING ORDER
C   FOR A GIVEN TRIANGULAR AREA
C
C...TO RUN THIS PROGRAM-
C                       AT,IMSLIB5/UN=LIBRARY
C                       X,LIBRARY,IMSLIB5
C
C...TAPE DIRECTORY-
C                   TAPE8 - 5YR DATA SORTED IN TRIANGULAR AREAS
C
C...COMMONS
      COMMON /CNSTS/ ALATR,DELOM02,GSCF,HRCONV
C
      DIMENSION XO(16),YO(13)
      DIMENSION IRVS(7001),IRVS4(7001),WK(1)
      DIMENSION AKILT(1000),AMILT(1000),ATBILT(1000)
      DIMENSION AKIUT(1000),AMIUT(1000),ATBIUT(1000)
      DIMENSION AKI(7001),AMI(7001),ATBI(7001)
      REAL KTARR(7001),AMARR(7001),TBARR(7001)
      REAL KT,K,KT1,TB1,TB,ION,IO,I02,ION2
      DATA XO/0.1,0.15,0.2,0.25,0.3,0.35,0.4,0.45,0.5,0.55,0.6,0.65,0.7,
     &0.75,0.8,0.85/
      DATA YO/1.0,1.5,2.0,2.5,3.0,3.5,4.0,4.5,5.0,5.5,6.0,6.5,7.0/
C
C...DATA TO BE CREATED
      WRITE(6,*) 'DATA TO BE CREATED BASED ON PLANE (INPUT- 1 ) '
      WRITE(6,*) 'OR ON A QUADRIC SURFACE (INPUT- 2 ) '
      READ(5,*) ISURF
C
C...INITIALIZATIONS
      IH=0
      IDU=1
      IPTSX=IPTSY=ITPTS=0
      IPTC=1
      ILOC=1
```

```
      IA=IB=2
      AKT=0.1
      AM=1.0
      DKT=0.01
      DAM=0.06
      IF (ISURF.EQ.1) DKT=0.6/70.0
      IC=0
      IP=1
C
C...INITIAL POINT AT (0.1,7,0)
      KTARR(1)=0.1
      AMARR(1)=7.0
      TBARR(1)=0.0
C
C...CREATE DATA BASE
      DO 10 I=1,70
            AKT=AKT+DKT
            DO 20 J=1,100
                  IC=IC+1
                  AM=AM+DAM
C                 EQUATION FOR A PLANE PASSING THROUGH
C                 (0.1,7,0)  (0.7,1,0)  (0.7,7,1)
                  IF (ISURF.EQ.1) THEN
                  TB=(6./3.6)*AKT+(0.6/3.6)*AM-(4.8/3.6)
                  END IF
C                 EQUATION FOR AN ELLIPTIC PARABOLOID
C                 CENTERED AT (0.5,4,0)
                  IF (ISURF.EQ.2) THEN
                  SUM1=(AKT-0.5)*(AKT-0.5)/(0.3*0.3)
                  SUM2=(AM-4.0)*(AM-4.0)/(2.5*2.5)
                  SUM=SUM1+SUM2
                  IF (SUM.GE.1.0) THEN
                     TB=0.0
                  ELSE
                     TB=SQRT(0.25*0.25*(1.0-SUM))
                  END IF
                      END IF
                  IF (TB.GE.0.0.AND.TB.LT.1.0) THEN
                      IP=IP+1
                      TBARR(IP)=TB
                      KTARR(IP)=AKT
                      AMARR(IP)=AM
                  ELSE
                      IP=IP+1
                      KTARR(IP)=AKT
                      AMARR(IP)=AM
                      TBARR(IP)=0.0
                  END IF
 20           CONTINUE
              AM=1.0
 10   CONTINUE
C
C...NUMBER OF DATA
           NPAIRS=IP
```

```
C
C
C              **** BEGIN TRIANGULATION OF DATA ****
C
      DO 400 IK=1,NPAIRS
C.....SEPARATE DATA IN KT BANDS START FROM 0.1 WITH 0.05 INCREMENTS
      IF (KTARR(IK).GT.XO(IA).OR.IK.EQ.NPAIRS) THEN
          IF (IK.EQ.NPAIRS) ITPTS=ITPTS+1
C           SORT DATA IN INCREASING AM
C           CALL IMSL SORTING SUBROUTINES
C           WE HAVE DETERMINED A NUMBER OF POINTS
C           WITHIN A KT BAND
            DO 223 IBC=IK-IPTSX,ITPTS
                   KTARR(IDU)=KTARR(IBC)
                   AMARR(IDU)=AMARR(IBC)
                   TBARR(IDU)=TBARR(IBC)
                   IDU=IDU+1
 223        CONTINUE
            DO 222 IBA=1,IDU-1
                   IRVS(IBA)=IBA
 222        CONTINUE
            CALL VSRTP(AMARR,IDU-1,IRVS)
            DO 555 IS=1,IDU-1
 555        IRVS4(IS)=IRVS(IS)
            CALL VSRTU(KTARR,IDU-1,IDU-1,1,1,IRVS,WK)
            CALL VSRTU(TBARR,IDU-1,IDU-1,1,1,IRVS4,WK)
C
             DO 401 IL=1,IDU-1
C.............SEPARATE DATA IN AM BANDS START FROM 1.0 WITH 0.5 INCREMENTS
             IF (AMARR(IL).GT.YO(IB).OR.IL.EQ.IDU-1) THEN
C           POINTS IN AM BAND
            IF (IL.LT.IDU-1) IPTY=IPTC-1
C            HAVE EXHAUSTED THE POINTS, THE IPTC COUNTER WAS NOT
C            INCREMENTED YET. THEREFORE HAVE TO ACCOUNT FOR THAT LOST POINT
            IF (IL.EQ.IDU-1) IPTY=IPTC
                   DO 402 IM=1,IPTY
                          IH=IH+1
                          AKI(IM)=KTARR(IH)
                          AMI(IM)=AMARR(IH)
                          ATBI(IM)=TBARR(IH)
 402                CONTINUE
C
C...DEFINE A QUADRILATERAL PLANE
C   WITH COORDINATES KT, AM
      AKI1=XO(IA-1)
      AMI1=YO(IB)
      AKI2=XO(IA-1)
      AMI2=YO(IB-1)
      AKI3=XO(IA)
      AMI3=YO(IB-1)
      AKI4=XO(IA)
      AMI4=YO(IB)
C
```

```
C...DEFINE A LOWER AND UPPER TRIANGLE
C    CALL SUBR. TRG TO SEPARATE DATA
       CALL TRG(AKI,AMI,ATBI,AKI1,AMI1,AKI3,AMI3,IPTY,
     & AKILT,AMILT,ATBILT,AKIUT,AMIUT,ATBIUT,NPTSLT,NPTSUT)
C
C...CREATE A DATA BASE WITH THE FOLLOWING INFORMATION-
C    NA - KT BAND COUNTER
C    NB - AM BAND COUNTER
C    IU - 0  LOWER TRIANGLE'S DATA
C         1  UPPE TRIANGLE'S DATA
C    KT,AM,TB CORRESPONDING DATA
       IF (NPTSLT.GT.0) THEN
       DO 100 I=1,NPTSLT
              ILOC=ILOC+1
              NA=IA-1
              NB=IB-1
              IU=0
              AKI(ILOC)=AKILT(I)
              AMI(ILOC)=AMILT(I)
              ATBI(ILOC)=ATBILT(I)
              WRITE(8,101) NA,NB,IU,AKI(ILOC),
     &         AMI(ILOC),ATBI(ILOC)
 101          FORMAT(3(2X,I2),3(2X,F16.14))
 100   CONTINUE
       END IF
C
       IF (NPTSUT.GT.0) THEN
       DO 200 II=1,NPTSUT
              ILOC=ILOC+1
              NA=IA-1
              NB=IB-1
              IU=1
              AKI(ILOC)=AKIUT(II)
              AMI(ILOC)=AMIUT(II)
              ATBI(ILOC)=ATBIUT(II)
              WRITE(8,101) NA,NB,IU,AKI(ILOC),
     &         AMI(ILOC),ATBI(ILOC)
 200   CONTINUE
       END IF
C
C...INCREMENT AM BAND COUNTER
       IB=IB+1
C...RESET POINT COUNTER
       IPTC=1
C
       END IF
C
C...TOTAL NUMBER OF POINTS IN ALL AM BANDS
       IPTSY=IPTSY+1
C...POINTS IN EACH AM BAND
       IPTC=IPTC+1
 401   CONTINUE
C          REINITIALIZE VARIABLES FOR NEXT KT BAND
           IPTSX=IPTSY=0
```

```
              IPTC=1
C             INCREMENT COUNTERS
              IA=IA+1
C             REINITIALIZE THE AM BAND COUNTER
              IB=2
              IDU=1
              IH=0
          END IF
C             NUMBER OF POINTS IN KT BANDS
              IPTSX=IPTSX+1
C             TOTAL NUMBER OF POINTS
              ITPTS=ITPTS+1
  400     CONTINUE
          STOP
          END
```

```
      PROGRAM DISPLAS(INPUT,OUTPUT,TAPE5=INPUT,TAPE6=OUTPUT,TAPE8,
     &                TAPE9,TAPE2)
C
C
C       C. BALARAS      4-24-88
C
C
C...PLOT A 3-D SURFACE USING DISSPLA
C   CONSTRUCT A SURFACE FROM SCATTERED POINTS
C   DISSPLA PROVIDES ROUTINES BGNMAT, GETMAT, AND ENDMAT TO
C   ENABLE THE USER TO CONSTRUCT A REGULAR Z MATRIX FROM THE
C   SCATTERED (X,Y,Z) VALUES. THIS CAN THEN BE GIVEN TO SURMAT
C   TO DRAW THE SURFACE
C   THE GOODNESS OF FIT IS ALSO CALCULATED
C
C   TAPE8 = DATA TAPE OF AN X,Y,Z ARRAY
C   TAPE9 = OUTPUT FILE OF SURFACE FIT NODES
C   TAPE2 = OUTPUT PLOT FILE
C
C...TO RUN THIS PROGRAM -
C                         AT,TAPE8
C                         AT,CALCOMP/UN=LIBRARY
C                         AT,DISSPLA/UN=LIBRARY
C                         X,LIBRARY,DISSPLA,CALCOMP
C                         FTN5,I=DISPLAS,L=0,REW
C
C...TO SUBMIT A JOB TO CALCOMP,
C             PLOTQ,TAPE2,PN=5,PA=0,FC=50
C             PN-PEN CODE, PA-PAPER CODE, FC-SCALLING
C...TO SUBMIT A JOB TO XEROX PRINTER,
C             EPIC,TAPE2
C
C...DIMENSIONS
      DIMENSION TBMAT(19,8),IBUF(512)
      DIMENSION TBARR(8112)
      DIMENSION XO(16),YO(5)
C...DECLARATIONS
      REAL KT
      DATA XO/0.1,0.15,0.2,0.25,0.3,0.35,0.4,0.45,0.5,
     &0.55,0.6,0.65,0.7,0.75,0.8,0.85/
      DATA YO/1.,2.,3.,4.,5./
C
C...INITIALIZATIONS
      SUMT=0.0
      NPAIRS=0
      SYY=0.
      RSS=0.
      IC=0
C...CHOOSE OUTPUT PLOTTING DEVICE
C     VERSATEC
C     CALL PVRSTC
C     CALL VRSTEC(IBUF,512,2)
C     CALCOMP
C     CALL PCLCMP
```

```
C      CALL CALCMP(IBUF,512,2)
C      XEROX PRINTER
       CALL PEPIC
       CALL EPIC(300.,0,7.0,7.0,2)
C...SELECT PLOT REDUCTION OR ENLARGEMENT FACTOR
       CALL BLOWUP(1.0)
C...CALL FOR SWISS-MEDIUM LETTERING STYLE
       CALL SWISSB
       CALL HEIGHT(0.2)
       CALL SHDCHR(90.,1,.002,1)
C...PLOTTING OF A 3-D SURFACE
C...PAGE SIZE BORDER
       CALL PAGE(12.0,15.0)
C...DEFINE SUBPLOT AREA
       CALL AREA2D(11.5,14.5)
C...DEFINE X,Y,Z WORKBOX IN INCHES
       CALL VOLM3D(5.0,4.0,5.0)
C...DEFINE 3-D AXIS LABELS
       CALL MIXALF('INSTRU')
       CALL X3NAME(' (H-1.5)CLEARNESS INDEX$',100)
       CALL Y3NAME(' (H-1.5)AIR MASS$',100)
       CALL Z3NAME(' (H-1.5)BEAM TRANSMITTANCE$',100)
C...DEFINE THE VIEW POINT
       CALL VUABS(-7.5,-6.0,7.5)
C...3-D GRAPH SETUP ROUTINES
       CALL GRAF3D(0.1,0.1,1.0,1.0,1.0,8.0,0.0,0.2,1.0)
C...3-D SURFACE DRAWING
C...DISSPLA CONSTRUCTS A REGULAR MATRIX FROM
C   A COLLECTION OF POINTS TO BE USED BY SURMAT
       CALL BGNMAT(19,8)
C...READ DATA
C      HAVE EXCLUDED THE THREE ERRONEOUS POINTS
       DO 1000 I=1,8109
       READ(8,10) KT,AM,TB
  10   FORMAT(12X,3(2X,F16.14))
       IF (AM.GT.5.0) GOTO 1000
C      NUMBER OF DATA TO USED
       NPAIRS=NPAIRS+1
C      SUM BEAM TRANSMITTANCE VALUES
       TBARR(NPAIRS)=TB
       SUMT=SUMT+TBARR(NPAIRS)
       CALL GETMAT(KT,AM,TB,1,0)
 1000  CONTINUE
       CALL ENDMAT(TBMAT,0)
C...REPORT SURFACE FIT NODES
       DO 1100 I=1,19
       DO 1200 J=1,8
       WRITE(9,20) I,J,TBMAT(I,J)
  20   FORMAT(' (',I2,',',I2,') ',F7.5)
 1200  CONTINUE
 1100  CONTINUE
       CALL SURMAT(TBMAT,1,19,1,8,0)
C
```

```
C...STATISTICAL ANALYSIS
C...POSITION CURSOR AT THE BEGINING OF THE DATA FILE
      REWIND(8)
C
C...READ DATA
      DO 1300 I=1,8109
      READ(8,30) NA,NB,IU,KT,AM,TB
 30   FORMAT(3(2X,I2),3(2X,F16.14))
C     SCREEN DATA
      IF (AM.GT.5.) GOTO 1300
      IC=IC+1
      IF (IU.EQ.0) THEN
C        EQN. OF TRG PLANE THAT ENCLOSES DATA
         CALL PLANEQ(XO(NA),YO(NB),TBMAT(NA,NB),
     &   XO(NA),YO(NB+1),TBMAT(NA,NB+1),
     &   XO(NA+1),YO(NB),TBMAT(NA+1,NB),A1,A2,A3,D)
C        DISTANCE OF DATA FROM PLANE
         H=ABS(A1*KT+A2*AM+A3*TB+D)/SQRT(A1*A1+A2*A2+A3*A3)
C        UNEXPLAINED VARIATION
         RSS=RSS+H*H
      END IF
      IF (IU.EQ.1) THEN
C        EQN OF TRG PLANE THAT ENCLOSES DATA
         CALL PLANEQ(XO(NA+1),YO(NB),TBMAT(NA+1,NB),
     &   XO(NA),YO(NB+1),TBMAT(NA,NB+1),
     &   XO(NA+1),YO(NB+1),TBMAT(NA+1,NB+1),A1,A2,A3,D)
C        DISTANCE OF DATA FROM PLANE
         H=ABS(A1*KT+A2*AM+A3*TB+D)/SQRT(A1*A1+A2*A2+A3*A3)
C        UNEXPLAINED VARIATION
         RSS=RSS+H*H
      END IF
 1300 CONTINUE
C
C     AVG. BEAM TRANSMITTANCE VALUE
      TAVE=SUMT/NPAIRS
C     TOTAL VARIATION
      DO 200 I=1,NPAIRS
            SYY=SYY+(TBARR(I)-TAVE)**2
 200  CONTINUE
C     EXPLAINED VARIATION
      SSREG=SYY-RSS
C     COEF. OF CORRELATION
      AR=SQRT(SSREG/SYY)
C     COEF. OF DETERMINATION
      AR2=AR*AR
C     REPORT RESULTS
      WRITE(9,*) ' '
      WRITE(9,*) 'NUMBER OF DATA USED = ',NPAIRS,'    IC= ',IC
      WRITE(9,*) 'TOTAL VARIATION SYY= ',SYY
      WRITE(9,*) 'RESIDUAL VARIATION RSS= ',RSS
      WRITE(9,*) 'EXPLAINED VARIATION SRR= ',SSREG
      WRITE(9,*) 'COEF. OF DETERMINATION R2= ',AR2
C
C...PLOT TERMINATION
```

```
CALL ENDPL(1)
CALL DONEPL
CALL EXIT
STOP
END
```

```
      PROGRAM IMSLFIT(INPUT,OUTPUT,TAPE5=INPUT,TAPE6=OUTPUT,TAPE7,
     &TAPE8,TAPE2)
C
C
C     C. BALARAS    14-4-88
C
C
C...SURFACE FITTING WITH IRREGULARLY DISTRIBUTED DATA POINTS
C   USING IMSL SUBROUTINE "IQHSCV"
C
C...THE DATA IN TAPE8 HAVE TO BE ACCORDINGLY COMPLETED
C   THAT IS REQUIRE SOME NULL DATA ON THE REFERENCE PLANE (X,Y,0)
C
C...TO RUN THIS PROGRAM,
C                       AT,TAPE8   (DATA FILE)
C                       AT,IMSLIB5/UN=LIBRARY
C                       AT,CALCOMP/UN=LIBRARY
C                       X,LIBRARY,CALCOMP,IMSLIB5
C
C...TAPE DIRECTORY,
C                  TAPE7  - OUTPUT FILE
C                  TAPE8  - INPUT FILE
C                  TAPE2  - PLOT FILE
C
C...DECLARATIONS
      REAL KTARR(8227),AMARR(8227),TBARR(8227)
      DIMENSION XO(16),YO(7),ZI(16,7)
      DIMENSION IWK(255149),WK(49362)
      DIMENSION IBUF(512),HID(304)
      REAL KT
C
      DATA XO/0.1,0.15,0.2,0.25,0.3,0.35,0.4,0.45,0.5,0.55,0.6,
     &0.65,0.7,0.75,0.8,0.85/
C
      DATA YO/1.0,2.0,3.0,4.0,5.0,6.0,7.0/
C
      NDATA=0
C
C...READ INPUT DATA
C
      DO 100 I=1,8227
            READ(8,20) KT,AM,TB
            IF (AM.GT.5.) GOTO 100
            NDATA=NDATA+1
            KTARR(NDATA)=KT
            AMARR(NDATA)=AM
            TBARR(NDATA)=TB
 20         FORMAT(12X,3(2X,F16.14))
 100  CONTINUE
C
C...CALL IMSL ROUTINE
      CALL IQHSCV(KTARR,AMARR,TBARR,NDATA,XO,16,YO,7,ZI,16,IWK,WK,IER)
C
```

```
C...REPORT RESULTS
      DO 200 I=1,16
      WRITE(7,*)  (ZI(I,J),J=1,7)
 200  CONTINUE
C
      STOP
      END
```

```
      PROGRAM TEMPV(INPUT,OUTPUT,TAPE5=INPUT,TAPE6=OUTPUT,TAPE9,
     &              TAPE8,TAPE3,TAPE2)
C
C
C       C. BALARAS        2-16-88
C       C. BALARAS        3-16-88
C       C. BALARAS        4-27-88
C
C
C...CALCULATE TEMPORAL VARIATION FACTOR (ETA)
C   THERE ARE THREE WAYS TO CALCULATE ETA,
C   ETA=SUM(I(PERIOD)-KT*IO(PERIOD))
C   ETA2=SUM(I(PERIOD)-IEST)
C   ETA3=SUM(I(PERIOD)-I(AVG))
C   THE CALCULATIONS ARE PERFORMED ON FIFTEEN MIN. BASIS
C   APPROPRIATE DATA HAS TO BE USED (I.E. QFILES) WHICH FIRST
C   HAVE BEEN PROCESSED THROUGH CREATE3 TO COMPLETE ANY MISSING
C   PERIODS. THE DATA WERE FINALL  WRITTEN IN TAPE3 AND COLLECTED IN
C   ANNUAL DATA FILES (DATA[YR]).
C   THE DATA ARE BEING PROCESSED S QUENTIALLY STARTING FROM
C   1979 JAN THE 1ST AND SO ON.
C
C...TO RUN THIS PROGRAM,
C                        AT,GDHR5Y
C                        C,GDHR5Y,TAPE9
C                        AT,QFILE
C                        C,QFILE,TAPE10
C                        G,CREATE3
C                        M77,I=CREATE3,L=0
C                       ************************************
C                       * COMPLETE QFILE HAVE BEEN         *
C                       * STORED UNDER 'DATA(YR)' FILES    *
C                       * AT,DATA(YR) ...                  *
C                       * C,DATA(YR),TAPE3                 *
C                       ************************************
C                        AT,IMSLIB5/UN=LIBRARY
C                        X,LIBRARY,IMSLIB5
C
C...TAPE DIRECTORY,
C                   TAPE2  - AVAILABLE
C                   TAPE10 - 15 MIN DATA (QFILE)
C                   TAPE3  - INPUT 15 MIN DATA (PROCESSED BY CREATE3)
C                   TAPE8  - OUTPUT
C                   TAPE9  - INPUT HOURLY DATA
C
C
      COMMON /CNSTS/ ALATR,DELOMO2,GSCF,HRCONV
      COMMON /CNSTS2/ QLO2
C
C...DIMENSIONS
      DIMENSION T(4),PIRAD(4)
      DIMENSION EXTR(4),DECL(4),W(4),EQT(4),A(4)
C
      REAL KT,K,KT1,TB1,TB,ION,IO,IO2,ION2
```

```
      INTEGER BADPER,YR,DAY,MO,HR,MIN
      INTEGER YR2,MO2,DAY2,HR2,MIN2
C
C...NO. OF HOURLY DATA FROM GD2H5Y (TAPE9)
      NPAIRS=8112
C
C
C...CONSTANTS
      ALATD=33.4046
      ALONGD=84.7478
      ALONST=75.0
      ZONE=5.0
      GSC=1367.
      PI=4.0*ATAN(1.0)
      DRCONV=PI/180.0
      HRCONV=12.0/PI
      ALATR=ALATD*DRCONV
      DLOMEGA=15.0*DRCONV
      DELOMO2=DLOMEGA/2.0
      GSCF=3.6*GSC*12.0/PI
C     FOR 15 MIN INTERVALS
      QLO=DLOMEGA/4.0
      QLO2=QLO/2.
C
C ***** BEGIN CALCULATIONS *****
C
      DO 100 I=1,NPAIRS
C...READ HOURLY DATA FROM GDHR5Y
      READ(9,20) YR,MO,DAY,HR,MIN,HRZTOT,DIR,PCT,BADPER
 20   FORMAT(5(1X,I2),2(2X,F7.1),2X,F4.2,1X,I2)
C
          IF (YR.NE.80) GOTO 100
C
C   RECORDED TIME IS FOR PERIOD ENDING
C   CALCULATE PERIOD ENDING TIME FOR 1ST 15 MIN PERIOD
      TIME=(HR+MIN/60.0)-0.75
C   ADJUST ACCORDINGLY FOR MISSING PERIOD
      IF (PCT.NE.0.0) THEN
         IF (BADPER.EQ.1) TIME=(HR+MIN/60.)-0.5
      END IF
C
C...CALCULATE AVG. HOURLY CLEARNESS INDEX AND HGIO
      CVLT=(HR+MIN/60.0)-0.5
      CALL HELGO(YR,MO,DAY,CVLT,ALONGD,ALATD,ALONST,ZONE,ALPHA,
     &           DELTA,EOT,OMEGA,R)
      CALL SUBI(OMEGA,ALATD,DELTA,BADPER,GSC,IFRST,R,HRZTOT,DIR,
     &           IO,KT,TB)
      CALL EXTRAD(DELTA,OMEGA,R,HBNIO,HGIO,AZCOS,AHANG,DLO2)
C
C...CALCULATE THE SOLAR ALTITUDE
      SINALT=AZCOS
      IF (SINALT.GE.0.0) THEN
         ALTAVE=ASIN(SINALT)
      ELSE
```

```
         ALTAVE=-99.0
       END IF
C...CALCULATE AIR MASS
       AM=AMASS(ALTAVE)
C...TEST FOR VALIDITY OF RESULTS
C    FOR NEGATIVE ALTITUDE, AM=1E50 SKIP CALCULATIONS
       IF (AM.GT.100.0) GOTO 100
C
C
C...IDENTIFY CORRESPONDING 15-MIN DATA
C    RESET COUNTER
       ICOUNT=0
 200   READ(3,30) YR2,MO2,DAY2,HR2,MIN2,FLG1,FLG2,FLG3
       READ(3,40) PYHEL1,PYHEL2,PYRAN
 30    FORMAT(12,5X,12,1X,12,1X,12,1X,12,44X,Z2,Z2,2X,Z2)
 40    FORMAT(23X,F5.0,F5.0,5X,F5.0)
C
       IF (YR2.EQ.80.AND.MO2.EQ.9.AND.DAY2.EQ.25.AND.HR2.EQ.10
      &.AND.MIN2.EQ.23) GOTO 1500
       ICOUNT=ICOUNT+1
C    PERIOD ENDING TIME OF 15 MIN PERIOD
       TIME2=(HR2+MIN2/60.0)
       DT=ABS(TIME-TIME2)
C    CROSS COMPARE DATA
       IF (YR2.NE.YR) GOTO 200
       IF (MO2.NE.MO) GOTO 200
       IF (DAY2.NE.DAY) GOTO 200
       IF (TIME2.NE.TIME.AND.DT.GT.0.00000000001) GOTO 200
C
C...NO. OF 15 MIN PERIODS
1500   NPER=4
       IF (BADPER.EQ.1) NPER=3
C...HOURLY INITIALIZATIONS
       SUM=0.
       SUM2=0.
       SUM3=0.
       NOP=0
       SUMI=0.
       SUMT=0.
       SUMT2=0.
       SUMIT=0.
C    15 MIN CALCULATIONS
       DO 300 IP=1,NPER
C              SKIP THIS PERIOD IF IT IS BAD
               IF (BADPER.EQ.IP.AND.BADPER.NE.1) GOTO 400
               CVLT=(HR2+MIN2/60.0)-0.125
               CALL HELGO(YR2,MO2,DAY2,CVLT,ALONGD,ALATD,ALONST,ZONE,
      &                   ALPHA,DELTA,EOT,OMEGA,R)
               CALL EXTRAD2(DELTA,OMEGA,R,HBNIO,HGIO,AZCOS,AHANG,DLO2)
C
               SUM=SUM+(PYRAN-KT*HGIO)**2
               SUMI=SUMI+PYRAN
               SUMT2=SUMT2+CVLT**2
               SUMT=SUMT+CVLT
```

```
                SUMIT=SUMIT+PYRAN*CVLT
                NOP=NOP+1
                T(NOP)=CVLT
                PIRAD(NOP)=PYRAN
                EXTR(NOP)=HGIO
                DECL(NOP)=DELTA
                A(NOP)=ALPHA
                EQT(NOP)=EOT
                W(NOP)=OMEGA
C               READ DATA FOR NEXT PERIOD
 400    IF (IP.LT.NPER) THEN
                READ(3,30) YR2,MO2,DAY2,HR2,MIN2,FLG1,FLG2,FLG3
                READ(3,40) PYHEL1,PYHEL2,PYRAN
        END IF
 300    CONTINUE
C
C
C...CALCULATE COEF. FOR BEST FIT
        C1=((SUMI*SUMT2)-(SUMT*SUMIT))/
     &     ((NOP*SUMT2)-(SUMT*SUMT))
        C2=((NOP*SUMIT)-(SUMT*SUMI))/
     &     ((NOP*SUMT2)-(SUMT*SUMT))
C
C...CALCULATE TEMPORAL VARIATION ETA
        IF (SUM.EQ.0.0) THEN
           ETA=0.0
        ELSE
           ETA=SQRT(SUM/HRZTOT**2)
        END IF
C...CALCULATE AVG. GLOBAL RAD VALUE FOR THE HOUR
        AVGI=0.
        DO 490 IP=1,NOP
                AVGI=AVGI+PIRAD(IP)
 490    CONTINUE
        AVGI=AVGI/NOP
C...CALCULATE TEMPORAL VARIATIONS ETA2 AND ETA3
        DO 500 IA=1,NOP
                IEST=C1+C2*T(IA)
                SUM2=SUM2+(PIRAD(IA)-IEST)**2
                SUM3=SUM3+(PIRAD(IA)-AVGI)**2
 500    CONTINUE
        IF (SUM2.EQ.0.0) THEN
           ETA2=0.
           ETA3=0.
        ELSE
           ETA2=SQRT(SUM2/HRZTOT**2)
           ETA3=SQRT(SUM3/HRZTOT**2)
        END IF
C   RECORD RESULTS
        WRITE(8,50) YR,MO,DAY,HR,MIN,KT,TB,ETA,ETA2,ETA3,AM,BADPER,NOP
 50     FORMAT(5(2X,I2),4X,6(F7.5,2X),2X,I2,2X,I2)
C
 100    CONTINUE
C
```

```
STOP
END
```

TABLE E.1

Coordinates of the Locally Weighted Least Square Error Fit Surface Using All the Five Year Data

Clearness Index	ETA1	Beam Transmittance	No. of Data
.10	.0	.0000	0
.10	.1	.0000	0
.15	.0	.0000	5
.15	.1	.0000	30
.10	.2	.0002	5
.15	.2	.0007	6
.10	.3	.0000	3
.15	.3	.0001	0
.10	.4	.0000	0
.15	.4	.0000	0
.10	.5	.0000	0
.15	.5	.0000	0
.20	.0	.0000	40
.20	.1	.0003	72
.20	.2	.0047	23
.20	.3	.0030	5
.20	.4	.0006	0
.20	.5	.0001	0
.25	.0	.0002	55
.25	.1	.0018	74
.25	.2	.0115	40
.25	.3	.0460	8
.25	.4	.0007	1
.25	.5	.0002	0
.30	.0	.0001	54
.30	.1	.0092	70
.30	.2	.0342	19
.30	.3	.0532	16
.30	.4	.1133	2
.30	.5	.0229	0
.35	.0	.0017	47
.35	.1	.0237	67
.35	.2	.0515	27
.35	.3	.0970	9
.35	.4	.0761	4
.35	.5	.0335	0
.40	.0	.0506	60
.40	.1	.0454	70
.40	.2	.0989	40
.40	.3	.1154	15
.40	.4	.1229	2
.40	.5	.0514	0
.45	.0	.0436	58
.45	.1	.0987	88

.45	.2	.1601	57
.45	.3	.1715	7
.45	.4	.1326	0
.45	.5	.0676	0
.50	.0	.0967	54
.50	.1	.1420	96
.50	.2	.2186	43
.50	.3	.2471	7
.50	.4	.1555	0
.50	.5	.0852	0
.55	.0	.2069	85
.55	.1	.2186	154
.55	.2	.2777	63
.55	.3	.3123	1
.55	.4	.1869	0
.55	.5	.1055	0
.60	.0	.2903	125
.60	.1	.2903	210
.60	.2	.4073	27
.60	.3	.3313	0
.60	.4	.2158	0
.60	.5	.1276	0
.65	.0	.4234	315
.65	.1	.3575	308
.65	.2	.3974	0
.65	.3	.3446	0
.65	.4	.2415	0
.65	.5	.1504	0
.70	.0	.5484	648
.70	.1	.3269	211
.70	.2	.3833	0
.70	.3	.3523	0
.70	.4	.2637	0
.70	.5	.1730	0
.75	.0	.6554	932
.75	.1	.4171	71
.75	.2	.3900	0
.75	.3	.3598	0
.75	.4	.2829	0
.75	.5	.1950	0
.80	.0	.7134	461
.80	.1	.4428	11
.80	.2	.4006	0
.80	.3	.3680	0
.80	.4	.2999	0
.80	.5	.2160	0
.85	.0	.7788	44
.85	.1	.5100	0
.85	.2	.4225	0
.85	.3	.3789	0
.85	.4	.3157	0
.85	.5	.2359	0

TABLE E.2

Coordinates of the Locally Weighted Least Square Error Fit Surface Using All the Five Year Data

Clearness Index	ETA2	Beam Transmittance	No. of Data
.10	.0	.0000	0
.10	.1	.0000	0
.15	.0	.0000	5
.15	.1	.0000	30
.10	.2	.0002	5
.15	.2	.0007	6
.10	.3	.0000	3
.15	.3	.0001	0
.10	.4	.0000	0
.15	.4	.0000	0
.10	.5	.0000	0
.15	.5	.0000	0
.20	.0	.0000	40
.20	.1	.0003	72
.20	.2	.0047	23
.20	.3	.0030	5
.20	.4	.0006	0
.20	.5	.0001	0
.25	.0	.0002	55
.25	.1	.0018	74
.25	.2	.0115	40
.25	.3	.0460	8
.25	.4	.0007	1
.25	.5	.0002	0
.30	.0	.0001	54
.30	.1	.0092	70
.30	.2	.0342	19
.30	.3	.0532	16
.30	.4	.1133	2
.30	.5	.0229	0
.35	.0	.0017	47
.35	.1	.0237	67
.35	.2	.0515	27
.35	.3	.0970	9
.35	.4	.0761	4
.35	.5	.0335	0
.40	.0	.0506	60
.40	.1	.0454	70
.40	.2	.0989	40
.40	.3	.1154	15
.40	.4	.1229	2
.40	.5	.0514	0
.45	.0	.0436	58
.45	.1	.0987	88
.45	.2	.1601	57

.45	.3	.1715	7
.45	.4	.1326	0
.45	.5	.0676	0
.50	.0	.0967	54
.50	.1	.1420	96
.50	.2	.2186	43
.50	.3	.2471	7
.50	.4	.1555	0
.50	.5	.0852	0
.55	.0	.2069	85
.55	.1	.2186	154
.55	.2	.2777	63
.55	.3	.3123	1
.55	.4	.1869	0
.55	.5	.1055	0
.60	.0	.2903	125
.60	.1	.2903	210
.60	.2	.4073	27
.60	.3	.3313	0
.60	.4	.2158	0
.60	.5	.1276	0
.65	.0	.4234	315
.65	.1	.3575	308
.65	.2	.3974	0
.65	.3	.3446	0
.65	.4	.2415	0
.65	.5	.1504	0
.70	.0	.5484	648
.70	.1	.3269	211
.70	.2	.3833	0
.70	.3	.3523	0
.70	.4	.2637	0
.70	.5	.1730	0
.75	.0	.6554	932
.75	.1	.4171	71
.75	.2	.3900	0
.75	.3	.3598	0
.75	.4	.2829	0
.75	.5	.1950	0
.80	.0	.7134	461
.80	.1	.4428	11
.80	.2	.4006	0
.80	.3	.3680	0
.80	.4	.2999	0
.80	.5	.2160	0
.85	.0	.7788	44
.85	.1	.5100	0
.85	.2	.4225	0
.85	.3	.3789	0
.85	.4	.3157	0
.85	.5	.2359	0

TABLE E.3

Coordinates of the Locally Weighted Least Square Error Fit Surface Using All the Five Year Data

Clearness Index	ETA3	Beam Transmittance	No. of Data
.10	.0	.0000	0
.10	.1	.0000	0
.15	.0	.0000	4
.15	.1	.0000	32
.10	.2	.0000	5
.15	.2	.0011	5
.10	.3	.0000	3
.15	.3	.0002	0
.10	.4	.0000	0
.15	.4	.0000	0
.10	.5	.0000	0
.15	.5	.0000	0
.20	.0	.0000	40
.20	.1	.0006	61
.20	.2	.0034	28
.20	.3	.0029	4
.20	.4	.0006	0
.20	.5	.0001	0
.25	.0	.0000	50
.25	.1	.0014	78
.25	.2	.0139	45
.25	.3	.0390	7
.25	.4	.0193	2
.25	.5	.0040	0
.30	.0	.0012	55
.30	.1	.0099	63
.30	.2	.0287	23
.30	.3	.0642	15
.30	.4	.1029	3
.30	.5	.0237	0
.35	.0	.0012	41
.35	.1	.0227	69
.35	.2	.0501	36
.35	.3	.1215	8
.35	.4	.0810	5
.35	.5	.0352	0
.40	.0	.0394	52
.40	.1	.0563	71
.40	.2	.0836	39
.40	.3	.1001	17
.40	.4	.1447	2
.40	.5	.0571	0
.45	.0	.0374	51
.45	.1	.0972	87

.45	.2	.1512	60
.45	.3	.2049	10
.45	.4	.1567	0
.45	.5	.0770	0
.50	.0	.0970	47
.50	.1	.1459	89
.50	.2	.2081	53
.50	.3	.2004	7
.50	.4	.1655	0
.50	.5	.0947	0
.55	.0	.1836	76
.55	.1	.2177	151
.55	.2	.2748	66
.55	.3	.2987	3
.55	.4	.1921	0
.55	.5	.1142	0
.60	.0	.2908	112
.60	.1	.2928	203
.60	.2	.3569	35
.60	.3	.3103	0
.60	.4	.2158	0
.60	.5	.1345	0
.65	.0	.3890	225
.65	.1	.4043	384
.65	.2	.0975	8
.65	.3	.2678	0
.65	.4	.2262	0
.65	.5	.1528	0
.70	.0	.5357	500
.70	.1	.4259	350
.70	.2	.1632	0
.70	.3	.2469	0
.70	.4	.2303	0
.70	.5	.1683	0
.75	.0	.6647	817
.75	.1	.5884	184
.75	.2	.2482	0
.75	.3	.2471	0
.75	.4	.2337	0
.75	.5	.1814	0
.80	.0	.7025	439
.80	.1	.6324	33
.80	.2	.3251	0
.80	.3	.2627	0
.80	.4	.2395	0
.80	.5	.1930	0
.85	.0	.8107	44
.85	.1	.6680	0
.85	.2	.3936	0
.85	.3	.2889	0
.85	.4	.2494	0
.85	.5	.2043	0

APPENDIX F

Table F.1 Coordinates of the Locally Weighted Least Square Error Fit Surface Using All Three Year Data from the National Observatory of Athens, Greece2

Table F.1

Coordinates of the Locally Weighted Least Square Error Fit Surface Using All Three Year Data from NOA

Clearness Index	Air Mass	Beam Transmittance	No. of Data
.10	1.0	.0000	0
.10	2.0	.0000	0
.15	1.0	.0097	7
.15	2.0	.0018	8
.10	3.0	.0078	6
.15	3.0	.0016	5
.10	4.0	.0000	8
.15	4.0	.0047	6
.10	5.0	.0000	4
.15	5.0	.0194	14
.20	1.0	.0199	11
.20	2.0	.0135	10
.20	3.0	.0095	8
.20	4.0	.0207	10
.20	5.0	.0381	12
.25	1.0	.0173	9
.25	2.0	.0217	23
.25	3.0	.0396	20
.25	4.0	.0473	17
.25	5.0	.0624	23
.30	1.0	.0360	34
.30	2.0	.0359	37
.30	3.0	.0451	22
.30	4.0	.0864	25
.30	5.0	.0733	13
.35	1.0	.0338	45
.35	2.0	.0433	44
.35	3.0	.0987	34
.35	4.0	.1232	16
.35	5.0	.1898	2
.40	1.0	.0763	56
.40	2.0	.0995	56
.40	3.0	.1693	61
.40	4.0	.1369	20
.40	5.0	.2219	3
.45	1.0	.0859	55
.45	2.0	.1668	63
.45	3.0	.2051	70
.45	4.0	.0837	10
.45	5.0	.0000	1
.50	1.0	.1454	61
.50	2.0	.2042	88
.50	3.0	.1999	47

.50	4.0	.1183	14
.50	5.0	.0000	2
.55	1.0	.2546	90
.55	2.0	.3375	159
.55	3.0	.2358	51
.55	4.0	.2749	9
.55	5.0	.2349	2
.60	1.0	.2778	131
.60	2.0	.3536	159
.60	3.0	.3507	25
.60	4.0	.1726	13
.60	5.0	.3188	2
.65	1.0	.4303	230
.65	2.0	.4090	196
.65	3.0	.3410	45
.65	4.0	.3140	22
.65	5.0	.1768	9
.70	1.0	.4675	402
.70	2.0	.4681	262
.70	3.0	.3885	58
.70	4.0	.3451	19
.70	5.0	.3990	13
.75	1.0	.5717	533
.75	2.0	.5055	235
.75	3.0	.4141	54
.75	4.0	.3984	14
.75	5.0	.3018	10
.80	1.0	.6676	235
.80	2.0	.5944	84
.80	3.0	.5702	32
.80	4.0	.5041	15
.80	5.0	.3778	10
.85	1.0	.5267	18
.85	2.0	.5435	5
.85	3.0	.5581	4
.85	4.0	.5116	5
.85	5.0	.8174	6

BIBLIOGRAPHY

Akima, H., "A Method of Bivariate Interpolation and Smooth Surface Fitting for Irregularly Distributed Data Points", ACM Transactions Mathematical Software, Vol. 4, pp. 148-159, 1978.

Angstrom, "Solar and Terrestrial Radiation", Quart. J. of Royal Meteorological Society, Vol. 50, p. 121, 1924.

Anscombe, F. J., "Rejection of Outliers", Technometrics, Vol.2, pp. 123-147, 1960.

Appelbaum, J., and Bergshtein, O., "Solar Radiation Distribution Sensor", Solar Energy, Vol. 39, p. 1, 1987.

Bahm, R. J., "An Evaluation of the Availability and Quality of Data on Solar Radiation", Proceedings of the AS/ISES Conference, pp. 2174 2177, 1980.

Balaras, C. A., Investigation of the Dependence of Atmospheric Transmittance for the Beam Radiation on Clearness Index, Master's Thesis, School of Mechanical Engineering, Georgia Institute of Technology, Sept. 1985.

Balaras, C. A., and Jeter, S. M., "A Model for the Beam Transmittance of the Atmosphere for Solar Energy Applications", Proceedings of the Solar Energy Applications Panhellenic Conference with European Participation, Patras, Greece, Sept. 14-17, 1987.

Barbaro, S., Coppolino, S., Leone, C., and Sinagra, E., "An Atmospheric Model for Computing Direct Beam and Diffuse Solar Radiation", Solar Energy, Vol. 22, pp. 225-228, 1979.

Barnhill, R. E., "Representation and Approximation of Surfaces", in J.R. Rice ed., Mathematical Software III, Academic Press, New York, 1977.

Beckman, W. A., Bugler, J. W., et. al., "Units and Symbols in Solar Energy", Solar Energy, Vol. 21, p. 65, 1978.

Bird, R. E., and Hulstrom, R. L., "Review, Evaluation, and Improvement of Direct Irradiance Models", Journal of Solar Energy Engineering, Vol. 103, p. 182, 1981.

Boes, E. C., Fundamentals of Solar Radiation in Solar Energy Handbook, J. F. Kreider and F. Kreith, editors, McGraw Hill, 1981.

Boes, E. C., Anderson, H. E., Hall, I. J., Prairie, R. R., and Stromberg, R. T., "Availability of Direct, Total, and Diffuse Solar Radiation to Fixed and Tracking Collectors in the U.S.A.", Sandia National Laboratories Report, No. SAND 77-0885, August, 1977.

Box, G. E. P., "Use and Abuse of Regression", Technometrics, Vol. 8, pp. 625-629, 1966.

Bruno, R., "A Correction Proceedure for Separating Direct and Diffuse Insolation on a Horizontal Surface", Solar Energy, Vol. 20, p. 97, 1978.

Brusa, R. W., and Frohlich, C., "Realization of the Absolute Scale of Total Irradiance", Scientific Discussions, Fourth International Pyrheliometer Comparisons, Davos, Switzerland, 1975.

Bugler, J. W., "The Determination of Hourly Insolation on an Inclined Plane Using a Diffuse Irradiance Model Based on an Hourly Measured Global Horizontal Insolation", Solar Energy, Vol. 19, pp. 477, 1977.

Carroll, J. J., "Global Transmissivity and Diffuse Fraction of Solar Radiation for Clear and Cloudy Skies as Measured and as Predicted by Bulk Transmissivity Models", Solar Energy, Vol. 35, pp. 105-118, 1985.

Castagnoli, C., Giraud, C., Longhetto, A., and Morra, O., "Correlation between Normal Direct Radiation and Global Radiation Depending on Cloudiness", Solar Energy, Vol. 28, pp. 289-292, 1982.

Choudhury, N. K. O., "Solar Radiation at New Delhi", Solar Energy, Vol. 7, pp. 44-52, 1963.

Collares-Pereira, M., and Rabl, A., "The Average Distribution of Solar Radiation Correlations Between Diffuse and Hemispherical and Between Daily and Hourly Insolation Values", Solar Energy, Vol. 22, p. 155, 1979.

Cooper, P. I., "The Absorption of Solar Radiation in Solar Stills", Solar Energy, Vol. 12, pp. 333-346, 1969.

Correc, Y., and Chapuis, E., "Fast Computation of Delaunay Triangulations", Advanced Engineering Software, Vol. 9, pp. 77-83, 1987.

Cotton, C. F., "ARL Models of Global Solar Radiation", U.S. Department of Commerce, 1979: SOLMET Volume 2 - Final Report, Department of Energy, Contract No. E(49-26)-1041, Asheville, NC, pp. 165-184.

Coulson, K. L., Solar and Terrestrial Radiation, Academic Press, New York, 1975.

Davies, J. A., Abdel-Wahab, M., and McKay, D. C., "Estimating Solar Irradiation on Horizontal Surfaces", International Journal of Solar Energy, Vol. 2, p. 405, 1984

Davies, J. A., and McKay, D. C., "Estimating Solar Irradiation and Components", Solar Energy, Vol. 29, pp. 55-64, 1982.

Dischinger, D. G., Solar Beam Radiation Model Development, Master's Thesis, School of Mechanical Engineering, Georgia Institute of Technology, June, 1984.

DISSPLA, Display Integrated Software System and Plotting Language, Integrated Software Systems Co., 1981.

Dogniaux, R., Grueter, J. W., Kasten, F., Page, J. K., Perrin De Brichambaut, Treble, F. C., and Palz, W., "Solar Meteorology (Units and Symbols)", International Journal of Solar Energy, Vol. 2, pp. 249-255, 1984.

Draper, N., and Smith, H., Applied Regression Analysis, 2nd edition, John Wiley, New York, 1981.

DSET Laboratories, Inc., Intercomparison of Absolute Cavity Pyrheliometers Seminar, Phoenix, Arizona, 1-3 November, 1978.

Duffie, J. A., and Beckman, W. A., Solar Engineering of Thermal Processes, John Wiley, New York, 1980.

Erbs, D. G., Klein, S. A., and Duffie J. A., "Estimation of the Diffuse Radiation Fraction for Hourly, Daily, and Monthly Average Global Radiation", Solar Energy, Vol. 28, p. 293, 1982.

Erbs, D. G., Stauter, R. C., and Duffie, J. A., "The Basis and Effects of Inaccuracies in Diffuse Radiation Correlations", Proceedings of the AS/ISES Annual Conference, Phoenix, arizona, G. E. Franta and B. H. Glenn, editors, 1980.

Faiman, D., Zemel, A., and Zangvil, A., "A Method for Monitoring in Remote Regions", Solar Energy, Vol. 38, pp. 327-333, 1987.

Farin, G., "Triangular Bernstein-Bezier Patches", Computer Aided Geometric Design, Vol. 3, pp. 83-127, 1986.

Fox, J., Linear Statistical Models and Related Methods, John Wiley, New York, 1984.

Frohlich, C., "Contemporary Measures of the Solar Constant", O.R. White (Ed.), Colorado Associated University Press, Boulder, 1977.

Garrison, J. D., "A Study of Solar Radiation Data for Six Sites", Solar Energy, Vol. 32, pp. 237-249, 1984.

Gautier, C., Diak, G., and Masse, S., "A Simple Physical Model to Estimate Incident Solar Radiation at the Surface from GOES Satellite Data", Journal of Applied Meteorology, Vol. 19, p. 1005, 1980.

Gilchrist, W., Statistical Modelling, John Wiley, Norwich, 1984.

Godske, G. J., Bergeron, T., Bjerknes, J., and Bundgaard, R., Dynamic Meteorology and Weather Forecasting, Boston: American Meteorological Society and Washington: Carnegie Institution of Washington, 1957.

Gordon, J. M., and Hochman, M., "On the Correlations Between Beam and Global Radiation", Solar Energy, Vol. 32, pp. 329-336, 1984.

Grether, D., et. al., "Measurement of Circumsolar Radiation, Proceedings of the ISES Meeting, Los Angeles, 1975.

Haurwitz, B. "Insolation in Relation to Cloud Type", Journal of Meteorology, Vol. 5, pp. 110-113, 1948.

Hay, J. E., "A Revised Method for Determining the Direct and Diffuse Components of the Total Short-Wave Radiation", Atmosphere, Vol. 14, pp. 278-287, 1976.

Hay, J. E., "Calculation of the Solar Radiation Incident on an Inclined Surface", Proceedings of the First Canadian Solar Radiation Data Workshop, J. E. Hay and T. K. Won, editors, Atmospheric Environment Service, Downsview, 1979.

Hay, J. E., "Calcualtion of Monthly Mean Solar Radiation for Horizontal and Inclined Surfaces", Solar Energy, Vol. 23, pp. 301-307, 1979.

Hickey, J. R., Stowe, L., Jacobowitz, H., Pellegrino, P., Maschhoff, R., House, F., and Vonder Haar, T., "Initial Solar Irradiance Determinations from Nimbus 7 Cavity Radiometer Measurements", Science, 208, pp. 281 - 283, 1980.

Hines, W. W., and Montgomery, D. C., Probability and Statistics in Engineering and Management Science, 2nd edition, John Wiley, New York, 1980.

Hollands, K.G.T., "A Deviation of the Diffuse Fraction's Dependence on the Clearness Index", Solar Energy, Vol. 35, pp. 131-136, 1985.

Hollands, K.G.T., "An Improved Model for Diffuse Radiation: Correction for Atmospheric Back-Scattering", Solar Energy, Vol. 38, pp. 233-236, 1987.

Hollands, K.G.T., and Crha, S. J., "A probability Density Function for the Diffuse Fraction, with Applications", Solar Energy, Vol. 38, pp. 237-246, 1987.

Hottel, H. C., "A Simple Model for Estimating the Transmittance of Direct Solar Radiation Through Clear Atmosphere", Solar Energy, Vol. 18, pp. 129-134, 1976.

Hussain, M., "Estimation of Global and Diffuse Irradiation from Sunshine Duration and Atmospheric Water Vapour Content", Solar Energy, Vol. 33, pp. 217-220. 1984.

IMSL Library, International Mathematical and Statistical Libraries, Inc., Houston, Texas, 1977.

Iqbal, M., "Estimation of the Monthly Average of the Diffuse Component of Total Insolation on a Horizontal Surface", Solar Energy, Vol. 20, pp. 101-105, 1978.

Iqbal, M., "A study of Canadian Diffuse and Total Solar Radiation Data-I. Monthly Average Daily Horizontal Radiation", Solar Energy, Vol. 22, pp. 81-86, 1979.

Iqbal, M., "Correlation of Average Diffuse and Beam Radiation with Hours of Bright Sunshine", Solar Energy, Vol. 23, pp. 169-173, 1979.

Iqbal, M., "Prediction of Hourly Diffuse Solar Radiation of Hourly Diffuse Solar Radiation from Measured Hourly Global Radiation on a Horizontal Surface", Solar Energy, Vol. 24, pp. 491-503, 1980.

Iqbal, M., An Introduction to Solar Radiation, Academic Press, New York, 1983.

Jeter, S. M., Craig, J. I., Hartman, T. L., and Hill, J. M., "Development of a Solar Model Year from National Service Chart Data", Proceedings of the ISES Silver Jubillee Congress, 1979.

Jeter, S. M., and Phan, C. N., "Site Specific Clear Day Solar Irradiance Model for Long Term Irradiance Data", AIAA Journal of Energy, Vol. 6, p. 115, 1981.

Jeter, S. M., and Balaras, C. A., A Five Year (1979-1983) Data Base and Solar Model Year for the West Central Georgia, Project Report Prepared for Georgia Power Co., School of Mechanical Engineering, Georgia Institute of Technology, 1986.

Jeter, S. M., and Balaras, C. A., "A Regression Model for the Beam Transmaittance of the Atmosphere Based on Data for Shenandoah, Georgia, U.S.A.", Solar Energy, Vol. 37, pp. 7-14, 1986.

Jeter, S. M., and Balaras, C. A., "Investigation of the Anisotropy of the Sky Radiation Using Tracking and Tilted Pyranometers", Proceedings of the ASES Annual Conference, Boulder, Colorado, 1986.

Jeter, S. M., Balaras, C. A., "Development of Models for the Beam Radiation Based on Data from Shenandoah, Georgia, U.S.A.", Proceedings of the ASES Annual Conference, SOLAR 87, pp. 403-407, 1987.

Johnson, F.S., "The Solar Constant", Journal of Meteorology, Vol. 11, p. 431, 1954.

Johnson, R. L., Subroutine SPOS, McDonnell Douglas Co., Private Communication, 1984.

Justus, C., Craig, J., and Schlag, J., "Program for Solar Energy Meteorological Research and Training Site (Region 3)", Annual Progress Report for the United States Department of Energy, No E-16-630, 1979.

Kaiser, J. A., and Hill R. H., Journal of Geophysical Research, Vol. 81, pp. 395-398, 1976.

Kennard, R. W., "A Note on the C_p Statistic", Technometrics, Vol. 13, p. 899, corrections Vol. 15, p. 657, 1973.

Khuri, A. I., and Comell J. A., Response Surface Designs and Analsyses, Marcel Dekker, Inc., New York, 1987.

Kondratyev, K., Radiation in the Atmosphere, New York, Academic, 1969.

Kosters, J. J., Kyle, T., and Murcray, D., "Attenuation of the Direct Solar Beam by Aerosols", J. Geoph. Res., Vol. 74, pp. 3379-3383, 1969.

Kreider, J. F., and Kreith, F., Solar Energy Handbook, McGraw Hill, pp. 5(10)-5(11), 1981.

Kreith, F., and Kreider, J. F., Principles of Solar Engineering, Series in Thermal and Fluids Engineering, McGraw Hill, New York, 1978.

Lalas, D., Petrakis, M., and Papadopoulos, C., "Correlations for the Estimation of the Diffuse Radiation Component in Greece", Solar Energy, Vol 39, p. 455, 1987.

Lamm, L. O., Adler, C. G., "A New Method for the Determination of Direct Insolation", Solar Energy, Vol. 39, pp. 109-112, 1987.

Lancaster, P., and Salkauskas, K., Curve and Surface Fitting, Academic Press, London, 1986.

Lewis, G., "Diffuse Irradiation over Zimbabwe", Solar Energy, Vol. 31, pp. 125-128, 1983.

Lewis, G., "The Applicability of Diffuse Solar Radiation Models to Huntsville, Alabama", Solar Energy, Vol. 38, pp. 55-57, 1987.

Liu, B.V.H., and Jordan, R.C., "Interrelationship and Characteristic Distribution of Direct, Diffuse and Total Solar Radiation", Solar Energy, Vol. 4, p. 1, 1960.

Lowry, W. P., Direct and Diffuse Solar Radiation: Variations with Atmospheric Turbidity and Altitude, Institute for Environmental Studies, University of Illinois, Urbana-Champaign, UILU-IES 80 0006, 1980.

Ma, C. C. Y., and Iqbal, M., "Statistical Comparison of Solar Radiation Correlations - Monthly Average Global and Diffuse Radiation on Horizontal Surfaces", Solar Energy, Vol. 33, pp. 143-148, 1984.

Mallows, C. L., "Some Comments on C_p", Technometrics, Vol. 15, pp. 661-675, 1973.

Massaquoi, J.G.M., "Predicting Diffuse Radiation when Only Data on Sunshine Duration is Available", Solar and Wind Technology, Vol. 4, pp. 205-210, 1987.

Maxwell, E. L., "A Quasi-Physical Model for Converting Hourly Global Horizontal to Direct Normal Insolation", Proceedings of the ASES Annual Conference, Portland, Oregon, pp. 35-46, 1987.

McClatchey, R. A., et. al., "Optical Properties of the Atmosphere, 3rd edition, Air Force Cambridge Research Laboratories, AFCRL-72-0497, Environmental Research Paper No. 411, 1972.

McDaniels, D. K., Pacific North West Solar Radiation Data, Published by the Solar Monitoring Lab, Physics Department-Solar Energy Center, University of Oregon, Eugene, Oregon, 1987.

McNally, D., Positional Astronomy, John Wiley and Sons, New York, 1974.

Modi, M., and Sukhatme, S. P., "Estimation of Daily Total and Diffuse Insolation in India from Weather Data", Solar Energy, Vol. 22, pp. 407-411, 1979.

Mujahid, A. M., and Turner, W. D., "Diffuse Sky Measurements and Determination of Corrected Shadow Band Multiplication Factors", ASME paper 80-WA/SOL-6, 1980.

Mujahid, A., and Turner, W. D., "Solar Radiation Modeling and Comparisons with Current Solar Radiation Models", Proceedings of the AS/ISES Annual Conference, Phoenix, Arizona, G.E. Franta and B.H. Glenn, editors, 1980.

National Almanac, United States Naval Observatory, Washington D.C., Annual Publication.

National Oceanic and Atmospheric Administration, Monthly Summary Solar Radiation Data, Vols. 1-4, National Climatic Center, Asheville, North Carolina.

Norris, D. J., "Solar Radiation on Inclined Surfaces", Solar Energy, Vol. 10, pp. 72-77, 1966.

Norris, D. J., "Correlation of Solar Radiation with Clouds", Solar Energy, Vol. 12, pp. 107-112, 1968.

Orgill, J. F., and Hollands, K.G.T., "Correlation Equation for Hourly Diffuse Radiation on a Horizontal Surface", Solar Energy, Vol. 19, pp. 357-359, 1977.

Page, J. K., "The Estimation of Monthly Mean Values of Daily Total Short-Wave Radiation on Vertical and Inclined Surfaces from Sunshine Records for Latitudes 40N to 40S", Proceedings of U.N. Conference on New Sources of Energy, Rome, Italy, 1961.

Perez, R., Seals, R., Ineichen, P., Stewart, R., and Menicucci, D., "A New Simplified Version of the Perez Diffuse Irradiance Model for Tilted Surfaces", Solar Energy, Vol. 39, pp. 221-231, 1987.

Phan, C. N., Procedures for Quality Control and Analysis of Data from a Solar Meteorological Monitoring Station, Master's Thesis, School of Mechanical Engineering, Georgia Institute of Technology, 1980.

Pinker, R. T., and Ewing, J. A., "Modeling Surface Solar Radiation: Model Formulation and Validation", Journal of Climate and Applied Meteorology, Vol. 24, p. 389, 1985.

Rabl, A., "Yearly Average Performance of the Principal Solar Collector Types", Solar Energy, Vol 27, p. 215, 1981

Randall, C. M., and Whitson, M. E., "Hourly Insolation and Meteorological Data BAses Including Improved Direct Insolation Measurements", Aerospace Corporation, Final Report ATR-78(7592)-1, 1977.

Rao, C.R.N., Bradley, W. A., and Lee, T. Y., "The Diffuse Component of the Daily Global Solar Irradiation at Corvallis, Oregon (U.S.A.)", Solar Energy, Vol. 35, pp. 637- 641, 1984.

Rao, C.R.N., Bradley, W. A., and Lee, T. Y., "Some Comments on Angstrom Type Regression Models for the Estimation of the Daily Global Solar Irradiation", Solar Energy, Vol. 34, pp. 117-119, 1985.

Rapp, D., and Hoffman, A.A.J., "On the Relation Between Insolation and Climatological Variables - I. Analysis of Insolation Patterns at Fort Worth, Texas", Energy Conservation, Vol. 16, pp. 1-11, 1976.

Raschke, E., and Bandeen, W., "The Radiation Balance of the Planet Earth from Radiation Measurements of the Satellite Nimbus II", Journal of Atmospheric Sciences, Vol. 9, pp. 215-238, 1970.

Rietveld, M. R., "A New Method for Estimating the Regression Coefficient in the Formula Relating Solar Radiation to Sunshine", Journal of Agricultural Meteorology, Vol. 19, pp. 243-252, 1978.

Roberts, C. K., and Boksenberg, A., The Astronomical Almanac U. S. Naval Observatory, Washington, D.C., 1985.

Robinson, N., ed., Solar Radiation, Elsevier, Amsterdam, 1966

Ruth, D. W., and Chant, R. W., "The Relationship of Diffuse Radiation to Total Radiation in Canada", Solar Energy, Vol. 18, pp. 153-154, 1976.

Shaw, N., Mannual of Meteorology. Vol. 3: The Physical Processes of Weather, Cambridge, Cambridge University Press, 1930.

Sherry, J. E., and Justus, C. G., "A Simple Hourly All-Sky Solar Radiation Model Based on Meteorological Parameters", Solar Energy, Vol. 32, p. 195, 1984.

Sloan, S. W., "A Fast Algorithm for Constructing Delaunay Triangulations in the Plane", Advanced Engineering Software, Vol. 9, pp. 34-55, 1987.

Smietana, P. J., Flocchini, R. G., Kennedy, R. L., and Hatfield, J. L., "A New Look at the Correlation of KD and KT Models Using One-Minute Measurements", Solar Energy, Vol. 32, pp. 111-114, 1979.

Smith, W. L., Hickey, J., Howell, H., Jacobowitz, H., Hilleary, D., and Drummond, A., "Nimbus-6 Earth Radiation Budget Experiment", Applied Optics, Vol. 16, p. 306, 1977.

Sofia, S., Demarque, P., and Endal, A., "From Solar Dynamo to Terrestrial Climate", American Scientist, Vol. 73, pp. 326-333, 1985.

Solar Energy Research Institute, Solar Radiation and Meteorological Data Collection Activities in the United States, SERI/SP-281-1973, Golden, CO., 1983.

SOLMET, Vol. 2, "Hourly Solar Radiation - Surface Meteorological Observations", TD-9724, National Climatic Center, Ashville, North Carolina, 1979.

Speigel, L. S., Total Horizontal Solar Radiation Use in Determining Radiation Values on a Tilted Solar Collecting Surface, Master's Thesis, School of Geophysical Sciences, Georgia Tech, 1981.

Spencer, J. W., "A Comparison of Methods for Estimating Hourly Diffuse Solar Radiation from Global Solar Radiation", Solar Energy, Vol. 29, pp. 19-32, 1982.

Stanhill, G. "Diffuse, Sky and Cloud Radiation in Israel", Solar Energy, Vol. 10, pp. 96-101, 1966.

Stauter, R., and Klein, S. A., presented in Solar Engineering of Thermal Processes, by J.A. Duffie, and W. Beckman, John Wiley, 1980.

Stephens, G. L., "Radiation Profiles in Extended Water Clouds. I: Theory", Journal of Atmospheric Sciences, Vol. 35, pp. 2111-2122, 1978.

Stephens, G. L., "Radiation Profiles in Extended Water Clouds. II: Parameterization Schemes", Journal of Atmospheric Sciences, Vol. 35, pp. 2123-2132, 1978.

Stuart, R. W., and Hollands, K.G.T., "A probability Density Function for the Beam Transmittance", Proceedings of the ASES Annual Conference, Portland, Oregon, pp. 52-58, 1987.

Suckling, P. W., and Hay, J. E., "Modeling Direct, Diffuse, and Total Solar Radiation for Cloudless Days", Atmosphere, Vol. 14, pp. 298-308, 1976.

Studies in Geophysics, Solar Variability, Weather, and Climate, edited by the Geophysics Study Committee, Geophysics Research Board, Commission on Physical Sciences, Mathematics, and Resources, National Research Council, National Academy Press, Washington D.C., 1982.

Tabor, H.,"Solar Energy-Dreams and Reality", Space Solar Power Review, Vol. 5, pp. 247-252, 1985

Tarpley, J. D., "Estimating Incident Solar Radiation at a Surface from Geostationary Satellite Data", Journal of Applied Meteorology, Vol. 18, p. 1172, 1979.

Thekaekara, M., "Solar Radiation Measurement: Techniques and Instrumentation", Solar Energy, Vol 18, p. 309, 1976

Tuller, S. E., "The relationship between Diffuse, Total and Extraterrestrial Solar Radiation", Solar Energy, Vol.18, pp. 259-263, 1976.

Turner, W. D., and Salim, M., "Comparison of Two Diffuse Sky Radiation Models", Solar Energy, Vol. 32, pp. 677 - 680, 1984.

Turner, W. D., and Mujahid, A. M., "Determination of Direct Normal Solar Radiation from Measured Global Values - Comparison of Models", Journal of Solar Energy Engineering, Vol. 107, pp. 39-44, 1985.

Twomey, S., "The Influence of Aerosols on Radiative Properties of Clouds", Climate Change and Variability, a Southern Perspective, Pittock et al., Eds., Cambridge University Press, pp. 281-282, 1976.

Vignola, F., and McDaniels, D. K., "Correlations Between Diffuse and Global Insolation for the Pacific Northwest", Solar Energy, Vol. 32, pp. 161-168, 1984.

Vignola, F., and McDaniels, D. K., "Beam-Global Correlations in the Pacific Northwest", Solar Energy, Vol. 36, pp. 409-418, 1986.

Vonder Haar, T. H., and Ellis, J. S., "Solar Energy Microclimate as Determined from Satellite Observation", Optics in Solar Energy Utilization, Vol. 68, pp. 18-22, 1975.

Watt, A. D., "On the Nature and Distribution of Solar Radiation", HCP/T2552-01, U.S. Department of Energy, Washington, D.C., U.S.G.P.O.., 1978.

Willson, R. C., Duncan, C., and Geist, J., "Direct Measurement of Solar Luminosity Variation", Science, Vol. 207, pp. 177-179, 1980.

World Meteorological Organization, Measurement of Radiation and Sunshine, Guide to Meteorological Instruments and Observing Practices, 4th edition, W.M.O., No. 8, T.P. 3, Geneva, Switzerland, 1971.

World Meteorological Organization, Commission for Instruments and Methods for Observation, Abridged Final Report of the Seventh Session, W.M.O., No. 490, 1978.

Yellott, J. I., "Solar Radiation Measurements", Application of Solar Energy for Heating and Cooling of Buildings, ASHRAE, New York, 1977.

VITA

Constantinos Agelou Balaras was born in Athens, Greece, on September 20, 1962. He attended the Varvakio Model School in Athens and upon graduation was admitted to the Mechanical Engineering Department of the Michigan Technological University, where he was awarded a foreign student scholarship. For two summers during his undergraduate studies he was employed at the Hellenic Shipyards Co., Skaramaga, Greece, as an engineering trainee.

Upon receiving his Bachelor of Science in Mechanical Engineering, with honors, September 1980 - February 1984, he was admitted to the graduate program at the George W. Woodruff School of Mechanical Engineering, Georgia Institute of Technology. He graduated with the degree of Master of Science in August 1985, and then continued towards his Ph.D. degree. During his graduate studies at Georgia Tech, he was a research assistant working in the area of solar radiation modeling. On the subject he completed a Master's thesis, the present Ph.D. dissertation, and a number of publications. Towards the end of his Ph.D. studies he was a consulting engineer at American Combustion Inc.

He is a member of the Sigma Xi (The Scientific Research Society), the Pi-Tau-Sigma (Honorary Mechanical Engineering Fraternity), ASME, AHRAE, ASES, and ISES.